The influence of collagen isolation, cross-linking and sterilisation on macrophage response

A thesis submitted to the National University of Ireland Galway for the degree of Doctor of Philosophy

By

Luis M. Delgado

Research Supervisor: Dr Dimitrios I. Zeugolis

March 2018

Regenerative, Modular & Developmental Engineering Laboratory (REMODEL)

Centre for Research in Medical Devices (CÚRAM)

National University of Ireland Galway (NUI Galway)

Table of contents

Plagiarism statement

I certify that the thesis is all my own work and I have not obtained a degree in this University, or elsewhere, on the basis of this work.

Luis M. Delgado

Table of figures

Chapter 1

Chapter 2

Chapter 4

Table of tables

Chapter 1

Chapter 3

List of abbreviations

AA: acetic acid;

APS: ammonium persulphate;

CD#: cluster of differentiation (#);

CFU: colony forming units;

CH: carbohydrate;

COL#: collagen type #;

DSC: differential scanning calorimetry;

ECM: extracellular matrix;

EDC: 1-ethyl-3-(3-dimethylaminopropyl) carbodiimide;

ELISA: enzyme-linked immunosorbent assay;

EO: ethylene oxide;

ET: ethanol;

DHT: dehydrothermal treatment;

DMEM: Dulbecco's modified Eagle's medium;

DPPA: diphenyl-phosphorylazide;

FBGCs: foreign body giant cells;

FBS: foetal bovine serum;

GAG: glycosaminoglycan;

GEN: genipin;

GI: gamma irradiation;

GP: gas plasma;

GTA: glutaraldehyde;

HBSS: Hank's balanced salt solution;

HCl or HC: hydrochloric acid;

HE: haematoxylin and eosin staining;

HIF 1α: hypoxia inducible factor 1 alpha;

HMDI: hexamethylene diisocyanate;

IF: immunofluorescence;

IFN-γ: interferon gamma;

IHC: immunohistochemistry;

IL-#: interleukin (#);

FITC: fluorescein isothiocyanate;

LDH: lactate dehydrogenase;

LPS: lipopolysaccharide;

MCP-#: monocyte chemo-attractant protein-#;

MIP-#: macrophage inflammatory protein-#;

MMC: macromolecular crowding;

MMP: matrix metalloproteinases;

MT: Masson's trichrome staining;

Mw: molecular weight;

NCL: non-cross-linked;

NHS: N-hydroxysuccinimide;

NO: nitric oxide;

NS: non-sterile;

OLE: oleuropein;

PBMCs: peripheral blood mononuclear cells;

PBS: phosphate buffered saline;

PCR: polymerase chain reaction;

PDGF: platelet-derived growth factor;

PEG: polyethylene glycol;

PF4: platelet factor 4;

PG: proteoglycan;

PMA: phorbol 12-myristate 13-acetate;

RANTES: regulated on activation, normal T cell expressed and secreted;

RAW264.7: mouse leukemic monocyte-macrophage cell line;

RGD: Arg-Gly-Asp or arginyl-glycyl-aspartic acid;

ROS: reactive oxygen species;

RPM: rotations per minute;

SDS: sodium dodecyl sulphate;

SDS-PAGE: sodium dodecyl sulphate polyacrylamide gel electrophoresis;

SEM: scanning electron microscopy;

SIS: small intestinal submucosa;

TCP: tissue culture plastic;

TEMED: tetramethylethylenediamine;

TGase: transglutaminase;

TGF-β: transforming growth factor beta;

THP-1: human derived leukemic monocyte cell line;

TIMP: tissue inhibitors of matrix metalloproteinases;

TNF-α: tumour necrosis factor alpha;

TSB: Tryptic soy broth;

U937: human leukemic lymphoma monocytes cell;

VEGF: vascular endothelial growth factor;

4SP: 4-arm PEG succinimidyl glutarate;

Acknowledgements

First of all, I would like to sincerely thank Dr Dimitrios Zeugolis for the opportunity to work in his research group with such exciting topic and for his valuable supervision, patience, huge support and encouragement even at very difficult moments. His impetus and great sense of humour have helped me to develop this project and to improve my research skills. I would also like to thank European Union Seventh Framework Programme (FP7/2007-2013) for the financial support, under the grant agreement number 263289 (Green Nano Mesh).

I would like to profoundly extend my thanks to Prof Abhay Pandit for his valuable scientific advice. Also, I wish to extend my gratitude to both former and current members of REMODEL, CURAM and NUIG, especially Dr Oliver Carroll, Dr Oonagh Dwane, Dr Manus Biggs, Dr Fitzgerald, Mr Vidoja Kovacevic, Ms Tara Cosgrave, Mr Anthony Slogan, Dr Enda O'Connell, Mr Maciej Doczyk, Mr Keith Feerick, Mr David Connolly and Mr William Kelly.

This thesis project would have been even harder to complete without the continuous, unconditional and unforgettable help from Mr Kieran Fuller, Ms Diana Gaspar, Ms Ayelen Helling, Mr Kyriakos Spanoudes, Ms Lígia Bré and Mr Joshua Chao. I do not have enough words to acknowledge what you have done for me, especially to you Kieran and Diana for getting me away from the late lab hours and for the kayaking hours.

I would like to thank the members of Phibo for the selfless training about the sterilisation treatment and regulatory. For their guidance since I was an undergraduate student who wanted to dedicate his life to research, I would like to sincerely extend my thanks to Prof F. Javier Gil, Prof Maria Pau Ginebra, Dr Conrado Aparicio, Dr Elisabeth Engel, Dr Marta Pegueroles and Dr Román Pérez.

I would like to thank my lab colleagues and Galway friends Marc, Tom, Estelle, Eleni, Andrew, Anna, Naledi, Christina, Diana P, Zhuning, Pramod, Abhigyan, Alex, Daniela, Peader, Aitor, Shane, Dilip, Akshay, Bill, Gianluca, Peter and Colm. I have a funny story from each one of you.

Finally, but not less important, I wish to thank my family. Thanks mum and dad for your support and education showing me the importance of love, work and knowledge. Thanks Miguel for your lessons and being an example of commitment and integrity. And, I am honestly grateful to my wife Irene. I still remember her sad face when I told her that I finally was moving to Ireland to perform this challenging project; it was tough, but we have reached the finish line. Although it was a very complex episode of our story, we had the fortune to receive such a great gift: our daughter Aina. Sincerely, thank you for your love, being behind me even living far away and giving me the greatest gift of life. I cannot imagine finishing this PhD thesis without you.

Abstract

Collagen-based devices are frequently associated with foreign body response. Although several pre- (e.g. species, state of animal, tissue, isolation protocol) and post- (e.g. cross-linking, scaffold architecture, sterilisation) scaffold fabrication factors have a profound effect on foreign body response, little is known about how collagen-based devices fabrication mediates macrophage response. In this thesis, we assessed biophysically, biochemically and biologically three different treatments during the fabrication of a collagen type I film: collagen isolation, cross-linking and sterilisation.

In the first phase of this thesis, we studied the influence of acetic acid and hydrochloric acid and the utilisation or not of pepsin or salt precipitation during collagen extraction on the yield, purity, free amines, denaturation temperature, resistance to collagenase degradation and macrophage response. Subsequently, as extracted collagen forms are usually subjected to chemical cross-linking to enhance their stability and the traditional cross-linking approaches are associated with toxicity and inflammation, we investigated the stabilisation capacity, cytotoxicity and inflammatory response of collagen scaffolds cross-linked with glutaraldehyde, carbodiimide, 4-arm polyethylene glycol succinimidyl glutarate, genipin and oleuropein. Therefore, as a step forward and given that there is still no single cross-linking method / sterilisation treatment that can be used universally for collagen-based devices, we assessed the influence of ethylene oxide, ethanol, gamma irradiation and gas plasma sterilisation on the structural, biophysical, biochemical and biological properties of self-assembled collagen films cross-linked with the optimised cross-linking agents from the previous part, 4-arm polyethylene glycol succinimidyl glutarate and genipin.

Acetic acid / pepsin extracted collagen exhibited the highest yield, purity and free amine content and the lowest denaturation temperature. No differences in resistance to collagenase digestion were detected between the different extraction groups. Although all treatments exhibited similar macrophage morphology comprised of round cells (M1 phenotype), elongated cells (M2 phenotype) and cell aggregates (foreign body response), significantly more elongated cells were observed on collagen films extracted using acetic acid. Moreover, cytokine analysis revealed that hydrochloric acid treatments induced significantly higher IL-1β and TNF-α release from macrophage with respect to acetic acid treatments. Salt precipitation did not influence the assessed parameters. Overall, our data suggest that collagen extraction variables affect the physicochemical and biological properties of collagen preparations.

Regarding collagen cross-linking, fibroblast cultures showed no significant difference between the treatments. Although direct cultures with human derived leukemic monocyte cells (THP-1) clearly demonstrated the cytotoxic effect of glutaraldehyde, THP-1 cultures supplemented with conditioned media from the various groups showed no significant difference between the treatments. No significant difference in secretion of pro-inflammatory (e.g. IL-1β, IL-8, TNF-α) and anti-inflammatory (e.g. VEGF) cytokines was observed between the non-cross-linked and the 4SP and genipin cross-linked groups, suggesting the suitability of these agents as collagen cross-linkers.

With regards to collagen sterilisation, our data clearly illustrate that gas plasma is not suitable for collagen-based devices. Ethylene oxide, after 4-arm polyethylene glycol succinimidyl glutarate cross-linking, resulted in significant reduction of the mechanical properties of the collagen films. Gamma irradiation and ethanol

sterilisation did not significantly affect thermal, degradation, solubility and mechanical properties of the collagen films. Human skin fibroblast and human macrophage cultures did not reveal any considerable differences as a function of the cross-linking method / sterilisation treatment. Overall, our data illustrate that genipin cross-linking maintains collagen stability even against the most severe sterilisation treatments.

Collectively, these data suggest that during collagen scaffold fabrication all processing variables should be monitored as, evidently, they affect collagen stability and biological response.

Keywords

Collagen; Collagen isolation; Acid extraction; Pepsin extraction; Salt precipitation; Collagen cross-linking; Mechanical resilience; Enzymatic stability; Macrophage response; Cytokine release; Foreign body response; Host response; Inflammation; Collagen sterilisation; Collagen stability.

Chapter 1: Introduction

Sections of this chapter have been published or are under submission at:

Delgado LM, Pandit A, Zeugolis DI. *Influence of sterilisation methods on collagen-based devices stability and properties.* Expert Rev Med Devices. 2014;11(3):305-314.

Delgado LM, Bayon Y, Pandit A, Zeugolis DI. *To cross-link or not to cross-link? Cross-linking associated foreign body response of collagen-based devices.* Tissue Eng Part B Rev. 2015;21(3):298-313.

Abbah SA*, **Delgado LM***, Azeem A, Fuller K, Shologu N, Keeney M, Biggs MJ, Pandit A, Zeugolis DI. *Harnessing Hierarchical Nano- and Micro-Fabrication Technologies for Musculoskeletal Tissue Engineering.* Adv Healthc Mater. 2015;4(16):2488-2499. *: S.A.A. and L.M.D. contributed equally to this work.

Sorushanova A, **Delgado LM**, Wu Z, Shologu N, Kshirsagar A, Raghunath RN, Mullen AM, Bayon Y, Pandit A, Raghunath M, Zeugolis DI. *New tricks for the old protein – Collagen biosynthesis, characterisation and device development.* Submitted.

1.1. Introduction

Collagen is one of the major structural extracellular matrix (ECM) proteins in mammals, constituting 20 to 30% of the total body proteins. To-date, 29 different collagen types have been identified [1], with all types sharing a unique and common triple-helical configuration with a repeated $[Gly\text{-}X\text{-}Y]_n$ sequence, where X- is often proline and Y- is frequently hydroxyproline [2, 3]. Among the different collagen types, collagen type I, predominantly localised in skin, tendon, cornea and bone, is the most abundant in the body and consequently the most widely studied. Collagen-based materials, in the form of tissue grafts and reconstituted scaffolds (Although scaffold has been traditionally defined as three-dimensional macroporous substrate, it could be currently defined as 2D or 3D engineered devices mimicking ECM properties and allowing cell and tissue infiltration), are attractive for biomedical applications such as wound healing, due to their natural composition and their well-tolerated degradation products, are perceived by the host as normal constituents rather than as foreign matter and therefore provide an acceptable host response [4]. In addition to their superior mechanical properties, collagen-based devices provide instructive cues to the cells, promoting this way functional tissue repair and regeneration [5, 6]. It is therefore not surprising that the collagen-based medical device market is estimated to reach US$ 3.7 billion by 2017 [7].

The natural cross-linking pathway of lysyl oxidase is responsible for mechanical resilience of tissues and their proteolytic resistance [8]. Given that the natural cross-linking pathway of lysyl oxidase does not occur *in vitro*, the harsh extraction / purification methods [9], scaffold fabrication technologies [10] and the subsequent sterilisation methods [11] necessitate the introduction of exogenous cross-links (chemical, physical or biological in nature) into the molecular structure of collagen

implants to control their degradation rate and enhance their mechanical stability [12-14]. However, such cross-linking approaches are associated with numerous shortfalls as a function of the cross-linking density / method, including cytotoxicity [15, 16], calcification [17-19] and foreign body response [20, 21], impairing wound healing.

The physico-chemical and biological factors need to be maintained after the final sterilization processing. Effective sterilization is required, as with every other medical device. However, current sterilisation methods may adversely affect material properties, release profile of therapeutic molecules, protease degradation and *in vivo* absorption rate [22-24], they simultaneously give rise to potentially beneficial changes with respect to cellular attachment and growth [25]. Indeed, both moist and dry heat are known to denature, albeit to different extent, the triple helical structure of collagen [12], resulting in the increased availability of the otherwise cryptic RGD motifs that are recognised by integrins, thus promoting cell attachment [26, 27].

In this chapter, the physiological and impaired wound healing, the collagen sources and extraction methods and the collagen cross-linking and sterilisation methods are discussed. The project rationale is also introduced.

1.2. Wound healing

1.2.1. Physiological wound healing

The wound healing process is the innate response of all tissues to any injury or device implantation. It is a complex process that is regulated by several cell types; growth factors; and cytokines that direct the four overlapping phases (**Figure 1.1** and **Figure 1.2**), namely haemostasis, inflammation, new tissue formation and tissue remodelling [28].

Haemostasis occurs immediately after injury or device implantation. Released factors from the tissue induce platelets to secrete clotting factors (e.g. mainly serotonin, thromboxane, PDGF, TGF-β) to promote coagulation and to develop a fibrin clot [29]. This provisional fibrin matrix acts as a scaffold for further cell migration. Simultaneously to the formation of the fibrin clot, a dynamic interaction between blood plasma proteins and the device surface occurs and a provisional matrix around the biomaterial surface is developed; this event is known as Vroman effect [30]. The initial protein adsorption depends on the surface properties of the device, including wettability [31, 32]; surface charge / chemistry [33, 34]; topography / roughness [35-37]; and stiffness [38], which modulate cell / inflammatory response and subsequent wound healing.

Following haemostasis, acute inflammation begins between 24 and 48 hours after injury. This phase is characterised by the recruitment of neutrophils and mast cells in response to chemokines (cytokines with chemo-attractive properties) and other chemo-attractants (mainly IL-1, IL-6, IL-8, MCP-1, MIP-1 and TNF-α) [39, 40]. Neutrophils and mast cells phagocytise foreign material, bacteria, dead cells and damaged matrix within the wound. The presence of contaminants / foreign matter at wound bed increases neutrophil presence, reactive oxygen species (ROS) and

cytokine signalling [39, 41]. Neutrophils secrete TGF-β, PDGF, PF4 and IL-1 to recruit further mast cells and monocytes. Mast cells secrete histamine and other cytokines that recruit leukocytes into the injury site. After 48-72 hours, monocytes migrate and differentiate into macrophages, which secrete TNF-α, IL-6, RANTES, MCP-1 and MIP-1 to recruit further macrophages and dominate the cell population at the injury site [42]. Initially, macrophages are mainly M1 phenotype, a pro-inflammatory or classically activated phenotype. M1 macrophages attack potential pathogens or phagocytise at the wound site, as a response to IFN-γ, TNF-α or bacterial lipopolysaccharides. Gradually, M1 macrophages change to M2 phenotype, an anti-inflammatory or alternatively activated phenotype. M2 macrophages have been described as displaying different sub-phenotypes or roles, which are anti-inflammatory (M2a), immunoregulatory or homeostatic (M2b) and pro-wound healing (M2c) [43-45]. The macrophage phenotype switch is induced by cytokines, such as IL-4, IL-10 and IL-13, and functional reconstruction depends on the timing of this change. Macrophage activation and polarisation is crucial in the coordination of the later inflammation and regeneration phases [46, 47]. Thus, macrophage polarisation and activation is at the forefront of scientific investigation, with various studies aiming to modulate it using biophysical cues (e.g. architectural features [48]; topographical patterns [36]); biochemical signals (e.g. incorporation of glycosaminoglycans [49] or drugs [50]); and biological means (e.g. gene therapy with lipoplexes [51] or polyplexes [52]).

New tissue formation begins 2-10 days after injury and is identified by migration and proliferation of different cell types that produce new ECM and form the initial wound. In skin, for example, keratinocytes migrate over the dermis and restore the barrier function of the epidermis [39], while fibroblasts, attracted by macrophage

cytokines, migrate to the injury site from the wound edge or bone marrow and differentiate into myofibroblasts, contributing to the wound contraction [53]. During this stage, fibroblasts and myofibroblasts interact, migrate, proliferate and secrete ECM proteins to replace the fibrin matrix and form new tissue, predominantly constituted by collagen type III and smaller amounts of fibronectin, elastin and proteoglycans [39, 54]. Meanwhile, macrophages and fibroblasts secrete VEGF and FGF2 respectively that promote endothelial and progenitor cells to produce new blood vessels [54, 55]. These new vessels start out from pre-existing vessels adjacent to the wound [39].

Tissue remodelling significantly increases 2-3 weeks after injury and could continue for over a year. The remodelling phase is characterised by different cell types undergoing reduction in cell activity and apoptosis and the creation of mature blood vessels. Collagen type III is gradually replaced by collagen type I, an event mainly controlled by matrix metalloproteinases (MMP), tissue inhibitors of matrix metalloproteinases (TIMP) and mechanical stress and strain. The properties of the tissue are partially recovered, but the new tissue hardly ever reaches the pre-injury state; for example, dermis reaches up to 70% of its pre-injury tensile strength [39].

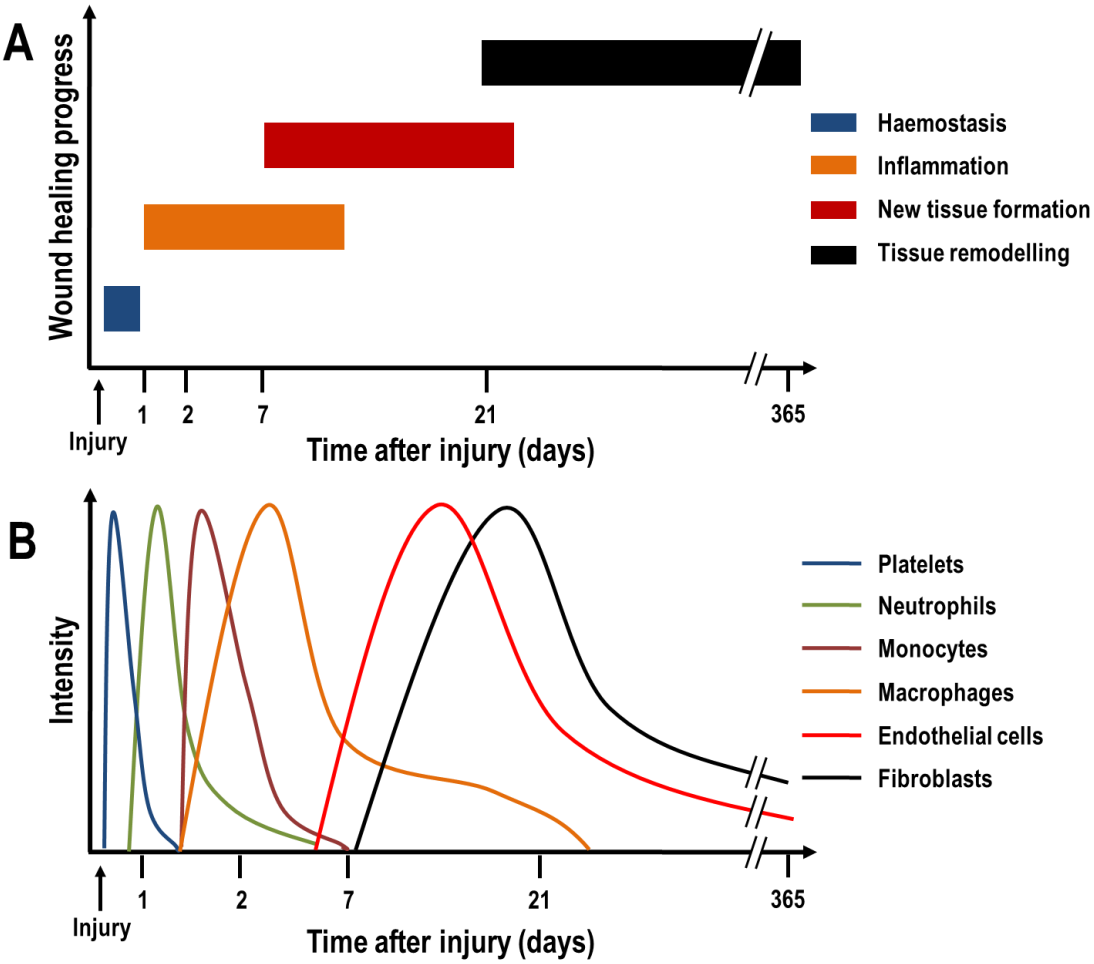

Figure 1.1. Temporal distribution of the four overlapping wound healing phases (A) and associated cell type (B).

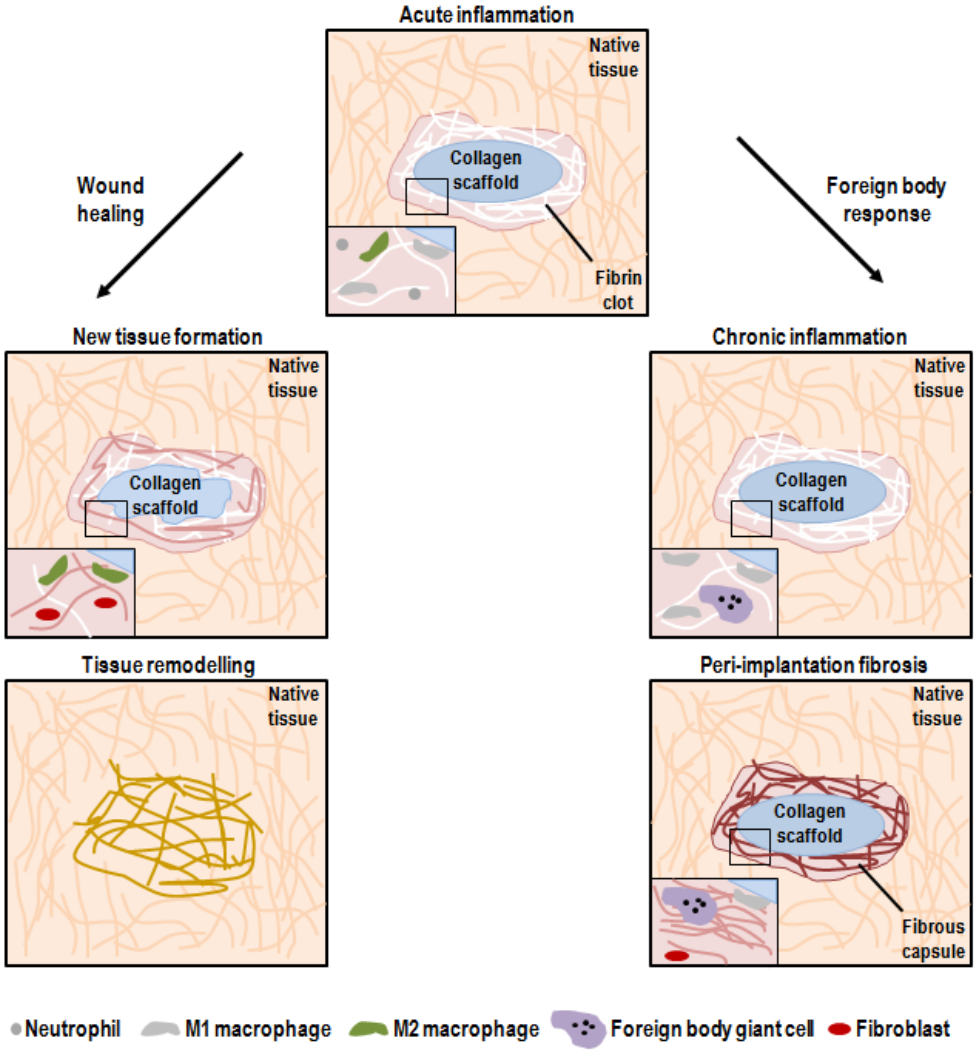

Figure 1.2. Acute inflammation is characterized by the presence of neutrophils, monocytes, and macrophages. Depending on the resolution of the acute inflammation, injury repair could lead to a wound healing process or a classical foreign body response. In wound healing, M2 macrophages attract fibroblast and endothelial cells to secrete a new vascularized tissue. This connective tissue replaces fibrin clot and degraded scaffold. Tissue remodelling is the last healing and could continue for over a year. In foreign body response, acute inflammation persists over time and M1 macrophages aggregate into foreign body giant cells (FBGCs). M1 macrophages and FBGCs fail to degrade the foreign scaffold, resulting in fibroblast recruitment and deposition of a fibrous connective tissue around the scaffold (peri-implantation fibrosis).

1.2.2. Impaired wound healing

Multiple potential factors, local (e.g. injury size, infection, device properties and degradation products) or systemic (e.g. nutrition, age, health state) [56] in nature can interfere with one or more wound healing stages resulting in improper or impaired wounds. The most common impaired wounds after device implantation are delayed acute wounds, chronic wounds and peri-implantation fibrosis, the hallmark of which is a patch of inflammatory cells, mainly macrophages and foreign body giant cells (FBGCs), and a disorganised extracellular matrix, mostly collagen [39, 56]. The foreign body response is composed of macrophages, foreign body giant cells and a fibrous connective tissue around the scaffold, this response is considered the end-stage response of a pro-inflammatory responses following implantation of a medical device [42]. On the other hand, chronic wounds are defined as wounds that fail to proceed through the normal wound healing phases in an orderly and timely manner, including excessive levels of pro-inflammatory cytokines, proteases, ROS, and senescent cells [57].

In severe burns, immunosuppression is brought about due to suppression of T-cell proliferation, large macrophage activation and high amount of pro-inflammatory cytokine and free radicals that predispose patients to impaired healing, infection and systemic organ failure [58, 59].

Local factors, such as bacterial contamination and foreign material that cannot be cleaned or degraded respectively, induce the inflammatory cells (monocytes, M1 macrophages and FBGCs) to remain at the device's interface, prolonging the inflammation phage to over months or years and leading into chronic inflammation and healing failure [39]. Systemic factors are associated with the overall health / disease state of the patient. Increased age is often associated with impaired wound

healing. For example, in healthy older adults, wound healing suffers a temporal delay associated with dysfunction of macrophage phagocytic capacity [60] and polarisation [61]; delayed angiogenesis [62]; and delayed collagen synthesis and re-epithelisation [63]. Obesity, that nowadays affects over 500 million people worldwide [64], induces hypoxia and high infection rate due to skin folds and partial suppression of T-cell function [65, 66]; prompts wound dehiscence by increasing tension on wound site [67]; and alters adipocytes and macrophages ratio in adipose tissue, inducing increased production of adipocytokines (e.g. TNF-α, IL-6, IL-8 and MCP-1)[68]. This increase of adipocytokines, in combination with the activation of granulocytes and monocytes that secrete free radicals and proteolytic enzymes [66], compromise the wound healing process. Diabetes, with over 382 million sufferers worldwide in 2013 [69], increases reactive oxygen species production and reduces antioxidant secretion, leading to oxidative stress [70], which when combined with the hypoxic stress of diabetic wounds [71], leads to an increased inflammatory response [56]. Further, diabetic patients have several dysregulated cellular functions, including reduction of inflammatory cell recruitment [72]; limited bacterial phagocytosis [73]; and dysfunction of macrophage polarisation (maintaining a strong M1 marker expression and function [74] or fibroblast dysfunction [75]) that result in an unbalanced expression of growth factors and MMPs that inhibit new tissue formation [76], compromising that way physiological wound healing.

1.3. State of the art of collagen

The term ‘collagen’ encompasses a large group (40 different genes form 29 homo- and hetero- trimeric molecules) of glycoproteins. In the human body, collagen is the major connective tissue component; it constitutes 75-90 % of the human skin, organic part of bone, cartilage, tendon and cornea and provides mechanical support/integrity and specific function of each tissue [77-87]. This abundance of collagen in human tissues has prompted scientific research and technological innovation into its utilisation as a scaffold fabrication material in tissue engineering applications due to its natural composition, favourable mechanical properties, low antigenicity and well-tolerated degradation products [4, 5, 12, 88-92]. In addition, collagen-based materials provide biological cues that support cell attachment, proliferation and growth, ultimately promoting functional repair and regeneration of tissues and organs *in vivo* [46, 93].

1.3.1. Collagen diversity

‘Collagen’ encapsulates a broad range of glycoproteins with some common characteristic features: all collagen types share a unique and common triple-helical configuration with $[Gly\text{-}X\text{-}Y]_n$ amino acid sequence where X is often proline and Y is frequently hydroxyproline. The triple-helical structure is based on a right-handed triple helix formed by three left-handed polyproline α chains of identical length, which determines the unique quaternary structure of collagen stability [12, 93]. These difference between collagens have been identified by minor alterations in the collagen molecule in terms of triple helix length, molecular weight, charge profile, interruptions of the triple helix, size and shape of the terminal globular domains, cleavage or retention of the latter aggregates, and variation in the post-translation

modifications [6, 82]. To-date, all collagens have been classified into four different types: fibrous collagens (types I, II, III, V, XI, XXIV and XXVII consist of quarter-staggered fibrils), non-fibrous collagens (types IV, VII and XXVIII with inabilities to form quarter-staggered fibrils by themselves), filamentous collagens (types VI, VIII and X) and fibril associated collagens with interrupted triple-helices (FACIT, types IX, XII-XVII, XIX–XXIII and XXV) [1].

1.3.2. Collagen structure and conformation

The triple-helical conformation is the common and unique structural element of all collagens, which was deduced from high angle X-ray fibre diffraction studies in tendon [94]. The collagen triple-helix (tertiary structure) has a coiled-coil structure made of three parallel polypeptide chains. Subsequently, each α-chain (secondary structure) is constituted by three collagen polypeptides which are wound around each other in a regular helix to generate a rope-like structure approximately (280nm in length and 1.4nm in diameter). In particular, collagen type I, present in the form of elongated fibres in skin, bone and tendon, present individual fibrils that can be longer than 500 μm with diameter about 500nm and contain more than 10 million molecules. The collagen fibrils possess a high level of axial alignment, which results in the characteristic D banding; this produces an average periodicity of 67 nm in the native hydrated state and 55-65 nm in dehydrated samples for electron microscopy [95-100].

Moreover, the intra-molecular hydrogen bonds between glycines in adjacent chains provide the helix stability. The hydroxyl groups of hydroxyproline residues are also involved in hydrogen bonding the stabilisation of triple helix structure. Specifically, the two hydrogen bonds formed within the chains are due to the attraction force

between the amine group of a glycyne residue and the carboxylic group of the residue in the second position of the triplet in the adjacent chain and the second bond is via the water molecule participating in the formation of additional hydrogen bonds with the help of the hydroxyl group of hydroxyproline in the third position. Each α-chain is a left-handed helix and the three chains are staggered by one residue relative to each other and are super-coiled around a central axis and form a right-handed super-helix [101-104]. At each end of the collagen molecule is a short non-helical region known as telopeptide. These telopeptide domains are crucial for the fibril formation and are involved in the collagen cross-linking process [105-107].

1.3.3. Collagen-based materials in Tissue Engineering

Collagenous materials, in various physical forms (tissue grafts, hydrogels, sponges, fibres, films, hollow spheres and tissue-engineered substitutes), are extensively used in Tissue Engineering.

Autologous, allogeneic or xenogeneic tissue grafts are commonly used for tissue repair as their similar biological structure and molecular composition that allows cell infiltration and tissue ingrowth and remodelling [108, 109]. Due to the restricted availability of autografts, allogeneic and xenogeneic tissue graft such as skin [110], small intestine submucosa [111], bladder [112], pericardium [113] or tendon [114] grafts are well established in clinical therapies and used as gold standards. Tissue grafts manufacturing process should be designed in order to maintain structure, mechanical integrity and bioactivity of the tissue to the best extent possible [115]. Most common process includes separation of surrounding tissues, decellularisation, cross-linking, disinfection and sterilisation. Decellularisation is a crucial step which combines chemical, biological and physical treatments to remove cells and to

minimize the amount of cellular debris and any other molecules with immunogenic capacity [116, 117]. Chemical cross-linking treatment is also commonly used to control mechanical properties and degradation profile. However, cross-linking should be optimized for each application to avoid cytotoxicity, predominant pro-inflammatory response and delayed wound healing or even peri-implantation fibrosis [46, 118]. Moreover, several different tissue grafts have been developed for each clinical application. For example, small intestine submucosa and bladder have been used for treatments, such as hernia, tendon, bladder and wound healing treatments, which require rapid cell infiltration, graft degradation and tissue remodelling with low mechanical performance [20, 112, 119-121]. On the other hand, skin derived tissue grafts are well established for ventral and abdominal hernia repair and infected wounds which require high mechanical performance and enzymatic resistance [20, 122-125].

Collagen hydrogels are a network of collagen fibrils which is held together by electrostatic and hydrophobic bonds. Collagen has the ability of self-assembling when diluted collagen solutions are reconstituted at physiological pH, ionic strength and temperature [126-132]. The fluency and fast assembly time allow collagen preparations to be used as injectable systems for cell and molecules delivery [133]. Furthermore, cross-linking is used to control mechanical stability and degradation rate [134, 135]. Specifically for hydrogels, mechanical properties can be improved by plastic compression [136-140]. Collagen hydrogels have been employed in numerous clinical applications. Stem cells from skeletal muscle encapsulated into a collagen type I hydrogel increased cardiac genes expression, contractile forces and calcium ion exchange as native cardiac cells [141]. Moreover, embryonic stem cells or cardiomyocytes loaded in collagen type I hydrogels and mechanically stimulated

differentiated into cardiomyocytes [142] or cardiac muscle bundles [143], respectively. In the neural treatment, collagen type I hydrogels with or without growth factors, have been shown to promote neural polarity, adhesion, survival and growth [144-147]. In the cartilage repair, collagen type II hydrogels have been demonstrated to maintain chondrocyte phenotype [148, 149] and drive mesenchymal stem cell differentiation towards chondrogenic lineage [150-152].

Collagen sponges are obtained by freeze-drying. Initially, collagen is entrapped within the developing ice crystals and then ice is sublimated. This process permits controlling pore size and distribution by modifying collagen concentration and freezing set-up [153-155]. Pores should be designed to allow cell migration and nutrients/debris diffusion [156, 157]. Several different cell types and biomolecules have been combined with collagen sponges with promising *in vitro* and *in vivo* results. For example, collagen sponges with glycosaminoglycans or calcium phosphate scaffolds have been shown to repair rat calvarial defects as effectively as natural bone materials or biomaterials with mesenchymal stem cells [158-160]. Collagen sponges have also shown to retain growth factor such as bone morphogenetic protein 2, enhancing bone healing in critical size rat calvarial defect [161]. Regarding skin wound healing, collagen sponge with skin cell precursors accelerated wound healing and enhanced local capillary regeneration in a diabetic wound mice model [162]. On the other hand, adult bone marrow mesenchymal stem cells loaded into collagen sponges increased vascularisation in a immuno-deficient mice model [163]. Collagen sponges functionalised with different fibroblast growth factor [164-166] or platelet lysate [167] have been shown to regenerate full-thickness defects in normal and diabetic wounds.

As collagen hydrogels, hollow collagen microspheres can be used as carrier systems for drug delivery with high reproducibility, surface area, cargo capacity, controlled size, shape, dispersity and degradation rates [168, 169]. These hollow microspheres are obtained by the collagen deposition on sulphonated polystyrene beads as templates, which afterwards are removed, leaving behind the hollow collagen shell [168-172]. These hollow collagen spheres have been used for gene [52, 170], growth factor [173] and drug [174] delivery or ROS scavenging [175, 176].

Collagen fibres have been explored using three different methods: electrospinning, extrusion and isoelectric focusing. Electrospinning allows the fabrication of matrix composed of nanofibres of gelatin, as the current process leads to irreversible denaturation [177, 178]. Collagen fibres within 50 - 400 μm diameter and structural and mechanical properties similar to native tissues can be obtained by the extrusion of collagen solution in a series of phosphate buffers at 37 °C [179-185]. Collagen fibres with high collagen fibril alignment are prepared by isoelectric focusing, which induces collagen monomers to align and to migrate at isoelectric focusing point, where the overall charge is neutral [186]. Extruded collagen fibres have been shown to promote cell alignment and bidirectional cell growth [187, 188] and neotissue formation [189-191]. In tendon repair, extruded collagen fibres were infiltrated by new tissue; however, the resorption degree was low due to the high cross-linking level [191]. On the other hand, isoelectric focused collagen fibres induced bidirectional growth of tenocytes and bone marrow stromal cells [192, 193] and to stimulate tenogenic differentiation of bone marrow stem cells [194, 195]. These fibres have also been shown to provide topographical cues for *in vitro* axonal guidance, even in the presence of myelin-associated glycoprotein that is known to inhibit neurite guidance [196].

Finally, collagen films, produced through evaporation with or without previous fibrillogenesis, have been used extensively in biomedicine for several applications [197, 198]. Moreover, several approaches, such as magnetic field, soft lithography, imprinting or reverse dialysis, have been explored to align the sub-fibrillar structure of collagen within collagen films. In particular, magnetic field between 1.9 to 12 T during 30-90 minutes induced collagen fibrils to align perpendicularly to the field direction due to the negative diamagnetic moment of the collagen α chains [199-206]. However, the superconducting magnets required to induce alignment have a high-cost and, therefore, iron oxide particles in combination with a low magnetic field of 0.0001 T have been explored to align collagen fibrils with partially satisfactory results [207, 208]. Given the high cost of this magnetic field technology, soft lithography has been explored for replicating topographical patterns such as grooves, pillars and holes [209, 210], even for cell encapsulation within patterns [211]. Molecular imprinting [212-214] and high speed spinning methods [214, 215] have also been used to align collagen fibrils through the introduction of high shear forces during the collagen impression on a substrate. Both molecular imprinting and high speed spinning result in slightly misaligned collagen film due to the fast collagen desiccation requirement to fix the fibril structure and alignment. Alternatively, reverse dialysis to obtained high collagen concentration and alignment have been explored successfully; however, further investigations are needed to increase the scaffold dimensions [213, 216].

Collagen films with or without gelatin, hyaluronic acid, carbodiimide cross-linked or lamellae-like sub-structure, exhibited similar properties to human cornea and supported growth of human corneal epithelial cells and stromal fibroblasts [217-219]. On the other hand, collagen films were used to guide pulmonary stem cell

attachment and growth [220], while same films functionalised with Ficoll™ and cross-linked with genipin supported WI38 fibroblasts attachment and proliferation [197]. Given that collagen films can be wrapped to obtain single channel tubes, they have been for peripheral nerve regeneration with successful neurite outgrowth from explants [221]. Even more, these wrapped collagen films have reached the clinical market as nerve guidance conduits such as NeuraWrap™, NeuroMend™, NeuroMatrix™, NeuraGen™ [222], reducing myofibroblast infiltration while guiding Schwann cell migration and axonal regrowth towards their distal targets smaller than 4 cm in length [223-225]. Furthermore, magnetically aligned collagen scaffolds in combination of proteoglycans or hyaluronic acid have been used to align human keratocytes [202] or to maintain primary chondrocytes [203] in culture, respectively.

1.4. Assessment of the inflammatory response to collagen-based devices

Herein, host / macrophage response is discussed, as a function and extent of the cross-linking density / method employed to stabilise collagen-based devices. The extent of cross-linking can be assessed by denaturation temperature, quantification of free amine groups, swelling, mechanical properties and / or resistance to enzymatic degradation. However, denaturation temperature is customarily used to assess cross-linking density due to the simplicity and accuracy of the technique. Thus, herein we define collagen materials that are slightly cross-linked; moderately cross-linked; and heavily cross-linked as those that have exhibited denaturation temperature of <65 °C; 65-70 °C; and >70 °C, respectively.

1.4.1. Methods for assessing *in vitro* inflammatory response to collagen-based devices

Although numerous cells (e.g. macrophages [113], monocytes [226], neutrophils [227], leukocytes [228] and dendritic cells [229]) are employed to study the *in vitro* inflammation response to biomaterials, macrophages appear to be the preferred cell population for collagen-based devices. This may be due to the determinant role of macrophages in the resolution of inflammation and wound healing and the availability of techniques to characterise macrophage sub-populations and response [230]. To date, the most reliable macrophage sources are those isolated from human peripheral blood mononuclear cells (PBMCs) [49] and immortalised cell lines, such as human derived leukemic monocyte cell line (THP-1) [52]; human leukemic lymphoma monocytes cell line (U937) [113]; and mouse leukemic monocyte-macrophage cell line (RAW264.7) [231]. The advantages of immortalised macrophage cell lines include higher accessibility; lower cell phenotype variability;

unnecessary addition of inflammatory mediators in media to prevent apoptosis; and cryopreservation without detrimental effect on cell viability and differentiation [232, 233]. Nonetheless, immortalised cell lines suffer from certain cell dysfunctions, such as adapted growth in culture, reduced cell-cell interaction and decreased protein secretion [234].

Our understanding of the host response to collagen-based materials is largely attributed to experimental data on macrophage activation and polarisation (**Figure 1.3**). Macrophages express different surface markers according to each sub-population; M1 macrophages are positive for CD80, CD86 and CCR7, whilst M2 express CD163 and CD206 [43, 46]. Furthermore, the different macrophage sub-populations direct inflammation and tissue repair by secreting cytokines and other reactive species. Specifically, M1 macrophages produce pro-inflammatory cytokines such as IL-1α, IL-1β, IL-6, IL-8, IL-12, IL-23 and TNF-α, whilst M2 macrophages secrete IL-1ra, IL-4, IL-10, IL-13, VEGF, TGF-β and arginase [43-46]. M1 macrophages regulate inflammation and collagen-based devices degradation by the secretion of nitrites, reactive oxygen species (ROS) and MMPs [113, 235].

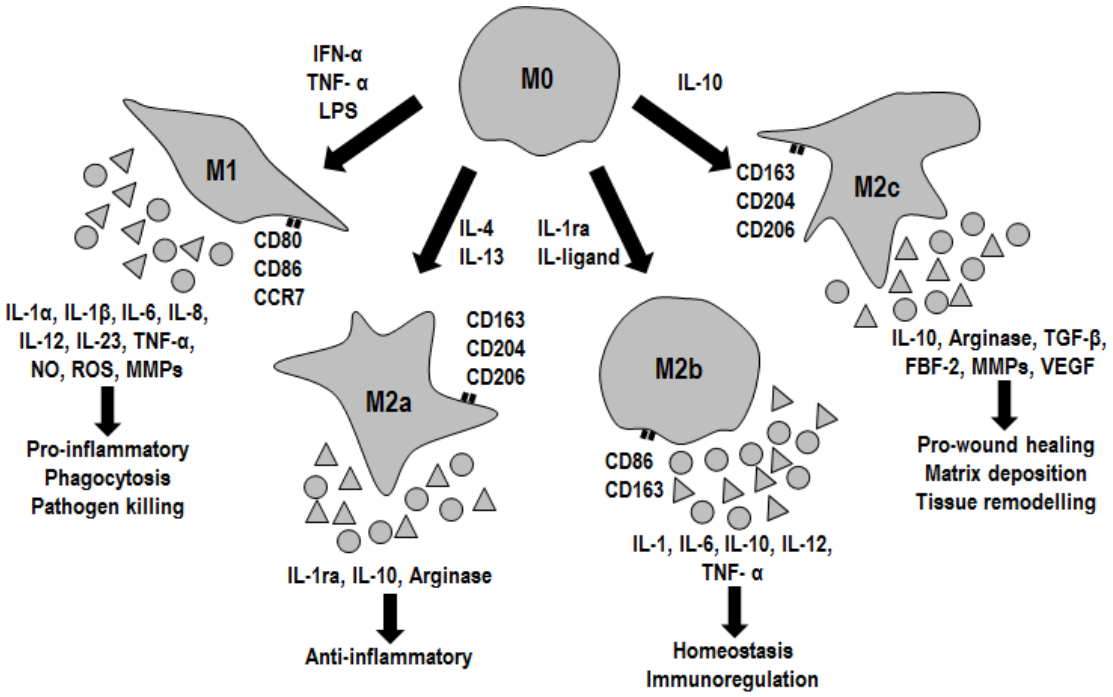

Figure 1.3. Macrophages polarized from M0 (non-polarised) to M1 (pro-inflammatory) or M2 (M2a, anti-inflammatory; M2b, homeostatic; M2c, wound healing) depending on inducing signals. Each macrophage subpopulation expresses different surface markers, cytokines, and reactive species. CD, cluster of differentiation; FBF-2, puf-domain RNA-binding protein; IFN, interferon; IL, interleukin; LPS, lipopolysaccharide; MMP, matrix metalloproteinases; NO, nitric oxide; ROS, reactive oxygen species; TGFb, transforming growth factor beta; TNF-a, tumour necrosis factor alpha; VEGF, vascular endothelial growth factor.

1.4.2. *In vitro* assessment of inflammatory response to collagen-based devices

Cross-linked collagen-based materials have been shown to preferentially alter macrophage response *in vitro* (**Table 1.1**). GTA cross-linked decellularised bovine pericardium (non-commercial material) induced moderate fibroblast cytotoxicity and THP-1 macrophage activation, which secreted higher amount of TNF-α and IL-6 than the non-cross-linked counterpart [236]. Additionally, this same material altered U937 macrophage morphology (cell area reduction and disrupted membrane), reduced attachment and viability, increased release of pro-inflammatory cytokines (TNF-α and IL-6) and changed MMP pattern secretion (up-regulated MMP-1 and down-regulated MMP-2 and MMP-9), whilst EDC cross-linked pericardium reduced the release of pro-inflammatory cytokines, altered MMP pattern and induced rounded macrophage [113], which morphology has been recently associated with M1 macrophages [237]. Moreover, PBMCs released higher amount of TNF-α and IL-6 than IL-10, when cultured on non-commercial GTA cross-linked porcine pulmonary valves [238]. With regard to reconstituted collagen materials, non-commercial EDC cross-linked collagen sponges have been shown to increase *in vitro* resistance to degradation by macrophages; however, these sponges promoted RAW 264.7 macrophage aggregation to form FBGCs that gradually degraded the sponges [239]. When incubated with human primary monocytes / macrophages, commercially available slightly cross-linked (HMDI) porcine dermis grafts (Permacol™ Surgical Implant, Covidien, denaturation temperature of 60-61 °C [110, 240], whilst its non-cross-linked counterpart has denaturation temperature of 56-57 °C [241]) induced low amount of pro-inflammatory (TNF-α, IL-1β, IL-6, MCP-3, MIP-1α) and anti-inflammatory (IL-1ra, CCL18, MIP-4) cytokines, when compared to other synthetic materials used for soft tissue repair, showing a low M1/M2 protein secretion index

[242]. Moreover, Permacol™ materials did not alter *in vitro* leukocyte viability, activation and reactive oxygen species expression. When they were exposed to fresh human peripheral whole blood, they behaved similarly to their non-cross-linked counterparts [228]. As EDC treatment, non-commercial DHT cross-linked collagen sponges induced FBGCs formation, although the treatment increased the enzymatic resistance [239].

Macrophage activation has also been associated with release of chemicals / processing by-products and surface modification. Specifically, released by-products from HMDI and EDC cross-linked porcine dermis grafts (Permacol™, and CollaMend™ FM Implant, Bard, denaturation temperature at 66 °C [110, 240]) were associated with the increase of pro-inflammatory (IL-1β, IL-6, IL-8) and vascular (VEGF) cytokine expression of human PBMCs [243]. However, a recent publication questioned this theory, as no cross-linking agent traces were detected by nuclear magnetic resonance spectroscopy on conditioned media with non-commercial GTA cross-linked collagen scaffold, and put forward the notion that the increase of pro-inflammatory cytokine expression may be induced by collagen surface modification as a function of cross-linking method employed [113]. Overall, cross-linking of collagen-based devices has been shown to induce a pro-inflammatory response: macrophage activation and increase of pro-inflammatory cytokine release. Despite the significant efforts and the advances in elegant readout systems, the mechanism by which cross-linking alters inflammation has not been elucidated as yet.

Table 1.1. *In vitro* inflammatory response associated with cross-linked collagen-based materials.

Cross-linking agent	Summary of *in vitro* results	References
GTA (i.e. Peri-Guard® & non-commercial materials)	Alteration of macrophage morphology (cell area reduction and membrane disruption) Reduction of macrophage attachment and viability Up-regulation of pro-inflammatory cytokines Alteration of MMP secretion	[113, 236, 238]
HMDI (i.e. Permacol™ & non-commercial materials)	Increase of enzymatic resistance Moderate up-regulation of pro-inflammatory and angiogenic factors/cytokines No alteration of leukocyte behaviour or release of reactive oxygen species	[228, 242, 243]
EDC (i.e. CollaMend™ & non-commercial materials)	Increase of enzymatic resistance Up-regulation of pro-inflammatory and angiogenic factors/cytokines Induction of rounded macrophages and macrophage aggregations that form FBGCs to degrade the scaffolds	[113, 239, 243]
DHT (i.e. non-commercial materials)	Increase of enzymatic resistance Induction rounded macrophages and of macrophage aggregations that form FBGCs to degrade the scaffolds	[239]

1.4.3. *In vivo* models for assessing host response to collagen-based devices

In vivo studies assessing host response can be roughly grouped based on the animal model employed (**Table 1.2**). Small animal models are primarily utilised to assess inflammatory response to novel devices, whilst large animal models are used 'as close' replicates of clinical setting. The most common small animal model for collagen-based devices *in vivo* characterisation is the subcutaneous implantation in mouse or rat for up to a month in duration [21, 112]. A rat full-thickness skin defect model has also been used to evaluate the wound healing ability of collagen materials combined with plastic dressings in acute and chronic wounds [244, 245]. The rabbit ear model has also been used to study specific wounds, such as burns [246] and hypertrophic scarring [247]. Inflammatory response and wound healing are evaluated by routine histological analysis that is sometimes complemented with immuno-staining and evaluation of protein and gene expression levels. Collagen-based devices have been extensively assessed in large animal abdominal muscle model repair with significant differences in the size of the defect, time points and characterisation methods (**Table 1.2**). However, rat abdominal model has also been used to evaluate collagen devices for soft tissue repair, despite the lower biomechanical stimulus of small animal models compared to large animals. Obviously, the type of the defect depends on the size of the animal; partial-thickness defect is induced in small animals [248], whilst full-thickness defect is used in large animals [249]. Furthermore, small animal models are primarily used to study early host response; thus such studies have more early time points (before 30 days). In contrary, large animal models are primarily focused on long-term response and therefore early time points (less than 30 days) are hardly ever of interest. Although routine histological analysis is carried out in both small and large animal models,

small animal models use more immunohistochemistry, ELISA and PCR assays to study inflammation cells, surface markers, proteins and cytokines, whilst large animal models study functional parameters, such as histomorphometry and mechanical properties of the new tissue. This deviation may be due to the lack of antibodies for large animal models, such as pig, sheep and bovine species.

Table 1.2. Overview of the animal models and experimental parameters used to study host response and wound healing associated with cross-linked collagen-based materials.

Model size	Species	Material	Model	Time points	Characterisation	Ref.
Small animal models	C57BL/6 mouse	Dermal sheep collagen disk (GTA, HMDI)	Subcutaneous implantation	2, 7, 14 and 21 days	Toluidine blue staining, PCR (IL-4, IL-6, IL-10, IL-13, IFN-γ, TGF-β, MCP-1, MIP-1), IHC (IL-10), zymography	[21, 250]
	Sprague-Dawley rat	Porcine bladder (EDC, GTA), porcine heart valve (GTA), bovine pericardium (GTA)	Subcutaneous implantation	7, 28, 63 and 180 days	HE and MT staining, quantitative stereological analysis	[112, 251]

Model size	Species	Material	Model	Time points	Characterisation	Ref.
Small animal models	Sprague-Dawley rat	SIS (EDC, non-cross-linked), porcine dermis (EDC, unknown, non-cross-linked),	Partial-thickness defect in abdominal muscle	7, 14, 28 and 112 days	MT staining and IHC (CD68, CD80, CD163, CCR7)	[20, 248]
	Wistar rat	Bovine pericardium (GTA, non-cross-linked)	Partial-thickness defect in abdominal muscle	21 and 90 days	HE and MT staining, IHC (CD80, CD163), lymphocyte transformation test	[252]
	Sprague-Dawley rat	Porcine dermis (EDC, HMDI) and human dermis (non-cross-linked)	Partial-thickness defect in abdominal muscle	3, 7, 14, 30, 90, and 180 days	HE, MT and Verhoeff's staining, IF (COLI, COLIII, FN, elastase and MMP-9)	[253]

Model size	Species	Material	Model	Time points	Characterisation	Ref.
Large animal models	Sprague-Dawley rat	Collagen hydrogel with or without growth factors	Full-thickness skin defect	3, 7 and 14 days	HE staining, IHC (CD68, COL IV), stereological analysis, wound contraction	[244, 245]
	New Zealand white rabbit	Porcine dermis (EDC, HMDI) and SIS (non-cross-linked)	Partial-thickness defect in abdominal oblique muscle	14, 30, 90 and 180 days	MT staining, IF and qRT-PCR for COLI and COLIII, tensile test	[254, 255]
	New Zealand white rabbit	Collagen sponge with or without growth factors	2nd degree-burn defect	15 days	HE staining, tensile test	[246]

Model size	Species	Material	Model	Time points	Characterisation	Ref.
Large animal models	Yucatan minipig	Porcine dermis (EDC, HMDI), bovine pericardium (non-cross-linked) and human dermis (non-cross-linked)	Full-thickness defect in abdominal muscle	30, 180 and 360 days	HE staining, stereological analysis, tensile test	[249, 256]
	Caribbean vervet monkey	Porcine dermis (EDC, HMDI) and SIS (non-cross-linked)	Full-thickness defect in abdominal muscle	180 days	HE staining, IHC (CD3, CD20, CD68), ELISA (immunoglobulin G and M), tensile test	[240, 257]

1.4.4. *In vivo* assessment of host response to collagen-based devices

Non-cross-linked (**Table 1.3**) acellular ECM tissue grafts have shown different host response depending on their origin. Commercially available porcine small intestinal submucosa (SIS; Surgisis™ Soft Tissue Graft, Cook, denaturation temperature of 61-62 °C [110, 240]) and porcine bladder commercially available (MatriStem, Acell) [20] or research grade [112, 251] promoted a dense mononuclear cell infiltration, predominantly neutrophils at week 1 and macrophages (more M2 macrophages than M1) at week 2. At week 4-5, SIS and bladder grafts were completely degraded and grafts were followed by constructive wound healing; grafts were totally replaced by organised collagenous connective tissue and skeletal muscle tissue. Evidence of FBGCs and peri-implantation fibrosis were not observed [20, 112] or the fibrous tissue surrounding the implants was slight, less than 52 µm [251]. In the same way, commercially available human, porcine and bovine dermis (Alloderm® Tissue Matrix, LifeCell, denaturation temperature 64 °C; Strattice™ Reconstructive Tissue Matrix, LifeCell, denaturation temperature 60 °C; SurgiMend™ Collagen Matrix for Soft Tissue Reconstruction, TEI Biosciences, denaturation temperature 57 °C [110]) demonstrated a dense mononuclear cell infiltration, higher M2 macrophage population than M1, and no presence of FBGCs or encapsulation [20, 253, 258, 259]. However, dermis grafts showed lower cell infiltration, degradation and new tissue formation than those of SIS and bladder [20, 253, 258, 259], prolonging graft remodelling over 12 months [258, 259]. This longer degradation may be due to the higher organisation and density of dermis compared to SIS or bladder. With regards to reconstituted collagen materials, non-cross-linked materials have been shown to be well-tolerated, to promote tissue regeneration with minimal inflammatory response [93]. Finally, the wound healing capacity (cell infiltration, new tissue

deposition and neovascularisation) of non-cross-linked collagen materials have also been confirmed in clinical setting [260].

Table 1.3. *In vivo* response associated with cross-linked collagen-based materials. The degree of cross-linking regulates scaffold stability and host response.

Cross-linking agent	Summary of *in vivo* results	Ref.
Non-cross-linked	**In general, non-cross-linked collagen materials:** Relevant initial cell infiltration High ratio M2/M1 macrophages Functional reconstruction, no encapsulation	[20, 256, 260-262]
	Porcine SIS and bladder (i.e. Surgisis™, MatriStem™ or other non-commercial materials): Fast degradation and remodelling ratio	[112, 248, 251]
	Human, porcine and bovine dermis (i.e. Strattice™ or other non-commercial materials): Lower cell infiltration and over-extended remodelling over 12 months	[20, 253, 259]
GTA	**Heavily cross-linked collagen-based materials (i.e. Peri-Guard® & non-commercial materials):** Reduced cell infiltration Low ratio M2/M1 macrophages Up-regulation of pro-inflammatory cytokines Foreign body response - Fibrous encapsulation	[21, 112, 249, 251, 252, 256, 263-265]

Cross-linking agent	Summary of *in vivo* results	Ref.
HMDI	**Slightly cross-linked collagen-based materials (i.e. Permacol™):** Reduced cell infiltration and similar early recruitment of mononuclear cells than its non-cross-linked counterpart and less than non-cross-linked SIS and bladder. Low degradation ratio, over 12-24 months (similar to non-cross-linked counterparts) Prolonged presence of macrophages around scaffold Prolonged remodelling and tissue support	[228, 253-255, 257-260, 262, 266-268]
HMDI	**Heavily cross-linked collagen-based materials (i.e. non-commercial materials):** Poor cell infiltration and low ratio M2/M1 macrophages Up-regulation of IL-10 from FBGCs Over-prolonged presence of macrophages and FBGCs Limited scaffold degradation over 2 years, chronic inflammation and fibrous encapsulation	[21, 250, 269]
EDC	**Slightly cross-linked collagen-based materials (i.e. non-commercial materials):** Relevant initial cell infiltration Scaffold degradation and remodelling over 180 days New connective tissue replace degraded scaffold	[112, 270-273]

Cross-linking agent	Summary of *in vivo* results	Ref.
	Moderately and heavily cross-linked collagen-based materials (i.e. CollaMend™ & non-commercial materials): Reduced cell infiltration Low ratio M2/M1 macrophages Limited scaffold degradation over 12 months Prolonged presence of macrophages and FBGCs around scaffold Chronic inflammation and fibrous encapsulation	[20, 240, 248, 253-255, 260, 262]
Genipin	**Slightly cross-linked collagen-based materials (i.e. non-commercial materials):** Moderate initial cell infiltration Scaffold degradation and remodelling up to 12 months New connective tissue replace degraded scaffold	[274]
	Heavily cross-linked collagen-based materials (i.e. non-commercial materials): Reduced cell infiltration Limited scaffold degradation at 12 months Prolonged presence of macrophages and FBGCs around scaffold and chronic inflammation	[274, 275]

Chemically cross-linked collagen-based devices demonstrated extended support on the defect area overtime, when compared to the non-cross-linked counterparts [276]. Commercially available GTA cross-linked tissue grafts (**Table 1.3**) (Peri-Guard® Repair Patch, Synovis, denaturation temperature 83 °C [110]) have been shown to elicit chronic inflammation and typical foreign reaction, as evidenced by the early dense accumulation of mononuclear cells and the prolonged presence of macrophages, FBGCs and fibrous encapsulation surrounding the implant [249, 256, 263]. GTA cross-linked bovine pericardium grafts reduced M2/M1 macrophage ratio during inflammation phase, as compared to non-cross-linked grafts [252]. Moreover, non-commercial GTA cross-linked sheep collagen disks induced a massive infiltration of neutrophils that secreted a high amount of MIP-1, MCP-1 and IFN-γ, recruiting and activating macrophages. As a result, macrophages upregulated IL-6 and downregulated IL-10, IL-13, promoting FBGC formation [21]. Additionally, commercially available GTA cross-linked collagen sponges for guided bone regeneration and guided tissue regeneration (BioMend® Extend™, Zimmer Dental) promoted ossification *in vivo*; however, the incidence of mucosa tissue perforation was increased [277]. This tissue perforation may be related to the prolonged degradation over 24 weeks, decreased tissue integration and vascularisation, and prolonged presence of macrophages and FBGCs around the material [278]. Similar to tissue grafts, non-commercial GTA cross-linked collagen hydrogels demonstrated a reduced *in vivo* degradation (20% degradation after 6 weeks), whilst their non-cross-linked counterparts were largely degraded within a week. However, GTA cross-linked hydrogels reduced cell infiltration and promoted a dense connective tissue layer with inflammatory cells around the hydrogel at an early stage [264]. The non-healing result of GTA cross-linked collagen materials has been attributed to the

toxicity of GTA residues [265] and the high cross-linking density that prohibit degradation and cell infiltration, even after 2 years of implantation [263].

Slightly cross-linked (HMDI) porcine dermis Permacol™ (**Table 1.3**) has displayed high resistance to degradation *in vivo* and in clinical applications, maintaining structural integrity for over 2 years [253, 266]. Permacol™ has also been shown to induce early recruitment of mononuclear cells around the graft and limited cell infiltration than its non-cross-linked counterpart [259]. However, this early inflammatory cell population recruitment has been shown to be lower for Permacol™ than non-cross-linked SIS and porcine and human dermis (Surgisis™, Strattice™ and Alloderm®, respectively). However, this response was normalised between all grafts over extended periods [255, 259]. Regarding cell infiltration, mononuclear cells were detected around Permacol™ and only infiltrated through material pores; only 20% of implants were colonised at day 14 and the totality of graft was colonised after 1 month [254, 255, 258]. At 90 days, Permacol™ showed a higher amount of macrophages (RAM-11 positive, specific antibody for rabbit macrophages) and FBGCs than non-cross-linked SIS graft (Surgisis™), but slightly lower macrophage recruitment than other cross-linked porcine dermis graft (CollaMend™) [254]. After 90 and 180 days of implantation, Permacol™ implants were surrounded by a new randomly organised connective tissue and fibroblast, supporting tissue integration in its immediate environment. This new tissue adhered to the implants, penetrated them through surface pores and showed a lower collagen density than that of the typical fibrous tissue [253, 255, 257]. Although Permacol™ demonstrated reduction of remodelling ratio, as non-cross-linked Strattice™ and Alloderm®, the absence of encapsulation may indicate that these materials are well tolerated and integrated, as they may be assimilated as a normal host matter.

Non-commercial heavily cross-linked (HMDI) dermal grafts (denaturation temperature of 74 °C) exhibited extended degradation resistance; induced a limited cell infiltration and demonstrated a prolonged delay in wound healing [269]. These observations may be related to the IL-10 upregulation from FBGCs, which is known to upregulate transcription of TIMP-1, preventing degradation by MMPs. This has also been observed in heavily cross-linked (HMDI) dermal sheep collagen disks [21] and heavily cross-linked (HMDI) bovine collagen type I disks [250]. Decellularisation and delipidation process can also dramatically influence the inflammatory profile of collagen grafts. Specifically, HMDI cross-linked porcine dermis grafts, that were decellularised and delipidated with sodium dodecyl sulphate (SDS) and non-cross-linked SIS (Surgisis™) have shown increased ROS expression as compared to non-cross-linked collagen grafts (Strattice™ and Alloderm™), Permacol™ and non-cross-linked Permacol™ [228]. This suggests that ROS increase may be processing-dependent. Finally, Permacol™ has been widely used for human hernia repair with favourable outcomes, as compared to synthetic implants [261]. Nonetheless, tissue grafts have been associated with a 10% failure rate and 14% chronic inflammation issues for the most complex surgery cases for which no ideal material exists as yet [266-268]. Commercially available HMDI cross-linked porcine dermis (Zimmer® Collagen Repair Patch, Zimmer) has been used for rotator cuff repair with significant improvement of tendon functionality [279]; however, chronic inflammation has been reported in few cases [280]. It is worth pointing out that these clinical studies were focused on visual observations of the wound and CT scans to evaluate seroma formation; hernia recurrence; and infection. The lack of systematic tissue analysis prohibits precise identification of the cause; is it the graft itself or the comorbidity of the patients?

EDC has also been studied extensively with *in vivo* degradation and host response depending on the tissue graft characteristics (**Table 1.3**). Commercially available EDC cross-linked porcine dermis grafts (CollaMend™) showed high resistance to degradation, with no degradation signs and no significant cell infiltration for over 180 days [255]. Further, CollaMend™ induced a disorganised connective tissue with a large amount of macrophages and FBGCs at the implant interface at day 7, reaching the highest cell amount by day 14. By day 30-35, these materials were encapsulated within a dense collagenous tissue and FBGCs [20, 253]; encapsulation and non-constructive remodelling layer were evidenced over 180 days, the longest published time point [240, 255]. Regarding macrophage polarisation, CollaMend™ implants presented the lowest population of M2 macrophages (CD206+) and the highest of M1 macrophages (CCR7+) [20]. EDC cross-linked porcine dermis has been employed for human abdominal wall reconstruction and clinical data showed similar recurrence to HMDI cross-linked porcine dermis, largely attributed to poor tissue integration and delay in wound healing [260, 262, 281]. However, these clinical studies did not assess inflammatory response in detail. Another commercially available EDC cross-linked SIS (CuffPatch™, Arthrotek) showed similar results to CollaMend™; a higher amount of M1 macrophages (CD80+ and CCR7+) than M2 macrophages (CD163+) and a prolonged presence of macrophages and FBGS over 16 weeks were reported [248]. Interestingly, further investigations demonstrated that the degree of EDC cross-linking of non-commercial decellularised porcine bladder modulated degradation rate, whilst it delayed the different stages of reconstructive wound healing [112]. Specifically, the low dose EDC cross-linked tissue grafts (0.0005 mmol per mg of tissue) were completely infiltrated with host cells by day 7 and remained intact, with new collagen being deposited after 28 days.

The degradation of these tissue grafts and new collagenous connective tissue deposition was evidenced up to 180 days. The high dose EDC cross-linked porcine bladder (0.0033 mmol per mg of tissue) displayed the same tendency than the low dose EDC with some delays in remodelling: low degradation at day 63 and partial degradation with new organised connective tissue by day 180 [112]. Authors of this study mentioned that the outstanding cellular infiltration and the remodelling features are due to the slight cross-linking degree and the fibroporous structure of these materials. Certainly, the introduction of interconnected porosity (30-40 μm pore size) in other synthetic bulk materials has been demonstrated to promote M2 macrophages and to increase integration of the materials [282]. Although porosity would be a relevant designing parameter modulating host response, it has not been explored in detail for collagenous materials.

The same host response tendency than EDC cross-linked tissue grafts was observed for EDC cross-linked collagen-elastin sponges (non-commercial materials) [270]; the low degree of EDC cross-linking (0.3 mM EDC) increased stability of the scaffolds and supported tissue regeneration, although it delayed the wound healing phases. In contrast, the medium degree of EDC cross-linking (0.5 mM EDC) impaired wound healing, induced more macrophages and FBGCs, and scarring was evidenced [270]. Furthermore, low dose EDC cross-linked collagen conduits and sponges (non-commercial materials) have been shown to increase guidance of regenerating axons through distal peripheral nerve sections without obvious macroscopic signs of inflammation or neuroma formation [271-273].

As with other cross-linking methods, genipin cross-linking (**Table 1.3**) has been shown to increase resistance to degradation for over a year of non-commercial collagen materials, which delayed wound healing [274, 275]. 0.00625, 0.05 and

0.625% genipin was used to cross-link bovine pericardium tissue grafts. 0.00625% genipin cross-linked grafts were unable to elicit tissue regeneration due to premature degradation and lack of cell support. 0.05% genipin cross-linked grafts promoted a dense layer of inflammatory cells surrounding the grafts and low cell infiltration at day 3. Cell ingrowth increased with time, reaching maximum by month 3. A gradual graft degradation and new tissue deposition were observed over time; the graft was totally degraded and replaced by connective tissue after 12 months. In contrast, 0.625% genipin cross-linked grafts presented more inflammatory cells; less graft degradation; and less tissue replacement; limited graft surface degradation was observed even after 12 months [274]. Ribose has also been used commercially to cross-link collagen sponges (Ossix®, ColBar LifeScience) for guided bone regeneration. This material has demonstrated prolonged degradation, limited cell integration and vascularisation, and to induce the presence of macrophages and FBGCs around the material for 24 weeks [278].

Overall, *in vivo* studies demonstrate that host response depends on the cross-linking density and methods employed. Indeed, slightly cross-linked with HMDI, EDC or genipin collagen-based materials support initial cell infiltration and ultimately scaffold replacement by new tissue. Nonetheless, delays in wound healing have also been reported. On the other hand, heavily cross-linked collagen-based materials promote a pro-inflammatory response (macrophage activation, predominant M1 macrophage population and increase of pro-inflammatory cytokine release) that results in impaired wounds or fibrous encapsulation. Despite the extensive investigation into alternative cross-linking methods, no host response studies have been reported as yet.

1.5. Collagen source and extraction

Collagen can be extracted from human, animal or fish tissues, *in vitro* mammalian cell cultures or recombinant synthesis technologies. In the biomaterials field, the mammalian skin or tendon and cartilage are the standard sources of collagen type I and type II, respectively; and the main origin of these tissues are porcine, bovine or human [12]. However, the tissue origin is one of the major drawbacks for clinical translation of these collagen products because of batch-to-batch variability, disease transmission, immunogenic reactions, microbial or virus contaminations and cultural or religious issues [283]. For these reasons, extensive research has been performed to extract collagen from *in vitro* cell culture, fish processing waste or recombinant protein systems.

As cells produce their own ECM proteins, several primary and immortalised cell types have been used for the production of various collagens. However, cell culture conditions have been modified to increase the collagen synthesis yield. Media supplementation with L-ascorbic acid was demonstrated to be essential given that ascorbate is a crucial cofactor in the hydroxylation of proline and lysine of collagen [284, 285]. The supplementation with growth factor and gene transfection was investigated between the 1980 and 1990s [286-288]; however, these strategies did not increase the collagen synthesis yield in a comparable amount to the tissue extraction. On the other hand, hypoxia condition has been demonstrated to increase significantly collagen synthesis, through the activation of hypoxia inducible factor 1 α (HIF 1α) and TGF-β1 [289, 290]. Macromolecular crowding (MMC) has also been shown to enhance ECM deposition in cell culture, mainly collagen type I [291, 292]. Interestingly, MMC and hypoxia condition has been demonstrated to increase synergistically the ECM protein deposition [293, 294].

Regarding recombinant collagen technologies, genetically modified microorganisms and plants have also been proposed as an alternative to collagen extracted from mammalian tissues, avoiding their main drawbacks [295]. Transgenic microorganisms (bacteria and yeasts) have been investigated due to their glycosylation capacity; however, the yield of this approach is below 260 mg/l [296-298] and their proteolytic resistance is lower than native collagen, even when collagen was expressed with a thermally stable triple helical structure [298, 299]. These issues were tackled with corn and tobacco plants that have been genetically modified to produce human recombinant procollagens which require complex post-translational modifications [300, 301].

Regarding collagen extraction, mammalian or fish tissues have a fibrillar structure with different amounts of covalent cross-links, which are makes difficult the collagen extraction. To this end, solubilisation using neutral salted, diluted acid with or without enzymes and alkaline solutions are used to isolate different types of collagen. However, not all treatments can break native collagen cross-links: dilute acids only disassociate intermolecular cross-links between triple helices (aldimide bonds) while enzymes, such as pepsin, can disassociate mature and more stable cross-links (ketoimine bonds), increasing extraction yields [9, 302, 303]. On the other hand, more severe procedures use heat combining acid or alkaline solution to dissolve collagen whilst tend to denature collagen into gelatin. Pepsin treatment also produces a lower collagen immune response due to a selectively cleavage of the non-helical N- and C- telopeptides, removing the antigenic P-determinant segment that is located in the telopeptides located [304-306]. Finally, solubilised collagen needs purification steps (salt precipitation, filtration or centrifugation and dialysis) to eliminate collagen telopeptides, protein aggregates, other proteins and proteoglycans,

pepsin and acid. Nonetheless, extracted and purified collagen is not completely safe because of the risk of disease transmission due to bacteria, virus or prion. Therefore, besides quality hazard tests, disinfection with sodium hydroxide and final product sterilisation treatments are performed whilst these treatments affect collagen stability [307, 308].

1.6. Collagen cross-linking

The hierarchical assembling of the collagen molecules provides structural stability and mechanical resilience to the collagen-based tissues. Additionally, the collagen packaging is stabilised by weak interactions and strong intermolecular cross-links that contributes to mechanical and enzymatic stability [12]. Collagen type I has four cross-linking types, two in the helical region and one more in each telopeptide where the action of lysyl oxidase catalyses aldehydes from lysine and hydroxylysine residues [8]. The resulting aldehydes react spontaneously with other lysines and hydroxylysines from adjacent chains of the same molecule or from other adjacent molecules. These cross-links between two different molecules result in head-to-tail bonding along fibrils, known as aldimide bridges [309]. However, the natural cross-linking mediated by lysyl oxidase would not occur *in vitro* [8] and, consequently, reconstituted forms of collagen can lack sufficient strength and may disintegrate upon handling or collapse under the pressure from surrounding tissue *in vivo*. Furthermore, the rate of biodegradation has to be customised based for the specific application. Thus, it is often necessary to introduce exogenous cross-linking (chemical, physical or biological in nature) into the molecular structure, in order to tune mechanical properties, to prevent the denaturation at 37°C and to control the degradation rate which may also determine tissue regeneration rate [14, 310] (**Table 1.4**). The fundamental principle of exogenous collagen cross-linking is the formation of covalent bonds between collagen molecules using chemical or natural reagents, biological cross-linkers or physical methods, which generally link either to the free amine or carboxyl groups of collagen.

Table 1.4. Mechanical properties of collagen-based devices as a function of cross-linking method and conformation.

	Type	Cross-linking method	Stress (MPa)	Strain (%)	E Modulus (MPa)	Ref.
Native tissue	Skin	-	1-27.5	30-180	4.6-20	[311-314]
	Tendon	-	5-86	5-22	1.9-1800	[315-317]
	Cornea	-	0.12-0.25	7-9	0.1-11.1	[318-320]
	Cartilage	-	0.5-1.0	7-10	0.5-0.9	[321, 322]
Biomaterial	Hydrogel	Non-cross-linked	0.020-0.027	25-30	0.001-0.100	[323-327]
		Glutaraldehyde	0.010-0.188	25-30	0.004-0.100	[323, 327]
		EDC-NHS	0.010-0.172	20-40	0.002-0.125	[327, 328]
		Transglutaminase	0.005-0.010	30-40	0.001-0.002	[324, 329, 330]
	Fibre	Non-cross-linked	0.2-4	12-40	1-5	[14, 331, 332]

	Type	Cross-linking method	Stress (MPa)	Strain (%)	E Modulus (MPa)	Ref.
		Glutaraldehyde	8-60	27-53	3-47	[14, 331]
		EDC-NHS	1-4	23-65	1-4	[14, 332]
		Genipin	4-60	15-43	2-500	[14, 333, 334]
	Film	Non-cross-linked	1.5-8	19-50	1.5-8	[197, 335]
		Glutaraldehyde	8-48	3-11	100-1000	[197, 336]
		EDC-NHS	4-20	30-60	5-35	[337, 338]
		Genipin	3.5-15	5-18	35-130	[197, 335]

1.6.1. Chemical cross-linking

The most widely used chemical cross-linking agents are aldehydes (e.g. glutaraldehyde, GTA) [113], isocyanates (e.g. hexamethylene diisocyanate, HMDI) [228], and carbodiimides (e.g. 1-ethyl-3-(3-dimethylaminopropyl)carbodiimide, EDC) [338]. All these agents have been employed to induce different extensions of collagen cross-linking, which depends on the processing parameters (cross-linking concentration and incubation time) and the cross-linking mechanism of each agent (**Figure 1.4** and **Figure 1.5**). For example, GTA has been shown to extensively stabilise collagen materials because of its self-polymerisation capacity, since these agents could cross-link high amounts of amines from lysine and hydroxylysine residues, including those that are relatively far apart [339-341]. However, unreacted GTA or hydrolytic or enzymatic degradation products may remain non-specifically bound to the matrix even after exhaustive rinsing, thereby introducing cytotoxic derivatives [342]. As GTA, isocyanates react with amine groups, HMDI forms urea linkages; this, however, is with superior cytocompatibility because there are no potentially toxic side products formed [343, 344] and the short half-life of the isocyanate group in water ensures that reactive groups will not be released from the treated surface over extended time periods [345, 346].

On the other hand, carboxyl groups of aspartic and glutamic acid residues from collagen chains can be used to cross-link collagen through acyl azides [269, 347-352] and carbodiimides [353-355]. Such approaches activate carboxyl groups which spontaneously bonds to amine groups of lysine and hydroxylysine residues of collagen. After extensive washing to completely remove by-products, foreign cross-linking molecules do not remain in the collagen protein and, therefore, these methods demonstrate less toxicity. These methods are less strong and less resistant to

proteolytic attack, as such methods can couple proximate collagen molecules; they are, however, less susceptible to calcification [356, 357].

Although chemical cross-linking agents are widely used in collagen-based industry and the research field, chemical cross-linking is associated with alteration of the normal wound healing, even at low concentration. High cross-linking densities are associated with numerous shortfalls as a function of the cross-linking density / method, including cytotoxicity [15, 16], calcification [17, 358, 359] and foreign body response [20, 310]. Therefore, natural and synthetic moieties have been advocated as alternatives to these common agents; the alternatives most commonly reported are acyl azide (e.g. diphenyl-phosphorylazide, DPPA [16]; photo-reactive agents (e.g. rose Bengal [360]; riboflavin [361]); carbohydrates (e.g. ribose [362], glucose [363]) and plant extracts (e.g. genipin [364, 365]; oleuropein [366]; and myrica rubra [331]). And, more recently, branched polyethylene glycol (PEG) polymers with various molecular weight and functional residues have been promoted to cross-link collagen-based devices [367-370]. Despite the extensive investigation into alternative cross-linking methods, no deep biological studies have been reported as yet.

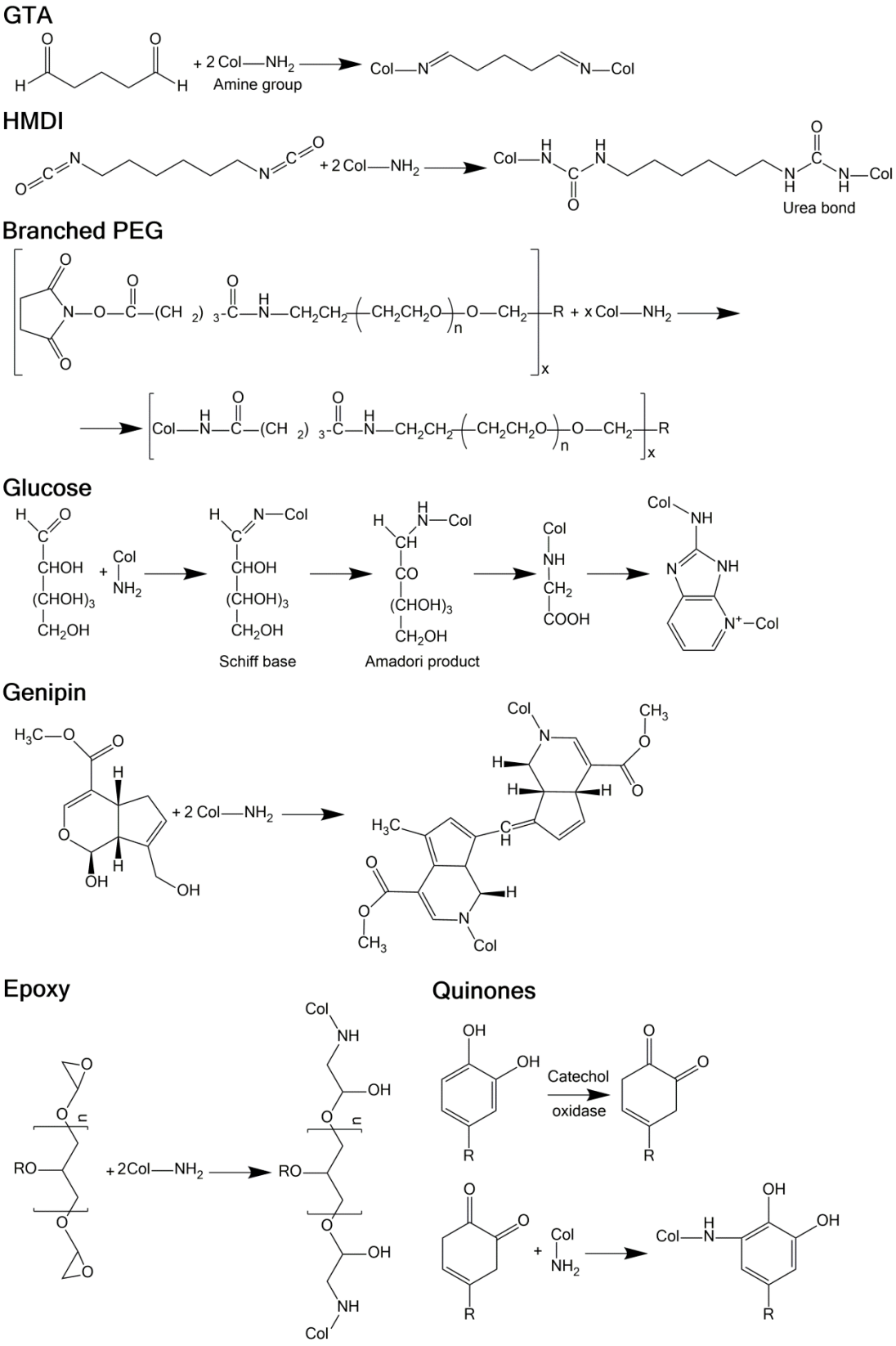

Figure 1.4. Chemical cross-linking of collagen reactions – Part 1. GTA: glutaraldehyde; HMDI: hexamethylene diisocyanate.

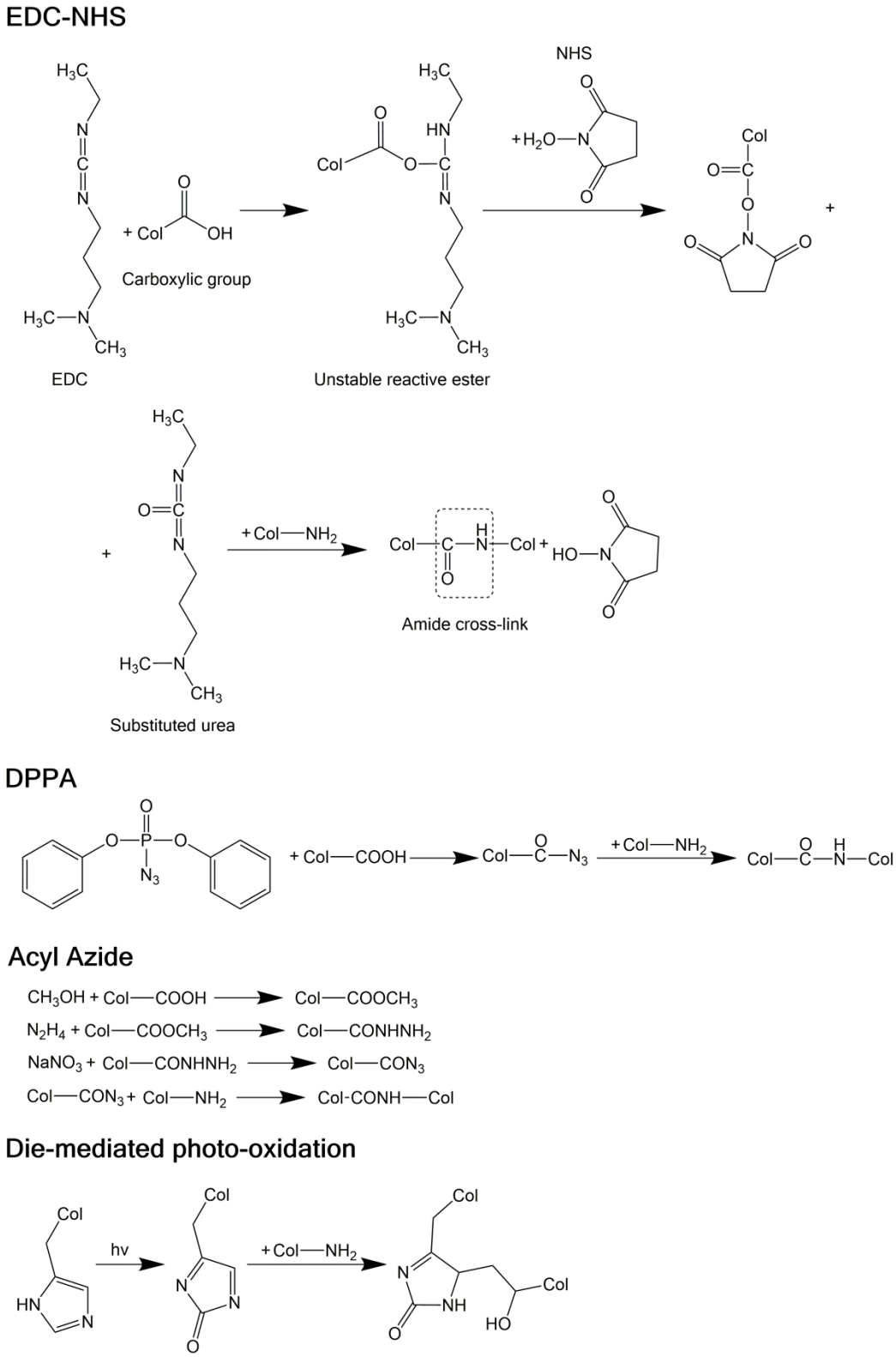

Figure 1.5. Chemical cross-linking of collagen reactions – Part 2. EDC: 1-ethyl-3-(3-dimethylaminopropyl)carbodiimide, NHS: N-hydroxysuccinimide; DPPA: diphenyl-phosphorylazide.

1.6.2. Physical cross-linking

To avoid cytotoxic effects associated with either the chemical cross-linker itself or its by-products, dehydrothermal [22, 181, 371-374] and UV irradiation [22, 375-378] have been assessed. Both treatments increase mechanical and proteolytic stability only slightly and have also been associated with collagen denaturation during processing. Dehydrothermal treatment uses high vacuum and temperatures over 100°C for several hours to promote severe collagen dehydration. Consequently, formation of inter-chain cross-links is induced as a result of condensation reactions either by amide formation or esterification between carboxyl and free amino and hydroxyl groups respectively (**Figure 1.6**). Prior to heat treatment, collagen-based materials are exposed to vacuum to remove as much water as possible to avoid collagen denaturation [22]. After dehydrothermal treatment, the helix-to-coil transition temperature is increased, enhancing the thermal stability of collagen without altering its triple helical structure [181]. Regarding UV cross-linking, this promotes bonds by free radical formation on tyrosine and phenylalanine residues, which in collagen are few. For that reason, UV cross-linking efficiency is considered negligible. The mechanism causes the formation of the hydroxyl radical ($OH^{\bullet}$) from water. The OH radical attacks the peptide backbone to produce peptide radicals (-NH-$C^{\bullet}$-CO-), which can interact to form a cross-link (**Figure 1.6**) [375, 376]. Moreover, UV irradiation is efficient for the introduction of cross-links which is especially useful for treatment of collagen solutions [378]. The efficiency of the reaction depends mainly on the sample preparation, the irradiation dose and time of exposure [379]. It has been reported that UV irradiation of wet collagen fibres causes rapid insolubility [380] and increases their tensile strength [381].

1.6.3. Biological cross-linking

Mimicking the *in vivo* collagen cross-linking, a more recent cross-linking strategy used tissue-type transglutaminase for catalysing covalent cross-linking of ECM proteins in a Ca^{2+} dependent manner [382-386]. Specifically, the transglutaminase reaction catalyses acyl donation from the γ-carboxamide group (glutaminyl residue) to the ε-amine group, resulting in the γ-glutamyl-lysine stabilising isopeptide between proteins (**Figure 1.6**) [387]. Collagen-based materials have been cross-linked with different transglutaminase sources, mammalian tissue or microbial extracted, and both types showed a moderate increase in denaturation temperature and mechanical and biological stability [324, 387, 388].

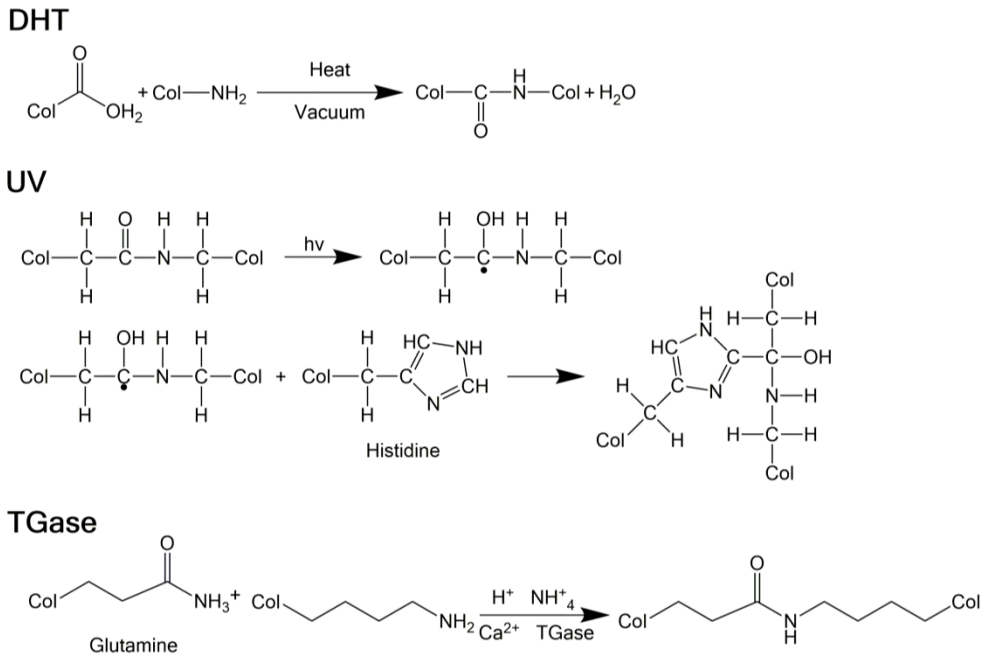

Figure 1.6. Physical (DHT and UV) and biological (TGase) cross-linking of collagen reactions. DHT: dehydrothermal treatment; TGase: transglutaminase.

1.7. Collagen sterilisation

As with every other medical device, effective sterilisation is required. ISO Standards for medical devices are already in place for radiation requirements and identification of optimal dose [329-331]; for ethylene oxide requirements and determination of residuals [332, 333]; and for microbiological methods to be performed when defining [197, 334], validating or maintaining a sterilisation method. However, sterilisation methods have been shown to have a variable cross-linking / biological effect on collagen-based devices (**Figure 1.7** and **Table 1.5**). For example, amino acid analysis indicates intensive reaction of ethylene oxide with lysine and hydroxylysine residues [389] and simultaneously necessitates appropriate post-treatment steps to avoid cytotoxicity [390]. Irradiation methods have been shown to induce both cross-linking, albeit weak, and polypeptide chain scission and in collagen-based devices [391-393]. Formation of cross-links is attributed to free radicals formed on aromatic amino acid residues (e.g. tyrosine and phenylalanine). However, these free radicals may initiate degradation of collagen chains [6, 394-396]. In the case of 70kGy irradiation, for example, damaging effects are induced on both mature and immature cross-links [397]. Given that such methods do not introduce any foreign substances, either as residual molecules or as compounds formed during *in vivo* degradation, they are considered biocompatible [12, 348, 398].

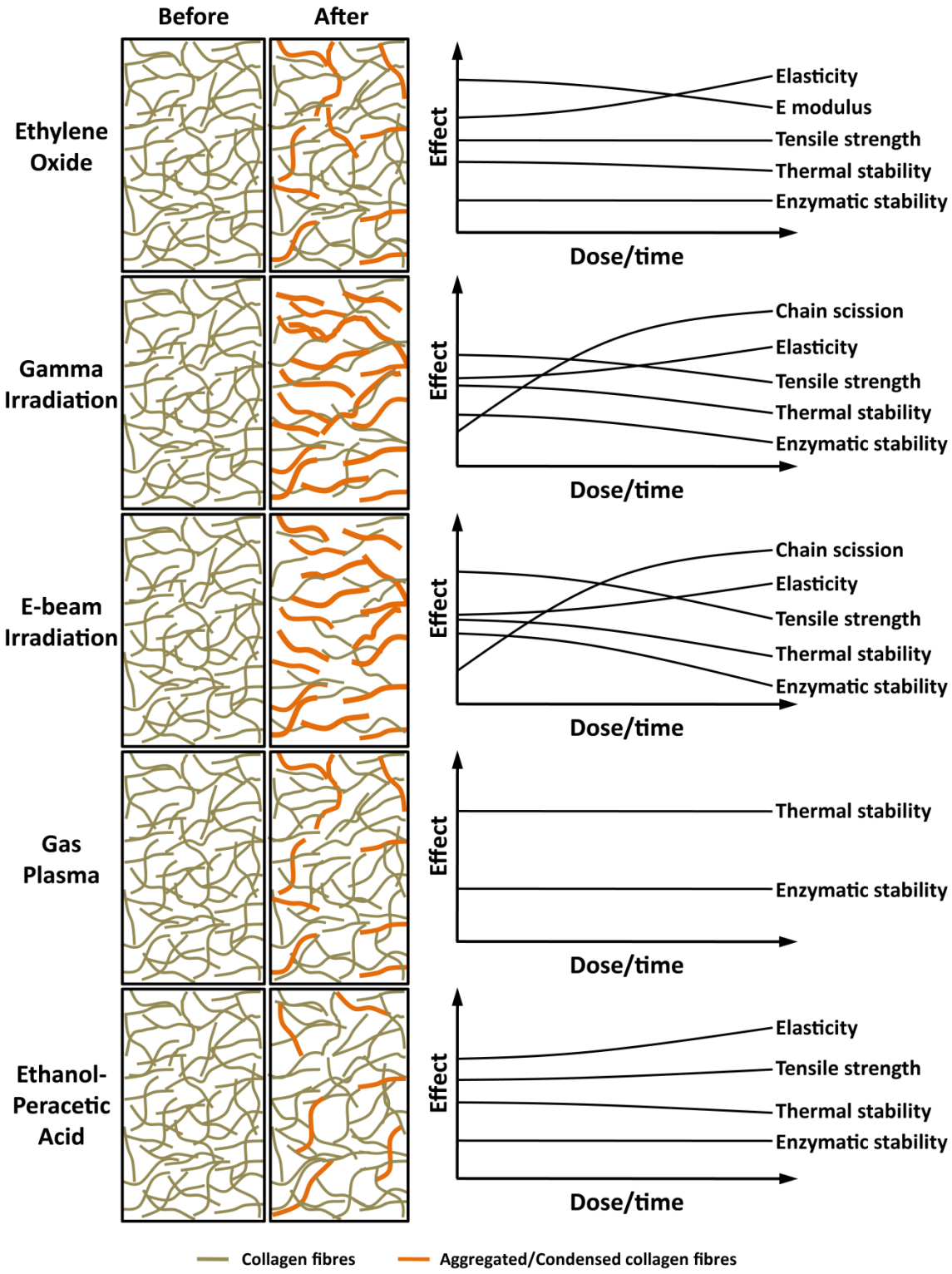

Figure 1.7. Schematic summary of the effects of different sterilization methods on structural, mechanical and biological stability of collagen-based devices.

Table 1.5. The influence of various sterilization methods on the properties of implantable devices.

Sterilisation method	Material form	Sterilisation parameters	State during sterilisation	Result	Ref.
Ethylene oxide	ECM matrix	750 mg/h for 16h.	Dry	Less reduction of mechanical properties than *γ*- and E-beam irradiation.	[399]
	Collagen sponge	24h at 35°C	Dry	Less degradation than *γ*- irradiation.	[400]
	Collagen sponge	100% EthO at 70% RH for 8 h at 55°C.	Dry	Structure and stability as untreated. No effect on cell proliferation, migration and morphology.	[401]
Gamma radiation	ECM matrix	2.0-30 kGy at 0.30 kGy/h and 22–25°C	Dry	Collagen condensation and hole formation, producing a reduction of swelling ratio, elasticity and stability.	[402]

Sterilisation method	Material form	Sterilisation parameters	State during sterilisation	Result	Ref.
Gamma radiation	Collagen solution	0.25, 0.5 and 1.0 kGy at 10 kGy/h and 30-35°C	Wet	γ-irradiation, at low dose (0–1 kGy), induced increased degradation and cross-linking.	[403]
	ECM matrix	0-32 kGy at 0.23 kGy/h	Dry	γ-irradiation caused significant damage to native dermis ECM, even at moderate dose (7–12 kGy).	[404]
	Tendon	25 and 50 kGy	Wet	Degradation (less severe for cross-linked samples).	[405]
E-beam radiation	ECM matrix	2.2 Mrad	Dry	Decreasing of uniaxial & biaxial strength, maximum tangential stiffness and energy dissipation.	[399]

Sterilisation method	Material form	Sterilisation parameters	State during sterilisation	Result	Ref.
E-beam radiation	Tendon	5 MeV	Wet	Degradation (less severe for cross-linked samples)	[405]
Gas plasma	Collagen sponge	6 mg/ml of H_2O_2 at 35°C for 30 min	Dry	Significant less degradation than gamma irradiated samples.	[400]
Peracetic acid	Human graft	2.5% peracetic acid and 25% ethanol in distilled water for 4 hours	Wet	No degradation evidence	[406]
	Tendon	0.1% peracetic acid	Wet	Porosity increased and collagen fibre pattern is slightly loosened.	[407]
Ethanol	Pericardium	70% ethanol	Wet	Thermal stability and tensile strength slightly increased and enzymatic degradation unaltered.	[408]

1.7.1. Ethylene oxide

Ethylene oxide has been used extensively to sterilise collagen-based devices with very reliable/reproducible results, subject to appropriate aeration step to minimise/eliminate residual ethylene oxide; to avoid cytotoxic side-effects; and to comply with regulatory limits [390]. Ethylene oxide has been shown to decrease helix stability of non-cross-linked, glutaraldehyde cross-linked and hexamethylene diisocyanate cross-linked collagen scaffolds, evidenced by reduction in shrinkage temperature [389]. Although significant decrease elastic modulus and increase of elongation capacity can be brought about, maximum mechanical resistance under uniaxial and biaxial loading conditions is not significantly altered in terminally sterilised porcine bladder derived scaffolds [399]. Furthermore, ethylene oxide sterilisation induces a lower rate of degradation as compared to non-sterilised collagenous materials [389] or other sterilization methods [400, 401]. The osteoinductivity of collagen type I and partially purified bone morphogenetic protein scaffold has also been shown to be reduced after ethylene oxide sterilisation at 37°C for 4h and at 55°C for 1 hour; however, the reduction induced by ethylene oxide at 29°C for 5 hours is about half of the control values, making this approach suitable for clinical use in sterilisation of bone morphogenetic protein [409]. In addition, ethylene oxide has a minor influence on collagen-induced platelet aggregation [400]; this factor could determine the success of devices for vascular applications. The porous structure and stability of ethylene oxide sterilised collagen sponges (dry materials) remains almost unaltered, whilst fibroblasts and endothelial cells have been shown to exhibit normal morphology [401]. It is worth pointing out that environmental humidity appears to be a critical variable in ethylene oxide sterilisation process. Recent studies indicate that sterilisation efficacy decreases

markedly below 30% and above 90%, as relative humidity is critical for the ethylene oxide diffusivity into the devices' structure [410].

1.7.2. Gamma irradiation

Gamma irradiation is a very attractive method for sterilisation of biopolymers due to its high efficacy and lack of residual chemicals that can cause cytotoxicity. Although it is considered as the most reliable sterilisation method available [411], it induces chain scission in non-cross-linked, glutaraldehyde cross-linked and hexamethylene diisocyanate cross-linked dermal sheep collagen, resulting in a decrease of tensile strength and high strain modulus values [389]. Furthermore, it has been observed in recent years that 31.7 kGy gamma irradiated bone has significantly less resistant to fatigue crack growth than the control bone tissue, whilst there was less micro-damage associated with fracture in the irradiated specimens than in the control specimens. The authors attributed these changes to ultra-structural alterations in the collagen matrix, caused by the irradiation, and concluded that gamma irradiation sterilised bone allografts may be more predisposed to fracture [412]. Similarly, gamma irradiation, at 2 Mrad (20kGy), has been reported to have no influence in the quarter-staggered arrangement of the collagen of patellar tendon allografts or to acetic acid solubility. However, an increased solubility in pepsin and a significantly lower shrinkage temperature were observed [413], both indicative of a compromised triple helical conformation [10]. Another study that assessed the influence of 25 kGy (2.5 Mrad) on mechanical, physicochemical and biological function of glutaraldehyde cross-linked tendon xenografts showed that the irradiation did not affect the ultimate tensile stress, but affected response to long-term collagenase degradation and thermal denaturation temperature. Of significant importance is the

finding that indicates that following 12 months implantation study, there was a slightly more active cellular response around irradiated tendon, but the mechanical properties of the retrieved implants were the same for irradiated and non-irradiated tissue grafts [414]. These results indicate that gamma irradiation may have a surface effect, whilst the bulk properties of the tissue graft remain unaffected. A mild surface denaturation may be beneficial, as cryptic RGD sequences may become available and may positively influence integration of the scaffold in the host tissue [415].

With respect to bone grafts, a dose-dependent decrease in mechanical properties has been established in the literature, when gamma dose is increased above 25 kGy for cortical bone or 60 kGy for cancellous bone. Therefore, a trend towards application of lower gamma dose has been observed the recent years. However, to substantiate the lower dose, an in depth investigation on the stability, mechanical properties, and biological function should be carried out to ensure safety and efficacy [416]. Other studies have suggested that gamma irradiation (0 and 1.0 kGy) brings about simultaneously chain degradation and cross-linking in fish and porcine gelatin and collagen in protein concentration and irradiation dose dependent manner [417]. Indeed, it has been reported that irradiation dosage of 1 Mrad (10 kGy) is less damaging to the collagen peptide backbone, whilst at higher dosage, although pronase resistance was observed, significant damage was clearly demonstrated, under enzymatic digestion, to non-cross-linked and chemically cross-linked collagen. The authors suggested caution on the interpretation of data from enzymatic assays and long-term experiments for functional changes assessment [418]. The osteoinductivity of collagen type I and partially purified bone morphogenetic protein scaffold was reduced considerably after sterilization by gamma irradiation at 2.5

Mrad (25 kGy), with collagen being far more labile than the bone morphogenic protein [409].

Gamma irradiation sterilised sponges (2.5 Mrad, 25 kGy) showed a dramatic decrease of resistance against enzyme degradation and severe shrinkage after cell seeding. Collapsed porosity inhibited fibroblasts and barred completely the human umbilical vein endothelial cell ingrowth into the sponges [401]. These results indicate that irradiation compromised the triple helical structure of collagen and upon immersion in the culture media, the scaffold collapsed. Suboptimal results have also been obtained for synthetic devices. For example, gamma irradiation (25, 75 or 125 kGy) sterilised polylactic acid (PLA) meshes induced milder inflammatory response and more orderly collagen deposition than ethylene oxide treated meshes during degradation, but tissue healing after 12 months was not of sufficient strength to prevent hernia recurrences [419].

A recent study demonstrated that gamma irradiation did not induce morphological changes, nor did it have an effect on the amount of primary amine groups, or the amount of heparin covalently attached to collagen scaffolds. However, irradiation (15 and 25 kGy) did result in collagen degradation products, a decrease in collagen denaturation temperature, and an increase in proteolytic degradation in a dose dependent fashion. These parameters were hardly influenced by ethylene oxide treatment. Both methods had hardly any effect on tensile strength and the cytocompatibility of the cross-linked collagen scaffolds, indicating that aspects like cost, safety and practicality of use may be taken into account in the choice of sterilisation method [420]. Gamma irradiation in inert environment (e.g. argon, nitrogen, vacuum) as means to minimise oxidation has also been proposed [421]. However, argon gas protection of gamma irradiated (2.5 Mrad) deep-frozen canine

bone-ACL-bone allografts demonstrated reduced mechanical properties and slight hyper-vascularity, as compared with the non-irradiated grafts at 12 months post implantation [422, 423], possibly due to free radical production and associated chain scission, thus questioning whether the use of argon gas protection is actually necessary.

1.7.3. E-beam irradiation

E-beam irradiation has been introduced as an alternative sterilisation method to ethylene oxide and gamma irradiation for sterilisation of human tissue graft in tissue banks [424]. However, results today have not demonstrated significant improvement over the aforementioned methods; e-beam has been shown to affect the structural properties of scaffolds composed of extracellular matrix. Specifically, e-beam sterilisation has been shown to decrease the uniaxial and biaxial maximum strength, stiffness and dissipation energy, increasing elongation capacity or altering porous structure in urinary bladder matrix, bone or tendon [399, 405, 424]. Moreover, when porcine small intestinal submucosa (SIS) samples were sterilised with ethylene oxide, gamma irradiation and e-beam irradiation and were subsequently subjected to hydrolytic degradation conditions for specific periods of time, all sterilisation methods resulted in an increase in the rate of sample degradation, with e-beam irradiation causing the greatest percentage of weight loss. All sterilisation methods caused an increase in both cellular protein production and metabolic activity, with ethylene oxide causing the greatest effect at short time points, but this was decreased after 28 days in culture [425]. To minimise material degradation by e-beam, irradiation dose, temperature of irradiation and defatting procedure have been evaluated. For that purpose, human femur rings were defatted in alcohol solution and

frozen in dry ice before e-beam sterilisation at 25 or 35 kGy. Temperature and defatting procedure was shown to be ineffective in reducing degradation phenomena, and the decrease in mechanical properties was similar for both irradiation doses [424]. However, it has been shown that e-beam sterilised extracellular matrix scaffolds (derived from porcine urinary bladder) are able to maintain mechanical strength and stability after 12 month of storage at room temperature or refrigerated conditions, following e-beam sterilisation [426]. Finally, e-beam sterilised tendon allografts have been shown to decrease the biomechanical properties and increased the remodelling ratio at early implantation time, when used in anterior cruciate ligament reconstruction. Further, this study demonstrated that e-beam treated tendons did not promote a recovery of the biomechanical function and authors concluded that e-beam irradiation cannot be recommended for soft tissue allograft sterilisation [427].

1.7.4. Radioprotectants

Given that physical irradiation method impair the mechanical strength and the enzymatic degradation of implantable devices, due to free radical reactions with the molecular structure of collagen [428, 429], radioprotectant (e.g. L-cysteine, N-acetyl-L-cysteine, L-cysteine-ethyl-ester) utilisation has been proposed to reduce radiation damage. It is hypothesised that reducing the presence or viability of free radicals, with pre-treatment of the device with radioprotecting free radical scavengers, will reduce the damaging effects of irradiation [430, 431]. Free radical scavengers inhibit free radical damage to the target molecule either by directly chemically reacting with the radical or by minimising / inhibiting the formation of the radical [428]. Although the use of thiourea as a radioprotectant has been shown

to significantly improve biochemical and biomechanical properties of irradiated bone [428] compared to bone irradiated without thiourea, the vast majority of studies assess the sterilisation efficacy of radioprotectants, rather their beneficiary effects on the properties of the device [432]. Performing irradiation (50 kGy), on radioprotectant pre-treated tissues, at dry ice temperature, a condition believed to substantially limit the diffusion of free radicals, resulted in tissue integrity as good as allografts treated with low irradiation dose (18 kGy) [433]. Moreover, free radical scavenging has been compared with exogenous chemical cross-linking techniques in order to stabilize materials prior to irradiation. After gamma and e-beam irradiation at 25 and 50 kGy, samples cross-linked with 1-ethyl-3-(3-dimethylaminopropyl) carbodiimide showed higher strength and higher resistance to enzymatic degradation than scavenger-treated and unprotected samples. Although free radical scavenging treatment with ascorbate and riboflavin showed protective effects up to 25 kGy [405]. Further studies demonstrated that combination of exogenous cross-linked and free radical scavenged rabbit tendons increased mechanical properties and degradation resistance compared to cross-linking or scavenger-treated only [434]. This increase in stability of the irradiated treated samples was validated successfully in a rabbit *in vivo* model and a dynamic bioreactor system, which combined dynamic loading and collagenase degradation [435]. It is worth pointing out that there is limited literature about the biological effect of radioprotectant techniques on the biological behaviour of medical devices and therefore the potential application of radioprotectant technology is subject to further investigation. Given that free radical scavengers, such as ascorbate, riboflavin, tocopherol, have received FDA clearance, it is worth investigating further their free radical scavenging capacity, following irradiation.

1.7.5. Gas plasma

The use of gas plasma sterilisation has been advocated as means to avoid denaturation issues associated with gamma and e-beam irradiation and toxicity issues associated with ethylene oxide residues. The non-degrading effect of gas plasma sterilisation was evidenced to be as minimal as ethylene oxide and less significant than gamma irradiation, using SDS-PAGE assays [400]. The authors also demonstrated that although ethylene oxide sterilisation was most comparable to non-sterilised collagen platelet aggregation, plasma treatment and gamma irradiation were not significantly different [400]. One of the distinct advantages of plasma sterilisation is that can be achieved at low temperatures (<50°C), preserving the integrity of temperature sensitive polymers [436]. An important characteristic of plasma sterilisation is the limitation of efficacy to only thin materials, as any material covering the microorganisms, including packaging, will slow down the process [437]. Another limitation is that the process will not work with moist materials; plasma techniques require vacuum which cannot be achieved in the presence of any moisture [438]. An argon gas plasma glow-discharge system (5W for 5min) effectively sterilised non-degradable and biodegradable, mono- and multi-filament, natural and synthetic sutures (except plain and chromic catguts) without changing mechanical properties [439]. Although the preliminary results are promising [440], detailed *in vitro* and *in vivo* studies are still to be carried out. No data has been found regarding to the influence of gas plasma on mechanical properties of collagen-based devices.

1.7.6. Peracetic acid

Peracetic acid sterilisation is an alternative method for tissue banks with the purpose of avoiding denaturation phenomena associated with gamma and e-beam irradiation. Peracetic acid has been shown to be an efficient way to disinfect collagen-based electro-spun films, skin grafts, tendon grafts, and small intestinal submucosa without producing harmful reaction residues [441-446]. Another study has demonstrated that peracetic acid treatment is as efficient on virus inactivation as gamma irradiation [447]. 2.5% peracetic acid-treated amnion showed the highest moisture vapour permeability and oxygen permeability, the highest tensile strength and the lowest sulphur content and thickness; however collagen types V and VII were preserved best in the control (non-sterilised) group [406]. Other studies have shown that the structural integrity of tendon grafts was maintained after 0.1% peracetic acid sterilisation, although the collagen fibrils pattern was slightly loosened. Moreover, peracetic acid incubation caused significant changes in pore size of tendon grafts [407]. Regarding mechanical properties alterations, sterilisation with a mix of 0.1% peracetic acid and 4% ethanol has been shown to increase the biaxial strength of a canine submucosa tissue while it decreased the biaxial strength of porcine bladder tissue [443]. It is worth pointing out that non-cytotoxic response was observed with 0.1% peracetic acid-treated tendon graft after appropriated rinsing step [441]. Peracetic acid has also been used successfully as a decellularisation sterilisation method [444].

1.7.7. Ethanol

Ethanol is a common sterilisation methods for collagen-based materials, such as films [197], sponges [239, 448, 449], fibres and tissue graft [274, 275, 450], prior to

in vitro and *in vivo* experiments. Reconstituted collagen forms are usually immersed into 70% between 15 and 30 minutes [197, 239, 449], whilst tissue graft are sterilised with gradual increase in ethanol concentration from 20 to 75% over a period of 4 hours [274, 275]. Data to-date indicate that ethanol sterilisation does not degrade porcine pericardium; whilst denaturation temperature and tensile strength were slightly increased and enzymatic degradation was unaffected [408]. Ethanol treatment slightly increased porosity, but did not affect biomechanical properties and cytocompatibility of equine tendon grafts [451]. A contradictory to these observations study demonstrated that ethanol sterilisation of sericin scaffold resulted in significant changes in pore size and mechanical properties, resulting from shrinkage of the scaffold [452]. A study that assessed the influence of different sterilisation methods on the *in vivo* osteoinductive properties of partially demineralised bone matrix demonstrated that the osteoinductive properties were not reduced after ethanol sterilisation and 3 and 6 weeks post-implantation, ethanol sterilised bone graft showed osteoclastic and osteoblastic activity and new bone lamellae formation adjacent to the implanted bone graft [453].

1.8. Project rationale and hypothesis

In the last 20 years, the biomaterials field has seen tremendous progress, especially in the area of fabrication. Indeed, we now have the capability to fabricate 3D implantable devices that closely imitate the architectural features of native tissue supramolecular assemblies, offer control over cellular functions (e.g. attachment, growth, migration, differentiation, lineage commitment) at the nano- and micro-scale biointerface and, ultimately, direct neotissue formation. However, there are significant challenges that should be addressed to enable clinical translation and commercialisation. For example, collagen extraction protocols need to reduce batch-to-batch variability and a better understanding of how the extraction parameters influence reconstituted scaffolds is required. Self-assembled collagen-based devices should gain sufficient mechanical resilience and degradation resistance, whilst modulating inflammatory response through a more pro-wound healing scenario. All fabrication methods need to provide readily functionalisation opportunities to aid tissue repair. Moreover, sterilization and scalability should also be incorporated into the developmental plans for the production of industrial-relevant prototypes. These challenges are likely to be surmounted over the years as the promise of clinical translation and commercialization of these ground-breaking technologies is compelling. In this context, the overall goal of this project was to develop an optimal type I collagen film capable of modulating macrophage response. It was hypothesised that the modulation of pre-, during- and post- fabrication parameters (e.g. collagen extraction, film fabrication, cross-linking, sterilisation) will induce a collagen film with sufficient mechanical and enzymatic stability, avoiding toxicity and ultimately reducing pro-inflammatory macrophage activation.

To achieve this goal, the thesis project was divided into three phases (**Figure 1.8**): collagen extraction and purification (Phase I), scaffold fabrication and cross-linking (Phase II), and scaffold sterilisation (Phase III). Each phase has its specific hypothesis and objectives that we ventured to validate herein.

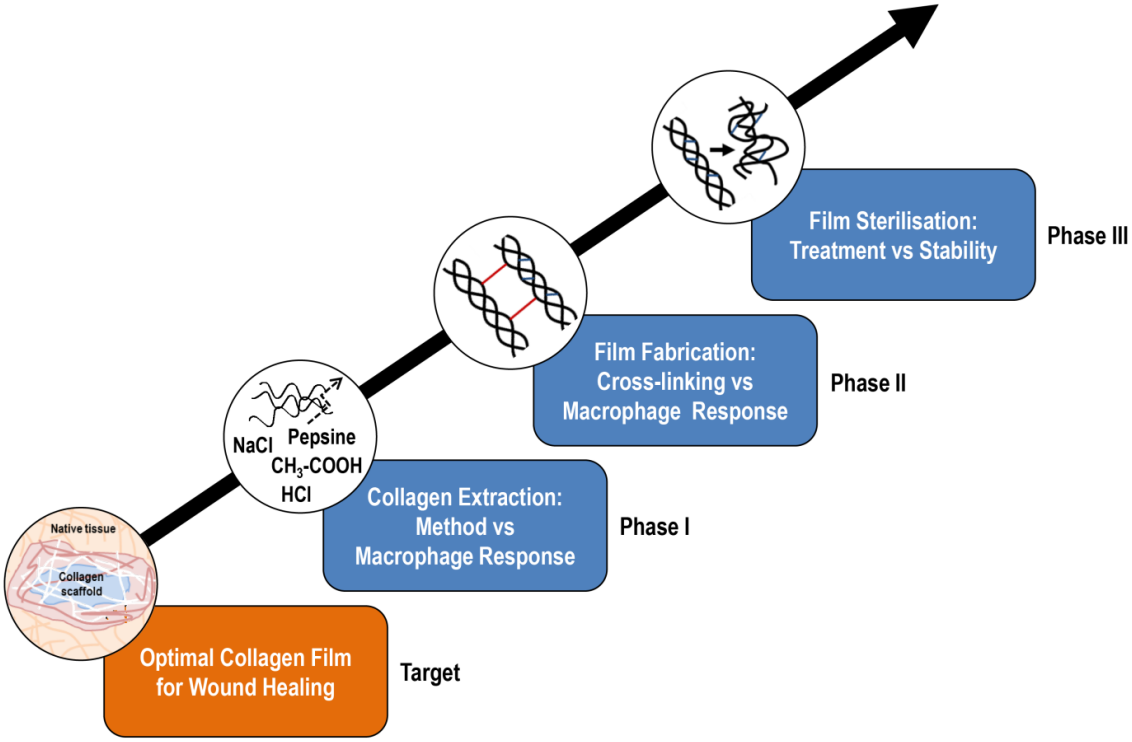

Figure 1.8. Thesis overview. The project developed herein is composed of three different research phases: collagen extraction and purification (Phase I – Chapter 2), scaffold fabrication and cross-linking (Phase II – Chapter 3), and scaffold sterilisation (Phase III – Chapter 4).

1.8.1. Phase I (Chapter 2)

Overall aim: To assess the influence of different collagen extraction methods on the structural, biochemical, biophysical and biological properties of collagen-based devices.

Hypothesis: The usage of acetic acid or hydrochloric acid, pepsin and salt precipitation during collagen type I extraction can affect the collagen ultrastructure and enzymatic stability, and can modulate the *in vitro* macrophage response.

Specific Objectives:

1. To extract collagen using acetic acid and hydrochloric acid, pepsin and salt precipitation.
2. To assess the structural, biochemical, biophysical and biological properties of collagen-based devices as a function of the extraction method used.

1.8.2. Phase II (Chapter 3)

Overall aim: To assess the influence of different collagen cross-linking methods on the structural, biochemical, biophysical and biological properties of collagen-based devices.

Hypothesis: The collagen chemical cross-linking method used can affect the fibrillar structure, free amine content, enzymatic and mechanical stability, and *in vitro* macrophage response of collagen-based devices.

Specific Objectives:

1. To cross-link collagen devices using different cross-linking methods.
2. To assess the structural, biochemical, biophysical and biological properties of collagen-based devices as a function of the cross-linking method used.

1.8.3. Phase III (Chapter 4)

Overall aim: To assess the influence of different collagen sterilisation methods on the structural, biochemical, biophysical and biological properties of collagen-based devices.

Hypothesis: Physical and chemical sterilisation method used can affect the collagen ultrastructure, free amine content, enzymatic and mechanical stability, and macrophage response of collagen-based devices.

Specific Objectives:

1. To sterilise collagen devices using different sterilisation methods.
2. To assess the structural, biochemical, biophysical and biological properties of collagen-based devices as a function of the sterilisation method used.

1.9. References

[1] Zeugolis DI, Raghunath M. Collagen: Materials analysis and implant uses. In: Ducheyne P, Healy KE, Hutmacher DW, Grainger DW, Kirkpatrick CJ, editors. Comprehensive biomaterials: Elsevier; 2011. p. 261-278.

[2] van der Rest M, Garrone R, Herbage D. Collagen: A family of proteins with many facets. In: Kleinman HK, editor. Advances molecular cell biology: JAI Press Inc; 1993. p. 1-67.

[3] Kielty CM, Grant ME. The collagen family: Structure, assembly and organization in the extracellular matrix. In: Royce PM, Steinmann B, editors. Connective tissue and its heritable disorders: Molecular, genetic and medical aspects. 2nd ed. New York: John Wiley Inc; 2002. p. 159-221.

[4] Lee CH, Singla A, Lee Y. Biomedical applications of collagen. Int J Pharm 2001;221:1-22.

[5] Fratzl P, Weinkamer R. Nature's hierarchical materials. Progress Mat Sci 2007;52:1263-1334.

[6] Paul RG, Bailey AJ. Chemical stabilisation of collagen as a biomimetic. ScientificWorldJournal 2003;3:138-155.

[7] Global Industry Analysts Inc. Collagen and HA-based biomaterials - Global strategic business report. MCP-1209 2013:1-617.

[8] Smith-Mungo LI, Kagan HM. Lysyl oxidase: Properties, regulation and multiple functions in biology. Matrix Biol 1998;16:387-398.

[9] Zeugolis DI, Paul RG, Attenburrow G. Factors influencing the properties of reconstituted collagen fibers prior to self-assembly: Animal species and collagen extraction method. J Biomed Mater Res A 2008;86A:892-904.

[10] Zeugolis DI, Khew ST, Yew ESY, Ekaputra AK, Tong YW, Yung L-YL, et al. Electro-spinning of pure collagen nano-fibres - Just an expensive way to make gelatin? Biomaterials 2008;29:2293-2305.

[11] Delgado L, Pandit A, DI Z. Influence of sterilisation methods on collagen-based devices stability and properties. Expert Rev Med Devices 2014;11:305-314.

[12] Friess W. Collagen--biomaterial for drug delivery. Eur J Pharm Biopharm 1998;45:113-136.

[13] Ramshaw JAM, Werkmeister JA, Glattauer V. Collagen-based biomaterials. Biotechnol Genet Eng Rev 1996;13:335-382.

[14] Zeugolis DI, Paul GR, Attenburrow G. Cross-linking of extruded collagen fibers - A biomimetic three-dimensional scaffold for tissue engineering applications. J Biomed Mater Res A 2009;89:895-908.

[15] Gough JE, Scotchford CA, Downes S. Cytotoxicity of glutaraldehyde crosslinked collagen/poly(vinyl alcohol) films is by the mechanism of apoptosis. J Biomed Mater Res 2002;61:121-130.

[16] van Wachem PB, Zeeman R, Dijkstra PJ, Feijen J, Hendriks M, Cahalan PT, et al. Characterization and biocompatibility of epoxy-crosslinked dermal sheep collagens. J Biomed Mater Res 1999;47:270-277.

[17] Levy RJ, Schoen FJ, Sherman FS, Nichols J, Hawley MA, Lund SA. Calcification of subcutaneously implanted type I collagen sponges. Effects of formaldehyde and glutaraldehyde pretreatments. Am J Pathol 1986;122:71-82.

[18] Vasudev SC, Chandy T. Effect of alternative crosslinking techniques on the enzymatic degradation of bovine pericardia and their calcification. J Biomed Mater Res 1997;35:357-369.

[19] McPherson J, Sawamura S, Armstrong R. An examination of the biologic response to injectable, glutaraldehyde cross-linked collagen implants. J Biomed Mater Res 1986;20:93-107.

[20] Brown BN, Londono R, Tottey S, Zhang L, Kukla KA, Wolf MT, et al. Macrophage phenotype as a predictor of constructive remodeling following the implantation of biologically derived surgical mesh materials. Acta Biomater 2012;8:978-987.

[21] Ye Q, Harmsen MC, van Luyn MJ, Bank RA. The relationship between collagen scaffold cross-linking agents and neutrophils in the foreign body reaction. Biomaterials 2010;31:9192-9201.

[22] Weadock KS, Miller EJ, Bellincampi LD, Zawadsky JP, Dunn MG. Physical crosslinking of collagen fibers: Comparison of ultraviolet irradiation and dehydrothermal treatment. J Biomed Mater Res 1995;29:1373-1379.

[23] Weadock KS, Miller EJ, Keuffel EL, Dunn MG. Effect of Physical crosslinking methods on collagen-fiber durability in proteolytic solutions. J Biomed Mater Res 1996;32:221-226.

[24] Abraham GA, Frontini PM, Cuadrado TR. Physical and mechanical behavior of sterilized biomedical segmented polyurethanes. J Appl Polym Sci 1997;65:1193-1203.

[25] Andrews KD, Hunt JA, Black RA. Effects of sterilisation method on surface topography and in-vitro cell behaviour of electrostatically spun scaffolds. Biomaterials 2007;28:1014-1026.

[26] Egles C, Shamis Y, Mauney J, Volloch V, Kaplan D, Garlick J. Denatured collagen modulates the phenotype of normal and wounded human skin equivalents. J Invest Dermatol 2008;128:1830-1837.

[27] Abraham LC, Dice JF, Lee K, Kaplan DL. Phagocytosis and remodeling of collagen matrices. Exp Cell Res 2007;313:1045-1055.

[28] Zeng Q, Macri LK, Prasad A, Clark RAF, Zeugolis DI, Hanley C, et al. Skin tissue engineering. In: Ducheyne P, editor. Comprehensive biomaterials. Oxford: Elsevier; 2011. p. 467-499.

[29] Martin P. Wound healing--Aiming for perfect skin regeneration. Science 1997;276:75-81.

[30] Vroman L, Adams AL, Fischer GC, Munoz PC. Interaction of high molecular weight kininogen, factor XII, and fibrinogen in plasma at interfaces. Blood 1980;55:156-159.

[31] Xu LC, Siedlecki CA. Effects of surface wettability and contact time on protein adhesion to biomaterial surfaces. Biomaterials 2007;28:3273-3283.

[32] Hallab NJ, Bundy KJ, O'Connor K, Moses RL, Jacobs JJ. Evaluation of metallic and polymeric biomaterial surface energy and surface roughness characteristics for directed cell adhesion. Tissue Eng 2001;7:55-71.

[33] MacDonald DE, Deo N, Markovic B, Stranick M, Somasundaran P. Adsorption and dissolution behavior of human plasma fibronectin on thermally and chemically modified titanium dioxide particles. Biomaterials 2002;23:1269-1279.

[34] Schutte RJ, Parisi-Amon A, Reichert WM. Cytokine profiling using monocytes/macrophages cultured on common biomaterials with a range of surface chemistries. J Biomed Mater Res A 2009;88:128-139.

[35] Deligianni DD, Katsala N, Ladas S, Sotiropoulou D, Amedee J, Missirlis YF. Effect of surface roughness of the titanium alloy Ti-6Al-4V on human bone marrow cell response and on protein adsorption. Biomaterials 2001;22:1241-1251.

[36] Chen S, Jones Ja, Xu Y, Low H-Y, Anderson JM, Leong KW. Characterization of topographical effects on macrophage behavior in a foreign body response model. Biomaterials 2010;31:3479-3491.

[37] Waterfield JD, Ali TA, Nahid F, Kusano K, Brunette DM. The effect of surface topography on early NFkappaB signaling in macrophages. J Biomed Mater Res A 2010;95:837-847.

[38] Blakney AK, Swartzlander MD, Bryant SJ. The effects of substrate stiffness on the in vitro activation of macrophages and in vivo host response to poly(ethylene glycol)-based hydrogels. J Biomed Mater Res A 2012;100:1375-1386.

[39] Li J, Chen J, Kirsner R. Pathophysiology of acute wound healing. Clin Dermatol 2007;25:9-18.

[40] Peterson JM, Pizza FX. Cytokines derived from cultured skeletal muscle cells after mechanical strain promote neutrophil chemotaxis in vitro. J Appl Physiol 2009;106:130-137.

[41] Bryan N, Ahswin H, Smart N, Bayon Y, Wohlert S, Hunt JA. Reactive oxygen species (ROS)--a family of fate deciding molecules pivotal in constructive inflammation and wound healing. Eur Cell Mater 2012;24:249-265.

[42] Anderson JM, Rodriguez A, Chang DT. Foreign body reaction to biomaterials. Semin Immunol 2008;20:86-100.

[43] Mantovani A, Sica A, Sozzani S, Allavena P, Vecchi A, Locati M. The chemokine system in diverse forms of macrophage activation and polarization. Trends Immunol 2004;25:677-686.

[44] Gordon S, Taylor PR. Monocyte and macrophage heterogeneity. Nat Rev Immunol 2005;5:953-964.

[45] Mosser DM, Edwards JP. Exploring the full spectrum of macrophage activation. Nat Rev Immunol 2008;8:958-969.

[46] Brown BN, Badylak SF. Expanded applications, shifting paradigms and an improved understanding of host-biomaterial interactions. Acta Biomater 2013;9:4948-4955.

[47] Lucas T, Waisman A, Ranjan R, Roes J, Krieg T, Muller W, et al. Differential roles of macrophages in diverse phases of skin repair. J Immunol 2010;184:3964-3977.

[48] Garg K, Pullen Na, Oskeritzian Ca, Ryan JJ, Bowlin GL. Macrophage functional polarization (M1/M2) in response to varying fiber and pore dimensions of electrospun scaffolds. Biomaterials 2013;34:4439-4451.

[49] Franz S, Allenstein F, Kajahn J, Forstreuter I, Hintze V, Moller S, et al. Artificial extracellular matrices composed of collagen I and high-sulfated hyaluronan promote phenotypic and functional modulation of human pro-inflammatory M1 macrophages. Acta Biomater 2013;9:5621-5629.

[50] Vacanti NM, Cheng H, Hill PS, Guerreiro JDT, Dang TT, Ma M, et al. Localized delivery of dexamethasone from electrospun fibers reduces the foreign body response. Biomacromolecules 2012;13:3031-3038.

[51] Bartneck M, Peters FM, Warzecha KT, Bienert M, van Bloois L, Trautwein C, et al. Liposomal encapsulation of dexamethasone modulates cytotoxicity, inflammatory cytokine response, and migratory properties of primary human macrophages. Nanomedicine 2014;10:1209-1220.

[52] Helary C, Browne S, Mathew A, Wang W, Pandit A. Transfection of macrophages by collagen hollow spheres loaded with polyplexes: A step towards modulating inflammation. Acta Biomater 2012;8:4208-4214.

[53] Tomasek JJ, Gabbiani G, Hinz B, Chaponnier C, Brown RA. Myofibroblasts and mechano-regulation of connective tissue remodelling. Nat Rev Mol Cell Biol 2002;3:349-363.

[54] Gurtner GC, Werner S, Barrandon Y, Longaker MT. Wound repair and regeneration. Nature 2008;453:314-321.

[55] Spiller KL, Anfang RR, Spiller KJ, Ng J, Nakazawa KR, Daulton JW, et al. The role of macrophage phenotype in vascularization of tissue engineering scaffolds. Biomaterials 2014;35:4477-4488.

[56] Guo S, Dipietro LA. Factors affecting wound healing. J Dent Res 2010;89:219-229.

[57] Frykberg RG, Banks J. Challenges in the treatment of chronic wounds. Adv Wound Care 2015;4:560-582.

[58] Alexander M, Chaudry IH, Schwacha MG. Relationships between burn size, immunosuppression, and macrophage hyperactivity in a murine model of thermal injury. Cell Immunol 2002;220:63-69.

[59] Schwacha MG, Nickel E, Daniel T. Burn injury-induced alterations in wound inflammation and healing are associated with suppressed hypoxia inducible factor-1alpha expression. Mol Med 2008;14:628-633.

[60] Swift ME, Burns AL, Gray KL, DiPietro LA. Age-related alterations in the inflammatory response to dermal injury. J Invest Dermatol 2001;117:1027-1035.

[61] Mahbub S, Deburghgraeve CR, Kovacs EJ. Advanced age impairs macrophage polarization. J Interferon Cytokine Res 2012;32:18-26.

[62] Swift ME, Kleinman HK, DiPietro LA. Impaired wound repair and delayed angiogenesis in aged mice. Lab Invest 1999;79:1479-1487.

[63] Gosain A, DiPietro LA. Aging and wound healing. World J Surg 2004;28:321-326.

[64] World Health Organisation. Fact sheet N311. World Health Organisation 2014.

[65] Anaya DA, Dellinger EP. The obese surgical patient: A susceptible host for infection. Surg Infect 2006;7:473-480.

[66] Nieman DC, Henson DA, Nehlsen-Cannarella SL, Ekkens M, Utter AC, Butterworth DE, et al. Influence of obesity on immune function. J Am Diet Assoc 1999;99:294-299.

[67] Spiliotis J, Tsiveriotis K, Datsis AD, Vaxevanidou A, Zacharis G, Giafis K, et al. Wound dehiscence: is still a problem in the 21th century: A retrospective study. World J Emerg Surg 2009;4:12.

[68] Juge-Aubry CE, Henrichot E, Meier CA. Adipose tissue: A regulator of inflammation. Best Pract Res Clin Endocrinol Metab 2005;19:547-566.

[69] International Diabetes Federation. IDF diabetes atlas, 6th edn. Brussels, Belgium: International Diabetes Federation; 2013.

[70] Aouacheri O, Saka S, Krim M, Messaadia A, Maidi I. The investigation of the oxidative stress-related parameters in type 2 diabetes mellitus. Can J Diabetes 2014:44-49.

[71] Martin A, Komada MR, Sane DC. Abnormal angiogenesis in diabetes mellitus. Med Res Rev 2003;23:117-145.

[72] Galkowska H, Olszewski WL, Wojewodzka U, Rosinski G, Karnafel W. Neurogenic factors in the impaired healing of diabetic foot ulcers. J Surg Res 2006;134:252-258.

[73] Lecube A, Pachón G, Petriz J, Hernández C, Simó R. Phagocytic activity is impaired in type 2 diabetes mellitus and increases after metabolic improvement. PLoS One 2011;6:e23366.

[74] Olefsky JM, Glass CK. Macrophages, inflammation, and insulin resistance. Annu Rev Physiol 2010;72:219-246.

[75] Falanga V. Wound healing and its impairment in the diabetic foot. Lancet 2005;366:1736-1743.

[76] Wall SJ, Bevan D, Thomas DW, Harding KG, Edwards DR, Murphy G. Differential expression of matrix metalloproteinases during impaired wound healing of the diabetes mouse. J Invest Dermatol 2002;119:91-98.

[77] Hulmes D. Building collagen molecules, fibrils, and suprafibrillar structures. J Struct Biol 2002;137:2-10.

[78] van der Rest M, Garrone R, Herbage D. Collagen: A family of proteins with many facets. In: Kleinman H, editor. Advances in Molecular and Cell Biology. Greenwich, Connecticut: JAI Press Inc; 1993. p. 1-67.

[79] Kielty C, Grant M. The collagen family: Structure, assembly, and organization in the extracellular matrix. In: Royce P, Steinmann B, editors. Connective Tissue and Its Heritable Disorders: Molecular, Genetic, and Medical Aspects. Second ed. Hoboken, NJ, USA: John Wiley & Sons, Inc.; 2002. p. 159-221.

[80] Bella J. Collagen structure: new tricks from a very old dog. Biochem J 2016;473:1001-1025.

[81] Shoulders M, Raines R. Collagen structure and stability. Annu Rev Biochem 2009;78:929-958.

[82] Bailey A, Paul R, Knott L. Mechanisms of maturation and ageing of collagen. Mech Ageing Dev 1998;106:1-56.

[83] Kadler K, Holmes D, Trotter J, Chapman J. Collagen fibril formation. Biochem J 1996;316:1-11.

[84] Eyden B, Tzaphlidou M. Structural variations of collagen in normal and pathological tissues: Role of electron microscopy. Micron 2001;32:287-300.

[85] Starborg T, Lu Y, Kadler K, Holmes D. Electron microscopy of collagen fibril structure in vitro and in vivo including three-dimensional reconstruction. Methods Cell Biol 2008;88:319-345.

[86] Kalamajski S, Oldberg A. The role of small leucine-rich proteoglycans in collagen fibrillogenesis. Matrix Biol 2010;29:248-253.

[87] Reed C, Iozzo R. The role of decorin in collagen fibrillogenesis and skin homeostasis. Glycoconj J 2002;19:249-255.

[88] Ellingsworth LR, DeLustro F, Brennan JE, Sawamura S, McPherson J. The human immune response to reconstituted bovine collagen. J Immunol 1986;136:877-882.

[89] Lynn AK, Yannas IV, Bonfield W. Antigenicity and immunogenicity of collagen. J Biomed Mater Res B 2004;71B:343-354.

[90] Antoine E, Vlachos P, Rylander M. Review of collagen I hydrogels for bioengineered tissue microenvironments: Characterization of mechanics, structure, and transport. Tissue Eng Part B Rev 2014;20:683-696.

[91] Pawelec K, Best S, Cameron R. Collagen: A network for regenerative medicine. J Mater Chem B 2016;4:6484-6496.

[92] Ramshaw J. Biomedical applications of collagens. J Biomed Mater Res B Appl Biomater 2016;104:665-675.

[93] Abou Neel EA, Bozec L, Knowles JC, Syed O, Mudera V, Day R, et al. Collagen--emerging collagen based therapies hit the patient. Adv Drug Deliv Rev 2013;65:429-456.

[94] Ramshaw JAM, Werkmeister JA, Glattauer V. Collagen-based Biomaterials. Biotechnology and Genetic Engineering Reviews 1995;13:335-382.

[95] Birk DE, Fitch JM, Babiarz JP, Doane KJ, Linsenmayer TF. Collagen fibrillogenesis in vitro: interaction of types I and V collagen regulates fibril diameter. Journal of Cell Science 1990;95:649-657.

[96] El Feninat F, Ellis T, Sacher E, Stangel I. Moisture-dependent renaturation of collagen in phosphoric acid etched human dentin. J Biomed Mater Res 1998;42:549-553.

[97] Rosenblatt J, Devereux B, Wallace DG. Injectable collagen as a pH-sensitive hydrogel. Biomaterials 1994;15:985-995.

[98] Parkinson J, Brass A, Canova G, Brechet Y. The mechanical properties of simulated collagen fibrils. Journal of Biomechanics 1997;30:549-554.

[99] Chapman JA, Tzaphlidou M, Meek KM, Kadler KE. The collagen fibril--A model system for studying the staining and fixation of a protein. Electron Microscopy Reviews 1990;3:143-182.

[100] Kielty CM, Grant ME. The collagen family: Structure, assembly and organization in the extracellular matrix. In: Royce PM, Steinmann B, editors. Connective Tissue and Its Heritable Disorders: Molecular, Genetic and Medical Aspects. Second Edition ed: John Wiley Inc; 2002. p. 159-221.

[101] Sasaki N, Odajima S. Stress-strain curve and Young's modulus of a collagen molecule as determined by the X-ray diffraction technique. Journal of Biomechanics 1996;29:655-658.

[102] Paul RG, Bailey AJ. Chemical stabilisation of collagen as a biomimetic. The Scientific World journal 2003;3:138-155.

[103] Miles CA, Burjanadze TV, Bailey AJ. The Kinetics of the Thermal Denaturation of Collagen in Unrestrained Rat Tail Tendon Determined by Differential Scanning Calorimetry. Journal of Molecular Biology 1995;245:437-446.

[104] Bailey AJ, Paul RG. Collagen: A not so simple protein. Journal of the Society of Leather Technologists and Chemists 1998;82:104-110.

[105] Wess TJ, Hammersley AP, Wess L, Miller A. A Consensus Model for Molecular Packing of Type I Collagen. Journal of Structural Biology 1998;122:92-100.

[106] Wess TJ, Hammersley AP, Wess L, Miller A. Molecular Packing of type I Collagen in Tendon. Journal of Molecular Biology 1998;275:255-267.

[107] Woodley D, Yamauchi M, Wynn K, Mechanic G, Briggaman R. Collagen telopeptides (cross-linking sites) play a role in collagen gel lattice contraction. J Invest Dermatol 1991;97:580-585.

[108] Song JJ, Ott HC. Organ engineering based on decellularized matrix scaffolds. Trends Mol Med 2011;17:424-432.

[109] Chen FM, Liu X. Advancing biomaterials of human origin for tissue engineering. Prog Polym Sci 2015;53:86-168.

[110] Deeken CR, Eliason BJ, Pichert MD, Grant SA, Frisella MM, Matthews BD. Differentiation of biologic scaffold materials through physicomechanical, thermal, and enzymatic degradation techniques. Ann Surg 2012;255:595-604.

[111] Sandor M, Xu H, Connor J, Lombardi J, Harper JR, Silverman RP, et al. Host response to implanted porcine-derived biologic materials in a primate model of abdominal wall repair. Tissue Eng A 2008;14:2021-2031.

[112] Burugapalli K, Chan JC, Kelly JL, Pandit AS. Efficacy of crosslinking on tailoring in vivo biodegradability of fibro-porous decellularized extracellular matrix and restoration of native tissue structure: A quantitative study using stereology methods. Macromol Biosci 2014;14:244-256.

[113] McDade JK, Brennan-Pierce EP, Ariganello MB, Labow RS, Michael Lee J. Interactions of U937 macrophage-like cells with decellularized pericardial matrix materials: Influence of crosslinking treatment. Acta Biomater 2013;9:7191-7199.

[114] Omae H, Zhao C, Sun YL, An KN, Amadio PC. Multilayer tendon slices seeded with bone marrow stromal cells: A novel composite for tendon engineering. J Orthop Res 2009;27:937-942.

[115] Abou Neel EA, Bozec L, Knowles JC, Syed O, Mudera V, Day R, et al. Collagen -- Emerging collagen based therapies hit the patient. Adv Drug Deliv Rev 2013;65:429-456.

[116] Badylak SF, Gilbert TW. Immune response to biologic scaffold materials. Semin Immunol 2008;20:109-116.

[117] Kawecki M, Labus W, Klama-Baryla A, Kitala D, Kraut M, Glik J, et al. A review of decellurization methods caused by an urgent need for quality control of cell-free extracellular matrix' scaffolds and their role in regenerative medicine. J Biomed Mater Res B Appl Biomater 2018;106:909-923.

[118] Utomo L, Boersema GSA, Bayon Y, Lange JF, van Osch G, Bastiaansen-Jenniskens YM. In vitro modulation of the behavior of adhering macrophages by medications is biomaterial-dependent. Biomed Mater 2017;12:025006.

[119] Ricchetti ET, Aurora A, Iannotti JP, Derwin KA. Scaffold devices for rotator cuff repair. J Shoulder Elbow Surg 2012;21:251-265.

[120] Wang Y, Liao L. Histologic and functional outcomes of small intestine submucosa-regenerated bladder tissue. BMC Urol 2014;14:69.

[121] Valerio IL, Campbell P, Sabino J, Dearth CL, Fleming M. The use of urinary bladder matrix in the treatment of trauma and combat casualty wound care. Regen Med 2015;10:611-622.

[122] Warwick AM, Velineni R, Smart NJ, Daniels IR. Onlay parastomal hernia repair with cross-linked porcine dermal collagen biologic mesh: long-term results. Hernia 2016;20:321-325.

[123] Zhang Z, Lv L, Mamat M, Chen Z, Zhou Z, Liu L, et al. Xenogenic (porcine) acellular dermal matrix promotes growth of granulation tissues in the wound healing of Fournier gangrene. Am Surg 2015;81:92-95.

[124] Romain B, Story F, Meyer N, Delhorme JB, Brigand C, Rohr S. Comparative study between biologic porcine dermal meshes: risk factors of postoperative morbidity and recurrence. J Wound Care 2016;25:320-325.

[125] Abdelfatah MM, Rostambeigi N, Podgaetz E, Sarr MG. Long-term outcomes (>5-year follow-up) with porcine acellular dermal matrix (Permacol) in incisional hernias at risk for infection. Hernia 2015;19:135-140.

[126] Kadler KE, Hojima Y, Prockop DJ. Assembly of collagen fibrils de novo by cleavage of the type I pC-collagen with procollagen C-proteinase. Assay of critical concentration demonstrates that collagen self-assembly is a classical example of an entropy-driven process. J Biol Chem 1987;262:15696-15701.

[127] Kuivaniemi H, Tromp G, Prockop DJ. Mutations in fibrillar collagens (types I, II, III, and XI), fibril-associated collagen (type IX), and network-forming collagen (type X) cause a spectrum of diseases of bone, cartilage, and blood vessels. Hum Mutat 1997;9:300-315.

[128] Payne KJ, Veis A. Fourier transform IR spectroscopy of collagen and gelatin solutions: Deconvolution of the amide I band for conformational studies. Biopolymers 1988;27:1749-1760.

[129] Holmes DF, Graham HK, Trotter JA, Kadler KE. STEM/TEM studies of collagen fibril assembly. Micron 2001;32:273-285.

[130] Parkinson J, Brass A, Canova G, Brechet Y. The mechanical properties of simulated collagen fibrils. J Biomech 1997;30:549-554.

[131] Ngo P, Ramalingam P, Phillips JA, Furuta GT. Collagen gel contraction assay. Methods Mol Biol 2006;341:103-109.

[132] Silver FH, Freeman JW, Seehra GP. Collagen self-assembly and the development of tendon mechanical properties. J Biomech 2003;36:1529-1553.

[133] Wallace DG, Rosenblatt J. Collagen gel systems for sustained delivery and tissue engineering. Adv Drug Deliv Rev 2003;55:1631-1649.

[134] Rault I, Frei V, Herbage D, Abdul-Malak N, Huc A. Evaluation of different chemical methods for cros-linking collagen gel, films and sponges. J Mater Sci Mater Med 1996;7:215-221.

[135] Stratesteffen H, Kopf M, Kreimendahl F, Blaeser A, Jockenhoevel S, Fischer H. GelMA-collagen blends enable drop-on-demand 3D printablility and promote angiogenesis. Biofabrication 2017;9:045002.

[136] Hu K, Shi H, Zhu J, Deng D, Zhou G, Zhang W, et al. Compressed collagen gel as the scaffold for skin engineering. Biomed Microdevices 2010;12:627-635.

[137] Busby GA, Grant MH, Mackay SP, Riches PE. Confined compression of collagen hydrogels. J Biomech 2013;46:837-840.

[138] Braziulis E, Diezi M, Biedermann T, Pontiggia L, Schmucki M, Hartmann-Fritsch F, et al. Modified plastic compression of collagen hydrogels provides an

ideal matrix for clinically applicable skin substitutes. Tissue Eng C 2012;18:464-474.

[139] Engelhardt EM, Stegberg E, Brown RA, Hubbell JA, Wurm FM, Adam M, et al. Compressed collagen gel: A novel scaffold for human bladder cells. J Tissue Eng Regen Med 2010;4:123-130.

[140] Brown RA, Wiseman M, Chuo CB, Cheema U, Nazhat SN. Ultrarapid engineering of biomimetic materials and tissues: Fabrication of nano- and microstructures by plastic compression. Adv Funct Mater 2005;15:1762-1770.

[141] Clause KC, Tinney JP, Liu LJ, Gharaibeh B, Huard J, Kirk JA, et al. A three-dimensional gel bioreactor for assessment of cardiomyocyte induction in skeletal muscle-derived stem cells. Tissue Eng C 2010;16:375-385.

[142] Tulloch NL, Muskheli V, Razumova MV, Korte FS, Regnier M, Hauch KD, et al. Growth of engineered human myocardium with mechanical loading and vascular coculture. Circ Res 2011;109:47-59.

[143] Zimmermann WH, Schneiderbanger K, Schubert P, Didie M, Munzel F, Heubach JF, et al. Tissue engineering of a differentiated cardiac muscle construct. Circ Res 2002;90:223-230.

[144] Xie J, Pak K, Evans A, Kamgar-Parsi A, Fausti S, Mullen L, et al. Neurotrophins differentially stimulate the growth of cochlear neurites on collagen surfaces and in gels. Neural Regen Res 2013;8:1541-1550.

[145] Koppes AN, Keating KW, McGregor AL, Koppes RA, Kearns KR, Ziemba AM, et al. Robust neurite extension following exogenous electrical stimulation within single walled carbon nanotube-composite hydrogels. Acta Biomater 2016;39:34-43.

[146] Hiraoka M, Kato K, Nakaji-Hirabayashi T, Iwata H. Enhanced survival of neural cells embedded in hydrogels composed of collagen and laminin-derived cell adhesive peptide. Bioconjug Chem 2009;20:976-983.

[147] Moriarty N, Pandit A, Dowd E. Encapsulation of primary dopaminergic neurons in a GDNF-loaded collagen hydrogel increases their survival, re-innervation and function after intra-striatal transplantation. Sci Rep 2017;7:16033.

[148] Frazer A, Bunning RA, Thavarajah M, Seid JM, Russell RG. Studies on type II collagen and aggrecan production in human articular chondrocytes in vitro and effects of transforming growth factor-beta and interleukin-1beta. Osteoarthr Cartil 1994;2:235-245.

[149] Kontturi LS, Järvinen E, Muhonen V, Collin EC, Pandit AS, Kiviranta I, et al. An injectable, in situ forming type II collagen/hyaluronic acid hydrogel vehicle for chondrocyte delivery in cartilage tissue engineering. Drug Deliv Transl Res 2014;4:149-158.

[150] Bosnakovski D, Mizuno M, Kim G, Takagi S, Okumura M, Fujinaga T. Chondrogenic differentiation of bovine bone marrow mesenchymal stem cells (MSCs) in different hydrogels: Influence of collagen type II extracellular matrix on MSC chondrogenesis. Biotechnol Bioeng 2006;93:1152-1163.

[151] Lazarini M, Bordeaux-Rego P, Giardini-Rosa R, Duarte ASS, Baratti MO, Zorzi AR, et al. Natural Type II Collagen Hydrogel, Fibrin Sealant, and Adipose-Derived Stem Cells as a Promising Combination for Articular Cartilage Repair. Cartilage 2017;8:439-443.

[152] Parmar PA, St-Pierre JP, Chow LW, Spicer CD, Stoichevska V, Peng YY, et al. Enhanced articular cartilage by human mesenchymal stem cells in enzymatically

mediated transiently RGDS-functionalized collagen-mimetic hydrogels. Acta Biomater 2017;51:75-88.

[153] Chvapil M. Collagen sponge: Theory and practice of medical applications. J Biomed Mater Res 1977;11:721-741.

[154] O'Brien FJ, Harley BA, Yannas IV, Gibson LJ. Influence of freezing rate on pore structure in freeze-dried collagen-GAG scaffolds. Biomaterials 2004;25:1077-1086.

[155] Haugh MG, Murphy CM, O'Brien FJ. Novel freeze-drying methods to produce a range of collagen–glycosaminoglycan scaffolds with tailored mean pore sizes. Tissue Eng C 2009;16:887-894.

[156] Byrne EM, Farrell E, McMahon LA, Haugh MG, O'Brien FJ, Campbell VA, et al. Gene expression by marrow stromal cells in a porous collagen–glycosaminoglycan scaffold is affected by pore size and mechanical stimulation. J Mater Sci Mater Med 2008;19:3455-3463.

[157] Huang L, Zhu L, Shi X, Xia B, Liu Z, Zhu S, et al. A compound scaffold with uniform longitudinally oriented guidance cues and a porous sheath promotes peripheral nerve regeneration in vivo. Acta Biomater 2017:In Press.

[158] Keogh MB, Partap S, Daly JS, O'Brien FJ. Three hours of perfusion culture prior to 28 days of static culture, enhances osteogenesis by human cells in a collagen GAG scaffold. Biotechnol Bioeng 2011;108:1203-1210.

[159] Alhag M, Farrell E, Toner M, Lee TC, O'Brien FJ, Claffey N. Evaluation of the ability of collagen-glycosaminoglycan scaffolds with or without mesenchymal stem cells to heal bone defects in Wistar rats. Oral Maxillofac Surg 2012;16:47-55.

[160] Lyons FG, Al-Munajjed AA, Kieran SM, Toner ME, Murphy CM, Duffy GP, et al. The healing of bony defects by cell-free collagen-based scaffolds compared to stem cell-seeded tissue engineered constructs. Biomaterials 2010;31:9232-9243.

[161] Quinlan E, Thompson EM, Matsiko A, O'Brien FJ, López-Noriega A. Long-term controlled delivery of rhBMP-2 from collagen-hydroxyapatite scaffolds for superior bone tissue regeneration. J Control Release 2015;207:112-119.

[162] Onuma-Ukegawa M, Bhatt K, Hirai T, Kaburagi H, Sotome S, Wakabayashi Y, et al. Bone marrow stromal cells combined with a honeycomb collagen sponge facilitate neurite elongation in vitro and neural restoration in the hemisected rat spinal cord. Cell Transplant 2015;24:1283-1297.

[163] Markowicz M, Koellensperger E, Neuss S, Koenigschulte S, Bindler C, Pallua N. Human bone marrow mesenchymal stem cells seeded on modified collagen improved dermal regeneration in vivo. Cell Transplant 2006;15:723-732.

[164] Kanda N, Morimoto N, Takemoto S, Ayvazyan AA, Kawai K, Sakamoto Y, et al. Efficacy of novel collagen/gelatin scaffold with sustained release of basic fibroblast growth factor for dermis-like tissue regeneration. Ann Plast Surg 2012;69:569-574.

[165] Kanda N, Morimoto N, Ayvazyan AA, Takemoto S, Kawai K, Nakamura Y, et al. Evaluation of a novel collagen-gelatin scaffold for achieving the sustained release of basic fibroblast growth factor in a diabetic mouse model. J Tissue Eng Regen Med 2014;8:29-40.

[166] Ayvazyan A, Morimoto N, Kanda N, Takemoto S, Kawai K, Sakamoto Y, et al. Collagen-gelatin scaffold impregnated with bFGF accelerates palatal wound healing of palatal mucosa in dogs. J Surg Res 2011;171:e247-e257.

[167] Ito R, Morimoto N, Pham LH, Taira T, Kawai K, Suzuki S. Efficacy of the controlled release of concentrated platelet lysate from a collagen/gelatin scaffold for dermis-like tissue regeneration. Tissue Eng A 2013;19:1398-1405.

[168] Rethore G, Pandit A. Use of templates to fabricate nanoscale spherical structures for defined architectural control. Small 2010;6:488-498.

[169] Shi X, Wang S, Chen X, Meshinchi S, Baker JR, Jr. Encapsulation of submicrometer-sized 2-methoxyestradiol crystals into polymer multilayer capsules for biological applications. Mol Pharm 2006;3:144-151.

[170] Browne S, Fontana G, Rodriguez BJ, Pandit A. A protective extracellular matrix-based gene delivery reservoir fabricated by electrostatic charge manipulation. Mol Pharm 2012;9:3099-3106.

[171] Dash BC, Rethore G, Monaghan M, Fitzgerald K, Gallagher W, Pandit A. The influence of size and charge of chitosan/polyglutamic acid hollow spheres on cellular internalization, viability and blood compatibility. Biomaterials 2010;31:8188-8197.

[172] Dash BC, Mahor S, Carroll O, Mathew A, Wang W, Woodhouse KA, et al. Tunable elastin-like polypeptide hollow sphere as a high payload and controlled delivery gene depot. J Control Release 2011;152:382-392.

[173] Kraskiewicz H, Breen B, Sargeant T, McMahon S, Pandit A. Assembly of protein-based hollow spheres encapsulating a therapeutic factor. ACS Chem Neurosci 2013;4:1297-1304.

[174] Likhitpanichkul M, Kim Y, Torre OM, See E, Kazezian Z, Pandit A, et al. Fibrin-genipin annulus fibrosus sealant as a delivery system for anti-TNFα drug. Spine J 2015;15:2045-2054.

[175] Milcovich G, Contessotto P, Marsico G, Ismail S, Pandit A. Synthetic/ECM-inspired hybrid platform for hollow microcarriers with ROS-triggered nanoporation hallmarks. Sci Rep 2017;7:13138.

[176] Tapeinos C, Larranaga A, Sarasua JR, Pandit A. Functionalised collagen spheres reduce H2O2 mediated apoptosis by scavenging overexpressed ROS. Nanomedicine 2017:In Press.

[177] Yang L, Fitié C, van der Werf K, Bennink M, Dijkstra P, Feijen J. Mechanical properties of single electrospun collagen type I fibers. Biomaterials 2008;29:955-962.

[178] Zeugolis DI, Khew ST, Yew ES, Ekaputra AK, Tong YW, Yung LY, et al. Electro-spinning of pure collagen nano-fibres - Just an expensive way to make gelatin? Biomaterials 2008;29:2293-2305.

[179] Kato YP, Christiansen D, Hahn RA, Shieh SJ, Goldstein JD, Silver FH. Mechanical properties of collagen fibres: A comparison of reconstituted and rat tail tendon fibres. Biomaterials 1989;10:38-42.

[180] Kato YP, Silver FH. Formation of continuous collagen fibres: Evaluation of biocompatibilily and mechanical properties. Biomaterials 1990;11:169-175.

[181] Wang MC, Pins GD, Silver FH. Collagen fibres with improved strength for the repair of soft tissue injuries. Biomaterials 1994;15:507-512.

[182] Pins GD, Christiansen DL, Patel R, Silver FH. Self-assembly of collagen fibers. Influence of fibrillar alignment and decorin on mechanical properties. Biophys J 1997;73:2164-2172.

[183] Pins GD, Huang EK, Christiansen DL, Silver FH. Effects of static axial strain on the tensile properties and failure mechanisms of self-assembled collagen fibers. J Appl Polym Sci 1997;63:1429-1440.

[184] Christiansen DL, Huang EK, Silver FH. Assembly of type I collagen: Fusion of fibril subunits and the influence of fibril diameter on mechanical properties. Matrix Biol 2000;19:409-420.

[185] Gentleman E, Lay AN, Dickerson DA, Nauman EA, Livesay GA, Dee KC. Mechanical characterization of collagen fibers and scaffolds for tissue engineering. Biomaterials 2003;24:3805-3813.

[186] Marino AA, Becker RO. The effect of electric current on rat tail tendon collagen in solution. Calcif Tissue Res 1969;4:330-338.

[187] Cornwell KG, Downing BR, Pins GD. Characterizing fibroblast migration on discrete collagen threads for applications in tissue regeneration. J Biomed Mater Res A 2004;71:55-62.

[188] Sanami M, Sweeney I, Shtein Z, Meirovich S, Sorushanova A, Mullen AM, et al. The influence of poly(ethylene glycol) ether tetrasuccinimidyl glutarate on the structural, physical, and biological properties of collagen fibers. J Biomed Mater Res B 2016;104:914-922.

[189] Kato YP, Dunn MG, Zawadsky JP, Tria AJ, Silver FH. Regeneration of Achilles tendon with a collagen tendon prosthesis. Results of a one-year implantation study. J Bone Joint Surg Am 1991;73:561-574.

[190] Cavallaro JF, Kemp PD, Kraus KH. Collagen fabrics as biomaterials. Biotechnol Bioeng 1994;43:781-791.

[191] Enea D, Gwynne J, Kew S, Arumugam M, Shepherd J, Brooks R, et al. Collagen fibre implant for tendon and ligament biological augmentation. In vivo study in an ovine model. Knee Surg, Sports Traumatol, Arthrosc 2013;21:1783-1793.

[192] Gurkan UA, Cheng X, Kishore V, Uquillas JA, Akkus O. Comparison of morphology, orientation, and migration of tendon derived fibroblasts and bone marrow stromal cells on electrochemically aligned collagen constructs. J Biomed Mater Res A 2010;94:1070-1079.

[193] Kishore V, Uquillas JA, Dubikovsky A, Alshehabat MA, Snyder PW, Breur GJ, et al. In vivo response to electrochemically aligned collagen bioscaffolds. J Biomed Mater Res B 2012;100:400-408.

[194] Kishore V, Bullock W, Sun X, van Dyke WS, Akkus O. Tenogenic differentiation of human MSCs induced by the topography of electrochemically aligned collagen threads. Biomaterials 2012;33:2137-2144.

[195] Younesi M, Islam A, Kishore V, Anderson JM, Akkus O. Tenogenic Induction of Human MSCs by Anisotropically Aligned Collagen Biotextiles. Adv Funct Mater 2014;24:5762-5770.

[196] Abu-Rub MT, Billiar KL, van Es MH, Knight A, Rodriguez BJ, Zeugolis DI, et al. Nano-textured self-assembled aligned collagen hydrogels promote directional neurite guidance and overcome inhibition by myelin associated glycoprotein. Soft Matter 2011;7:2770-2781.

[197] Satyam A, Subramanian GS, Raghunath M, Pandit A, Zeugolis DI. In vitro evaluation of Ficoll-enriched and genipin-stabilised collagen scaffolds. J Tissue Eng Regen Med 2014;8:233-241.

[198] Kumar P, Satyam A, Cigognini D, Pandit A, Zeugolis D. Low oxygen tension and macromolecular crowding accelerate extracellular matrix deposition in human corneal fibroblast culture. J Tissue Eng Regen Med 2016:In Press.

[199] Murphy CM, O'Brien FJ. Understanding the effect of mean pore size on cell activity in collagen-glycosaminoglycan scaffolds. Cell Adh Migr 2010;4:377-381.

[200] Torbet J, Ronziere MC. Magnetic alignment of collagen during self-assembly. Biochem J 1984;219:1057-1059.

[201] Worcester DL. Structural origins of diamagnetic anisotropy in proteins. Proc Natl Acad Sci U S A 1978;75:5475-5477.

[202] Torbet J, Malbouyres M, Builles N, Justin V, Roulet M, Damour O, et al. Orthogonal scaffold of magnetically aligned collagen lamellae for corneal stroma reconstruction. Biomaterials 2007;28:4268-4276.

[203] Novak T, Voytik-Harbin SL, Neu CP. Cell encapsulation in a magnetically aligned collagen-GAG copolymer microenvironment. Acta Biomater 2015;11:274-282.

[204] Eguchi Y, Ogiue-Ikeda M, Ueno S. Control of orientation of rat Schwann cells using an 8-T static magnetic field. Neurosci Lett 2003;351:130-132.

[205] Ceballos D, Navarro X, Dubey N, Wendelschafer-Crabb G, Kennedy WR, Tranquillo RT. Magnetically aligned collagen gel filling a collagen nerve guide improves peripheral nerve regeneration. Exp Neurol 1999;158:290-300.

[206] Yang Y, Ahearne M, Wimpenny I, Torbet J. Monitoring the effect of magnetically aligned collagen scaffolds on tendon tissue engineering by PSOCT. SPIE BiOS: Biomedical Optics: International Society for Optics and Photonics; 2009. p. 717903-717903-717907.

[207] Guo C, Kaufman LJ. Flow and magnetic field induced collagen alignment. Biomaterials 2007;28:1105-1114.

[208] Xu B, Chow MJ, Zhang Y. Experimental and modeling study of collagen scaffolds with the effects of crosslinking and fiber alignment. Int J Biomater 2011;2011:172389.

[209] Tang MD, Golden AP, Tien J. Fabrication of collagen gels that contain patterned, micrometer-scale cavities. Adv Mater 2004;16:1345-1348.

[210] Vernon RB, Gooden MD, Lara SL, Wight TN. Native fibrillar collagen membranes of micron-scale and submicron thicknesses for cell support and perfusion. Biomaterials 2005;26:1109-1117.

[211] Nelson CM, Inman JL, Bissell MJ. Three-dimensional lithographically defined organotypic tissue arrays for quantitative analysis of morphogenesis and neoplastic progression. Nat Protocs 2008;3:674-678.

[212] Mosser G, Anglo A, Helary C, Bouligand Y, Giraud-Guille MM. Dense tissue-like collagen matrices formed in cell-free conditions. Matrix Biol 2006;25:3-13.

[213] Kirkwood JE, Fuller GG. Liquid crystalline collagen: A self-assembled morphology for the orientation of mammalian cells. Langmuir 2009;25:3200-3206.

[214] Saeidi N, Sander EA, Ruberti JW. Dynamic shear-influenced collagen self-assembly. Biomaterials 2009;30:6581-6592.

[215] Saeidi N, Sander EA, Zareian R, Ruberti JW. Production of highly aligned collagen lamellae by combining shear force and thin film confinement. Acta Biomater 2011;7:2437-2447.

[216] Muthusubramaniam L, Peng L, Zaitseva T, Paukshto M, Martin GR, Desai TA. Collagen fibril diameter and alignment promote the quiescent keratocyte phenotype. J Biomed Mater Res A 2012;100:613-621.

[217] Liu Y, Ren L, Yao H, Wang YJ. Collagen films with suitable physical properties and biocompatibility for corneal tissue engineering prepared by ion leaching technique. Mater Lett 2012;87:1-4.

[218] Liu Y, Ren L, Wang Y. Crosslinked collagen-gelatin-hyaluronic acid biomimetic film for cornea tissue engineering applications. Mater Sci Eng C 2013;33:196-201.

[219] Crabb RA, Chau EP, Evans MC, Barocas VH, Hubel A. Biomechanical and microstructural characteristics of a collagen film-based corneal stroma equivalent. Tissue Eng 2006;12:1565-1575.

[220] Huang CJ, Chien YL, Ling TY, Cho HC, Yu J, Chang YC. The influence of collagen film nanostructure on pulmonary stem cells and collagen-stromal cell interactions. Biomaterials 2010;31:8271-8280.

[221] Yao L, de Ruiter GC, Wang H, Knight AM, Spinner RJ, Yaszemski MJ, et al. Controlling dispersion of axonal regeneration using a multichannel collagen nerve conduit. Biomaterials 2010;31:5789-5797.

[222] Li ST, Archibald SJ, Krarup C, Madison RD. Peripheral nerve repair with collagen conduits. Clin Mater 1992;9:195-200.

[223] Lundborg G. A 25-year perspective of peripheral nerve surgery: Evolving neuroscientific concepts and clinical significance. J Hand Surg Am 2000;25:391-414.

[224] Daly W, Yao L, Zeugolis D, Windebank A, Pandit A. A biomaterials approach to peripheral nerve regeneration: Bridging the peripheral nerve gap and enhancing functional recovery. J R Soc Interface 2012;9:202-221.

[225] de Ruiter GC, Malessy MJ, Yaszemski MJ, Windebank AJ, Spinner RJ. Designing ideal conduits for peripheral nerve repair. Neurosurg Focus 2009;26:E5.

[226] Kajahn J, Franz S, Rueckert E, Forstreuter I, Hintze V, Moeller S, et al. Artificial extracellular matrices composed of collagen I and high sulfated hyaluronan

modulate monocyte to macrophage differentiation under conditions of sterile inflammation. Biomatter 2012;2:226-w236.

[227] Velard F, Laurent-Maquin D, Braux J, Guillaume C, Bouthors S, Jallot E, et al. The effect of zinc on hydroxyapatite-mediated activation of human polymorphonuclear neutrophils and bone implant-associated acute inflammation. Biomaterials 2010;31:2001-2009.

[228] Bryan N, Ashwin H, Smart N, Bayon Y, Scarborough N, Hunt JA. The innate oxygen dependant immune pathway as a sensitive parameter to predict the performance of biological graft materials. Biomaterials 2012;33:6380-6392.

[229] Sprague L, Muccioli M, Pate M, Meles E, McGinty J, Nandigam H, et al. The interplay between surfaces and soluble factors define the immunologic and angiogenic properties of myeloid dendritic cells. BMC Immunol 2011;12:35.

[230] Brown BN, Ratner BD, Goodman SB, Amar S, Badylak SF. Macrophage polarization: An opportunity for improved outcomes in biomaterials and regenerative medicine. Biomaterials 2012;33:3792-3802.

[231] Ren JD, Fan L, Tian FZ, Fan KH, Yu BT, Jin WH, et al. Involvement of a membrane potassium channel in heparan sulphate-induced activation of macrophages. Immunology 2014;141:345-352.

[232] Heil TL, Volkmann KR, Wataha JC, Lockwood PE. Human peripheral blood monocytes versus THP-1 monocytes for in vitro biocompatibility testing of dental material components. J Oral Rehabil 2002;29:401-407.

[233] Qin Z. The use of THP-1 cells as a model for mimicking the function and regulation of monocytes and macrophages in the vasculature. Atherosclerosis 2012;221:2-11.

[234] Pan C, Kumar C, Bohl S, Klingmueller U, Mann M. Comparative proteomic phenotyping of cell lines and primary cells to assess preservation of cell type-specific functions. Mol Cell Proteomics 2009;8:443-450.

[235] Kwon J, Kim J, Park S, Khang G, Kang PM, Lee D. Inflammation-responsive antioxidant nanoparticles based on a polymeric prodrug of vanillin. Biomacromolecules 2013;14:1618-1626.

[236] Umashankar PR, Mohanan PV, Kumari TV. Glutaraldehyde treatment elicits toxic response compared to decellularization in bovine pericardium. Toxicol Int 2012;19:51-58.

[237] McWhorter FY, Wang T, Nguyen P, Chung T, Liu WF. Modulation of macrophage phenotype by cell shape. Proc Natl Acad Sci U S A 2013;110:17253-17258.

[238] Bayrak A, Tyralla M, Ladhoff J, Schleicher M, Stock UA, Volk HD, et al. Human immune responses to porcine xenogeneic matrices and their extracellular matrix constituents in vitro. Biomaterials 2010;31:3793-3803.

[239] Yahyouche A, Zhidao X, Czernuszka JT, Clover AJ. Macrophage-mediated degradation of crosslinked collagen scaffolds. Acta Biomater 2011;7:278-286.

[240] Sandor M, Xu H, Connor J, Lombardi J, Harper JR, Silverman RP, et al. Host response to implanted porcine-derived biologic materials in a primate model of abdominal wall repair. Tissue Eng Part A 2008;14:2021-2031.

[241] Ashwin H, Hunt J, Mausy E, Migliozzi J, Beers D, Wohlert S. Influence of varying HMDI crosslinking parameters on porcine dermis. In TCES meeting. Eur Cell Mater 2012;23:64.

[242] Grotenhuis N, Bayon Y, Lange JF, Van Osch GJ, Bastiaansen-Jenniskens YM. A culture model to analyze the acute biomaterial-dependent reaction of human primary macrophages. Biochem Biophys Res Commun 2013;433:115-120.

[243] Orenstein SB, Qiao Y, Klueh U, Kreutzer DL, Novitsky YW. Activation of human mononuclear cells by porcine biologic meshes in vitro. Hernia 2010;14:401-407.

[244] Pandit A, Ashar R, Feldman D, Thompson A. Investigation of acidic fibroblast growth factor delivered through a collagen scaffold for the treatment of full-thickness skin defects in a rabbit model. Plast Reconstr Surg 1998;101:766-775.

[245] Dong Y, Hassan WU, Kennedy R, Greiser U, Pandit A, Garcia Y, et al. Performance of an in situ formed bioactive hydrogel dressing from a PEG-based hyperbranched multifunctional copolymer. Acta Biomater 2014;10:2076-2085.

[246] Lee AR. Enhancing dermal matrix regeneration and biomechanical properties of 2nd degree-burn wounds by EGF-impregnated collagen sponge dressing. Arch Pharm Res 2005;28:1311-1316.

[247] Hong SJ, Jia SX, Xie P, Xu W, Leung KP, Mustoe TA, et al. Topically delivered adipose derived stem cells show an activated-fibroblast phenotype and enhance granulation tissue formation in skin wounds. PLoS One 2013;8:e55640.

[248] Badylak SF, Valentin JE, Ravindra AK, McCabe GP, Stewart-Akers AM. Macrophage phenotype as a determinant of biologic scaffold remodeling. Tissue Eng Part A 2008;14:1835-1842.

[249] Deeken CR, Melman L, Jenkins ED, Greco SC, Frisella MM, Matthews BD. Histologic and biomechanical evaluation of crosslinked and non-crosslinked biologic meshes in a porcine model of ventral incisional hernia repair. J Am Coll Surg 2011;212:880-888.

[250] Ye Q, van Amerongen MJ, Sandham JA, Bank RA, van Luyn MJ, Harmsen MC. Site-specific tissue inhibitor of metalloproteinase-1 governs the matrix metalloproteinases-dependent degradation of crosslinked collagen scaffolds and is correlated with interleukin-10. J Tissue Eng Regen Med 2011;5:264-274.

[251] Burugapalli K, Pandit A. Characterization of tissue response and in vivo degradation of cholecyst-derived extracellular matrix. Biomacromolecules 2007;8:3439-3451.

[252] Umashankar PR, Arun T, Kumary TV. Effect of chronic inflammation and immune response on regeneration induced by decellularized bovine pericardium. J Biomed Mater Res A 2013;101:2202-2209.

[253] Broderick G, McIntyre J, Noury M, Strom HM, Psoinos C, Christakas A, et al. Dermal collagen matrices for ventral hernia repair: Comparative analysis in a rat model. Hernia 2012;16:333-343.

[254] Bellon JM, Rodriguez M, Gomez-Gil V, Sotomayor S, Bujan J, Pascual G. Postimplant intraperitoneal behavior of collagen-based meshes followed by laparoscopy. Surg Endosc 2012;26:27-35.

[255] Pascual G, Rodriguez M, Sotomayor S, Moraleda E, Bellon JM. Effects of collagen prosthesis cross-linking on long-term tissue regeneration following the repair of an abdominal wall defect. Wound Repair Regen 2012;20:402-413.

[256] Melman L, Jenkins ED, Hamilton NA, Bender LC, Brodt MD, Deeken CR, et al. Early biocompatibility of crosslinked and non-crosslinked biologic meshes in a porcine model of ventral hernia repair. Hernia 2011;15:157-164.

[257] Connor J, McQuillan D, Sandor M, Wan H, Lombardi J, Bachrach N, et al. Retention of structural and biochemical integrity in a biological mesh supports tissue remodeling in a primate abdominal wall model. Regen Med 2009;4:185-195.

[258] Bryan N, Ahswin H, Smart N, Bayon Y, Wohlert S, Hunt JA. The in vivo evaluation of tissue-based biomaterials in a rat full-thickness abdominal wall defect model. J Biomed Mater Res B Appl Biomater 2014;102:709-720.

[259] Bryan N, Ashwin H, Smart NJ, Wohlert S, Bayon Y, Hunt JA. Characterisation and comparison of the host response of 6 tissue-based surgical implants in a subcutaneous in vivo rat model. J Appl Biomater Funct Mater 2014;18:35-42.

[260] Harth KC, Rosen MJ. Major complications associated with xenograft biologic mesh implantation in abdominal wall reconstruction. Surg Innov 2009;16:324-329.

[261] Smart NJ, Marshall M, Daniels IR. Biological meshes: A review of their use in abdominal wall hernia repairs. Surgeon 2012;10:159-171.

[262] Shah BC, Tiwari MM, Goede MR, Eichler MJ, Hollins RR, McBride CL, et al. Not all biologics are equal! Hernia 2011;15:165-171.

[263] Badylak S, Kokini K, Tullius B, Simmons-Byrd A, Morff R. Morphologic study of small intestinal submucosa as a body wall repair device. J Surg Res 2002;103:190-202.

[264] Pilipchuk SP, Vaicik MK, Larson JC, Gazyakan E, Cheng MH, Brey EM. Influence of crosslinking on the stiffness and degradation of dermis-derived hydrogels. J Biomed Mater Res A 2013;101:2883-2895.

[265] Saito H, Murabayashi S, Mitamura Y, Taguchi T. Characterization of alkali-treated collagen gels prepared by different crosslinkers. J Mater Sci Mater Med 2008;19:1297-1305.

[266] O'Brien JA, Ignotz R, Montilla R, Broderick GB, Christakis A, Dunn RM. Long-term histologic and mechanical results of a Permacol abdominal wall explant. Hernia 2011;15:211-215.

[267] Hsu PW, Salgado CJ, Kent K, Finnegan M, Pello M, Simons R, et al. Evaluation of porcine dermal collagen (Permacol) used in abdominal wall reconstruction. J Plast Reconstr Aesthet Surg 2009;62:1484-1489.

[268] Parker DM, Armstrong PJ, Frizzi JD, North JH, Jr. Porcine dermal collagen (Permacol) for abdominal wall reconstruction. Curr Surg 2006;63:255-258.

[269] van Wachem PB, van Luyn MJ, Olde Damink LH, Dijkstra PJ, Feijen J, Nieuwenhuis P. Biocompatibility and tissue regenerating capacity of crosslinked dermal sheep collagen. J Biomed Mater Res 1994;28:353-363.

[270] Boekema BK, Vlig M, Olde Damink L, Middelkoop E, Eummelen L, Buhren AV, et al. Effect of pore size and cross-linking of a novel collagen-elastin dermal substitute on wound healing. J Mater Sci Mater Med 2014;25:423-433.

[271] Daly WT, Yao L, Abu-rub MT, O'Connell C, Zeugolis DI, Windebank AJ, et al. The effect of intraluminal contact mediated guidance signals on axonal mismatch during peripheral nerve repair. Biomaterials 2012;33:6660-6671.

[272] Yao L, Daly W, Newland B, Yao S, Wang W, Chen BK, et al. Improved axonal regeneration of transected spinal cord mediated by multichannel collagen conduits functionalized with neurotrophin-3 gene. Gene Ther 2013;20:1149-1157.

[273] Bozkurt A, Lassner F, O'Dey D, Deumens R, Bocker A, Schwendt T, et al. The role of microstructured and interconnected pore channels in a collagen-based nerve guide on axonal regeneration in peripheral nerves. Biomaterials 2012;33:1363-1375.

[274] Liang HC, Chang Y, Hsu CK, Lee MH, Sung HW. Effects of crosslinking degree of an acellular biological tissue on its tissue regeneration pattern. Biomaterials 2004;25:3541-3552.

[275] Chang Y, Tsai CC, Liang HC, Sung HW. In vivo evaluation of cellular and acellular bovine pericardia fixed with a naturally occurring crosslinking agent (genipin). Biomaterials 2002;23:2447-2457.

[276] Gaertner WB, Bonsack ME, Delaney JP. Experimental evaluation of four biologic prostheses for ventral hernia repair. J Gastrointest Surg 2007;11:1275-1285.

[277] Tal H, Kozlovsky A, Artzi Z, Nemcovsky CE, Moses O. Long-term bio-degradation of cross-linked and non-cross-linked collagen barriers in human guided bone regeneration. Clin Oral Implants Res 2008;19:295-302.

[278] Rothamel D, Schwarz F, Sager M, Herten M, Sculean A, Becker J. Biodegradation of differently cross-linked collagen membranes: An experimental study in the rat. Clin Oral Implants Res 2005;16:369-378.

[279] Badhe SP, Lawrence TM, Smith FD, Lunn PG. An assessment of porcine dermal xenograft as an augmentation graft in the treatment of extensive rotator cuff tears. J Shoulder Elbow Surg 2008;17:35S-39S.

[280] Soler JA, Gidwani S, Curtis MJ. Early complications from the use of porcine dermal collagen implants (Permacol) as bridging constructs in the repair of massive rotator cuff tears. A report of 4 cases. Acta Orthop Belg 2007;73:432-436.

[281] Chavarriaga LF, Lin E, Losken A, Cook MW, Jeansonne LO, White BC, et al. Management of complex abdominal wall defects using acellular porcine dermal collagen. Am Surg 2010;76:96-100.

[282] Madden LR, Mortisen DJ, Sussman EM, Dupras SK, Fugate JA, Cuy JL, et al. Proangiogenic scaffolds as functional templates for cardiac tissue engineering. Proc Natl Acad Sci U S A 2010;107:15211-15216.

[283] Báez J, Olsen D, Polarek JW. Recombinant microbial systems for the production of human collagen and gelatin. Appl Microbiol Biotechnol 2005;69:245-252.

[284] Stassen FL, Cardinale GJ, Udenfriend S. Activation of prolyl hydroxylase in L-929 fibroblasts by ascorbic acid. Proc Natl Acad Sci U S A 1973;70:1090-1093.

[285] Sullivan TA, Uschmann B, Hough R, Leboy PS. Ascorbate modulation of chondrocyte gene expression is independent of its role in collagen secretion. J Biol Chem 1994;269:22500-22506.

[286] Canalis E. Effect of insulinlike growth factor I on DNA and protein synthesis in cultured rat calvaria. J Clin Invest 1980;66:709-719.

[287] Fine A, Goldstein RH. The effect of transforming growth factor-beta on cell proliferation and collagen formation by lung fibroblasts. J Biol Chem 1987;262:3897-3902.

[288] Thornton FJ, Schäffer MR, Witte MB, Moldawer LL, MacKay SL, Abouhamze A, et al. Enhanced collagen accumulation following direct transfection of the inducible nitric oxide synthase gene in cutaneous wounds. Biochem Biophys Res Commun 1998;246:654-659.

[289] Falanga V, Zhou L, Yufit T. Low oxygen tension stimulates collagen synthesis and COL1A1 transcription through the action of TGF-beta1. J Cell Physiol 2002;191:42-50.

[290] Aro E, Khatri R, Gerard-O'Riley R, Mangiavini L, Myllyharju J, Schipani E. Hypoxia-inducible factor-1 (HIF-1) but not HIF-2 is essential for hypoxic induction of collagen prolyl 4-hydroxylases in primary newborn mouse epiphyseal growth plate chondrocytes. J Biol Chem 2012;287:37134-37144.

[291] Kumar P, Satyam A, Fan X, Collin E, Rochev Y, Rodriguez BJ, et al. Macromolecularly crowded in vitro microenvironments accelerate the production of extracellular matrix-rich supramolecular assemblies. Sci Rep 2015;5:8729.

[292] Satyam A, Kumar P, Fan X, Gorelov A, Rochev Y, Joshi L, et al. Macromolecular crowding meets tissue engineering by self-assembly: A paradigm shift in regenerative medicine. Adv Mater 2014;26:3024-3034.

[293] Kumar P, Satyam A, Cigognini D, Pandit A, Zeugolis DI. Low oxygen tension and macromolecular crowding accelerate extracellular matrix deposition in human corneal fibroblast culture. J Tissue Eng Regen Med 2016:In Press.

[294] Satyam A, Kumar P, Cigognini D, Pandit A, Zeugolis DI. Low, but not too low, oxygen tension and macromolecular crowding accelerate extracellular matrix deposition in human dermal fibroblast culture. Acta Biomater 2016;44:221-231.

[295] Olsen D, Yang C, Bodo M, Chang R, Leigh S, Baez J, et al. Recombinant collagen and gelatin for drug delivery. Adv Drug Deliv Rev 2003;55:1547-1567.

[296] Tang Y, Yang X, Hang B, Li J, Huang L, Huang F, et al. Efficient production of hydroxylated human-like collagen via the co-expression of three key genes in escherichia coli origami (DE3). Appl Biochem Biotechnol 2016;178:1458-1470.

[297] Vuorela A, Myllyharju J, Nissi R, Pihlajaniemi T, Kivirikko KI. Assembly of human prolyl 4-hydroxylase and type III collagen in the yeast pichia pastoris: Formation of a stable enzyme tetramer requires coexpression with collagen and assembly of a stable collagen requires coexpression with prolyl 4-hydroxylase. EMBO J 1997;16:6702-3712.

[298] Ruggiero F, Koch M. Making recombinant extracellular matrix proteins. Methods 2008;45:75-85.

[299] Majsterek I, McAdams E, Adachi E, Dhume ST, Fertala A. Prospects and limitations of the rational engineering of fibrillar collagens. Protein Sci 2003;12:2063-2072.

[300] Zhang C, Baez J, Pappu KM, Glatz CE. Purification and characterization of a transgenic corn grain-derived recombinant collagen type I alpha 1. Biotechnol Prog 2009;25:1660-1668.

[301] Stein H, Wilensky M, Tsafrir Y, Rosenthal M, Amir R, Avraham T, et al. Production of bioactive, post-translationally modified, heterotrimeric, human recombinant type-I collagen in transgenic tobacco. Biomacromolecules 2009;10:2640-2645.

[302] Cliche S, Amiot J, Avezard C, Gariepy C. Extraction and characterization of collagen with or without telopeptides from chicken skin. Poult Sci 2003;82:503-509.

[303] Pacak CA, Powers JM, Cowan DB. Ultrarapid purification of collagen type i for tissue engineering applications. Tissue Eng Part C Methods 2011;17:879-885.

[304] Rubin AL, Pfahl D, Speakman PT, Davison PF, Schmitt FO. Tropocollagen: Significance of protease-induced alterations. Science 1963;139:37-39.

[305] Kuznetsova N, Leikin S. Does the triple helical domain of type I collagen encode molecular recognition and fiber assembly while telopeptides serve as catalytic domains? Effect of proteolytic cleavage on fibrillogenesis and on collagen-collagen interaction in fibers. J Biol Chem 1999;274:36083-36088.

[306] Lynn AK, Yannas IV, Bonfield W. Antigenicity and immunogenicity of collagen. J Biomed Mater Res B Appl Biomater 2004;71:343-354.

[307] Forest P, Morfin F, Bergeron E, Dore J, Bensa S, Wittmann C, et al. Validation of a viral and bacterial inactivation step during the extraction and purification process of porcine collagen. Biomed Mater Eng 2007;17:199-208.

[308] Whitaker J, Feeney R. Chemical and physical modification of proteins by the hydroxide ion. Crit Rev Food Sci Nutr 1983;19:173-212.

[309] Bailey AJ, Light ND, Atkins ED. Chemical cross-linking restrictions on models for the molecular organization of the collagen fibre. Nature 1980;288:408-410.

[310] Delgado L, Bayon Y, Pandit A, Zeugolis DI. To cross-link or not to cross-link? Cross-linking associated foreign body response of collagen-based devices. Tissue Eng Part B Rev 2014;21:298-313.

[311] Manschot JFM, Brakkee AJM. The measurement and modelling of the mechanical properties of human skin in vivo—I. The measurement. J Biomech 1986;19:511-515.

[312] Agache PG, Monneur C, Leveque JL, De Rigal J. Mechanical properties and young's modulus of human skin in vivo. Arch Dermatol Res 1980;269:221-232.

[313] Annaidh AN, Ottenio M, Bruyère K, Destrade M, Gilchrist MD. Mechanical properties of excised human skin. In: Lim CT, Goh JCH, editors. 6th World Congress of Biomechanics (WCB 2010) August 1-6, 2010 Singapore: Springer Berlin Heidelberg; 2010. p. 1000-1003.

[314] Edsberg LE, Mates RE, Baier RE, Lauren M. Mechanical characteristics of human skin subjected to static versus cyclic normal pressures. J Rehabil Res Dev 1999;36:133-141.

[315] Lomas AJ, Ryan CN, Sorushanova A, Shologu N, Sideri AI, Tsioli V, et al. The past, present and future in scaffold-based tendon treatments. Adv Drug Deliv Rev 2014;84:257-277.

[316] Lewis G, Shaw KM. Tensile properties of human tendo Achillis: Effect of donor age and strain rate. J Foot Ankle Surg 1997;36:435-445.

[317] Couppe C, Suetta C, Kongsgaard M, Justesen L, Hvid LG, Aagaard P, et al. The effects of immobilization on the mechanical properties of the patellar tendon in younger and older men. Clin Biomech 2012;27:949-954.

[318] Jayasuriya AC, Ghosh S, Scheinbeim JI, Lubkin V, Bennett G, Kramer P. A study of piezoelectric and mechanical anisotropies of the human cornea. Biosens Bioelectron 2003;18:381-387.

[319] Wollensak G, Spoerl E, Seiler T. Stress-strain measurements of human and porcine corneas after riboflavin–ultraviolet-A-induced cross-linking. J Cataract Refractive Surg 2003;29:1780-1785.

[320] Elsheikh A, Anderson K. Comparative study of corneal strip extensometry and inflation tests. J R Soc Interface 2005;2:177-185.

[321] Athanasiou KA, Rosenwasser MP, Buckwalter JA, Malinin TI, Mow VC. Interspecies comparisons of in situ intrinsic mechanical properties of distal femoral cartilage. J Orthop Res 1991;9:330-340.

[322] Roberts CR, Rains JK, Paré PD, Walker DC, Wiggs B, Bert JL. Ultrastructure and tensile properties of human tracheal cartilage. J Biomech 1997;31:81-86.

[323] Calderon L, Collin E, Velasco-Bayon D, Murphy M, O'Halloran D, Pandit A. Type II collagen-hyaluronan hydrogel--a step towards a scaffold for intervertebral disc tissue engineering. Eur Cell Mater 2010;20:134-148.

[324] O Halloran DM, Collighan RJ, Griffin M, Pandit AS. Characterization of a microbial transglutaminase cross-linked type II collagen scaffold. Tissue Eng 2006;12:1467-1474.

[325] Helary C, Bataille I, Abed A, Illoul C, Anglo A, Louedec L, et al. Concentrated collagen hydrogels as dermal substitutes. Biomaterials 2010;31:481-490.

[326] Dewavrin JY, Hamzavi N, Shim VP, Raghunath M. Tuning the architecture of three-dimensional collagen hydrogels by physiological macromolecular crowding. Acta Biomater 2014;10:4351-4359.

[327] Madhavan K, Belchenko D, Motta A, Tan W. Evaluation of composition and crosslinking effects on collagen-based composite constructs. Acta Biomater 2010;6:1413-1422.

[328] Chen S, Hirota N, Okuda M, Takeguchi M, Kobayashi H, Hanagata N, et al. Microstructures and rheological properties of tilapia fish-scale collagen hydrogels with aligned fibrils fabricated under magnetic fields. Acta Biomater 2011;7:644-652.

[329] Nomura Y, Toki S, Ishii Y, Shirai K. Effect of transglutaminase on reconstruction and physicochemical properties of collagen gel from shark type I collagen. Biomacromolecules 2001;2:105-110.

[330] Fortunati D, Chau DY, Wang Z, Collighan RJ, Griffin M. Cross-linking of collagen I by tissue transglutaminase provides a promising biomaterial for promoting bone healing. Amino Acids 2014;46:1751-1761.

[331] Zeugolis DI, Paul RG, Attenburrow G. The influence of a natural cross-linking agent (Myrica rubra) on the properties of extruded collagen fibres for tissue engineering applications. Mater Sci Eng C Mater Biol Appl

2010;30:190-195.

[332] Shepherd JH, Ghose S, Kew SJ, Moavenian A, Best SM, Cameron RE. Effect of fiber crosslinking on collagen-fiber reinforced collagen-chondroitin-6-sulfate materials for regenerating load-bearing soft tissues. J Biomed Mater Res A 2013;101:176-184.

[333] Cheng X, Gurkan UA, Dehen CJ, Tate MP, Hillhouse HW, Simpson GJ, et al. An electrochemical fabrication process for the assembly of anisotropically oriented collagen bundles. Biomaterials 2008;29:3278-3288.

[334] Uquillas JA, Kishore V, Akkus O. Genipin crosslinking elevates the strength of electrochemically aligned collagen to the level of tendons. J Mech Behav Biomed Mater 2012;15:176-189.

[335] Kumar VA, Caves JM, Haller CA, Dai E, Li L, Grainger S, et al. Collagen-based substrates with tunable strength for soft tissue engineering. Biomater Sci 2013;1:1193-1202.

[336] Koide T, Daito M. Effects of various collagen crosslinking techniques on mechanical properties of collagen film. Dent Mater J 1997;16:1-9.

[337] Grover CN, Gwynne JH, Pugh N, Hamaia S, Farndale RW, Best SM, et al. Crosslinking and composition influence the surface properties, mechanical stiffness and cell reactivity of collagen-based films. Acta Biomater 2012;8:3080-3090.

[338] Olde Damink LH, Dijkstra PJ, van Luyn MJ, van Wachem PB, Nieuwenhuis P, Feijen J. Cross-linking of dermal sheep collagen using a water-soluble carbodiimide. Biomaterials 1996;17:765-773.

[339] Gorham SD. Collagen. In: Byrom D, editor. Biomaterials Novel materials from biological sources. New York: Macmillan Publishers Ltd and ICI Biological Products Business; 1991. p. 55-122.

[340] Hey KB, Lachs CM, Raxworthy MJ, Wood EJ. Crosslinked fibrous collagen for use as a dermal implant: Control of the cytotoxic effects of glutaraldehyde and dimethylsuberimidate. Biotechnol Appl Biochem 1990;12:85-93.

[341] Chapman JA, Tzaphlidou M, Meek KM, Kadler KE. The collagen fibril--a model system for studying the staining and fixation of a protein. Electron Microsc Rev 1990;3:143-182.

[342] Lee CR, Grodzinsky AJ, Spector M. The effects of cross-linking of collagen-glycosaminoglycan scaffolds on compressive stiffness, chondrocyte-mediated contraction, proliferation and biosynthesis. Biomaterials 2001;22:3145-3154.

[343] Damink LHHO, Dijkstra PJ, van Luyn MJA, van Wachem PB, Nieuwenhuis P, Feijen J. Crosslinking of dermal sheep collagen using hexamethylene diisocyanate. J Mater Sci Mater Med 1995;6:429-434.

[344] van Luyn MJA, van Wachem PB, Damink LHHO, Dijkstra PJ, Feijen J, Nieuwenhuis P. Secondary cytotoxicity of cross-linked dermal sheep collagens during repeated exposure to human fibroblasts. Biomaterials 1992;13:1017-1024.

[345] Panza JL, Wagner WR, Rilo HL, Rao RH, Beckman EJ, Russell AJ. Treatment of rat pancreatic islets with reactive PEG. Biomaterials 2000;21:1155-1164.

[346] Deible CR, Petrosko P, Johnson PC, Beckman EJ, Russell AJ, Wagner WR. Molecular barriers to biomaterial thrombosis by modification of surface proteins with polyethylene glycol. Biomaterials 1998;19:1885-1893.

[347] Petite H, Duval JL, Frei V, Abdul-Malak N, Sigot-Luizard MF, Herbage D. Cytocompatibility of calf pericardium treated by glutaraldehyde and by the acyl azide methods in an organotypic culture model. Biomaterials 1995;16:1003-1008.

[348] Zahedi S, Bozon C, Brunel G. A 2-year clinical evaluation of a diphenylphosphorylazide-cross-linked collagen membrane for the treatment of buccal gingival recession. J Periodontol 1998;69:975-981.

[349] Chevallay B, Abdul_Malak N, Herbage D. Mouse fibroblasts in long-term culture within collagen three-dimensional scaffolds: Influence of crosslinking with

diphenylphosphorylazide on matrix reorganization, growth, and biosynthetic and proteolytic activities. J Biomed Mater Res A 2000;49:448-459.

[350] Roche S, Ronziere M-C, Herbage D, Freyria A-M. Native and DPPA cross-linked collagen sponges seeded with fetal bovine epiphyseal chondrocytes used for cartilage tissue engineering. Biomaterials 2001;22:9-18.

[351] Marinucci L, Lilli C, Guerra M, Belcastro S, Becchetti E, Stabellini G, et al. Biocompatibility of collagen membranes crosslinked with glutaraldehyde or diphenylphosphoryl azide: An in vitro study. J Biomed Mater Res A 2003;67:504-509.

[352] Jorge-Herrero E, Fernandez P, Turnay J, Olmo N, Calero P, Garcia R, et al. Influence of different chemical cross-linking treatments on the properties of bovine pericardium and collagen. Biomaterials 1999;20:539-545.

[353] Girardot JM, Girardot MN. Amide cross-linking: An alternative to glutaraldehyde fixation. J Heart Valve Dis 1996;5:518-525.

[354] Pieper JS, Hafmans T, Veerkamp JH, van Kuppevelt TH. Development of tailor-made collagen-glycosaminoglycan matrices: EDC/NHS crosslinking, and ultrastructural aspects. Biomaterials 2000;21:581-593.

[355] Powell HM, Boyce ST. EDC cross-linking improves skin substitute strength and stability. Biomaterials 2006;27:5821-5827.

[356] Sung HW, Chang WH, Ma CY, Lee MH. Crosslinking of biological tissues using genipin and/or carbodiimide. J Biomed Mater Res A 2003;64:427-438.

[357] Barnes CP, Pemble CW, Brand DD, Simpson DG, Bowlin GL. Cross-linking electrospun type II collagen tissue engineering scaffolds with carbodiimide in ethanol. Tissue Eng 2007;13:1593-1605.

[358] Vasudev SC, Chandy T. Effect of alternative crosslinking techniques on the enzymatic degradation of bovine pericardia and their calcification. J Biomed Mater Res 1997;35:357-369.

[359] McPherson JM, Sawamura S, Armstrong R. An examination of the biologic response to injectable, glutaraldehyde cross-linked collagen implants. J Biomed Mater Res 1986;20:93-107.

[360] Cherfan D, Verter EE, Melki S, Gisel TE, Doyle FJ, Jr., Scarcelli G, et al. Collagen cross-linking using rose bengal and green light to increase corneal stiffness. Invest Ophthalmol Vis Sci 2013;54:3426-3433.

[361] Ibusuki S, Halbesma GJ, Randolph MA, Redmond RW, Kochevar IE, Gill TJ. Photochemically cross-linked collagen gels as three-dimensional scaffolds for tissue engineering. Tissue Eng 2007;13:1995-2001.

[362] Roy R, Boskey A, Bonassar LJ. Processing of type I collagen gels using nonenzymatic glycation. J Biomed Mater Res A 2010;93:843-851.

[363] Mentink CJ, Hendriks M, Levels AA, Wolffenbuttel BH. Glucose-mediated cross-linking of collagen in rat tendon and skin. Clin Chim Acta 2002;321:69-76.

[364] Huang LL, Sung HW, Tsai CC, Huang DM. Biocompatibility study of a biological tissue fixed with a naturally occurring crosslinking reagent. J Biomed Mater Res 1998;42:568-576.

[365] Sung HW, Chang Y, Chiu CT, Chen CN, Liang HC. Mechanical properties of a porcine aortic valve fixed with a naturally occurring crosslinking agent. Biomaterials 1999;20:1759-1772.

[366] Antunes APM, Attenburrow G, Covington AD, Ding J. Utilisation of oleuropein as a crosslinking agent in collagenic films. J Leather Sci 2008;2:1-12.

[367] Collin EC, Grad S, Zeugolis DI, Vinatier CS, Clouet JR, Guicheux JJ, et al. An injectable vehicle for nucleus pulposus cell-based therapy. Biomaterials 2011;32:2862-2870.

[368] Cosgriff-Hernandez E, Hahn MS, Russell B, Wilems T, Munoz-Pinto D, Browning MB, et al. Bioactive hydrogels based on designer collagens. Acta Biomater 2010;6:3969-3977.

[369] Ward J, Kelly J, Wang W, Zeugolis DI, Pandit A. Amine functionalization of collagen matrices with multifunctional polyethylene glycol systems. Biomacromolecules 2010;11:3093-3101.

[370] Taguchi T, Xu L, Kobayashi H, Taniguchi A, Kataoka K, Tanaka J. Encapsulation of chondrocytes in injectable alkali-treated collagen gels prepared using poly(ethylene glycol)-based 4-armed star polymer. Biomaterials 2005;26:1247-1252.

[371] Matsumoto K, Nakamura T, Shimizu Y, Ueda H, Sekine T, Yamamoto Y, et al. A novel surgical material made from collagen with high mechanical strength: A collagen sandwich membrane. ASAIO J 1999;45:288-292.

[372] Cote MF, Doillon CJ. Wettability of cross-linked collagenous biomaterials: *In vitro* study. Biomaterials 1992;13:612-616.

[373] Koide M, Osaki K, Konishi J, Oyamada K, Katakura T, Takahashi A, et al. A new type of biomaterial for artificial skin: Dehydrothermally cross-linked composites of fibrillar and denatured collagens. J Biomed Mater Res 1993;27:79-87.

[374] Collins RL, Christiansen D, Zazanis GA, Silver FH. Use of collagen film as a dural substitute: Preliminary animal studies. J Biomed Mater Res 1991;25:267-276.

[375] Sionkowska A. Modification of collagen films by ultraviolet irradiation. Polym Degrad Stabil 2000;68:147-151.

[376] Sionkowska A, Wess T. Mechanical properties of UV irradiated rat tail tendon (RTT) collagen. Int J Biol Macromol 2004;34:9-12.

[377] Metreveli N, Namicheishvili L, Jariashvili K, Mrevlishvili G, Sionkowska A. Mechanisms of the influence of UV irradiation on collagen and collagen-ascorbic acid solutions. Int J Photoenergy 2006;2006:1-4.

[378] Vizarova K, Bakos D, Rehakova M, Macho V. Modification of layered atelocollagen by ultraviolet irradiation and chemical cross-linking: Structure stability and mechanical properties. Biomaterials 1994;15:1082-1086.

[379] Sionkowska A, Wess T. Mechanical properties of UV irradiated rat tail tendon (RTT) collagen. International Journal of Biological Macromolecules 2004;34:9-12.

[380] Paul RG, Bailey AJ. Chemical stabilisation of collagen as a biomimetic. Sci World J 2003;24:138-155.

[381] Bellincampi LD, Closkey RF, Prasad R, Zawadsky JP, Dunn MG. Viability of fibroblast-seeded ligament analogs after autogenous implantation. J Orthop Res 1998;16:414-420.

[382] Babin H, Dickinson E. Influence of transglutaminase treatment on the thermoreversible gelation of gelatin. Food Hydrocoll 2001;15:271-276.

[383] Raghunath M, Hennies HC, Velten F, Wiebe V, Steinert PM, Reis A, et al. A novel in situ method for the detection of deficient transglutaminase activity in the skin. Arch Dermatol Res 1998;290:621-627.

[384] Raghunath M, Cankay R, Kubitscheck U, Fauteck JD, Mayne R, Aeschlimann D, et al. Transglutaminase activity in the eye: Cross-linking in epithelia and connective tissue structures. Invest Ophthalmol Vis Sci 1999;40:2780-2787.

[385] Sakamoto H, Kumazawa Y, Motoki M. Strength of protein gels prepared with microbial transglutaminase as related to reaction conditions. J Food Science 1994;59:866-871.

[386] Fuchsbauer HL, Gerber U, Engelmann J, Seeger T, Sinks C, Hecht T. Influence of gelatin matrices cross-linked with transglutaminase on the properties of an enclosed bioactive material using beta-galactosidase as model system. Biomaterials 1996;17:1481-1488.

[387] Zeugolis DI, Panengad PP, Yew ES, Sheppard C, Phan TT, Raghunath M. An in situ and in vitro investigation for the transglutaminase potential in tissue engineering. J Biomed Mater Res A 2010;92:1310-1320.

[388] Lee PF, Bai Y, Smith RL, Bayless KJ, Yeh AT. Angiogenic responses are enhanced in mechanically and microscopically characterized, microbial transglutaminase crosslinked collagen matrices with increased stiffness. Acta Biomater 2013;9:7178-7190.

[389] Olde Damink L, Dijkstra P, Van Luyn M, PB VW, Nieuwenhuis P, Feijen J. Influence of ethylene oxide gas treatment on the in vitro degradation behavior of dermal sheep collagen. J Biomed Mater Res 1995;29:149-155.

[390] Vink P, Pleijsier K. Aeration of ethylene oxide sterilized polymers. Biomaterials 1986;7:225-230.

[391] Dziedzic-Goclawska A KA, Uhrynowska-Tyszkiewicx I, Michalik J, Stachowicz, W. Radiation sterilization of human tissue grafts. In: Trends in radiation sterilization of healthcare products: International Atomic Energy Agency; 2008.

[392] Jiang B, Wu Z, Zhao H, Tang F, Lu J, Wei Q, et al. Electron beam irradiation modification of collagen membrane. Biomaterials 2006;27:15-23.

[393] Bailey AJ, Rhodes DN, Cater CW. Irradiation-induced crosslinking of collagen. Radiation Res 1964;22:606-621.

[394] Sionkowska A. Thermal denaturation of UV-irradiated wet rat tail tendon collagen. Int J Biol Macromol 2005;35:145-149.

[395] Sionkowska A, Skopińska J, Wisniewski M. Photochemical stability of collagen/poly(vinyl alcohol) blends. Polym Degrad Stabil 2004;83:117-125.

[396] Sionkowska A. The influence of UV light on collagen/poly(ethylene glycol) blends. Polym Degrad Stabil 2006;91:305-312.

[397] Barth HD, Zimmermann EA, Schaible E, Tang SY, Alliston T, Ritchie RO. Characterization of the effects of x-ray irradiation on the hierarchical structure and mechanical properties of human cortical bone. Biomaterials 2011;32:8892-8904.

[398] Zahedi S, Legrand R, Brunel G, Albert A, Dewe W, Coumans B, et al. Evaluation of a diphenylphosphorylazide-crosslinked collagen membrane for guided bone regeneration in mandibular defects in rats. J Periodontol 1998;69:1238-1246.

[399] Freytes DO, Stoner RM, Badylak SF. Uniaxial and biaxial properties of terminally sterilized porcine urinary bladder matrix scaffolds. J Biomed Mater Res B Appl Biomater 2008;84B:408-414.

[400] Geutjes PJ, van der Vliet JA, Faraj KA, de Vries N, van Moerkerk HT, Wismans RG, et al. Preparation and characterization of injectable fibrillar type I collagen and evaluation for pseudoaneurysm treatment in a pig model. J Vasc Surg 2010;52:1330-1338.

[401] Noah E, Chen J, Jiao X, Heschel I, Pallua N. Impact of sterilization on the porous design and cell behavior in collagen sponges prepared for tissue engineering. Biomaterials 2002;23:2855-2861.

[402] Gouk SS, Lim TM, Teoh SH, Sun WQ. Alterations of human acellular tissue matrix by gamma irradiation: Histology, biomechanical property, stability, in vitro cell repopulation, and remodeling. J Biomed Mater Res B Appl Biomater 2008;84:205-217.

[403] Hara M, Koshimizu N, Yoshida M, Haug IJ, Ulset A-ST, Christensen BE. Cross-linking and depolymerisation of gamma-irradiated fish gelatin and porcine gelatin studied by SEC-MALLS and SDS-PAGE: A comparative study. J Biomater Sci Polym Ed 2010;21:877-892.

[404] Sun WQ, Leung P. Calorimetric study of extracellular tissue matrix degradation and instability after gamma irradiation. Acta Biomater 2008;4:817-826.

[405] Seto A, Gatt CJ, Dunn MG. Radioprotection of tendon tissue via crosslinking and free radical scavenging. Clin Orthop Relat Res 2008;466:1788-1795.

[406] Versen-Hoeynck Fv, Steinfeld AP, Becker J, Hermel M, Rath W, Hesselbarth U. Sterilization and preservation influence the biophysical properties of human amnion grafts. Biologicals 2008;36:248-255.

[407] Huang NF, Okogbaa J, Lee JC, Jha A, Zaitseva TS, Paukshto MV, et al. The modulation of endothelial cell morphology, function, and survival using anisotropic nanofibrillar collagen scaffolds. Biomaterials 2013:1-10.

[408] Sung HW, Hsu HL, Hsu CS. Effects of various chemical sterilization methods on the crosslinking and enzymatic degradation characteristics of an epoxy-fixed biological tissue. J Biomed Mater Res 1997;37:376-383.

[409] Ijiri S, Yamamuro T, Nakamura T, Kotani S, Notoya K. Effect of sterilization on bone morphogenetic protein. J Orthop Res 1994;12:628-636.

[410] Mendes GCC, Brandao TRS, Silva CLM. Ethylene oxide sterilization of medical devices: A review. Am J Infect Control 2007;35:574-581.

[411] Gorham SD. Collagen. In: Byrom D, editor. Biomaterials. New York: Stockton Press; 1991. p. 55-122.

[412] Mitchell E, Stawarz A, Kayacan R, Rimnac C. The effect of gamma radiation sterilization on the fatigue crack propagation resistance of human cortical bone. J Bone Joint Surg Am 2004;86:2648-2657.

[413] DeDeyne P, Haut R. Some effects of gamma irradiation on patellar tendon allografts. Connect Tissue Res 1991;27:51-62.

[414] Roe SC, Milthorpe BK, True K, Rogers GJ, Schindhelm K. The effect of gamma irradiation on a xenograft tendon bioprosthesis. Clin Mater 1992;9:149-154.

[415] Petrie TA, Raynor JE, Reyes CD, Burns KL, Collard DM, Garcia AJ. The effect of integrin-specific bioactive coatings on tissue healing and implant osseointegration. Biomaterials 2008;29:2849-2857.

[416] Nguyen H, Morgan DAF, Forwood MR. Sterilization of allograft bone: Effects of gamma irradiation on allograft biology and biomechanics. Cell Tissue Bank 2007;8:93-105.

[417] Hara M, Koshimizu N, Yoshida M, Haug I, Ulset A, Christensen B. Cross-linking and depolymerisation of gamma-irradiated fish gelatin and porcine gelatin studied by SEC-MALLS and SDS-PAGE: A comparative study. J Biomater Sci Polym Ed 2010;21:877-892.

[418] Cheung D, Perelman N, Tong D, Nimni M. The effect of gamma-irradiation on collagen molecules, isolated alpha-chains, and crosslinked native fibers. J Biomed Mater Res 1990;24:581-589.

[419] de Tayrac R, Letouzey V, Garreau H, Guiraud I, Vert M, Mares P. Tissue healing during degradation of a long-lasting bioresorbable gamma-ray-sterilised poly(lactic acid) mesh in the rat: A 12-month study. Eur Surg Res 2010;44:102-110.

[420] Faraj KA, Brouwer KM, Geutjes PJ, Versteeg EM, Wismans RG, Deprest JA, et al. The effect of ethylene oxide sterilisation, beta irradiation and gamma irradiation on collagen fibril-based scaffolds. J Tissue Eng Reg Med 2011;8:460-470.

[421] Aquino K. Sterilization by gamma irradiation. In: Gamma radiation.: Adrovic F (Ed. InTech); 2012.

[422] Goertzen MJ, Clahsen H, Burrig KF, Schulitz KP. Sterilisation of canine anterior cruciate allografts by gamma irradiation in argon. Mechanical and neurohistological properties retained one year after transplantation. J Bone Joint Surg Br 1995;77:205-212.

[423] Goertzen MJ, Clahsen H, Schulitz KP. Anterior cruciate ligament reconstruction using cryopreserved irradiated bone-ACL-bone-allograft transplants. Knee Surg Sports Traumatol Arthrosc 1994;2:150-157.

[424] Kaminski A, Grazka E, Jastrzebska A, Marowska J, Gut G, Wojciechowski A, et al. Effect of accelerated electron beam on mechanical properties of human cortical bone: Influence of different processing methods. Cell Tissue Bank 2012;13:375-386.

[425] Grimes M, Pembroke J, McGloughlin T. The effect of choice of sterilisation method on the biocompatibility and biodegradability of SIS (small intestinal submucosa). Biomed Mater Eng 2005;15:65-71.

[426] Freytes DO, Tullius RS, Badylak SF. Effect of storage upon material properties of lyophilized porcine extracellular matrix derived from the urinary bladder. J Biomed Mater Res B Appl Biomater 2006;78B:327-333.

[427] Schmidt T, Hoburg A, Broziat C, Smith M, Gohs U, Pruss A, et al. Sterilization with electron beam irradiation influences the biomechanical properties

and the early remodeling of tendon allografts for reconstruction of the anterior cruciate ligament (ACL). Cell Tissue Bank 2012;13:387-400.

[428] Akkus O, Belaney R, Das P. Free radical scavenging alleviates the biomechanical impairment of gamma radiation sterilized bone tissue. J Orthop Res 2005;23:838-845.

[429] Hawkins C, MJ D. Oxidative damage to collagen and related substrates by metal ion/hydrogen peroxide systems: Random attack or site-specific damage? Biochimica et Biophysica Acta 1997;1360:84-96.

[430] Grieb T, Forng R, Bogdansky S, Ronholdt C, Parks B, Drohan W, et al. High-dose gamma irradiation for soft tissue allografts: High margin of safety with biomechanical integrity. J Orthop Res 2006;24:1011-1018.

[431] Grieb T, Forng R, Stafford R, Lin J, Almeida J, Bogdansky S, et al. Effective use of optimized, high-dose (50 kGy) gamma irradiation for pathogen inactivation of human bone allografts. Biomaterials 2005;26:2033-2042.

[432] Kattaya SA, Akkus O, Slama J. Radioprotectant and radiosensitizer effects on sterility of gamma-irradiated bone. Clin Orthop Relat Res 2008;466:1796-1803.

[433] Grieb TA, Forng RY, Forsell J, Burgess WH. Microbial sterilization and viral inactication in bone and soft tissue alografts using novel applications of high-dose gamma irradiation: Report on the preservation of structural integrity and biocompatibility. Pittsburgh Bone Symposium2003.

[434] Seto A, Gatt CJ, Jr., Dunn MG. Improved tendon radioprotection by combined cross-linking and free radical scavenging. Clin Orthop Relat Res 2009;467:2994-3001.

[435] Seto AU, Gatt CJ, Jr., Dunn MG. Sterilization of tendon allografts: A method to improve strength and stability after exposure to 50 kGy gamma radiation. Cell Tissue Bank 2013;14:349-357.

[436] Moisan M, Barbeau J, Moreau S, Pelletier J, Tabrizian M, Yahia LH. Low-temperature sterilization using gas plasmas: A review of the experiments and an analysis of the inactivation mechanisms. Int J Pharm 2001;226:1-21.

[437] Moisan M, Barbeau J, Crevier M-C, Pelletier J, Philip N, Saoudi B. Plasma sterilization. Methods and mechanisms. Pure Appl Chem 2002;74:349-358.

[438] Rutala WA, Weber DJ. Guideline for disinfection and sterilization in healthcare facilities. Healthcare Infection Control Practices Advisory Committee (HICPAC); 2008.

[439] Ayhan F, Ayhan H, Piskin E. Sterilization of sutures by low temperature argon plasma. J Bioact Compat Polym 1998;13:65-72.

[440] Markowicz M, Koellensperger E, Steffens G, Frentz M, Schrage N, Pallua N. The impact of vacuum freeze-drying on collagen sponges after gas plasma sterilization. J Biomater Sci Polym Ed 2006;17:61-75.

[441] Huang Q, Ingham E, Rooney P, Kearney JN. Production of a sterilised decellularised tendon allograft for clinical use. Cell Tissue Bank In Press.

[442] Hong Y, Takanari K. An elastomeric patch electrospun from a blended solution of dermal extracellular matrix and biodegradable polyurethane for rat abdominal wall repair. Tissue Eng Part C Methods 2012;18:122-132.

[443] Freytes DO, Badylak SF, Webster TJ, Geddes LA, Rundell AE. Biaxial strength of multilaminated extracellular matrix scaffolds. Biomaterials 2004;25:2353-2361.

[444] Brown B, Lindberg K, Reing J, Stolz DB, Badylak SF. The basement membrane component of biologic scaffolds derived from extracellular matrix. Tissue Eng 2006;12:519-526.

[445] Scheffler S, Trautmann S, Smith M, Kalus U, von Versen R, Pauli G, et al. No influence of collagenous proteins of Achilles tendon, skin and cartilage on the virus-inactivating efficacy of peracetic acid-ethanol. Biologicals 2007;35:355-359.

[446] Chan J, Burugapalli K, Naik H, Kelly JL, Pandit A. Amine functionalization of cholecyst-derived extracellular matrix with generation 1 PAMAM dendrimer. Biomacromolecules 2008;9:528-536.

[447] Pruss A, Hansen A, Kao M, Gurtler L, Pauli G, Benedix F, et al. Comparison of the efficacy of virus inactivation methods in allogeneic avital bone tissue transplants. Cell Tissue Bank 2001;2:201-215.

[448] Holladay C, Power K, Sefton M, O'Brien T, Gallagher WM, Pandit A. Functionalized scaffold-mediated interleukin 10 gene delivery significantly improves survival rates of stem cells in vivo. Molecular Therapy 2011;19:969-978.

[449] Xu C, Lu W, Bian S, Liang J, Fan Y, Zhang X. Porous collagen scaffold reinforced with surfaced activated PLLA nanoparticles. ScientificWorldJournal 2012;2012:695137.

[450] Chan-Myers HB, Guida SH, Roberts CG, Thyagarajan K, Tu R, Quijano RC. Sterilization of a small caliber vascular graft with a polyexpoxy compound. ASAIO J 1992;38:116-119.

[451] Youngstrom DW, Barrett JG, Jose RR, Kaplan DL. Functional characterization of detergent-decellularized equine tendon extracellular matrix for tissue engineering applications. PLoS One 2013;8:e64151.

[452] Siritientong T, Srichana T, Aramwit P. The effect of sterilization methods on the physical properties of silk sericin scaffolds. AAPS Pharm Sci Tech 2011;12:771-781.

[453] Hallfeldt KK, Stutzle H, Puhlmann M, Kessler S, Schweiberer L. Sterilization of partially demineralized bone matrix: The effects of different sterilization techniques on osteogenetic properties. J Surg Res 1995;59:614-620.

Chapter 2: Collagen extraction

Sections of this chapter have been published at:

Delgado LM, Shologu N, Fuller K, Zeugolis DI. *Acetic acid and pepsin result in high yield, high purity and low macrophage response collagen for biomedical applications.* Biomedical Materials. 2017;12(6):065009.

2.1. Introduction

Collagen for food, cosmetics, drug delivery and tissue engineering applications is primarily extracted from land animals; to a lesser extent is extracted from marine sources or synthesised recombinantly [1, 2]. A typical protocol for collagen extraction involves solubilisation using neutral / slightly alkaline salt, acidic, alkaline or acidic / proteolytic enzymes solutions followed by repeated salt precipitation. Neutral / slightly alkaline salt (e.g. phosphate) solubilisation, albeit simple and economical, it is of low yield, as most tissues contain little amount of salt-extractable collagen [3, 4]. Dilute acids (e.g. acetic acid, hydrochloric acid), although they can break intra-molecular cross-links (aldimine type), resulting in higher yields than salt-extracted collagen, they cannot disassociate stable / mature (e.g. ketoimine) cross-links [5, 6]. To this end, alkaline solutions (e.g. sodium hydroxide, sodium sulphate) are employed [7, 8]. However, alkaline extracted collagen has several disadvantages (e.g. high hydrolysis level, hydroxyl amino acids are destroyed) that reduce its applicability in food and medical industries [9]. As such, acidic / proteolytic enzymes (e.g. pepsin) solutions are extensively used, as they increase significantly the yield [10-17] and through the cleavage of the non-helical ends, the antigenic P-determinant is removed [13, 14].

Salt precipitation is an inherent part of the collagen purification due to the physico-chemical properties of the different collagen types that permit their precipitation by adjusting the pH and the salt concentration [18]. For example, sodium chloride at 0.9 M and at acidic pH has been used to purify collagen type I from porcine [19], rat [12] and bovine [20] tendons. Collagen type II has been extracted using 5 M sodium chloride at neutral pH from articular cartilage of calf legs [21] and 0.7 to 0.9 M sodium chloride at acidic pH from chicken cartilage [22]. Collagen type III from

chicken skin and collagen type IV from human and murine basement membranes have also been purified using 1.8 M sodium chloride at alkaline pH [5] or 1.2 to 3.0 M sodium chloride at neutral pH [23, 24], respectively.

Although subsequent dialysis steps reduce the acidity and remove small molecular weight impurities (e.g. salt), still, a collagen material with reduced inflammatory potential is not produced. For example, collagen scaffolds produced from acetic acid / pepsin / salt precipitated collagen exhibited low inflammatory profile [25] or similar *in vivo* inflammation response to the non-treated control [26]. On the other hand, collagen scaffolds produced from hydrochloric acid / pepsin induced granulomatous inflammation up to 8 months after implantation [27] and a dense infiltration of inflammatory cells was observed for up to 21 days [28]. However, other studies have demonstrated that collagen extracted using hydrochloric acid / pepsin promoted a similar low *in vivo* inflammation response to the non-treated control [29, 30]. Further, hydrochloric acid extracted collagen without pepsin and without salt precipitation induced low macrophage infiltration after 4 and 8 weeks of implantation [31]. These data suggest that the acid used to extract the collagen and the use or not of pepsin or salt in the extraction process may determine the inflammation potential of the resultant scaffold. Thus, herein, we ventured to assess the influence of acetic acid (AA), hydrochloric acid (HC), pepsin (P) and salt precipitation (S) on the biophysical, biochemical and biological properties of collagen-based devices. These two acids (AA and HC) were selected because of their different acid strength and the different ion residues that will remain in the collagen after the purification process that may have an influence on the biochemical and biological properties.

2.2. Materials and methods

2.2.1. Materials

Porcine tendons were collected from a local abattoir and transferred in ice to our laboratory. All other materials and reagents were purchased from Sigma-Aldrich (Ireland), unless otherwise stated.

2.2.2. Type I collagen isolation

Collagen extraction was based on well-established protocols [32, 33] with slight modifications; see Appendix R for further optimisation data. **Figure 2.1** summarises the extraction process of the different collagen preparations used in this study. Briefly, the tendons were dissected from the surrounding fascia, cryo-milled (Freezer/Mill 6870, SPEX SamplePrep, USA) and washed with 1X phosphate buffered saline (PBS) solution. The milled tendons were either dissolved in 0.5 M acetic acid or 0.003 M HCl under orbital agitation for 72 h at 4 °C. Due to the different acid strength, the concentrations were adjusted to obtain a solution at pH 2-3 which is known to be more efficient dissociating intermolecular cross-links (aldimine type) [3]. Enzymatic digestion (when used) was carried out using pepsin from porcine gastric mucosa at a ratio of 80 U/mg of milled tendon. After incubation at 4 °C for 72 h under stirring, soluble collagen was collected through filtration and centrifugation (16,800 g at 4 °C for 20 min). Collagen purification (when used) was performed using salt precipitation at 0.9 M NaCl, as collagen type I precipitates at this acidic pH and specific salt concentration [18]. Precipitated collagen was collected after centrifugation (16,800 g at 4 °C for 20 min) and re-suspended in 1.0 M acetic acid or 0.006 M HCl. The final collagen solutions were dialysed (Mw 8,000

cut off) repeatedly against 1 mM acetic acid or 0.006 mM HCl. Dialysed collagen solutions were then freeze-dried (Virtis Advantage 2.0, USA).

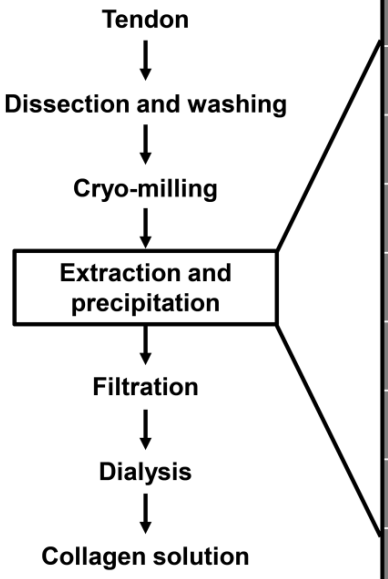

	Extraction and precipitation		
Group name	**Acid**	**Pepsin**	**Salt**
AA	Acetic Acid		
AAS	Acetic Acid		+
AAP	Acetic Acid	+	
AASP	Acetic Acid	+	+
HC	Hydrochloric Acid		
HCS	Hydrochloric Acid		+
HCP	Hydrochloric Acid	+	
HCSP	Hydrochloric Acid	+	+

Figure 2.1. Flow chart of the collagen extraction process and table describing the various groups assessed in this study.

2.2.3. Collagen purity assessment

Sodium dodecyl sulphate polyacrylamide gel electrophoresis (SDS-PAGE) was used to assess the purity of the produced collagen preparations, as has been described previously [33-35]. Freeze-dried samples were dissolved in 0.5 M acetic acid at 1 mg/ml. 0.1 mg/ml commercial type I bovine collagen (Symatese Biomateriaux, France) was used as control / standard. The samples were neutralised using NaOH and denatured at 95 °C for 5 min. Subsequently, the samples were loaded onto 5 % running and 3 % stacking acrylamide gels and run using the Bio-Rad Protean II® system (Bio-Rad Laboratories, UK). Gels were stained with the SilverQuest® kit (Invitrogen, USA) following the manufacturer's protocol. Densitometric analysis of gels was performed using a gel analyser plugin of ImageJ 1.48v software (National Institutes of Health, USA). Collagen bands [α_1(I) and α_2(I)] were quantified after defining each band with the rectangular tool and subtracting the background.

2.2.4. Free amine assessment

The amount of free primary amine groups of the type I collagen was quantified using ninhydrin assay, as has been described previously [36]. Briefly, 3 mg of each sample were mixed with 200 μl of deionized water and 1 ml of running buffer, which contained one part of 4 % (w/v) ninhydrin in 2-ethoxyethanol and one part of 200 mM citric acid with 0.16 % (w/v) tin (II) chloride at pH 5.0. After incubation at 95 °C for 30 min, the reaction was stopped by cooling down in ice and the addition of 250 μl of 50 % isopropanol. Tubes were vortexed and the absorbance of the developed purple colour was read at 570 nm. Glycine, at different concentrations, was used for the standard curve.

2.2.5. Denaturation temperature assessment

The denaturation temperature was assessed using a differential scanning calorimeter (DSC-60, Shimadzu, Japan), as has been described previously [37]. Briefly, 20 mg of each freeze-dried collagen sample were incubated in 1X PBS at room temperature overnight, blotted using filter paper to remove water excess and sealed in aluminium pans. Samples were subjected to a single constant heating ramp at 5 °C/min in the range of 25-90 °C, with an empty pan as reference. Denaturation temperature was determined as the maximum heat absorption of the endothermic peak.

2.2.6. Enzymatic stability assessment

Enzymatic degradation was assessed using the collagenase assay, as has been described previously [38]. Briefly, 5 mg of each collagen sample were incubated at 37 °C for 3, 6, 9 and 24 h in 0.1 M Tris-HCl and 5 mM $CaCl_2$ at pH 7.4 containing 50 U/ml of reconstituted bacterial collagenase type I from *Clostridium histolyticum*. Subsequently, centrifugation at 10,000 g for 5 min was carried out; supernatant was discarded and the pellets were freeze-dried. Scaffold degradation (% weight loss) was determined from the weight of remaining scaffolds after collagenase degradation and expressed as a percentage of the original weight.

2.2.7. *In vitro* inflammatory response assessment

In vitro inflammatory response was assessed, as has been described previously [39, 40]. Briefly, human derived leukemic monocyte cells (THP-1, ATCC, USA) were grown in RPMI-1640 supplemented with 10 % foetal bovine serum (FBS), 1 % penicillin / streptomycin. 200 μl of each collagen solution (1 mg/ml) were placed into each well of 24-well plates and let dry at room temperature for 24 h. Prior to

use, films were sterilised in 70 % ethanol for 30 min, followed by three washes in sterilized Hank's Balanced Salt Solution (HBSS). Cells were seeded onto collagen films at a density of 26 x 10^3 cells per cm^2. Mature macrophage-like state was induced by treating cells with phorbol 12-myristate 13-acetate (PMA) at 100 ng/ml for 6 h. Subsequently, adherent cells were washed with HBSS and incubated with supplemented media at 37 °C, 5 % CO_2 and 95 % humidified air for 24 and 48 h. Activated control was induced with 100 ng/ml of lipopolysaccharide (LPS) in supplemented media.

Macrophage response was characterised by cell morphology, proliferation, metabolic activity and inflammatory cytokine release. Macrophage morphology analysis was performed using the cell counter plugin of Image J software (National Institute of Health, USA). Elongated cells and total amount of cells were quantified by a single blind operator, counting 5 different regions per condition (50 ± 10 cells per region). Morphology measurements were made considering the R-ratio, an elongation factor that compares the length of major axis with the length of minor axis of a cell. A perfectly round cell has a R factor of 1 while an elongated cell has R factor greater than 2.5 [41]. Proliferation was assessed using Quant-iT™ PicoGreen® dsDNA kit (Invitrogen, USA), while cell metabolic activity was measured by 2 h incubation at 37 °C with 10 % alamarBlue® (Invitrogen, USA) following manufacturer's instructions. Cell metabolic activity was expressed in terms of reduction of alamarBlue®, considering metabolic activity of cells in TCP at each time point as 100 %. Inflammatory cytokines (IL-1β, IL-4, IL-6, IL-10, IL-12p70, IL-13, TNF-α, VEGF) were measured using Meso Scale Discovery (MSD®, USA) electrochemoluminescense assay as per manufacturer's guidelines. Briefly, cell free supernatants of each sample and supplied standard curve were incubated on MSD

plates for 2 h followed by a wash. Then, plates were incubated with detection antibody solution for 2 h. The plates were then washed and read using a Meso™ QuickPlex SQ120 instrument (MSD, USA).

2.2.8. Statistical analysis

Numerical data are expressed as mean ± standard deviation. Statistical analysis was performed using MINITAB® (version 16.2, Minitab Inc.). One way analysis of variance (ANOVA) followed by Fisher's post-hoc test were employed after confirming normal distribution from each sample population (Anderson-Darling normality test) and equality of variances (Bartlett's and Levene's tests for homogeneity of variance). Non-parametric statistics were used when either or both of the above assumptions were violated and, consequently, Kruskal-Wallis, for multiple comparisons, test was carried out. Statistical significance was accepted at $p < 0.05$.

2.3. Results

2.3.1. Collagen purity assessment

SDS-PAGE (**Figure 2.2a**) and complementary densitometric analysis of the α_1(I) and α_2(I) bands (**Figure 2.2b**) revealed that significantly more ($p < 0.05$) collagen came into solution when AA was used (as opposed to when HC was used). For both AA and HC preparations, the use of pepsin significantly increased ($p < 0.001$) yield. Pepsin decreased the cross-links of the AAP and AASP collagen (in comparison to AA and AAS, respectively), as evidenced by reduction in β and γ bands (**Table 2.1**). The use of salt did not increase ($p > 0.05$) yield or purity.

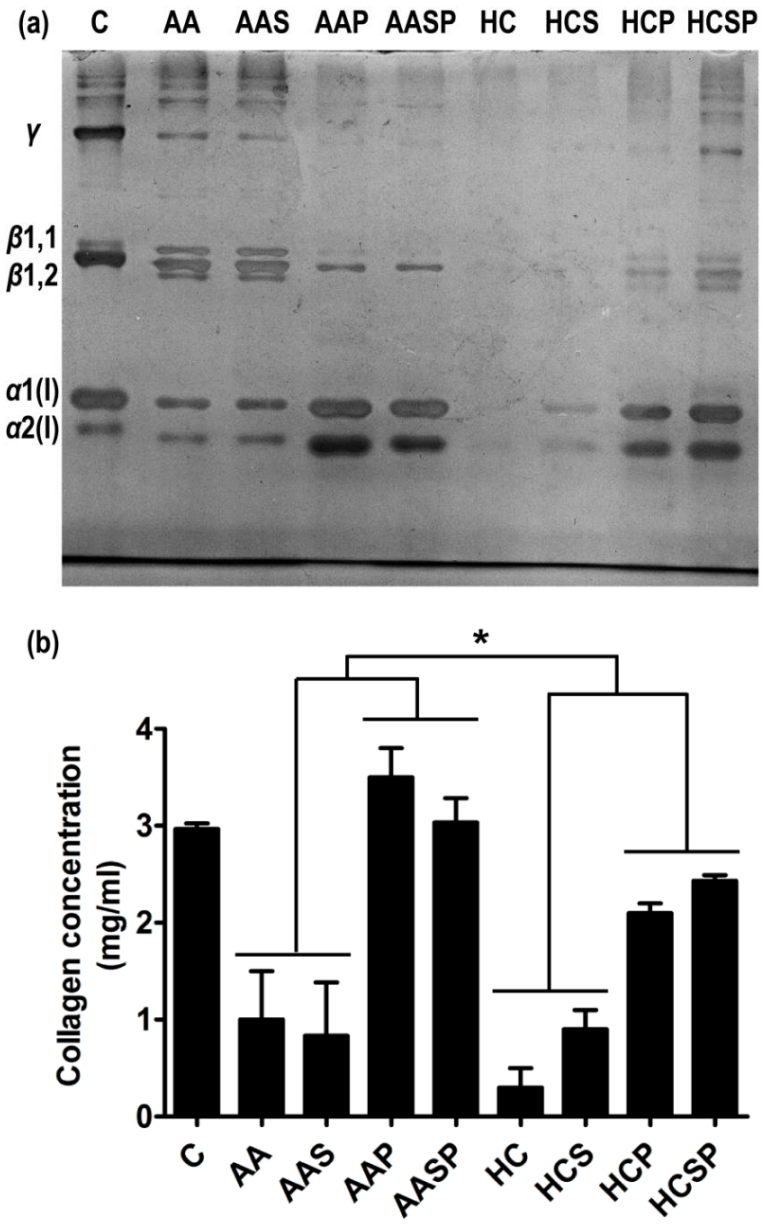

Figure 2.2. SDS-PAGE **(a)** and complementary densitometric analysis of α_1(I) and α_2(I) bands **(b)** revealed that significantly more ($p < 0.05$) collagen came into solution when AA was used. The use of pepsin, independently of the acid used, significantly increased ($p < 0.001$) yield. Pepsin also reduced the cross-links in the AAP and AASP (as compared to AA and AAS, respectively), as evidenced by the reduction in β and γ bands. Salt precipitation did not appear to induce a significant effect.

Table 2.1. Corresponding densitrometric analysis of type I collagen extracted with acetic acid and hydrochloric acid. Alpha bands increased and impurities decreased with pepsin treatment for all AA collagens. Alpha bands were lower for AA collagen without pepsin than HC collagen without pepsin. * indicates significant statistical difference respect to AA; #, respect to HC ($p < 0.05$).

Collagen extraction with acetic acid					
Bands	**Control**	**AA**	**AAS**	**AAP**	**AASP**
γ	23.3 ± 0.7	9.6 ± 1.5	5.9 ± 3.2	0.5 ± 0.4*	1.1 ± 0.3*
$\beta_{11} + \beta_{12}$	33.8 ± 0.6	47.1 ± 1.6	47.4 ± 1.7	11.4 ± 1.3*	10.6 ± 0.6*
$\alpha_{11} + \alpha_{12}$	42.2 ± 1.5	39.2 ± 1.3	42.4 ± 3.9	86.3 ± 1.5*	86.3 ± 0.6*
Impurities	0.7 ± 0.3	4.1 ± 0.4	4.4 ± 0.9	1.8 ± 0.3*	2.0 ± 0.2*
Collagen extraction with hydrochloric acid					
Bands	**Control**	**HC**	**HCS**	**HCP**	**HCSP**
γ	23.3 ± 0.7	7.9 ± 1.9	4.7 ± 2.5	1.5 ± 0.2#	4.2 ± 2.7
$\beta_{11} + \beta_{12}$	33.8 ± 0.6	15.3 ± 2.1	10.6 ± 2.5	17.0 ± 1.2	20.1 ± 1.8#
$\alpha_{11} + \alpha_{12}$	42.2 ± 1.5	67.1 ± 3.3	75.1 ± 4.0	77.6 ± 1.0#	69.9 ± 2.5
Impurities	0.7 ± 0.3	9.6 ± 2.0	9.1 ± 1.5	4.0 ± 0.2#	5.8 ± 0.7#

2.3.2. Free amine, denaturation temperature and enzymatic stability assessment

Ninhydrin assay was used to evaluate the amount of free amine groups (**Figure 2.3a**) and data obtained revealed that the highest % of free amines, for both AA and HC treatments, was detected for the AAP and the HCP groups ($p < 0.05$). DSC was used to assess the denaturation temperature / extend of cross-linking (**Figure 2.3b**) and data obtained revealed that the lowest denaturation temperature was detected for the AAP group ($p < 0.05$). Collagenase assay was used to assess resistance to enzymatic degradation (**Figure 2.3c**) and data obtained revealed no significant differences ($p > 0.05$) between the treatments.

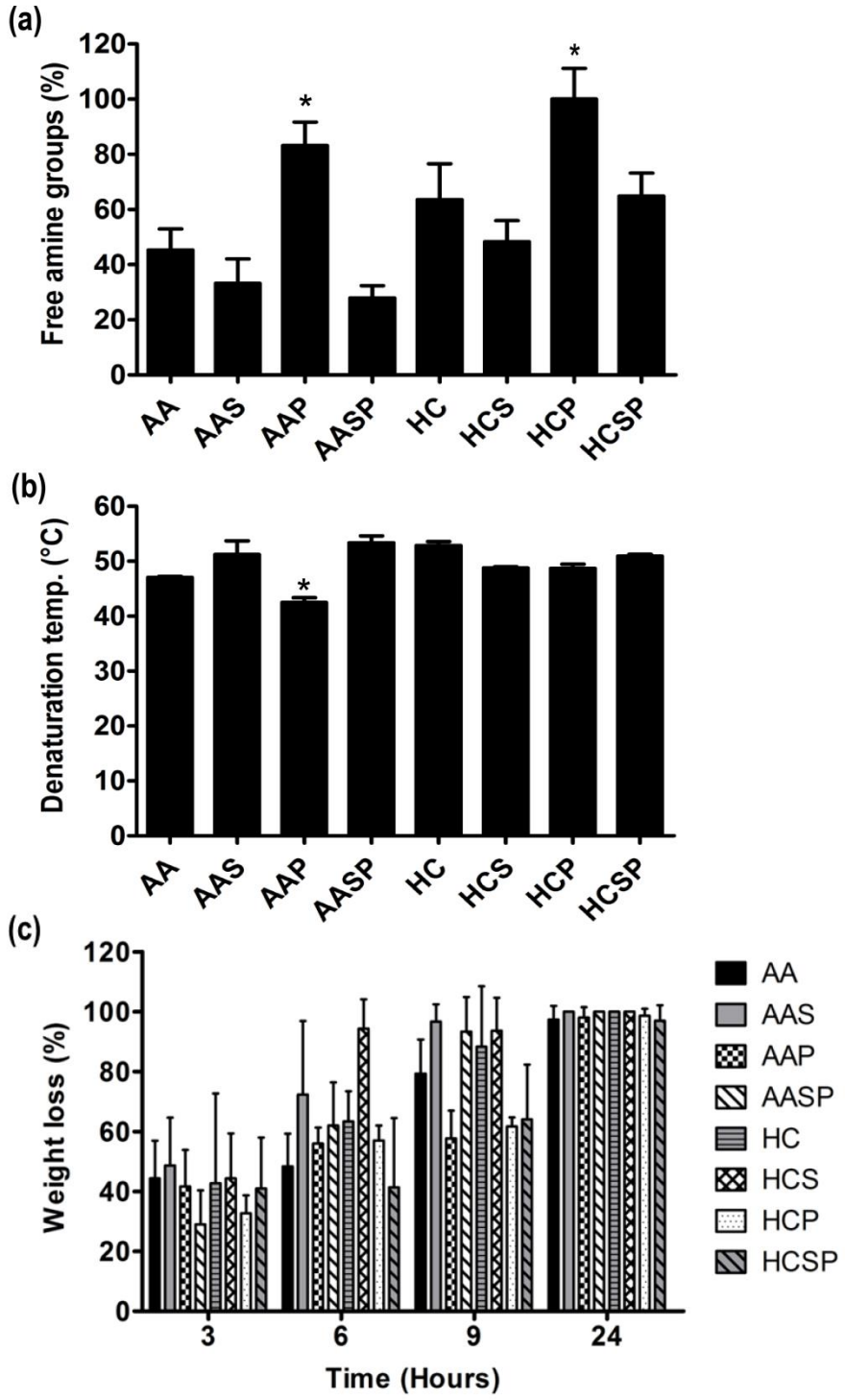

Figure 2.3. (a) The AAP and the HCP groups exhibited the highest % free amines ($p < 0.05$). **(b)** The AAP group exhibited the lowest denaturation temperature ($p < 0.05$). **(c)** No difference in resistance to collagenase degradation was observed between the groups ($p > 0.05$).

2.3.3. *In vitro* inflammatory response assessment

Phase contrast microscopy analysis demonstrated that most macrophages, independently of the treatment and time in culture, adopted a rounded morphology (**Figure 2.4**). Cells grown on TCP, LPS and all collagen preparations induced some macrophages to adopt an elongated morphology at both time points (**Figure 2.4**). Macrophage aggregates (5 or more cells) were also formed on TCP, LPS and all collagen preparations at both time points (**Figure 2.4**). At both time points, significantly more elongated macrophages were observed on AA films rather than on the HC films (**Figure 2.5a**).

Although DNA quantification analysis revealed that HC treatments exhibited significantly lower ($p < 0.001$) cell proliferation to the respective AA treatments at both time points (**Figure 2.5b**), no significant differences ($p > 0.05$) were observed between the groups in metabolic activity (**Figure 2.5c**).

Cytokine secretion analysis (**Figure 2.6** and **Figure 2.7**) revealed minimal / below detection limit release of IL-4, IL-6, IL-12, IL-13 and IL-10 and considerable release of IL-1β, TNF-α and VEGF at both time points. The secretion of TNF-α and VEGF was significantly increased ($p < 0.001$) from day 1 to day 2. LPS activated cells exhibited significantly higher ($p < 0.001$) levels of IL-1β and TNF-α at both time points, when compared to TCP. HC treatments exhibited significantly higher ($p < 0.001$) IL-1β and TNF-α to the respective AA treatments at both time points. Within the HC treatments, the HCP treatment induced significantly higher ($p < 0.001$) release of TNF-α at both time points.

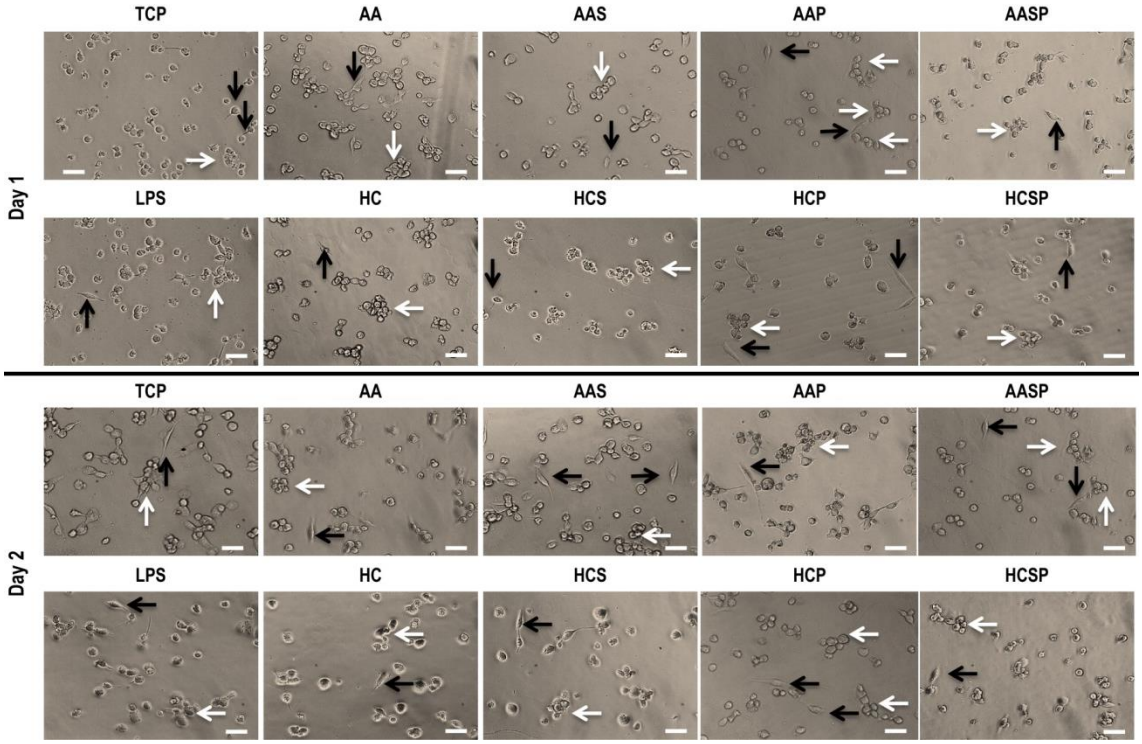

Figure 2.4. Phase contrast microscopy analysis demonstrated that most macrophages, independently of the treatment and time in culture, adopted a rounded morphology, although elongated cells (black arrows) and cell aggregates (white arrows) were evidenced. Scale bars: 50 μm.

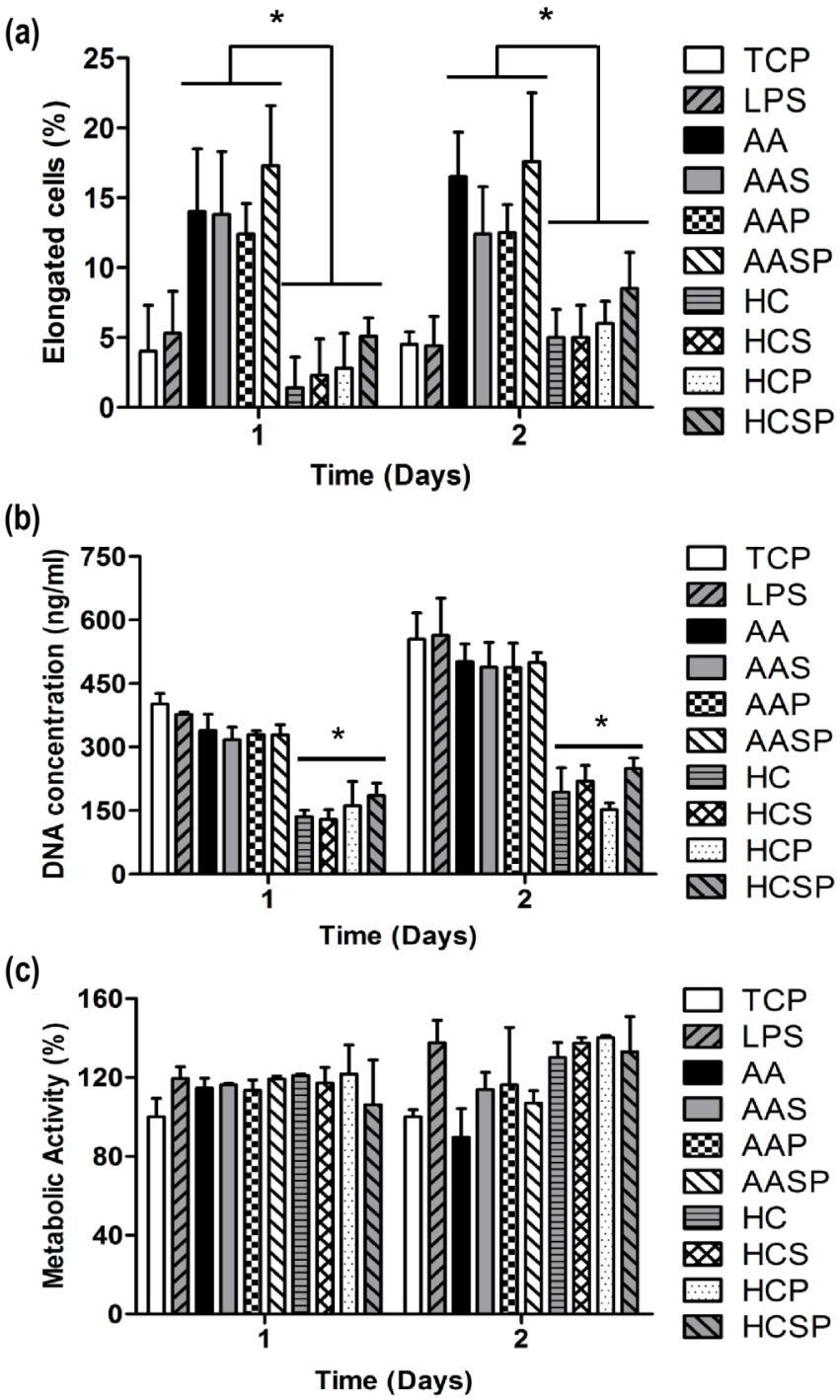

Figure 2.5. (a) Cell morphology analysis of the phase contrast images showed significantly more ($p < 0.001$) elongated macrophages on AA films rather than on HC films at both time points. **(b)** DNA quantification analysis revealed that HC treatments exhibited significantly lower ($p < 0.001$) cell proliferation to the respective AA treatments. **(c)** No significant differences ($p > 0.05$) were observed between the groups with respect to metabolic activity.

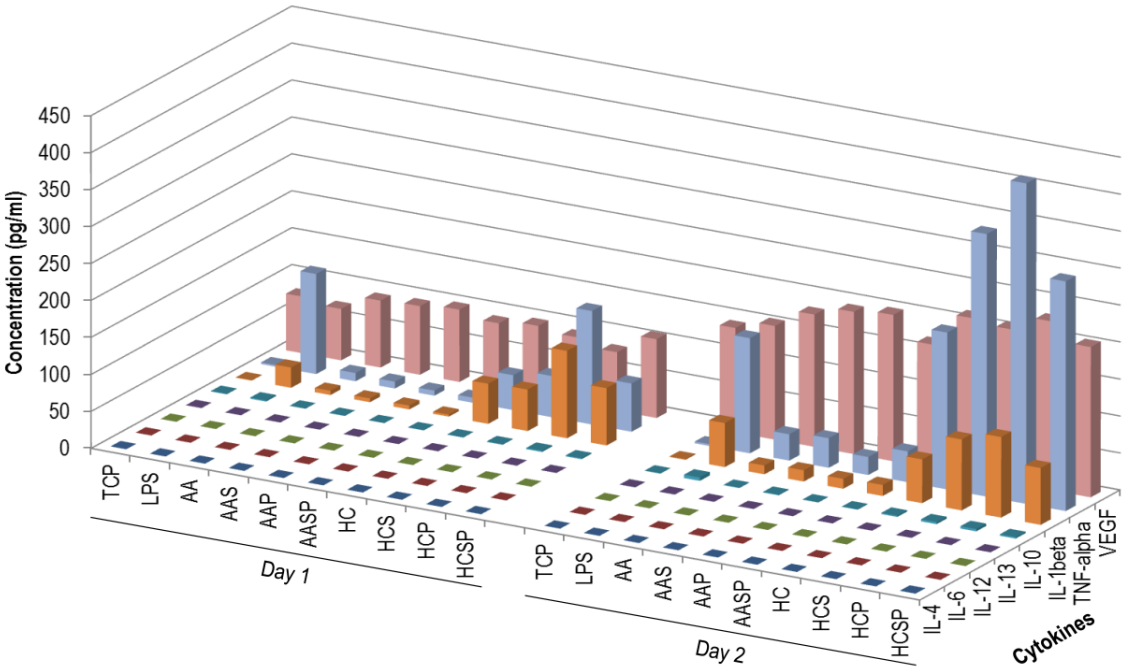

Figure 2.6. Multiplex ELISA on pro- and anti- inflammatory cytokines of THP-1 cells cultured on distinct collagen extractions for 1 and 2 days. Cytokine profile release analysis revealed that HC treatments exhibited significantly higher ($p < 0.001$) IL-1β and TNF-α secretion to the respective AA treatments at both time points.

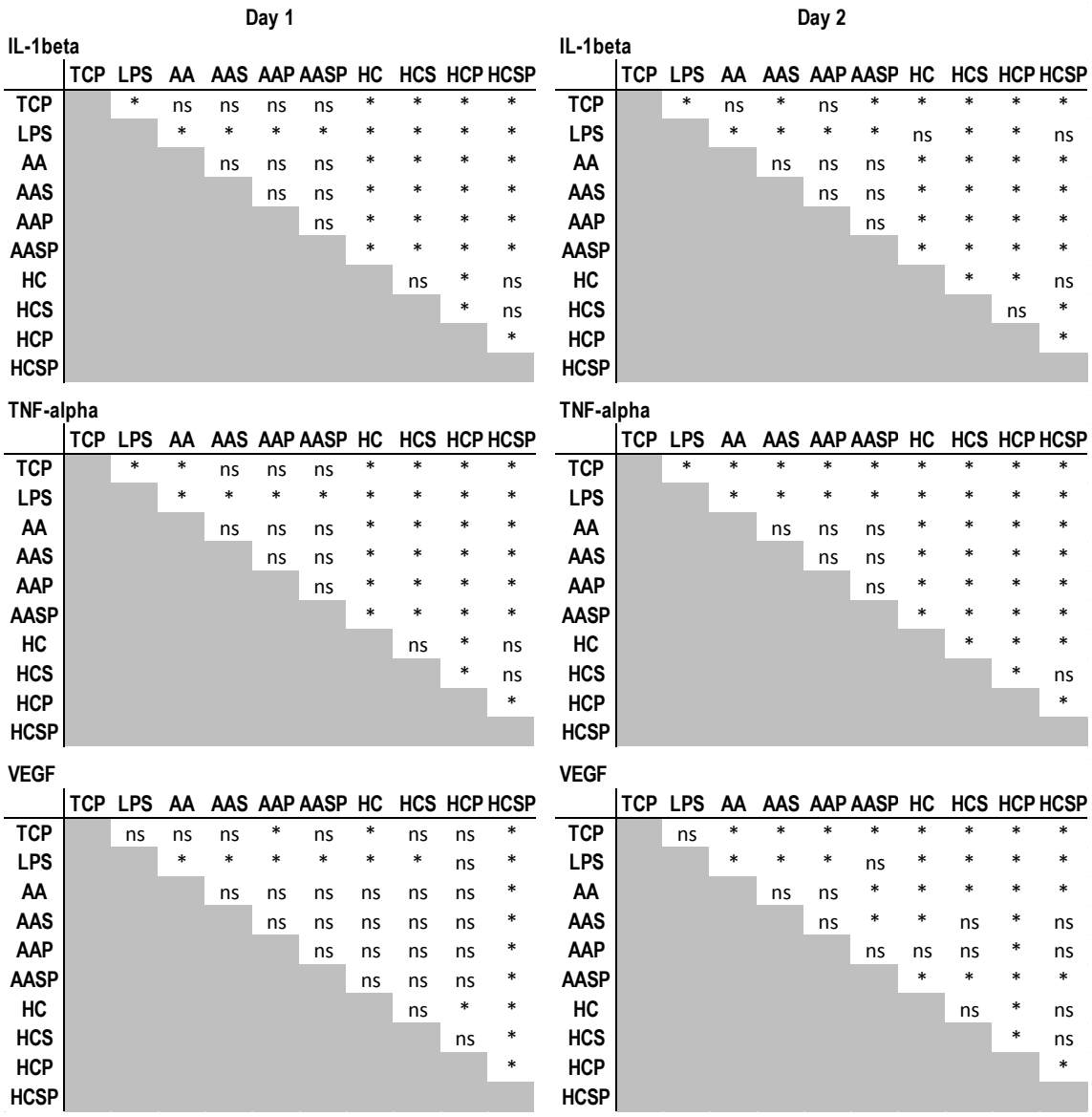

Figure 2.7. Multiplex ELISA on pro- and anti- inflammatory cytokines of THP-1 cells cultured on distinct films for 1 and 2 days. Multiple comparison tests for every pair of conditions (*: $p < 0.05$, ns: not significant).

2.4. Discussion

The term ‘collagen’ is used to epitomise a large family (40 different vertebrate collagen genes form 29 homo- and hetero- trimeric molecules) of glycoproteins with a characteristic $[Gly\text{-}X\text{-}Y]_n$ amino acid sequence (X is often proline and Y is frequently hydroxyproline). In vertebrates, collagen is the major connective tissue component; it constitutes 75 % to 90 % of the human skin, bone (organic matter), cartilage, tendon and cornea and is primarily responsible for the mechanical integrity and specific function of these tissues [42-57]. This abundance of collagen in human tissues has prompted scientific research and technological innovation into its utilisation as a scaffold fabrication material [58-64]. Indeed, bovine and porcine skin and tendon tissues are widely used to obtain collagen type I, the most abundant collagen family member. Traditionally, dilute acidic solutions (acetic acid or hydrochloric acid) are used to disassociate aldimine cross-links and dilute acidic solutions and proteolytic enzymes (e.g. pepsin) are used against the mature ketoimine cross-links, resulting in higher yields [10-17] and lower immune response [65-76]. Salt precipitation is also an integral part of the purification process, as by fine-tuning salt concentration / solution pH, different collagen types can be obtained [5, 12, 18-24]. Despite advances in the field of collagen as a biomaterial, collagen-based devices are frequently associated with foreign body response. Although exogenous cross-linking has been customarily blamed [77-80], several studies have suggested that other factors may also be responsible. For example, profound differences were observed in foreign body response of the same implant (hexamethylene diisocyanate cross-linked dermal sheep collagen), when it was assessed in rats and mice and within different strains of rats and mice [81]. Non-denatured and non-cross-linked collagen provoked completely different foreign body

reaction to gelatin [82]. Substantial biophysical, biological and immunological differences were also observed between different commercially available collagen preparations [83], possibly due to the different preparation protocols (e.g. different species / tissues from which the collagen was extracted from; different collagen types ratio present; different acids; utilisation or not of pepsin or salt). Thus, herein, we ventured to assess for first time whether the utilisation of different acids (AA and HC) and the utilisation or not of pepsin (P) or salt (S) could influence the yield, purity, free amines, denaturation temperature, resistance to collagenase degradation and macrophage response on collagen scaffolds. To eliminate species variability [12, 84], all experiments were conducted using collagen extracted from porcine tendons.

Starting with yield and purity assessment, we found that AA, possibly due to its weaker nature, brought more collagen into solution. This is in agreement with previous publication, where although HC has been shown to hydrolyse more collagen than AA, citric acid and lactic acid, higher yield and purity resulted from the lactic acid, followed by the AA, citric acid and HC [85]. In contrast to these data, more viscous collagen solutions and scaffolds with larger pores, higher compressive modulus, lower swelling and lower cell proliferation were resulted from HC extracted collagen, as opposed to AA extracted collagen [86]. This may be due to the acid concentration; previous studies have shown that maximum yield for collagen extracted from the skin of hybrid catfish *Clarias sp.* was obtained when 0.7 M AA was used; the yield was reduced at higher AA concentrations [87].

The use of pepsin, due to its capacity to break mature cross-links, brought more collagen into solution, as has been reported repeatedly in the literature [10-17]. Further, pepsin, having removed the telo-peptides regions that are involved in cross-linking [88-90], resulted in collagen preparations with less cross-links (as evidenced

by reduced β and γ bands in the AAP and AASP, as compared to AA and AAS, respectively), with higher free amine content and lower denaturation temperature, especially for the AAP group. In other words, pepsin induced higher disassociation of collagen ultrastructure and removed both telopeptides, reducing molecular stability and length which justify the lower denaturation temperature. Resistance to collagenase digestion was not able to detect any differences between the treatments, possibly due to the sensitivity of the assay. Other enzymes, such as trypsin and papain, have also been used in collagen extraction. However, trypsin has been shown to degrade collagen [91-93], whilst papain was not as efficient (yield wise) in comparison to pepsin [94-96].

Phase contrast microscopy analysis of macrophages seeded on the various collagen preparations revealed a mixed cell response, as evidenced by round cells, elongated cells and cell aggregates. Nonetheless, among the two acids, AA induced more macrophages to adopt an elongated morphology. Elongated macrophage morphology is associated with transition from M1 (round morphology; pro-inflammatory) to M2 (elongated morphology; anti-inflammatory) phenotype [97] and cell aggregates indicate foreign body response [98]. Such heterogeneous macrophage response has been reported as a function of different collagen cross-linking methods [39] and when macrophages were exposed to polyethylene particulate [99]. Macrophage phenotype variations may be responsible for this variable response [97, 100-102].

Although no difference in metabolic activity was observed between the two different acids, the DNA concentration was lower for the HC treatments. Cytokine analysis further corroborated the differences between the two acids: HC treatments exhibited higher IL-1β and TNF-α to the respective AA treatments at both time points. The observed DNA reduction may be related to the increased TNF-α release, which has

been associated with inducing apoptosis of adherent macrophage on biomaterials [103, 104]. These differences may be attributed to the strength of the acids and the variation of surface energy or hydrophilicity that they can cause. As hydrochloric acid is a strong acid, the HCl molecules instantly dissociate into ions and, therefore, higher amount of anions remain in the collagen network in comparison with the acetic acid. This fact could give a higher negative charge to the HCl collagen formulations; that is highly interesting because surface energy and charge were found to induce different macrophage response [105, 106]. The sensitivity of macrophage to surface charge has been also confirmed with endocytic assays with positive and negatively charged particles [107-109]. Although AAP increased the amount of free primary amine which are known to increase the positive charge balance and to affect macrophage response [110], our data do not reveal any influence on the macrophage morphology or cytokine release.

The different macrophage response can also be attributed to the different extent of cross-linking that results in different amounts of collagen released in the media, which has been shown to induce differential mononuclear cell activation *in vitro* [111]. We feel that pH could not be the reason, as HBSS was used for rinsing following sterilisation and its pH is between 7.1 and 7.4.

On the other hand, this study has some limitations regarding the assessment of macrophage adhesion and collagen degradation assisted by macrophages. For example, a recent publication demonstrated that macrophage polarisation can be controlled through integrin-mediated interactions between THP-1 macrophages and collagen matrix. Indeed, integrin α2β1 has a pivotal role to induce M2 phenotype, whereas inhibiting integrin α2β1 mechanism induces M1 phenotype [112]. Moreover, macrophages are known to degrade collagen matrix and it could have an

effect on their polarisation as a recent study showed that U937 macrophages recognise/respond to collagen fibril damage within tendon [113] and collagen debris [114]. Collagen degradation could be compared between conditions by direct staining of the collagen film or by SDS-PAGE of the supernatant in combination with the silver staining.

Salt precipitation did not appear to influence the parameters assessed due to the repeated dialysis step. In general, special attention should be paid when purifying collagen with salt precipitation, as even modest increase of sodium chloride salt in medium has been demonstrated to regulate the activation of mitogen-activated protein kinases and Akt, which potentiate macrophage apoptosis [115]. Furthermore, salt increase could lead to inhibition of endotoxin-induced stress fibre polymerisation *in vivo* [116].

2.5. Conclusions

Collagen-based devices are frequently associated with foreign body response. Pre- and post- extraction method variables have been shown to influence foreign body response. Herein, we demonstrated that during the extraction process variables could also affect the physicochemical and biological properties of collagen preparations. Our data suggest that high yield, high purity, low in innate cross-linking density and low in secretion of IL-1β and TNF-α collagen can be extracted using pepsin in acetic acid.

2.6. Reference

[1] Browne S, Zeugolis DI, Pandit A. Collagen: Finding a solution for the source. Tissue Eng Part A 2013;19:1491-1494.

[2] Zeugolis DI, Raghunath M. Collagen: Materials analysis and implant uses. In: Ducheyne P, Healy KE, Hutmacher DW, Grainger DW, Kirkpatrick CJ, editors. Comprehensive Biomaterials: Elsevier; 2011. p. 261-278.

[3] Friess W. Collagen--biomaterial for drug delivery. Eur J Pharm Biopharm 1998;45:113-136.

[4] Gross J, Highberger JH, Schmitt FO. Extraction of collagen from connective tissue by neutral salt solutions. Proc Natl Acad Sci U S A 1955;41:1-7.

[5] Cliche S, Amiot J, Avezard C, Gariepy C. Extraction and characterization of collagen with or without telopeptides from chicken skin. Poult Sci 2003;82:503-509.

[6] Pacak CA, Powers JM, Cowan DB. Ultrarapid purification of collagen type I for tissue engineering applications. Tissue Eng C 2011;17:879-885.

[7] Hattori S, Adachi E, Ebihara T, Shirai T, Someki I, Irie S. Alkali-treated collagen retained the triple helical conformation and the ligand activity for the cell adhesion via alpha2beta1 integrin. J Biochem 1999;125:676-684.

[8] Yoshimura K, Terashima M, Hozan D, Shirai K. Preparation and dynamic viscoelasticity characterization of alkali-solubilized collagen from shark skin. J Agric Food Chem 2000;48:685-690.

[9] Yang H, Shu Z. The extraction of collagen protein from pigskin. J Chem Pharmaceut Res 2014;6:683-687.

[10] Skierka E, Sadowska M. The influence of different acids and pepsin on the extractability of collagen from the skin of Baltic cod (Gadus morhua). Food Chem 2007;105:1302-1306.

[11] Nalinanon S, Benjakul S, Visessanguan W, Kishimura H. Use of pepsin for collagen extraction from the skin of bigeye snapper (Priacanthus tayenus). Food Chem 2007;104:593-601.

[12] Zeugolis DI, Paul RG, Attenburrow G. Factors influencing the properties of reconstituted collagen fibers prior to self-assembly: Animal species and collagen extraction method. J Biomed Mater Res A 2008;86A:892-904.

[13] Rubin AL, Pfahl D, Speakman PT, Davison PF, Schmitt FO. Tropocollagen: Significance of protease-induced alterations. Science 1963;139:37-39.

[14] Kuznetsova N, Leikin S. Does the triple helical domain of type I collagen encode molecular recognition and fiber assembly while telopeptides serve as catalytic domains? Effect of proteolytic cleavage on fibrillogenesis and on collagen-collagen interaction in fibers. J Biol Chem 1999;274:36083-36088.

[15] Muralidharan N, Jeya Shakila R, Sukumar D, Jeyasekaran G. Skin, bone and muscle collagen extraction from the trash fish, leather jacket (Odonus niger) and their characterization. J Food Sci Technol 2013;50:1106-1113.

[16] Ran XG, Wang LY. Use of ultrasonic and pepsin treatment in tandem for collagen extraction from meat industry by-products. J Sci Food Agric 2014;94:585-590.

[17] Aukkanit N, Garnjanagoonchorn W. Temperature effects on type I pepsin-solubilised collagen extraction from silver-line grunt skin and its in vitro fibril self-assembly. J Sci Food Agric 2010;90:2627-2632.

[18] Deyl Z, Miksik I, Eckhardt A. Preparative procedures and purity assessment of collagen proteins. J Chromatogr B 2003;790:245-275.

[19] Zeugolis DI, Panengad PP, Yew ES, Sheppard C, Phan TT, Raghunath M. An in situ and in vitro investigation for the transglutaminase potential in tissue engineering. J Biomed Mater Res A 2010;92:1310-1320.

[20] Zeugolis DI, Paul RG, Attenburrow G. The influence of a natural cross-linking agent (Myrica rubra) on the properties of extruded collagen fibres for tissue engineering applications. Mater Sci Eng C Mater Biol Appl

2010;30:190-195.

[21] Barnes CP, Pemble CW, Brand DD, Simpson DG, Bowlin GL. Cross-linking electrospun type II collagen tissue engineering scaffolds with carbodiimide in ethanol. Tissue Eng 2007;13:1593-1605.

[22] Deyl Z, Miksik I. Advanced separation methods for collagen parent alpha-chains, their polymers and fragments. J Chromatogr B 2000;739:3-31.

[23] Kleinman HK. Isolation of laminin-1 and type IV collagen from the EHS sarcoma. J Tissue Cult Meth 1994;16:231-233.

[24] Dixit SN, Stuart JM, Seyer JM, Risteli J, Timpl R, Kang AH. Type IV Collagens: Isolation and characterization of 7S collagen from human kidney, liver and lung. Coll Relat Res 1981;1:549-556.

[25] Holladay CA, Duffy AM, Chen X, Sefton MV, O'Brien TD, Pandit AS. Recovery of cardiac function mediated by MSC and interleukin-10 plasmid functionalised scaffold. Biomaterials 2012;33:1303-1314.

[26] Thomas D, Fontana G, Chen X, Sanz-Nogues C, Zeugolis DI, Dockery P, et al. A shape-controlled tuneable microgel platform to modulate angiogenic paracrine responses in stem cells. Biomaterials 2014;35:8757-8766.

[27] Kishore V, Uquillas JA, Dubikovsky A, Alshehabat MA, Snyder PW, Breur GJ, et al. In vivo response to electrochemically aligned collagen bioscaffolds. J Biomed Mater Res B Appl Biomater 2012;100:400-408.

[28] Garcia Y, Wilkins B, Collighan RJ, Griffin M, Pandit A. Towards development of a dermal rudiment for enhanced wound healing response. Biomaterials 2008;29:857-868.

[29] Kanda N, Morimoto N, Ayvazyan AA, Takemoto S, Kawai K, Nakamura Y, et al. Evaluation of a novel collagen–gelatin scaffold for achieving the sustained release of basic fibroblast growth factor in a diabetic mouse model. J Tissue Eng Regen Med 2014;8:29-40.

[30] Maeda M, Kadota K, Kajihara M, Sano A, Fujioka K. Sustained release of human growth hormone (hGH) from collagen film and evaluation of effect on wound healing in db/db mice. J Control Release 2001;77:261-272.

[31] Hong Y, Takanari K. An elastomeric patch electrospun from a blended solution of dermal extracellular matrix and biodegradable polyurethane for rat abdominal wall repair. Tissue Eng C 2012;18:122-132.

[32] Zeugolis D, Paul R, Attenburrow G. Extruded collagen-polyethylene glycol fibers for tissue engineering applications. J Biomed Mater Res B Appl Biomater 2008;85:343-352.

[33] Zeugolis D, Paul R, Attenburrow G. Post-self-assembly experimentation on extruded collagen fibres for tissue engineering applications. Acta Biomater 2008;4:1646-1656.

[34] Satyam A, Kumar P, Fan X, Gorelov A, Rochev Y, Joshi L, et al. Macromolecular crowding meets tissue engineering by self-assembly: A paradigm shift in regenerative medicine. Adv Mater 2014;26:3024-3034.

[35] Kumar P, Satyam A, Cigognini D, Pandit A, Zeugolis D. Low oxygen tension and macromolecular crowding accelerate extracellular matrix deposition in human corneal fibroblast culture. J Tissue Eng Regen Med In Press.

[36] Ward J, Kelly J, Wang W, Zeugolis DI, Pandit A. Amine functionalization of collagen matrices with multifunctional polyethylene glycol systems. Biomacromolecules 2010;11:3093-3101.

[37] Zeugolis D, Raghunath M. The physiological relevance of wet versus dry differential scanning calorimetry for biomaterial evaluation: A technical note. Polymer Int 2010;59:1403-1407.

[38] Helling A, Tsekoura E, Biggs M, Bayon Y, Pandit A, Zeugolis D. In vitro enzymatic degradation of tissue grafts and collagen biomaterials by matrix metalloproteinases: Improving the collagenase assay. ACS Biomater Sci Eng In Press.

[39] Delgado LM, Fuller K, Zeugolis DI. Collagen cross-linking - Biophysical, biochemical and biological response analysis. Tissue Eng Part A In Press;Epub.

[40] Fuller K, Gaspar D, Delgado L, Pandit A, Zeugolis D. Influence of porosity and pore shape on structural, mechanical and biological properties of poly ϵ-caprolactone electro-spun fibrous scaffolds. Nanomedicine 2016;11:1031-1040.

[41] Chen S, Jones Ja, Xu Y, Low H-Y, Anderson JM, Leong KW. Characterization of topographical effects on macrophage behavior in a foreign body response model. Biomaterials 2010;31:3479-3491.

[42] Hulmes D. Building collagen molecules, fibrils, and suprafibrillar structures. J Struct Biol 2002;137:2-10.

[43] van der Rest M, Garrone R, Herbage D. Collagen: A family of proteins with many facets. In: Kleinman H, editor. Advances in Molecular and Cell Biology. Greenwich, Connecticut: JAI Press Inc; 1993. p. 1-67.

[44] Kielty C, Grant M. The collagen family: Structure, assembly, and organization in the extracellular matrix. In: Royce P, Steinmann B, editors. Connective Tissue and Its Heritable Disorders: Molecular, Genetic, and Medical Aspects. Second ed. Hoboken, NJ, USA: John Wiley & Sons, Inc.; 2002. p. 159-221.

[45] Hulmes D. The collagen superfamily -- Diverse structures and assemblies. Essays Biochem 1992;27:49-67.

[46] Bella J. Collagen structure: new tricks from a very old dog. Biochem J 2016;473:1001-1025.

[47] Shoulders M, Raines R. Collagen structure and stability. Annu Rev Biochem 2009;78:929-958.

[48] Brodsky B, Persikov A. Molecular structure of the collagen triple helix. Adv Protein Chem 2005;70:301-339.

[49] Brodsky B, Ramshaw J. The collagen triple-helix structure. Matrix Biol 1997;15:545-554.

[50] Bailey A, Paul R, Knott L. Mechanisms of maturation and ageing of collagen. Mech Ageing Dev 1998;106:1-56.

[51] Bailey A. Molecular mechanisms of ageing in connective tissues. Mech Ageing Dev 2001;122:735-755.

[52] Kadler K, Holmes D, Trotter J, Chapman J. Collagen fibril formation. Biochem J 1996;316:1-11.

[53] Kadler K, Hill A, Canty-Laird E. Collagen fibrillogenesis: Fibronectin, integrins, and minor collagens as organizers and nucleators. Curr Opin Cell Biol 2008;20:495-501.

[54] Eyden B, Tzaphlidou M. Structural variations of collagen in normal and pathological tissues: Role of electron microscopy. Micron 2001;32:287-300.

[55] Starborg T, Lu Y, Kadler K, Holmes D. Electron microscopy of collagen fibril structure in vitro and in vivo including three-dimensional reconstruction. Methods Cell Biol 2008;88:319-345.

[56] Kalamajski S, Oldberg A. The role of small leucine-rich proteoglycans in collagen fibrillogenesis. Matrix Biol 2010;29:248-253.

[57] Reed C, Iozzo R. The role of decorin in collagen fibrillogenesis and skin homeostasis. Glycoconj J 2002;19:249-255.

[58] Glowacki J, Mizuno S. Collagen scaffolds for tissue engineering. Biopolymers 2008;89:338-344.

[59] Antoine E, Vlachos P, Rylander M. Review of collagen I hydrogels for bioengineered tissue microenvironments: Characterization of mechanics, structure, and transport. Tissue Eng Part B Rev 2014;20:683-696.

[60] Wallace D, Rosenblatt J. Collagen gel systems for sustained delivery and tissue engineering. Adv Drug Deliv Rev 2003;55:1631-1649.

[61] Pawelec K, Best S, Cameron R. Collagen: A network for regenerative medicine. J Mater Chem B 2016;4:6484-6496.

[62] Ramshaw J. Biomedical applications of collagens. J Biomed Mater Res B Appl Biomater 2016;104:665-675.

[63] Thomas D, Gaspar D, Sorushanova A, Milcovich G, Spanoudes K, Mullen A, et al. Scaffold and scaffold-free self-assembled systems in regenerative medicine. Biotechnol Bioeng 2016;113:1155-1163.

[64] Abbah S, Delgado L, Azeem A, Fuller K, Shologu N, Keeney M, et al. Harnessing hierarchical nano- and micro-fabrication technologies for musculoskeletal tissue engineering. Adv Healthc Mater 2015;4:2488-2499.

[65] Lynn A, Yannas I, Bonfield W. Antigenicity and immunogenicity of collagen. J Biomed Mater Res B Appl Biomater 2004;71:343-354.

[66] Na G, Butz L, Bailey D, Carroll R. In vitro collagen fibril assembly in glycerol solution: Evidence for a helical cooperative mechanism involving microfibrils. Biochemistry 1986;25:958-966.

[67] Gelman R, Poppke D, Piez K. Collagen fibril formation in vitro. The role of the nonhelical terminal regions. J Biol Chem 1979;254:11741-11745.

[68] Ishikawa H, Koshino T, Takeuchi R, Saito T. Effects of collagen gel mixed with hydroxyapatite powder on interface between newly formed bone and grafted achilles tendon in rabbit femoral bone tunnel. Biomaterials 2001;22:1689-1694.

[69] Alam M, Asahina I, Ohmamiuda K, Takahashi K, Yokota S, Enomoto S. Evaluation of ceramics composed of different hydroxyapatite to tricalcium phosphate ratios as carriers for rhBMP-2. Biomaterials 2001;22:1643-1651.

[70] Yamada N, Shioya N, Kuroyanagi Y. Evaluation of an allogeneic cultured dermal substitute composed of fibroblasts within a spongy collagen matrix as a wound dressing. Scand J Plast Reconstr Surg Hand Surg 1995;29:211-219.

[71] Hsu F, Chueh S, Wang Y. Microspheres of hydroxyapatite/reconstituted collagen as supports for osteoblast cell growth. Biomaterials 1999;20:1931-1936.

[72] Rodrigues C, Serricella P, Linhares A, Guerdes R, Borojevic R, Rossi M, et al. Characterization of a bovine collagen-hydroxyapatite composite scaffold for bone tissue engineering. Biomaterials 2003;24:4987-4997.

[73] Rosenblatt J, Rhee W, Wallace D. The effect of collagen fiber size distribution on the release rate of proteins from collagen matrices by diffusion. J Control Release 1989;9:195-203.

[74] Rosenblatt J, Devereux B, Wallace D. Injectable collagen as a ph-sensitive hydrogel. Biomaterials 1994;15:985-995.

[75] Wells M, Kraus K, Batter D, Blunt D, Weremowitz J, Lynch S, et al. Gel matrix vehicles for growth factor application in nerve gap injuries repaired with tubes: A comparison of biomatrix, collagen, and methylcellulose. Exp Neurol 1997;146:395-402.

[76] Pontz B, Meigel W, Rauterberg J, Kühn K. Localization of two species specific antigenic determinants on the peptide chains of calf skin collagen. Eur J Biochem 1970;16:50-54.

[77] McPherson J, Sawamura S, Armstrong R. An examination of the biologic response to injectable, glutaraldehyde cross-linked collagen implants. J Biomed Mater Res 1986;20:93-107.

[78] Ye Q, Harmsen M, van Luyn M, Bank R. The relationship between collagen scaffold cross-linking agents and neutrophils in the foreign body reaction. Biomaterials 2010;31:9192-9201.

[79] van Putten S, Ploeger D, Popa E, Bank R. Macrophage phenotypes in the collagen-induced foreign body reaction in rats. Acta Biomater 2013;9:6502-6510.

[80] Delgado LM, Bayon Y, Pandit A, Zeugolis DI. To cross-link or not to cross-link? Cross-linking associated foreign body response of collagen-based devices. Tissue Eng Part B Rev 2015;21:298-313.

[81] Khouw I, van Wachem P, Molema G, Plantinga J, de Leij L, van Luyn M. The foreign body reaction to a biodegradable biomaterial differs between rats and mice. J Biomed Mater Res 2000;52:439-446.

[82] Ye Q, Harmsen M, Ren Y, Bank R. The role of collagen receptors Endo180 and DDR-2 in the foreign body reaction against non-crosslinked collagen and gelatin. Biomaterials 2011;32:1339-1350.

[83] DeLustro F, Condell R, Nguyen M, McPherson J. A comparative study of the biologic and immunologic response to medical devices derived from dermal collagen. J Biomed Mater Res 1986;20:109-120.

[84] Angele P, Abke J, Kujat R, Faltermeier H, Schumann D, Nerlich M, et al. Influence of different collagen species on physico-chemical properties of crosslinked collagen matrices. Biomaterials 2004;25:2831-2841.

[85] Liu D, Lin Y, Chen M. Optimum condition of extracting collagen from chicken feet and its characteristics. Asian-Aust J Anim Sci 2001;14:1638-1644.

[86] Ratanavaraporn J, Kanokpanont S, Tabata Y, Damrongsakkul S. Effects of acid type on physical and biological properties of collagen scaffolds. J Biomater Sci Polym Ed 2008;19:945-952.

[87] Kiew P, Don M. The influence of acetic acid concentration on the extractability of collagen from the skin of hybrid Clarias sp. and its physicochemical properties: A preliminary study. Focus Mod Food Ind 2013;2:123-128.

[88] Woodley D, Yamauchi M, Wynn K, Mechanic G, Briggaman R. Collagen telopeptides (cross-linking sites) play a role in collagen gel lattice contraction. J Invest Dermatol 1991;97:580-585.

[89] Kalamajski S, Liu C, Tillgren V, Rubin K, Oldberg Å, Rai J, et al. Increased C-telopeptide cross-linking of tendon type I collagen in fibromodulin-deficient mice. J Biol Chem 2014;289:18873-18879.

[90] Tamiya M, Tokunaga S, Okada H, Suzuki H, Kobayashi M, Sasada S, et al. Prospective study of urinary and serum cross-linked N-telopeptide of type I collagen (NTx) for diagnosis of bone metastasis in patients with lung cancer. Clin Lung Cancer 2013;14:364-369.

[91] Stenman M, Ainola M, Valmu L, Bjartell A, Ma G, Stenman U, et al. Trypsin-2 degrades human type II collagen and is expressed and activated in mesenchymally transformed rheumatoid arthritis synovitis tissue. Am J Pathol 2005;167:1119-1124.

[92] van Deemter M, Kuijer R, Harm Pas H, Jacoba van der Worp R, Hooymans J, Los L. Trypsin-mediated enzymatic degradation of type II collagen in the human vitreous. Mol Vis 2013;19:1591-1599.

[93] Cassel J, Kanagy J. Studies on the purification of collagen. J Res Nation Bureau Stand 1949;42:557-565.

[94] Bakar J, Hartina M, Hashim D, Sazili A, Harvinder K. Collagen extraction from aquatic animals. 2010.

[95] Hashim P, Mohd Ridzwan M, Bakar J. Isolation and characterization of collagen from chicken feet. Int J Biol Biomol Agric Food Biotechn Eng 2014;8:250-254.

[96] Song W, Chen W, Yang Y, Li C, Qian G. Extraction optimization and characterization of collagen from the lung of soft-shelled turtle Pelodiscus sinensis. Int J Nutr Food Sc 2014;3:270-278.

[97] McWhorter FY, Wang T, Nguyen P, Chung T, Liu WF. Modulation of macrophage phenotype by cell shape. Proc Natl Acad Sci U S A 2013;110:17253-17258.

[98] Yahyouche A, Zhidao X, Czernuszka JT, Clover AJ. Macrophage-mediated degradation of crosslinked collagen scaffolds. Acta Biomater 2011;7:278-286.

[99] Xing S, Waddell J, Boynton E. Changes in macrophage morphology and prolonged cell viability following exposure to polyethylene particulate in vitro. Microsc Res Tech 2002;57:523-529.

[100] Buchacher T, Ohradanova-Repic A, Stockinger H, Fischer M, Weber V. M2 polarization of human macrophages favors survival of the intracellular pathogen Chlamydia pneumoniae. PLoS One 2015;10:e0143593.

[101] Féréol S, Fodil R, Labat B, Galiacy S, Laurent VM, Louis B, et al. Sensitivity of alveolar macrophages to substrate mechanical and adhesive properties. Cell Motil Cytoskeleton 2006;63:321-340.

[102] Sridharan R, Cameron AR, Kelly DJ, Kearney CJ, O'Brien FJ. Biomaterial based modulation of macrophage polarization: A review and suggested design principles. Materials Today 2015;18:313-325.

[103] Brodbeck WG, Shive MS, Colton E, Ziats NP, Anderson JM. Interleukin-4 inhibits tumor necrosis factor-alpha-induced and spontaneous apoptosis of biomaterial-adherent macrophages. J Lab Clin Med 2002;139:90-100.

[104] Chen S, Jones JA, Xu Y, Low HY, Anderson JM, Leong KW. Characterization of topographical effects on macrophage behavior in a foreign body response model. Biomaterials 2010;31:3479-3491.

[105] Anderson JM, Rodriguez A, Chang DT. Foreign body reaction to biomaterials. Semin Immunol 2008;20:86-100.

[106] Damink LHHO, Dijkstra PJ, van Luyn MJA, van Wachem PB, Nieuwenhuis P, Feijen J. Crosslinking of dermal sheep collagen using hexamethylene diisocyanate. J Mater Sci Mater Med 1995;6:429-434.

[107] Gustafson HH, Holt-Casper D, Grainger DW, Ghandehari H. Nanoparticle Uptake: The Phagocyte Problem. Nano today 2015;10:487-510.

[108] Yu SS, Lau CM, Thomas SN, Jerome WG, Maron DJ, Dickerson JH, et al. Size- and charge-dependent non-specific uptake of PEGylated nanoparticles by macrophages. International Journal of Nanomedicine 2012;7:799-813.

[109] Oh N, Park J-H. Endocytosis and exocytosis of nanoparticles in mammalian cells. International Journal of Nanomedicine 2014;9:51-63.

[110] Makino K, Yamamoto N, Higuchi K, Harada N, Ohshima H, Terada H. Phagocytic uptake of polystyrene microspheres by alveolar macrophages: effects of the size and surface properties of the microspheres. Colloids and Surfaces B: Biointerfaces 2003;27:33-39.

[111] Orenstein SB, Qiao Y, Klueh U, Kreutzer DL, Novitsky YW. Activation of human mononuclear cells by porcine biologic meshes in vitro. Hernia 2010;14:401-407.

[112] Cha BH, Shin SR, Leijten J, Li YC, Singh S, Liu JC, et al. Integrin-Mediated Interactions Control Macrophage Polarization in 3D Hydrogels. Adv Healthc Mater 2017;6:Epub.

[113] Veres SP, Brennan-Pierce EP, Lee JM. Macrophage-like U937 cells recognize collagen fibrils with strain-induced discrete plasticity damage. J Biomed Mater Res A 2015;103:397-408.

[114] Londono R, Dziki JL, Haljasmaa E, Turner NJ, Leifer CA, Badylak SF. The effect of cell debris within biologic scaffolds upon the macrophage response. J Biomed Mater Res A 2017;105:2109-2118.

[115] Kerby GS, Cottin V, Accurso FJ, Hoffmann F, Chan ED, Fadok VA, et al. Impairment of macrophage survival by NaCl: Implications for early pulmonary inflammation in cystic fibrosis. Am J Physiol Lung Cell Mol Physiol 2002;283:L188-L197.

[116] Cuschieri J, Gourlay D, Garcia I, Jelacic S, Maier RV. Hypertonic preconditioning inhibits macrophage responsiveness to endotoxin. J Immunol 2002;168:1389-1396.

Chapter 3: Collagen cross-linking

Sections of this chapter have been published at:

Delgado LM, Fuller K, Zeugolis DI. *Collagen Cross-Linking: Biophysical, Biochemical, and Biological Response Analysis.* Tissue Eng Part A. 2017;23(19-20):1064-1077.

3.1. Introduction

Collagen, in the form of tissue grafts or reconstituted scaffolds, is one of the most widely used biomaterial in tissue engineering applications due to its natural composition, favourable mechanical properties, low antigenicity and well-tolerated degradation products [1-5]. In addition, collagen-based materials provide biological cues that support cell attachment, proliferation and growth, ultimately promoting functional repair and regeneration of tissues and organs *in vivo* [6, 7]. Exogenous cross-linking methods, primarily chemical in nature, are customarily used as a means to control the mechanical stability and the degradation rate of collagen-based biomaterials. However, chemical cross-linking of collagen is associated with a predominant pro-inflammatory macrophage response, inhibition of macrophage polarisation, reduced cell infiltration, increased pro-inflammatory cytokine expression and delayed wound healing, resulting in cytotoxicity, reduced biocompatibility and peri-implantation fibrosis [7-10].

The mechanism behind the inflammatory and wound healing response to collagen cross-linking is still poorly understood. Macrophages have been described as a ‘rapid response’ cell type, with crucial role in coordinating later inflammatory response and regeneration phases following implantation [11]. Interestingly, recent studies indicate that macrophage response can be modulated by the physicomechanical properties of an engineered scaffold and, in particular, the architectural [12, 13], topographical [14] and chemical [15] properties that can be variably affected as a function of the cross-linking method employed.

Macrophage phenotype switching is controlled by numerous factors, including disease and disease state, drugs, growth factors, cytokines, chemokines, hormones, cell shape, scaffold present and its properties [16-21]. Through direct interactions

[12] and via released by-products [22], cross-linked collagen devices directly modulate macrophage response *in vitro*. M1 macrophages (pro-inflammatory or classically activated) are activated by bacterial lipopolysaccharide (LPS), tumour necrosis factor α (TNF-α) and interferon γ (IFN-γ) to stimulate the secretion of large amounts of pro-inflammatory interleukin (e.g. IL-1α, IL-1β, IL-6, IL-8, IL-12, IL-23) and TNF-α cytokines, reactive oxygen species and matrix metalloproteinases to attack and phagocytise pathogens or foreign matter [23-25]. M2 macrophages (anti-inflammatory or alternatively activated) are activated by IL-4, IL-10 and IL-13 or a combination of these, to produce IL-1ra, IL-4, IL-10, IL-13, vascular endothelial growth factor (VEGF), transforming growth factor β (TGF-β), arginase and scavenging molecules [23-25]. Critically, M2 macrophages display differential functions according to the cellular sub-phenotype [e.g. anti-inflammatory (M2a), homeostatic (M2b) and pro-wound healing (M2c)]. In instances that macrophages fail to remodel the substrate or to degrade foreign matter (frustrated phagocytosis), they aggregate and form foreign body giant cells, which are generally accepted as cells with higher degradation / resorption capacity than monocytes / macrophages. Furthermore, giant cells are related to peri-implantation fibrosis and foreign body response [26, 27], often encountered with heavily cross-linked collagen devices. The mechanism behind this transformation is unclear, however, hydrophobicity, ionic charge and soluble fusion mediators (e.g. receptor activator of nuclear factor kappa-B ligand, macrophage colony-stimulating factor, TNF-α, IL-1, IL-4, IL-13) are believed to be important in the formation of foreign body giant cells [28].

Customarily used collagen cross-linking approaches, such as glutaraldehyde (GTA) and 1-ethyl-3-(3-dimethylaminopropyl) carbodiimide (EDC), have been associated with cytotoxicity [29, 30], calcification [31, 32] and foreign body response [8, 33].

To this end, the use of alternative methods [multi-branched polyethylene glycol (PEG) polymers [34, 35] and plant extracts (e.g. genipin (GEN) [36], myrica rubra [37], oleuropein (OLE) [38]] has been advocated as a means to enhance mechanical and enzymatic stability, whilst reducing cytotoxicity. However, their immune response has yet to be assessed. Herein, the structural, physical and biological properties of non-cross-linked (NCL) and GTA, EDC, 4-arm PEG succinimidyl glutarate (4SP), GEN and OLE cross-linked collagen films were assessed.

3.2. Materials and methods

3.2.1. Materials

Bovine Achilles tendons were collected from a local abattoir (steers aged 24 months). 4-arm polyethylene glycol (PEG) succinimidyl glutarate (4SP, Mw 10,000), genipin (GEN) and oleuropein (OLE) were purchased from JenKem Technology (USA), Challenge Bioproducts (Taiwan), and Extrasynthese (France), respectively. All other materials and reagents were purchased from Sigma-Aldrich (Ireland), unless otherwise stated.

3.2.2. Type I collagen isolation

Bovine type I collagen was extracted from Achilles tendons by adapting a previously described protocol [39]. Briefly, the tendons were manually separated from the surrounding fascia, cryo-milled (Freezer/Mill 6870, SPEX SamplePrep, USA) and washed with 1X phosphate buffered saline (PBS) solution. Milled tendon tissue was dissolved in 1.0 M acetic acid under orbital agitation for 48 hours at 4 °C. Subsequently, pepsin (from porcine gastric mucosa) was added in the solution at ratio of 80 U/mg of milled tendon. The solution was incubated at 4 °C for 72 hours under stirring. Insoluble tendon was separated by filtration and centrifugation (21,000 g at 4°C for 20 min). Collagen solution was purified by repeated salt precipitation (0.9 M NaCl), centrifugation and re-suspension in 1.0 M acetic acid. The final atelocollagen solution was dialysed (Mw 8,000 cut off) against 1 mM acetic acid and the final solution was kept at 4°C. Collagen concentration was determined using hydroxyproline assay (~5 mg/ml) [40] and collagen purity was assessed using sodium dodecyl sulphate polyacrylamide gel electrophoresis (SDS-PAGE) followed by silver staining [41] (**Figure 3.1**).

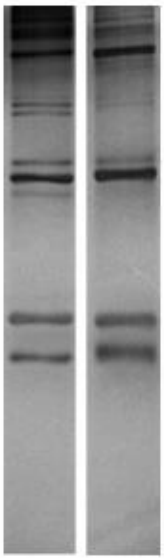

Figure 3.1. The purity of the extracted type I collagen was assessed using sodium dodecyl sulphate polyacrylamide gel electrophoresis (SDS-PAGE) followed by silver staining. SDS-PAGE analysis revealed the purity of the extracted collagen solution (left lane) was ~ 96 %, similar to commercially available BD Biosciences (right lane) type I collagen (~ 97 %).

3.2.3. Collagen film fabrication

Typical protocols for the fabrication of collagen films were followed [42], with slight modifications. Briefly, the pH of the collagen solution was adjusted to ~ 7.3 using 1.0 M NaOH and 10X PBS. Cross-linking was conducted as per established protocols (**Table 3.1**) in order to obtain about 80% free amine reduction. The final solutions were placed in silicone moulds and incubated for 1 hour at 37 °C to induce gelation. Subsequently, the water content was evaporated overnight at 25 °C.

Table 3.1. Cross-linking methods employed to stabilise collagen films in order to obtain about 80% free amine reduction. Treatments: non-cross-linked collagen film (NCL), collagen films cross-linked with glutaraldehyde (GTA), carbodiimide (EDC), 4-arm PEG succinimidyl glutarate (4SP), genipin (GEN) and oleuropein (OLE).

Cross-linking agent	Method	Ref.
NCL	No cross-linker in 1X PBS	-
GTA	0.625 % in 1X PBS	[36]
EDC	50 mM EDC / 10 mM N-hydroxysuccinimide (NHS) in 50 mM 2 (N-morpholino) ethanesulfonic acid (MES) in 1X PBS	[36]
4SP	1 mM in 1X PBS	[43]
GEN	0.625 % in 1X PBS	[36]
OLE	5.0 % in 1X PBS (After activation with 0.5 U/ml β-glucosidase at 25 ºC for 2 hours)	[38]

3.2.4. Structural characterisation

Morphological analysis of the produced films was analysed using a Stereo Microscope (SZX16, Olympus, UK) and a Hitachi S-4700 Scanning Electron Microscope (SEM, Hitachi, UK). Prior to SEM analysis, collagen films were incubated in 1X PBS overnight, dehydrated in ascending ethanol concentrations (50 %, 70 %, 90 %, 96 % and 100 %) and gold-coated (Emitech K-550X Sputter Coater, Emitech, UK).

3.2.5. Quantification of free amines

Free amines were quantified using ninhydrin assay, as has been described previously [44]. Briefly, ~ 3 mg of each film were mixed with 200 μl of deionised water and 1 ml of running buffer, which contained one part of 4 % (w/v) ninhydrin in 2-ethoxyethanol and one part 200 mM citric acid with 0.16 % (w/v) tin (II) chloride at pH 5.0. The mixtures were incubated at 95 °C for 30 min. The reaction was stopped by cooling down in ice and the addition of 250 μl of 50 % isopropanol. After vortexing, the absorbance was read at 570 nm (Varioskan Flash Multimode Reader, Thermo Scientific). Glycine, at different concentrations, was used for the standard curve and the % of free amines of each condition was normalised against to the NCL collagen films.

3.2.6. Quantification of denaturation temperature

The denaturation temperature was evaluated using a differential scanning calorimeter (DSC-60, Shimadzu, Japan), as has been described previously [45]. Briefly, collagen films were incubated in 1X PBS at room temperature overnight and then, they were quickly blotted using filter paper to remove surface / unbound water. The samples

were then hermetically sealed in aluminium pans and were subjected to a single constant heating ramp at 5 °C/min in the range of 25 to 90 °C. An empty pan was used as reference. Denaturation temperature was determined as the maximum heat absorption of the endothermic peak.

3.2.7. Quantification of enzymatic degradation

Resistance to enzymatic degradation was quantified as has been described previously [46]. Briefly, collagen films were weighed and hydrated for 2 hours in 0.1 M Tris-HCl and 5 mM $CaCl_2$ at pH 7.4. Subsequently, the films were incubated in 10 U/ml bacterial collagenase type IV (*Clostridium histolyticum*), reconstituted in the same buffer. After 24 hours of incubation at 37 °C, centrifugation was carried out (10,000g for 5 min), the supernatant was removed, the remaining films were freeze-dried and weighed. Enzymatic degradation was quantified as weight loss.

3.2.8. Quantification of mechanical properties

Uniaxial tensile test of hydrated (overnight incubation at 37 °C in phosphate buffer saline and brief bloating in tissue paper prior to testing to remove surface liquid) films was performed using an electromechanical testing machine (Z2.5, Zwick, Germany). Uniform strips were prepared and, using a micrometer screw gauge, the width and thickness of the samples were measured. The grips of the testing machine were covered with a rubber film to avoid breakage at contact points. Samples that broke at contact points were excluded. The grips were set at 20 mm distance. The samples were deformed to complete failure (deformation rate of 10 mm/min, 10 N static load cell). The following parameters were assessed: force at break, stress at break, strain at break and elastic modulus.

3.2.9. Human skin fibroblast response

Basic cellular functions were assessed using human skin fibroblasts [WS1, American Type Culture Collection (ATCC), USA]. WS1 fibroblasts were grown in Eagle's Minimum Essential Medium supplemented with 10 % foetal bovine serum (FBS), 1 % penicillin and streptomycin. Films were sterilised in 70 % ethanol for 30 minutes, followed by three washes in sterilised Hank's Balanced Salt Solution (HBSS). Cells were seeded onto the samples at 16 x 10^3 cells/cm^2 and incubated at 37 °C, 5 % CO_2 and 95 % humidified air for 1, 3 and 7 days. Phase contrast microscopy images were obtained using an inverted microscope (Leica microsystem, Germany) and images were analysed with the LAS EZ 2.0.0 software. Cell proliferation was assessed using Quant-iT™ PicoGreen® dsDNA kit (Invitrogen, USA), as per manufacturer's guidelines. Cell metabolic activity was assessed after two hours incubation at 37 °C with 10 % alamarBlue® (Invitrogen, USA), as per manufacturer's protocol. Cell metabolic activity was expressed in terms of % reduction of alamarBlue® and normalised considering metabolic activity of cells in tissue culture plastic (TCP) at each time point as 100 %. Cell viability was evaluated using Live/Dead® assay. Briefly, samples were incubated in HBSS with 4 μM calcein and 2 μM ethidium homodimer for 30 min. Stained samples were visualised using an inverted fluorescence microscope (IX 51, Olympus, UK). Five images were captured per film. Viable (green) and dead (red) cells were counted using ImageJ 1.48v software (National Institutes of Health, USA).

3.2.10. Human macrophage response and cytokine release

Human derived leukemic monocyte cells (THP-1, ATCC, USA) were grown in RPMI-1640 supplemented with 10 % FBS, 1 % penicillin and streptomycin. Cells

were seeded onto the various samples at 26 x 10^3 cells/cm^2 and mature macrophage-like state was induced through treatment with phorbol 12-myristate 13-acetate (PMA) at 100 ng/ml for 6 hours, as has been described previously [47-49]. Subsequently, adherent cells were washed with HBSS and incubated with supplemented media at 37 °C, 5 % CO_2 and 95 % humidified air for 1 and 2 days. Activated positive control phenotype was induced with 100 ng/ml of LPS in supplemented media for 24 hours. Cell proliferation and metabolic activity were determined as described in section 3.2.9. Cellular viability was quantified using CytoTox 96® Non-Radioactive Cytotoxicity Assay (Promega, USA) to measure released lactate dehydrogenase (LDH) in the supernatant from dead cells. Phase contrast microscopy images were obtained using an inverted microscope (Leica microsystem, Germany) and images were analysed with the LAS EZ 2.0.0 software.

Inflammatory cytokines (IL-1β, IL-4, IL-6, IL-8, IL-10, IL-12p70, IL-13, TNF-α, VEGF) were measured using Meso Scale Discovery (MSD, USA) electrochemoluminescense assay, as per manufacturer's guidelines. Briefly, cell free supernatants of each sample and supplied standard curve were incubated on MSD plates for 2 hours followed by a wash. The plates were then incubated with detection antibody solution for 2 hours. Subsequently, the plates were washed and read using a Meso™ QuickPlex SQ120 instrument (MSD).

The potential effect of released / degradation sub-products of cross-linked collagen films was investigated using the pre-conditioned media. Cross-linked films were incubated in supplemented RPMI-1640 media at 37 °C and 5 % CO_2 for 6 days prior to be exposed to cells. THP-1 cells were seeded at 26 x 10^3 cells/cm^2 with 100 ng/ml of PMA for 6 hours. Subsequently, plastic-adherent cells were washed with HBSS and incubated with pre-conditioned media at 37 °C, 5 % CO_2 and 95 % humidified

air for 48 hours. An activated control was induced with 100 ng/ml of LPS for 24 hours. Characterisation of macrophage cells was performed as described above.

3.2.11. Statistical analysis

All experiments were carried out in triplicate, except swelling, denaturation temperature and tensile test assays that were carried out in quintuplicate. Numerical data are expressed as mean ± standard deviation. Statistical analysis was performed using MINITAB® (version 16.2, Minitab Inc., USA). One way analysis of variance (ANOVA) followed by Fisher's post-hoc test were employed after confirming normal distribution from each sample population (Anderson-Darling normality test) and the equality of variances (Bartlett's and Levene's tests for homogeneity of variance). Nonparametric statistics were used when either or both of the above assumptions were violated and, consequently, Kruskal-Wallis for multiple comparison analysis was carried out. Statistical significance was accepted at $p < 0.05$.

3.3. Results

3.3.1. Structural characterisation

Non-cross-linked collagen films (NCL) and cross-linked collagen films with carbodiimide (EDC) and 4-arm PEG succinimidyl glutarate (4SP) were colourless and totally transparent, glutaraldehyde (GTA) and oleuropein (OLE) cross-linking made the films yellow / brown and semi-transparent and genipin (GEN) cross-linking resulted in dark blue and totally opaque films (**Figure 3.2**). SEM analysis revealed that NCL and 4SP cross-linked films maintained the fibrillar structure of collagen, which was diminished in EDC, GTA, GEN and OLE cross-linked films (**Figure 3.2**).

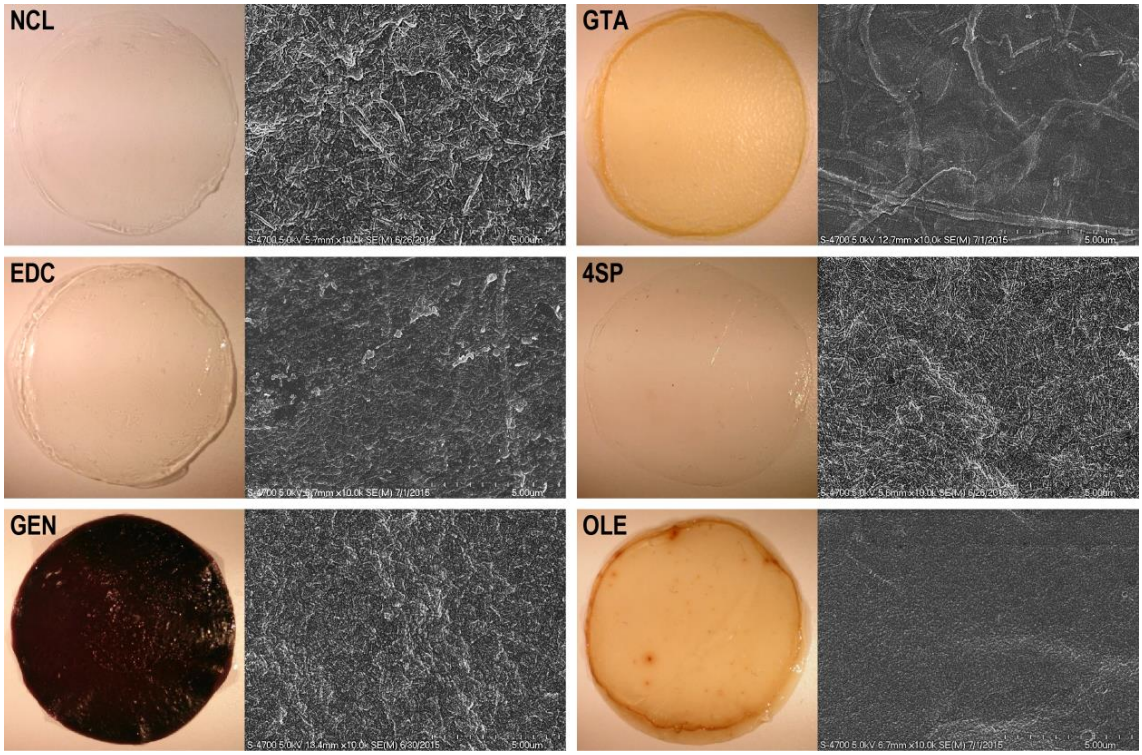

Figure 3.2. Optical and SEM images of the different collagen films. NCL, EDC and 4SP films were colourless, whilst GTA and OLE cross-linking induced a yellow / brown hue and GEN cross-linking resulted in dark blue hue. SEM analysis revealed that only NCL and 4SP cross-linked films maintained the fibrillar structure of collagen. Treatments: non-cross-linked collagen film (NCL), collagen films cross-linked with glutaraldehyde (GTA), carbodiimide (EDC), 4-arm PEG succinimidyl glutarate (4SP), genipin (GEN) and oleuropein (OLE).

3.3.2. Quantification of free amines

Collagen cross-linking involves the formation of covalent bonds between the free amine or carboxyl groups of collagen with the cross-linking agent; reduction in free amines can be used as a cross-linking efficiency indicator. A significant ($p < 0.001$) decrease in free amine groups was observed for all cross-linked collagen films (**Figure 3.3**). Among the cross-linked groups, GTA, EDC, 4SP and GEN brought about an approximate 80 % reduction in free amines, whilst OLE induced an approximate 40 % reduction in the amount of free amines (**Figure 3.3**).

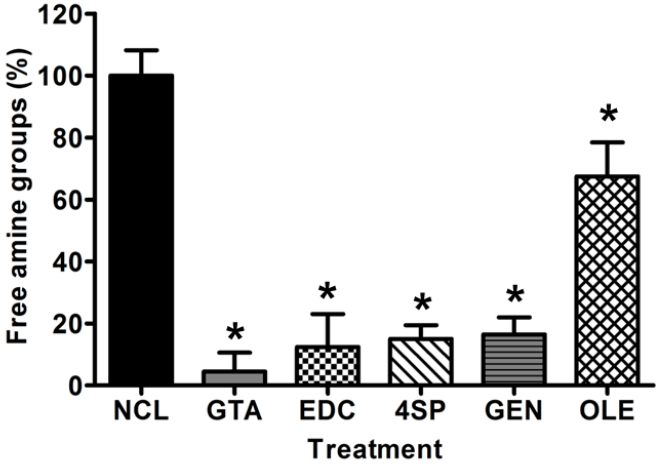

Figure 3.3. Quantification of free amine group of collagen films cross-linked with glutaraldehyde (GTA), carbodiimide (EDC), 4-arm PEG succinimidyl glutarate (4SP), genipin (GEN) and oleuropein (OLE); non-cross-linked collagen film (NCL) was used as control. *: Denotes significant difference ($p < 0.05$) from the control group (NCL).

3.3.3. Quantification of denaturation temperature

DSC analysis revealed that all cross-linking methods, but EDC ($p > 0.05$), significantly increased ($p < 0.001$) the denaturation temperature of the produced collagen films, as compared to the NCL films (**Figure 3.4**).

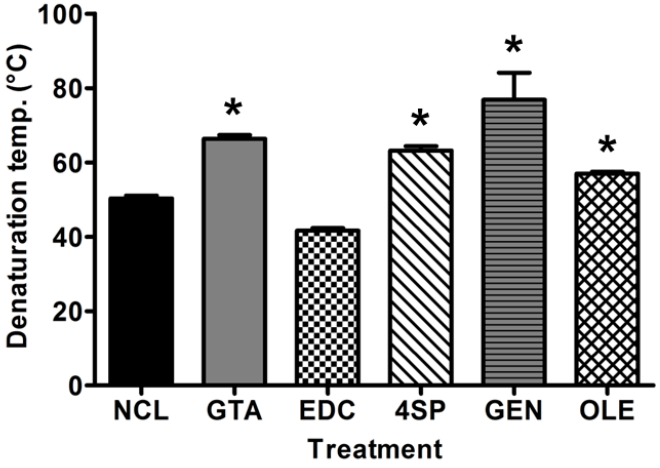

Figure 3.4. Denaturation temperature measured by differential scanning calorimetry (DSC) of collagen films cross-linked with glutaraldehyde (GTA), carbodiimide (EDC), 4-arm PEG succinimidyl glutarate (4SP), genipin (GEN) and oleuropein (OLE); non-cross-linked collagen film (NCL) was used as control. *: Denotes significant difference ($p < 0.05$) from the control group (NCL).

3.3.4. Quantification of enzymatic degradation

In vitro enzymatic degradation analysis (**Figure 3.5**) revealed that NCL, EDC and OLE films were almost completely degraded within 24 h, whilst GTA, 4SP and GEN induced a very high resistance to enzymatic degradation (less than 20 % was degraded).

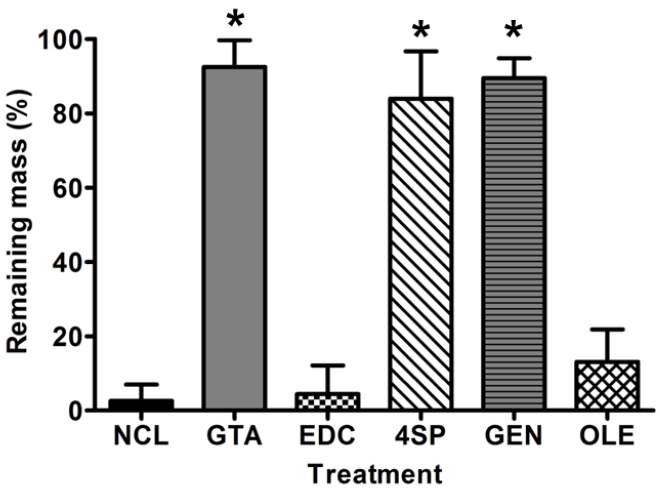

Figure 3.5. Degradation by collagenase after 24 hours incubation. of collagen films cross-linked with glutaraldehyde (GTA), carbodiimide (EDC), 4-arm PEG succinimidyl glutarate (4SP), genipin (GEN) and oleuropein (OLE); non-cross-linked collagen film (NCL) was used as control. *: Denotes significant difference ($p < 0.05$) from the control group (NCL).

3.3.5. Quantification of mechanical properties

Stress-strain curves consisted of a small toe region, a region of steeply rising stress and a long region of constant gradient until fracture (**Figure 3.6**). GEN stabilised films exhibited the highest ($p < 0.001$) force at break, stress at break and E modules values, whilst EDC cross-linked films exhibited the highest ($p < 0.001$) strain at break values (**Table 3.2**). EDC stabilised films exhibited the lowest ($p < 0.001$) force at break, stress at break and E modules values, whilst GTA cross-linked films exhibited the lowest ($p < 0.001$) strain at break values (**Table 3.2**).

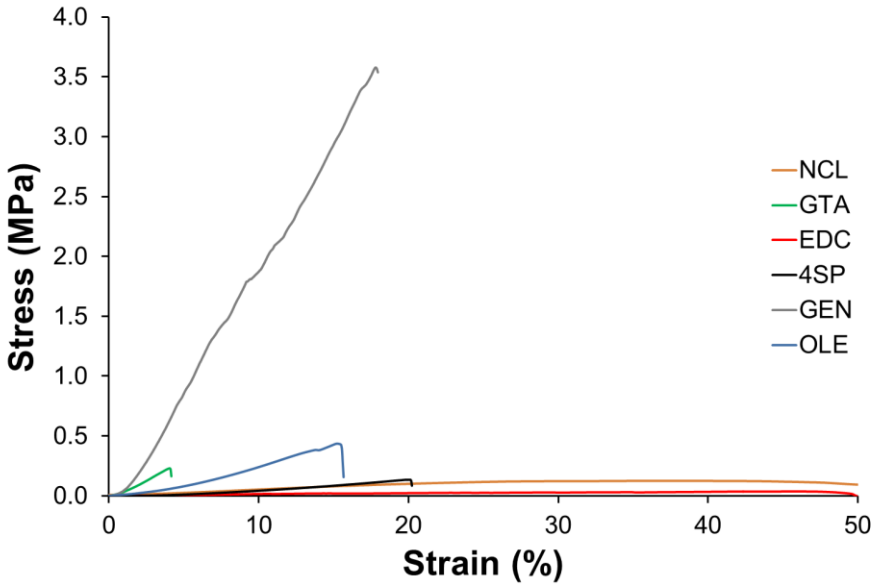

Figure 3.6. Tensile test stress-strain deformation mechanism of the produced collagen films. Stress-strain curves consisted of a small toe region, a region of steeply rising stress and a long region of constant gradient until fracture. Treatments: non-cross-linked collagen film (NCL), collagen films cross-linked with glutaraldehyde (GTA), carbodiimide (EDC), 4-arm PEG succinimidyl glutarate (4SP), genipin (GEN) and oleuropein (OLE).

Table 3.2. Mechanical data of the produced collagen films. The highest ($p < 0.001$; +) force at break, stress at break, strain at break and E modules values were obtained from the GEN, GEN, EDC and GEN cross-linked films, respectively. The lowest ($p < 0.001$; #) force at break, stress at break, strain at break and E modules values were obtained from the EDC, EDC, GTA and EDC cross-linked films, respectively. Treatments: non-cross-linked collagen film (NCL), collagen films cross-linked with glutaraldehyde (GTA), carbodiimide (EDC), 4-arm PEG succinimidyl glutarate (4SP), genipin (GEN) and oleuropein (OLE).

Cross-linking agent	Force at break (N/cm)	Stress at break (MPa)	Strain at break (%)	E Modulus (MPa)
NCL	0.35 ± 0.09	0.10 ± 0.03	40.82 ± 13.52	0.64 ± 0.63
GTA	0.26 ± 0.11	0.13 ± 0.09	5.77 ± 2.51 #	3.51 ± 2.47
EDC	0.23 ± 0.06 #	0.03 ± 0.01 #	51.60 ± 4.49 +	0.08 ± 0.02 #
4SP	0.47 ± 0.24	0.08 ± 0.04	15.22 ± 3.84	0.45 ± 0.13
GEN	5.59 ± 1.10 +	3.28 ± 1.37 +	16.49 ± 4.50	20.21 ± 5.01 +
OLE	1.22 ± 0.66	0.41 ± 0.22	15.46 ± 1.87	2.02 ± 0.89

3.3.6. Human skin fibroblast response

Phase contrast microscopy analysis revealed that human skin fibroblasts maintained their spindle-shaped morphology, independently of the cross-linking method and culture time (**Figure 3.7**). By day 7, DNA quantification [**Figure 3.8A**; only OLE was significantly higher ($p < 0.001$) to the non-cross-linked control], cell metabolic activity (**Figure 3.8B**) and cell viability (**Figure 3.8C**) assays revealed no apparent differences between the non-cross-linked and cross-linked groups ($p > 0.05$).

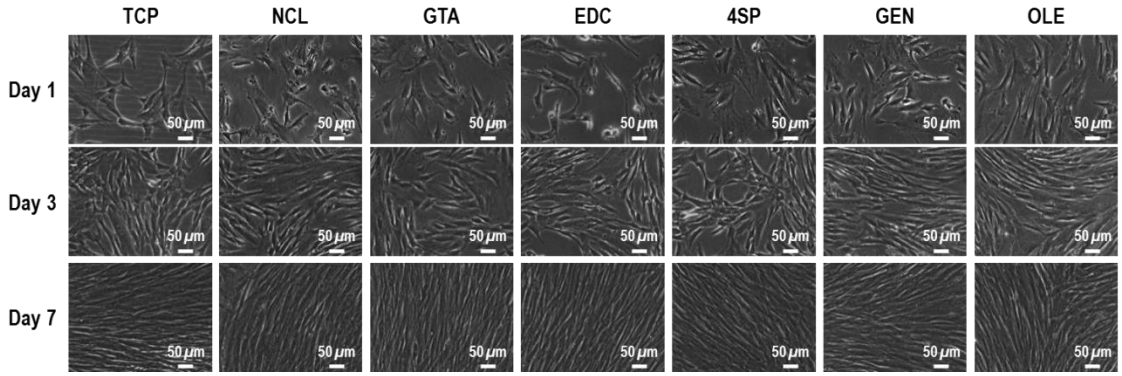

Figure 3.7. Phase contrast microscopic images of human skin fibroblasts cultured onto cross-linked collagen films for 1, 3 and 7 days. Human skin fibroblasts maintained their spindle-shaped morphology, independently of the treatment and the time in culture. Treatments: non-cross-linked collagen film (NCL), collagen films cross-linked with glutaraldehyde (GTA), carbodiimide (EDC), 4-arm PEG succinimidyl glutarate (4SP), genipin (GEN) and oleuropein (OLE). Tissue culture plastic (TCP) was used as control.

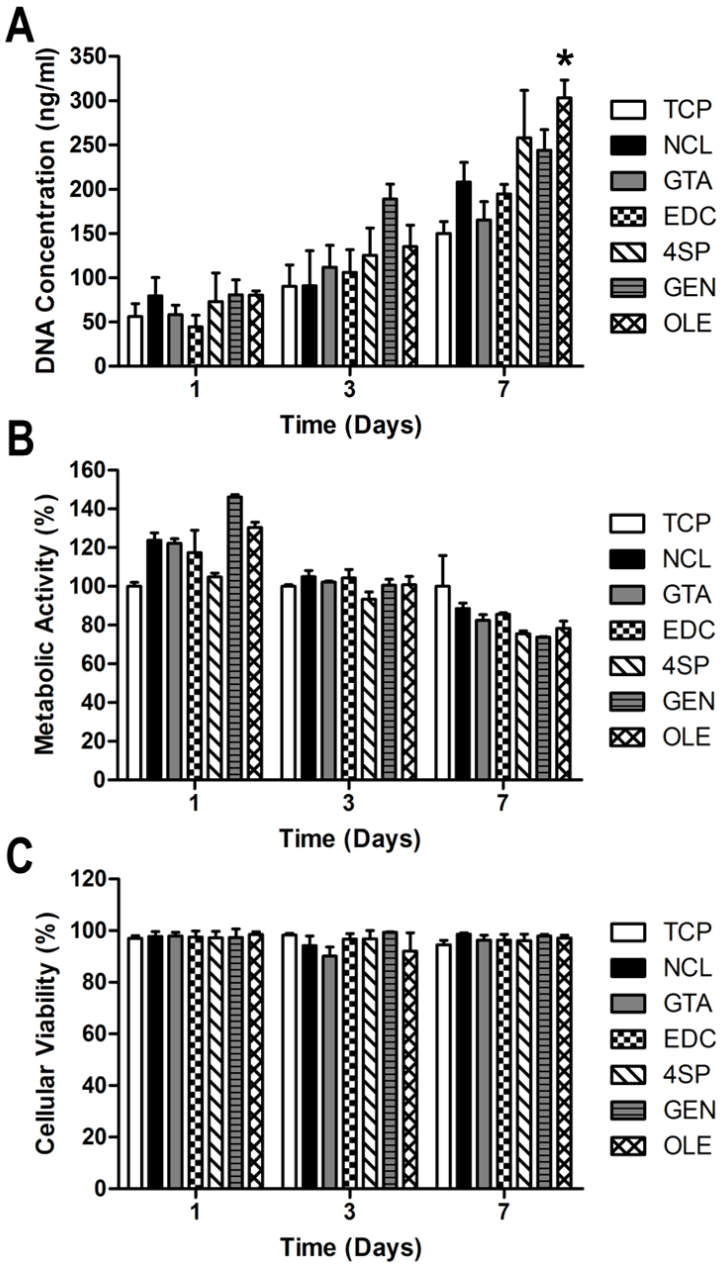

Figure 3.8. Human skin fibroblasts onto cross-linked collagen films after 1, 3 and 7 days of culture. Cellular proliferation was assessed through DNA concentration quantification **(A)**. Metabolic activity was assessed using alamarBlue® **(B)**. Cellular viability was assessed via Live/Dead® **(C)**. Treatments: non-cross-linked collagen film (NCL), collagen films cross-linked with glutaraldehyde (GTA), carbodiimide (EDC), 4-arm PEG succinimidyl glutarate (4SP), genipin (GEN) and oleuropein (OLE). Tissue culture plastic (TCP) was used as control. *: Denotes significant difference ($p < 0.05$) from the control group (NCL).

3.3.7. Human macrophage response and cytokine release

Phase contrast microscopy analysis revealed that by day 2 (a) most macrophages, independently of the treatment and time in culture, adopted a round morphology; (b) some elongated cells were observed on TCP, GEN, LPS, 4SP and OLE; and (c) all treatments, but GTA, formed aggregates (**Figure 3.9**). Cells grown on TCP, LPS and NCL exhibited significantly higher ($p < 0.001$) DNA concentration than cells grown on GTA, EDC, 4SP, GEN at day 1, whilst at day 2, cells grown on TCP, LPS and NCL exhibited significantly higher ($p < 0.001$) DNA concentration than cells grown on GTA, EDC, 4SP, GEN and OLE (**Figure 3.10A**). GTA cross-linked films induced the lowest ($p < 0.001$) cell metabolic activity at both time points, TCP, LPS and OLE induced the highest ($p < 0.001$) cell metabolic activity at day 1 and TCP, LPS, GEN and OLE induced the highest ($p < 0.001$) cell metabolic activity at day 2 (**Figure 3.10B**). GTA cross-linked films induced the lowest cell viability ($p < 0.001$) at both time points, no significant difference was observed between EDC, 4SP, GEN and OLE at both time points (**Figure 3.10C**).

When THP-1 cells were seeded on the various substrates, no significant difference ($p > 0.05$) in secretion of IL-1beta, IL-8, TNF-alpha and VEGF was detected between NCL, 4SP and genipin groups at both time points (**Figure 3.11 and Figure 3.12**). Cytokine release of IL-4, IL-6, IL-12, IL-13 and IL-10 was below the detection limit for all treatments for both time points (**Figure 3.11**). Cytokine release from cells seeded on GTA films was very low (**Figure 3.11**) due to the low cell number (**Figure 3.10C**).

Phase contrast microscopy analysis revealed that by day 2: (a) most macrophages, independently of the treatment, adopted a round morphology; (b) some elongated cells were observed on all samples, but TCP and OLE; and (c) all treatments, but

OLE, formed aggregates (**Figure 3.13**). All cross-linking treatments exhibited significantly higher ($p < 0.05$) DNA concentration (**Figure 3.14A**) and metabolic activity (**Figure 3.14B**) than the NCL counterparts, whilst no significant difference ($p > 0.05$) was observed in cell viability (**Figure 3.14C**). With respect to inflammatory cytokine release, only pre-conditioned media with GTA and OLE cross-linked films significantly increased ($p < 0.05$) IL-8 release (**Figure 3.15**), in comparison to the non-cross-linked samples. No significant difference ($p > 0.05$) was detected for VEGF, TNF-alpha and IL-1beta between the treatments (**Figure 3.15**). Cytokine release of IL-4, IL-6, IL-12, IL-13 and IL-10 was below the detection limit for all treatments (**Figure 3.15** and **Figure 3.16**).

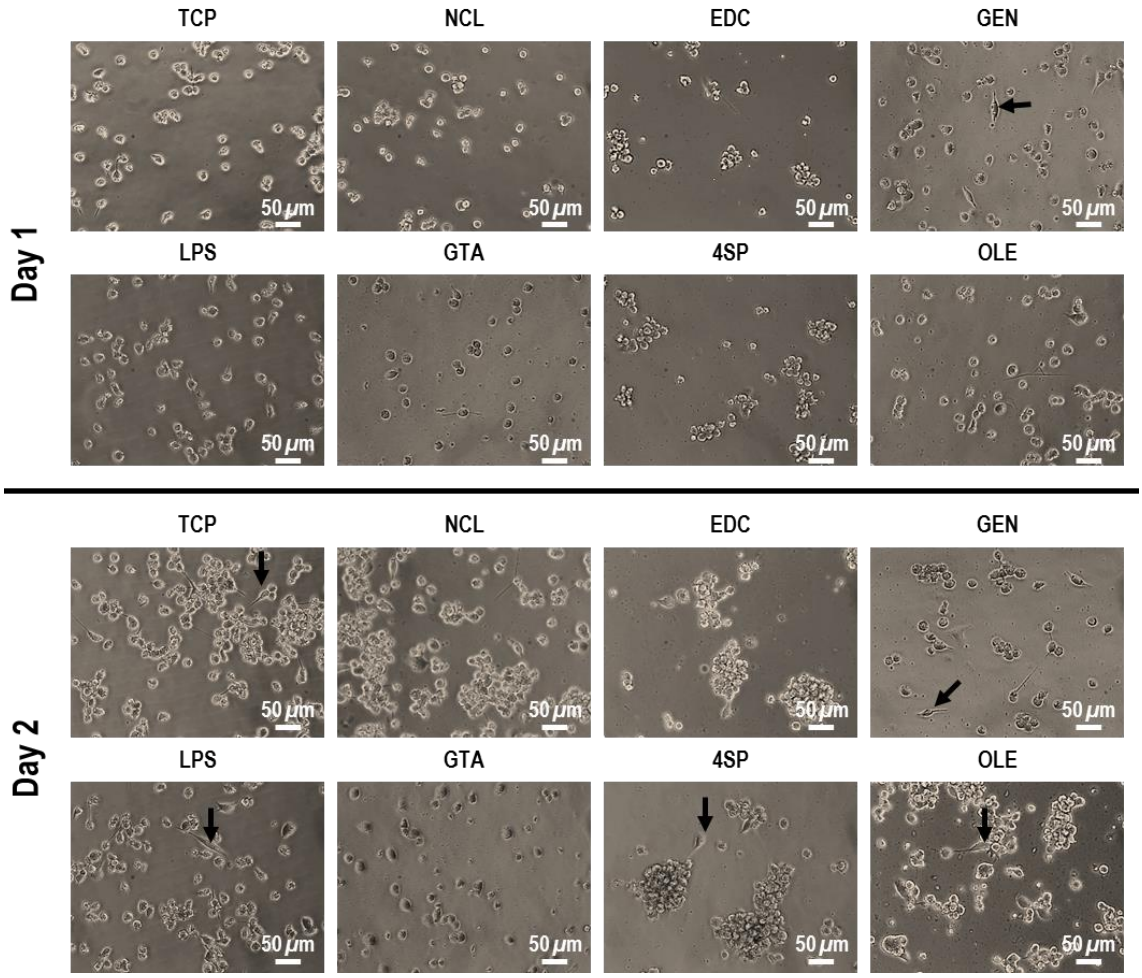

Figure 3.9. Phase contrast microscopic images of THP-1 cells cultured onto cross-linked collagen films for 1 and 2 days. The macrophages adopted a round morphology and formed aggregates, independently of the treatment and time in culture. Some elongated cells were also detected (indicative examples are highlighted using arrows). Treatments: non-cross-linked collagen film (NCL), collagen films cross-linked with glutaraldehyde (GTA), carbodiimide (EDC), 4-arm PEG succinimidyl glutarate (4SP), genipin (GEN) and oleuropein (OLE). Tissue culture plastic (TCP) and LPS stimulated TCP (LPS) were used as controls.

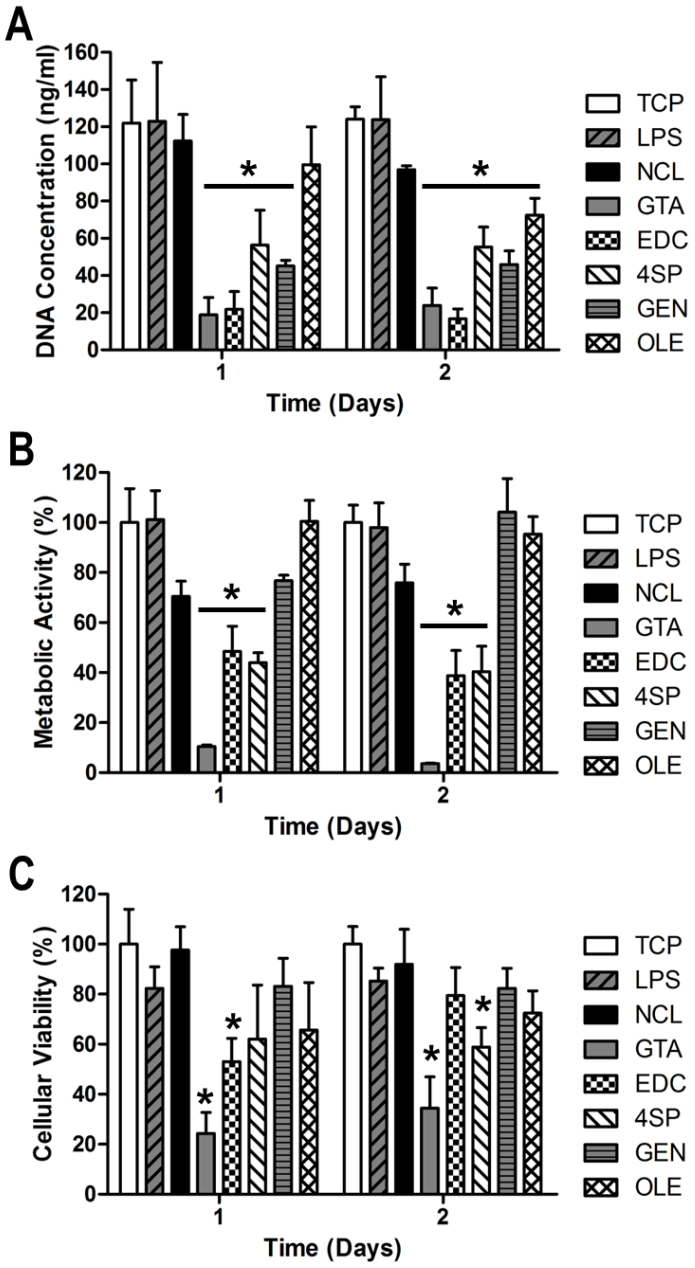

Figure 3.10. THP-1 cells onto cross-linked collagen films after 1 and 2 days of culture. Cellular proliferation was assessed through DNA concentration quantification **(A)**. Metabolic activity was assessed using alamarBlue® **(B)**. Cellular viability was assessed via Live/Dead® **(C)**. Treatments: non-cross-linked collagen film (NCL), collagen films cross-linked with glutaraldehyde (GTA), carbodiimide (EDC), 4-arm PEG succinimidyl glutarate (4SP), genipin (GEN) and oleuropein (OLE). Tissue culture plastic (TCP) and LPS stimulated TCP (LPS) were used as controls. *: Denotes significant difference ($p < 0.05$) from the control group (NCL).

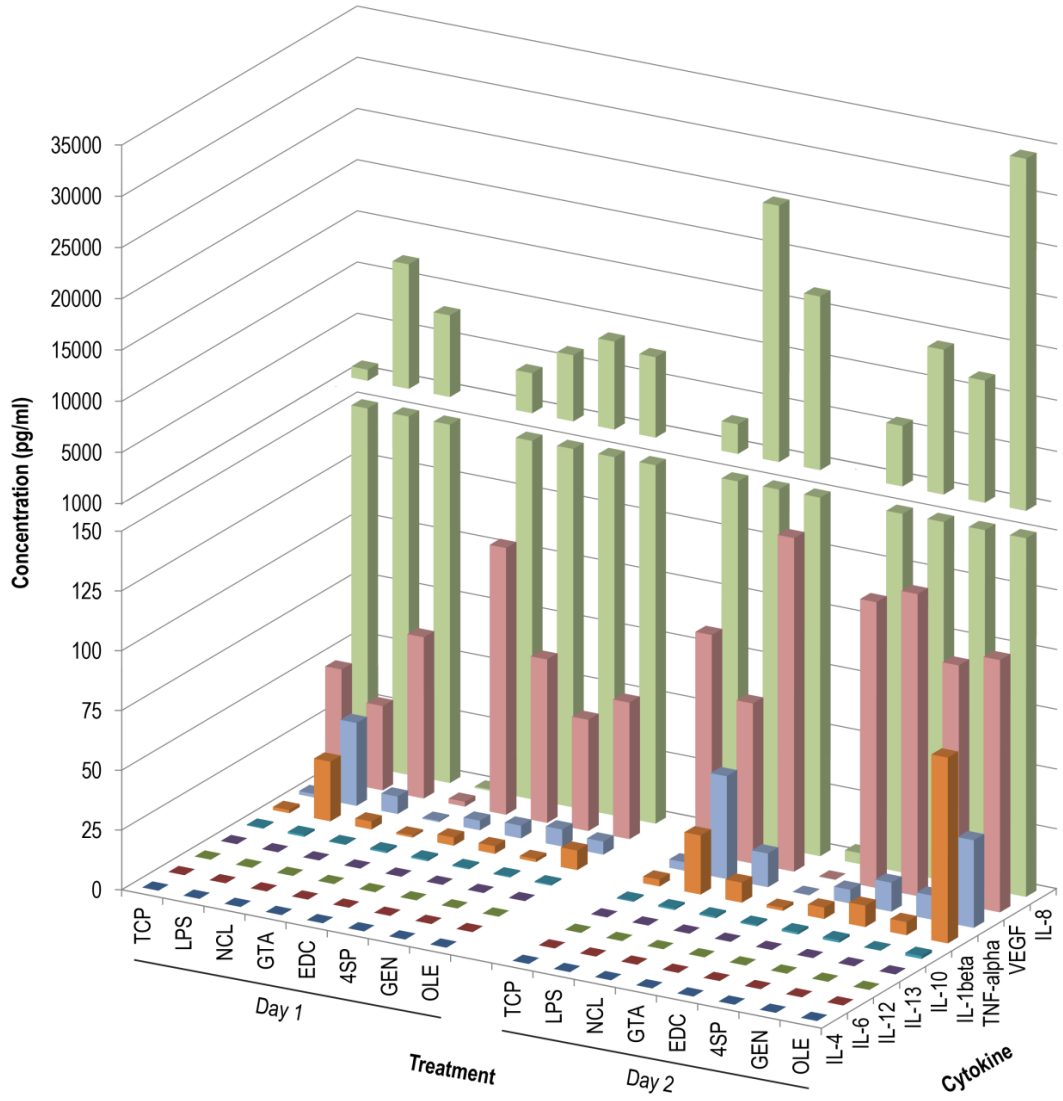

Figure 3.11. Multiplex ELISA on pro- and anti- inflammatory cytokines of THP-1 cells cultured on distinct films for 1 and 2 days. The bar represents the average. Treatments: non-cross-linked collagen film (NCL), collagen films cross-linked with glutaraldehyde (GTA), carbodiimide (EDC), 4-arm PEG succinimidyl glutarate (4SP), genipin (GEN) and oleuropein (OLE). Tissue culture plastic (TCP) and LPS stimulated TCP (LPS) were used as controls.

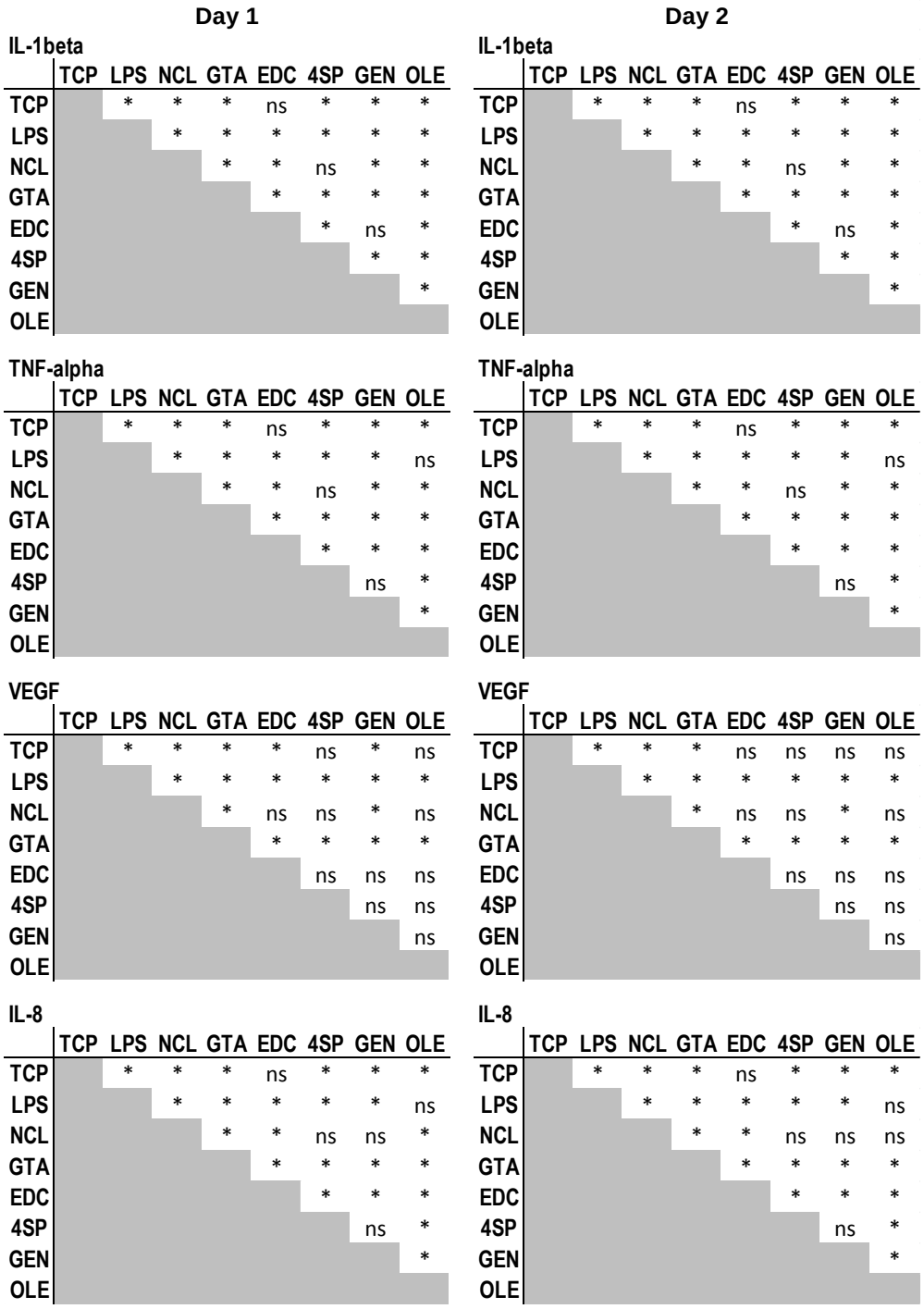

Figure 3.12. Multiplex ELISA, multiple comparison tests for every pair of conditions (* $p < 0.05$, ns: not significant). Treatments: non-cross-linked collagen film (NCL), collagen films cross-linked with glutaraldehyde (GTA), carbodiimide (EDC), 4-arm PEG succinimidyl glutarate (4SP), genipin (GEN) and oleuropein (OLE). Tissue culture plastic (TCP) and LPS stimulated TCP (LPS) were used as controls.

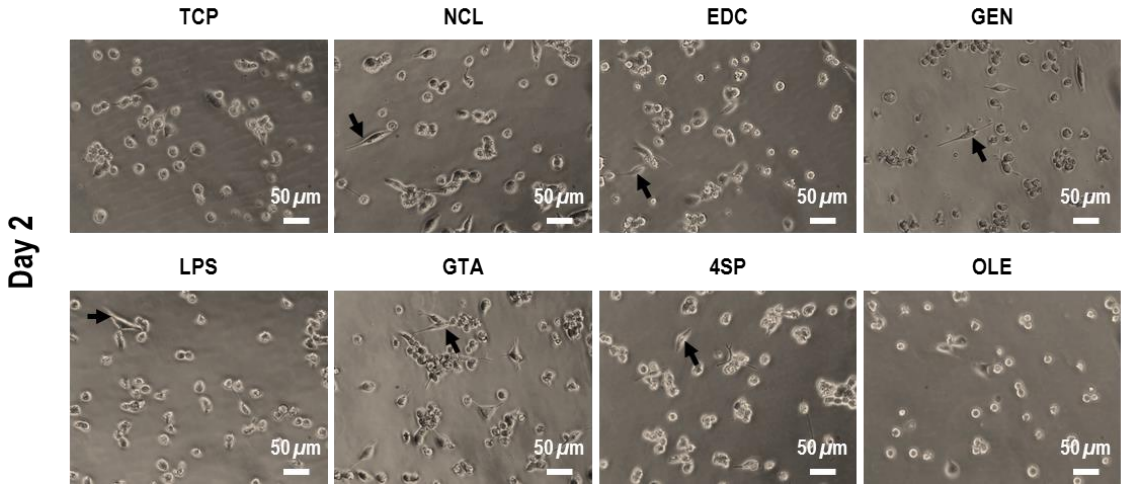

Figure 3.13. Phase contrast microscopic images of THP-1 cells cultured for 2 days with pre-conditioned media from the cross-linked collagen films. Macrophages adopted a round morphology and only cells on GTA films formed aggregates. Some elongated cells were also detected (indicative examples are highlighted using arrows). Treatments: non-cross-linked collagen film (NCL), collagen films cross-linked with glutaraldehyde (GTA), carbodiimide (EDC), 4-arm PEG succinimidyl glutarate (4SP), genipin (GEN) and oleuropein (OLE). Tissue culture plastic (TCP) and LPS stimulated TCP (LPS) were used as controls.

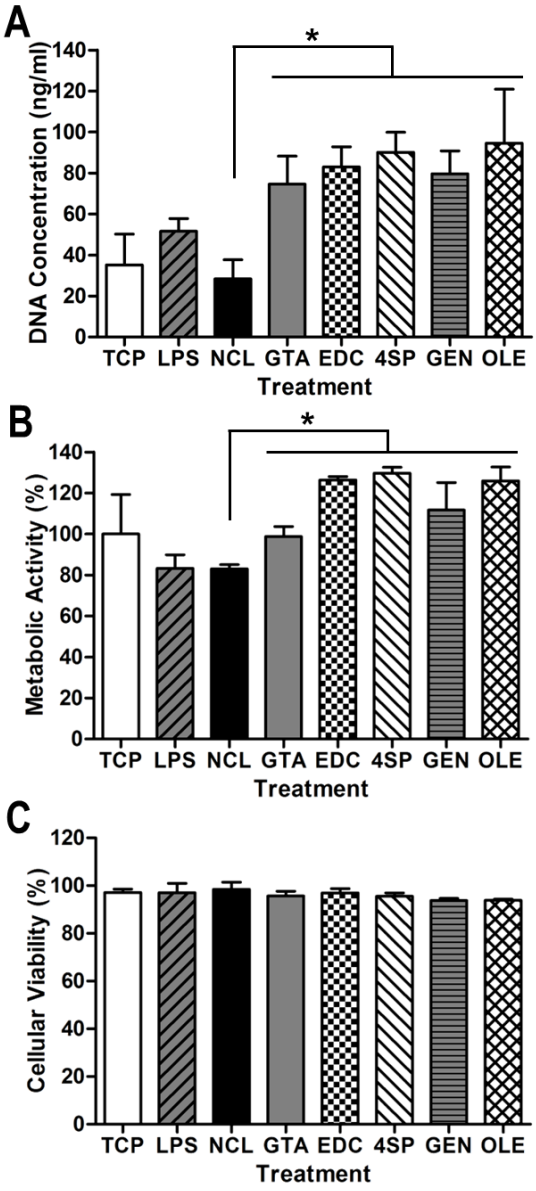

Figure 3.14. THP-1 cells cultured with pre-conditioned media from the cross-linked collagen films after 2 days of culture. Cellular proliferation was assessed through DNA concentration quantification **(A)**. Metabolic activity was assessed using alamarBlue® **(B)**. Cellular viability was assessed via Live/Dead® **(C)**. Treatments: non-cross-linked collagen film (NCL), collagen films cross-linked with glutaraldehyde (GTA), carbodiimide (EDC), 4-arm PEG succinimidyl glutarate (4SP), genipin (GEN) and oleuropein (OLE). Tissue culture plastic (TCP) and LPS stimulated TCP (LPS) were used as controls. *: Denotes significant difference ($p < 0.05$) from the control group (NCL).

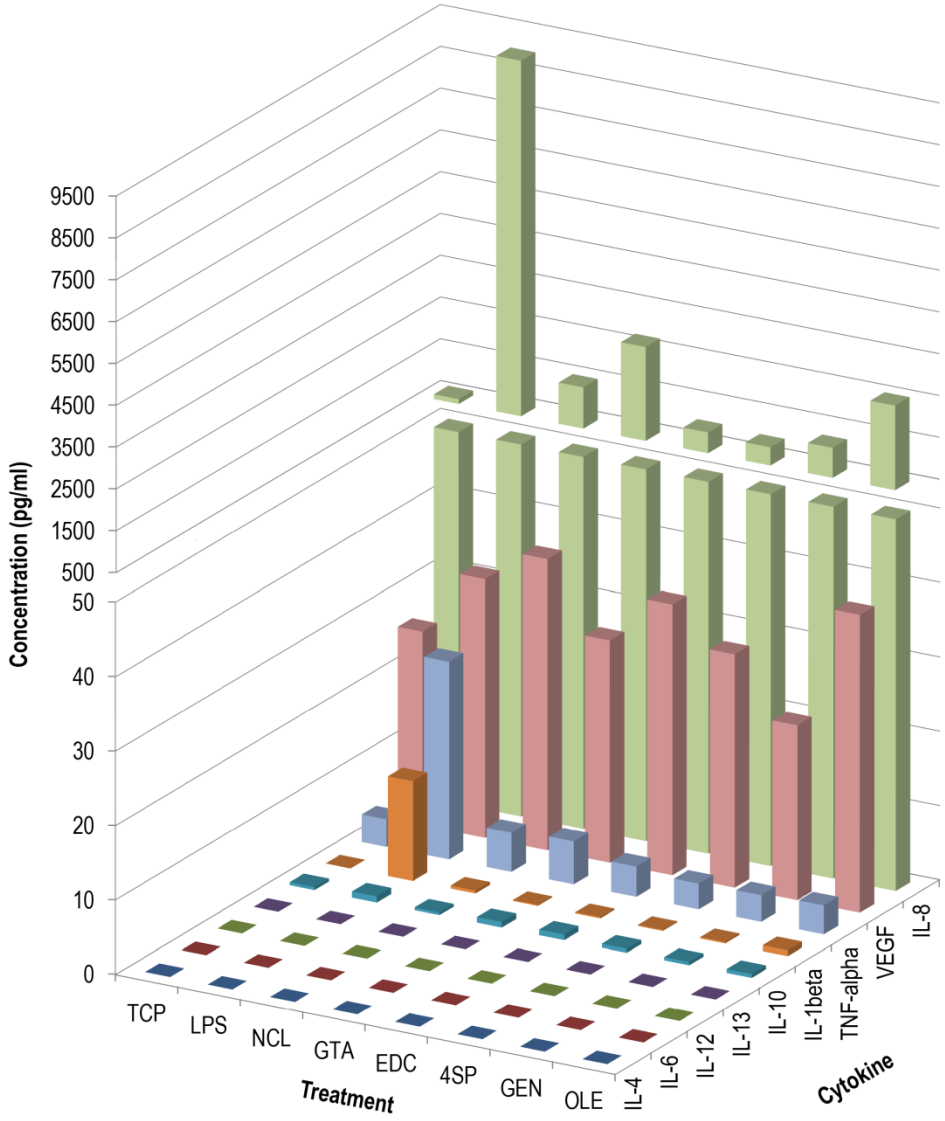

Figure 3.15. Multiplex ELISA on pro- and anti- inflammatory cytokines of THP-1 cells cultured with pre-conditioned media from the cross-linked collagen films after 2 days of culture. The bar represents the average. Treatments: non-cross-linked collagen film (NCL), collagen films cross-linked with glutaraldehyde (GTA), carbodiimide (EDC), 4-arm PEG succinimidyl glutarate (4SP), genipin (GEN) and oleuropein (OLE). Tissue culture plastic (TCP) and LPS stimulated TCP (LPS) were used as controls.

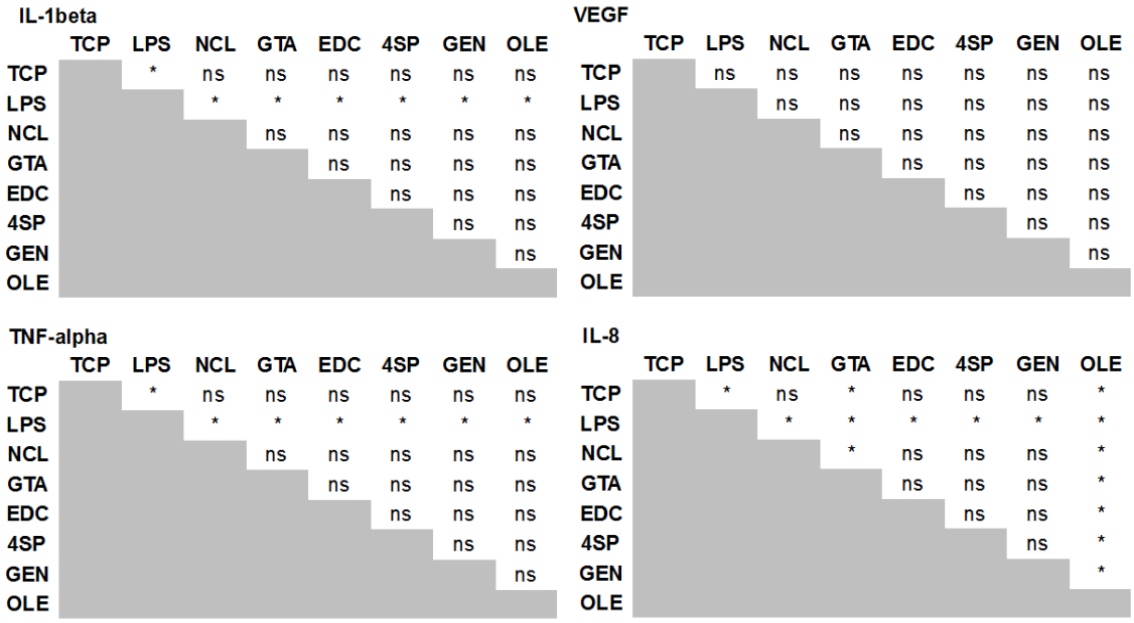

Figure 3.16. Multiplex ELISA, multiple comparison tests for every pair of conditions (* $p < 0.05$, ns: not significant). Treatments: non-cross-linked collagen film (NCL), collagen films cross-linked with glutaraldehyde (GTA), carbodiimide (EDC), 4-arm PEG succinimidyl glutarate (4SP), genipin (GEN) and oleuropein (OLE). Tissue culture plastic (TCP) and LPS stimulated TCP (LPS) were used as controls.

3.4. Discussion

Collagen-based devices represent one of the largest subsets of biomaterials currently in clinical practice [50]. Chemical cross-linking methods [51-53] are customarily employed to induce stability and to offer control over enzymatic degradation, yet collagen biomaterials are commonly associated with persistent and chronic activity of M1 macrophages [33], resulting in inflammation, suboptimal *in vivo* performance and, in several cases, implant failure [7, 8]. Herein, we ventured to assess the influence of various cross-linking methods (e.g. GTA, EDC, 4SP, GEN, OLE) on the structural, biochemical, biophysical and biological properties of collagen-based films (**Table 3.3** summarises around findings).

Although collagen can be cross-linked through its free amine or carboxyl groups, each cross-linking method has a unique mode of action, which consequently would be responsible for the properties of the resultant scaffold. GTA, for example, is considered a potent, but cytotoxic, collagen cross-linker that, in physiological conditions, reacts with the amine groups (primarily lysine, hydroxylysine, histidine, arginine and tyrosine) to form Schiff bases. Carboxylic acid groups of aspartic and glutamic acid residues in collagen react with EDC and then NHS; the NHS-activated carboxylic acid groups then react with the amine groups of lysine and hydroxylysine residues and release the NHS. EDC has limited cross-linking ability due to its short length structure and inability to polymerise, but is not as cytotoxic as GTA. The succinimidyl groups of 4SP react with the amine groups present on the collagen molecule. 4SP is not as potent as GTA, but it is significantly more cytocompatible. GEN cross-links free amine groups (e.g. lysine, hydroxylysine, arginine) and forms intra- and inter- molecular cross-links with collagen. OLE is an iridoid glycoside that contains a glucose molecule, which is cleaved by β-glucosidase to produce an

aglycone, which then reacts with the lysine residues of proteins. Both GEN and OLE are almost as efficient cross-linkers as GTA and less cytotoxic. A direct comparison though between these prominent collagen cross-linkers has yet to be reported.

Non-cross-linked collagen films (NCL) and cross-linked collagen films with carbodiimide (EDC) and 4-arm PEG succinimidyl glutarate (4SP) were clear and transparent, cross-linked collagen films with glutaraldehyde (GTA) and oleuropein (OLE) were brown and cross-linked films with genipin (GEN) were dark blue. The observed discolouration is attributed to the reaction between the cross-linking agents and the amino acids of collagen, as has been reported previously [36, 38, 43, 54, 55]. OLE presented a few brown dots that we attributed to clusters of the β-glucosidase enzyme used to active oleuropein aglycones, which bind to collagen amines [38]. The surface morphology was found to be cross-linking dependent, as it has been reported previously [43, 56-58], but in general a typical fibrous surface [59] was observed. GTA and OLE exhibited the least fibrous surface / smoothest surface, which is in agreement with previous observations, where cross-linking reduced / preferentially altered surface roughness [42, 60, 61].

Overall, cross-linking reduced the % free amines and increased the denaturation temperature and the resistance to enzymatic degradation of the collagen films. 4SP and GEN exhibited similar values to GTA, further advocating previous studies on their use as collagen cross-linking agents [34, 35, 43, 54, 55, 62, 63]. Although EDC is used extensively as a GTA alternative [64-68], herein EDC samples despite exhibiting lower % of free amines in comparison to the NCL samples, neither the denaturation temperature nor the resistance to enzymatic degradation was improved. In our case, this low stabilisation capacity of EDC could be attributed to the pH adjustment. Analysing the reaction, it could be observed that the optimal pH for the

substitution of the carbodiimide by NHS requires an acidic pH, around 5.5 [69], and in our case pH was around 7 to induce fibrillogenesis. Therefore, EDC cross-linking reaction was partially inhibited. This finding indicates that not all cross-linking agents can be used initially when fibrillogenesis is induced. Certainly, EDC-NHS crosslinking is commonly used to stabilise final forms of collagen such as fibres or sponges [70, 71] or to covalently bind functional molecules to collagen [72]. Further, although OLE has been claimed to be a potent collagen cross-linker [38, 73], herein it reduced the % of free amines and increased the denaturation temperature, but did not improve resistance to enzymatic degradation. Indeed, the commercially available form of oleuropein does not contain a reactive aglycone as genipin does and, therefore, oleuropein requires a pre-activation with β-glucosidase in the lab. Although a previous published protocol was used [38], the cross-linking efficiency was lower than the commercially available cross-linking agents. Even more, although we tried to improve the pre-activation by increasing the time and temperature and by introducing ultrasounds, the efficiency did not improve. Overall, these data illustrate that an array of assays should be conducted to assess the potential of a collagen cross-linking agent.

Even though several collagen deformation mechanisms have been proposed [74-77], the most widely accepted may be those of the Fratzl's model [78]. The relation between stress-induced structural changes and the J-shape stress-strain curve of collagen can be divided into four regions: toe or low strain region, the heel region, elastic or linear region and fibre failure. The region of low strain corresponds to the gradual removal of a macroscopic crimp in the collagen fibrils and this is visible in the light microscope. The crimp has been shown to act as a buffer or a shock absorber, permitting small longitudinal elongation of individual fibrils without

damage to the tissue [79]. This phenomenon results in a very low stiffness [80]. The second stage starts at strains typically beyond 2%, the effective elastic modulus increases progressively and, therefore, it is called the heel region. X-ray studies have demonstrated D-period distance increasing and lateral molecular packing of collagen molecules within fibrils, occurring as a result of the straightening of kinks. The straightening of the kinks allows an elongation of the fibrils and a resulting reduction in entropic disorder, which provides the force acting against the elongation. The entropic forces increase as the number of kinks decreases leading to the typical upwards curvature of the stress-strain curve [81-83]. The elastic region starts when collagen is stretched beyond the heel region, most kinks are straightened out and no further extension is possible by the entropic mechanism described above [78]. For larger strains, the exact mechanism by which mechanical energy is translated into molecular and fibrillar deformation is still unclear; most probably, large strain rates indicate stretching of the triple helixes and slippage occurs, resulting in increases in the length of the gap region with respect to the length of the overlap region, implying a side-by-side gliding of proteoglycans matrix that is around collagen fibrils [78, 84]. During loading at large strains, collagen hierarchical structure is extensively deformed and fibrils could split into individual microfibrils. Then, the collagen network disrupts when several microfibrils break up, a process termed defibrillation [82, 85-88].

The mechanical properties of the cross-linked scaffolds also appeared to be method dependent, with EDC producing the most extendable scaffolds and GEN resulting in scaffolds with the highest force at break, stress at break and elastic modulus values. Although both GTA [71, 89-91] and EDC [92-94] have been reported repeatedly to produce scaffolds with superior mechanical properties to non-cross-linked

counterparts and/or other cross-linkers, our data are in agreement with previous observations, where GEN significantly improved mechanical resilience [95-98] of collagen-based scaffolds and EDC failed to yield scaffolds with similar strength to more potent cross-linkers [43, 99, 100]. With respect to deformation mechanism, typical stress-strain curves of collagen materials that yield and undergo plastic flow were observed. The low modulus of the toe region, which is succeeded by the non-linear stress-strain curve, has been attributed to reorientation and uncramping of the collagen fibrils and the initiation of stretching of the triple helix, the non-helical ends and the cross-links [36, 101-103].

With respect to human skin fibroblast compatibility assessment, none of the cross-linking methods affected cell morphology (in all cases, human skin fibroblasts maintained their spindle shaped morphology) and they were not cytotoxic (no significant reductions were detected in DNA concentration, cell viability and cell proliferation at a given time point between non-cross-linked and cross-linked scaffolds). Previous studies have reported both cytotoxic [104] and non-cytotoxic [105] effects of EDC and GTA cross-linked collagen scaffolds. These contradictive data suggest that the cross-linking concentration / post-cross-linking treatments (e.g. number, duration and composition of washing bath) should be optimised for a specific device to identify the optimal cross-linker concentration with the desired cell response.

Macrophage polarisation has been closely linked to their shape. For example, macrophage elongation has been associated with transition from a pro-inflammatory M1 phenotype into an anti-inflammatory M2 phenotype [18], whilst cell aggregates are indicative of fusogenic phenotype and foreign body response [26]. Qualitative cell shape analysis revealed that most THP-1 macrophages exhibited a round

morphology, whilst some elongated THP-1 cells were also identified. Further, THP-1 aggregates were also formed. Such heterogeneous macrophage populations have been reported previously, when mature human monocyte-derived macrophages were exposed to polyethylene particulate [106] and have been associated with macrophage phenotype variations [18, 107-109].

By day 2, all cross-linked scaffolds significantly reduced THP-1 DNA concentration; GTA, EDC and 4SP significantly reduced THP-1 metabolic activity; and GTA and 4SP significantly reduced THP-1 viability in comparison to the NCL samples. When macrophages treated with pre-conditioned media, NCL media significantly reduced THP-1 DNA concentration and metabolic activity, whilst cell viability was not affected. Reduction in cell proliferation, viability and metabolic activity as a function of cross-linking method employed indicates cytotoxicity, as has been observed previously for macrophages exposed to GTA cross-linked bovine pericardium-derived scaffold [12], but was not verified herein with dermal fibroblasts and was not verified with the pre-conditioned media. Although previous data have demonstrated the influence of substrate rigidity on macrophage response [110, 111], no clear correlation was observed herein between scaffold rigidity, as a function of the different cross-linking method utilised, and macrophage response. Previous studies have demonstrated the influence of surface topography and chemistry on macrophage response [112-115]. We believe that this may be the reason for the variable cell response to the various scaffolds, but more detailed analysis (e.g. scaffolds with very specific topography; cross-linkers with similar chemistry) is required to verify this assumption.

THP-1 cells seeded on collagen scaffolds secreted significant amounts of 1L-1β (pro-inflammatory), TNF-α (pro-inflammatory), IL-8 (pro-inflammatory) and VEGF

(pro-angiogenesis), with OLE samples exhibiting the highest 1L-1β, TNF-α and IL-8 values and EDC and 4SP samples exhibiting the highest VEGF values. Previous studies have demonstrated high IL-1β, IL-6 and TNF-α secretion when GTA was used [116, 117]; this was not verified here due to the toxicity of the cross-linker [although GTA due to its self-polymerisation capacity can cross-link amines that are relatively far apart [118, 119], degradation products and unreacted GTA result in high cytotoxicity [29, 120] and calcification [121, 122]]. With respect to EDC, similarly to our work, previous studies have demonstrated comparable to the control bovine pericardium tissue pro-inflammatory cytokine profile [12]. *In vitro* data for GEN are not available, however previous *in vivo* studies have shown inflammatory response to GEN cross-linked bovine pericardium as a function of cross-linking concentration [123]. Although in our hands OLE films exhibited similar TNF-α production to LPS, previous studies have shown OLE to attenuate IL-1β, IL-6 and TNF-α secretion in LPS activated macrophages [124]. With respect to 4SP, *in vitro* data are available as yet, with respect to inflammatory response. To-date though, all published papers have shown promise in various clinical indications, including tendon [43], nucleus pulposus [35], cartilage [34, 125] and cornea [126].

Table 3.3. Summary table of the properties of the produced scaffolds to the performed assays. = denotes non-significant ($p > 0.05$) alterations with respect to the NCL group; ↑ denotes a significant ($p < 0.05$) increase with respect to NCL group; and ↓ denotes a significant ($p < 0.05$) reduction with respect to the NCL group. Treatments: non-cross-linked collagen film (NCL), collagen films cross-linked with glutaraldehyde (GTA), carbodiimide (EDC), 4-arm PEG succinimidyl glutarate (4SP), genipin (GEN) and oleuropein (OLE).

Cross-linking agent	GTA	EDC	4SP	GEN	OLE
Structure	↓	↓	=	=	↓
Free amine	↓	↓	↓	↓	↓
Denaturation temperature	↑	=	↑	↑	↑
Enzymatic degradation	↑	=	↑	↑	=

Cross-linking agent	GTA	EDC	4SP	GEN	OLE
Mechanical properties	Stress at break =	Stress at break ↓	Stress at break =	Stress at break ↑	Stress at break ↑
	Strain at break ↓	Strain at break ↑	Strain at break ↓	Strain at break ↓	Strain at break ↓
	E modulus ↑	E modulus ↓	E modulus =	E modulus ↑	E modulus ↑
***In vitro* fibroblast response**	=	=	=	=	=
***In vitro* macrophage response to direct contact**	Proliferation ↓	Proliferation ↓	Proliferation ↓	Proliferation ↓	Proliferation ↓
	Metabolic activity ↓	Metabolic activity ↓	Metabolic activity ↓	Metabolic activity ↓	Metabolic activity ↓
	Viability ↓	Viability =	Viability =	Viability =	Viability =

Cross-linking agent	GTA	EDC	4SP	GEN	OLE
***In vitro* macrophage response to direct contact**	Pro-inflammatory cytokine -	Pro-inflammatory cytokine ↓	Pro-inflammatory cytokine =	Pro-inflammatory cytokine =	Pro-inflammatory cytokine ↑
***In vitro* macrophage response to indirect contact**	Proliferation ↑	Proliferation ↑	Proliferation ↑	Proliferation ↑	Proliferation ↑
	Metabolic activity ↑	Metabolic activity ↑	Metabolic activity ↑	Metabolic activity ↑	Metabolic activity ↑
	Viability =	Viability =	Viability =	Viability =	Viability =
	Pro-inflammatory cytokine ↑ (only IL-8)	Pro-inflammatory cytokine =	Pro-inflammatory cytokine =	Pro-inflammatory cytokine =	Pro-inflammatory cytokine ↑ (only IL-8)

3.5. Conclusions

During the extraction and purification of collagen, native cross-linking is degraded. In order to reinstate integrity to reconstituted forms of collagen, exogenous cross-links are incorporated into the supramolecular structure, primary through chemical approaches. However, traditional cross-linking methods (e.g. glutaraldehyde, carbodiimide) are often linked to poor cytocompatibility, high inflammation and poor tissue integration. Herein we assessed the stability and biological response of collagen-based devices stabilised with glutaraldehyde, carbodiimide, 4-arm polyethylene glycol succinimidyl glutarate, genipin and oleuropein. All cross-linking methods reduced free amine groups. Denaturation temperature, resistance to collagenase digestion and mechanical properties were cross-linking method dependent. No significant differences were observed between the treatments in fibroblast cultures. Only the glutaraldehyde-cross-linked scaffolds were cytotoxic to human derived leukemic monocyte cells, whilst cultures supplemented with conditioned media from the various groups showed no significant difference between the treatments. No significant difference in pro-inflammatory and anti-inflammatory cytokines was observed between the non-cross-linked and the 4-arm polyethylene glycol succinimidyl glutarate and genipin cross-linked groups, suggesting the suitability of these agents as collagen cross-linkers.

3.6. References

[1] Fratzl P, Weinkamer R. Nature's hierarchical materials. Progress Mat Sci 2007;52:1263-1334.

[2] Friess W. Collagen--biomaterial for drug delivery. Eur J Pharm Biopharm 1998;45:113-136.

[3] Ellingsworth LR, DeLustro F, Brennan JE, Sawamura S, McPherson J. The human immune response to reconstituted bovine collagen. J Immunol 1986;136:877-882.

[4] Lynn AK, Yannas IV, Bonfield W. Antigenicity and immunogenicity of collagen. J Biomed Mater Res B 2004;71B:343-354.

[5] Lee CH, Singla A, Lee Y. Biomedical applications of collagen. Int J Pharm 2001;221:1-22.

[6] Abou Neel EA, Bozec L, Knowles JC, Syed O, Mudera V, Day R, et al. Collagen--emerging collagen based therapies hit the patient. Adv Drug Deliv Rev 2013;65:429-456.

[7] Brown BN, Badylak SF. Expanded applications, shifting paradigms and an improved understanding of host-biomaterial interactions. Acta Biomater 2013;9:4948-4955.

[8] Delgado LM, Bayon Y, Pandit A, Zeugolis DI. To cross-link or not to cross-link? Cross-linking associated foreign body response of collagen-based devices. Tissue Eng Part B 2015;21:298-313.

[9] Li J, Chen J, Kirsner R. Pathophysiology of acute wound healing. Clin Dermatol 2007;25:9-18.

[10] Guo S, Dipietro LA. Factors affecting wound healing. J Dent Res 2010;89:219-229.

[11] Brown BN, Ratner BD, Goodman SB, Amar S, Badylak SF. Macrophage polarization: An opportunity for improved outcomes in biomaterials and regenerative medicine. Biomaterials 2012;33:3792-3802.

[12] McDade JK, Brennan-Pierce EP, Ariganello MB, Labow RS, Michael Lee J. Interactions of U937 macrophage-like cells with decellularized pericardial matrix materials: Influence of crosslinking treatment. Acta Biomater 2013;9:7191-7199.

[13] Garg K, Pullen Na, Oskeritzian Ca, Ryan JJ, Bowlin GL. Macrophage functional polarization (M1/M2) in response to varying fiber and pore dimensions of electrospun scaffolds. Biomaterials 2013;34:4439-4451.

[14] Chen S, Jones Ja, Xu Y, Low H-Y, Anderson JM, Leong KW. Characterization of topographical effects on macrophage behavior in a foreign body response model. Biomaterials 2010;31:3479-3491.

[15] Franz S, Allenstein F, Kajahn J, Forstreuter I, Hintze V, Moller S, et al. Artificial extracellular matrices composed of collagen I and high-sulfated hyaluronan promote phenotypic and functional modulation of human pro-inflammatory M1 macrophages. Acta Biomater 2013;9:5621-5629.

[16] Lucas T, Waisman A, Ranjan R, Roes J, Krieg T, Muller W, et al. Differential roles of macrophages in diverse phases of skin repair. J Immunol 2010;184:3964-3977.

[17] Martinez FO, Gordon S. The M1 and M2 paradigm of macrophage activation: Time for reassessment. F1000Prime Reports 2014;6:13.

[18] McWhorter FY, Wang T, Nguyen P, Chung T, Liu WF. Modulation of macrophage phenotype by cell shape. Proc Natl Acad Sci U S A 2013;110:17253-17258.

[19] Tabas I, Bornfeldt K. Macrophage phenotype and function in different stages of atherosclerosis. Circ Res 2016;118:653-667.

[20] Patel U, Rajasingh S, Samanta S, Cao T, Dawn B, Rajasingh J. Macrophage polarization in response to epigenetic modifiers during infection and inflammation. Drug Discov Today In Press.

[21] Ferrante C, Leibovich S. Regulation of macrophage polarization and wound healing. Adv Wound Care 2012;1:10-16.

[22] Orenstein SB, Qiao Y, Klueh U, Kreutzer DL, Novitsky YW. Activation of human mononuclear cells by porcine biologic meshes in vitro. Hernia 2010;14:401-407.

[23] Mantovani A, Sica A, Sozzani S, Allavena P, Vecchi A, Locati M. The chemokine system in diverse forms of macrophage activation and polarization. Trends Immunol 2004;25:677-686.

[24] Gordon S, Taylor PR. Monocyte and macrophage heterogeneity. Nat Rev Immunol 2005;5:953-964.

[25] Mosser DM, Edwards JP. Exploring the full spectrum of macrophage activation. Nat Rev Immunol 2008;8:958-969.

[26] Yahyouche A, Zhidao X, Czernuszka JT, Clover AJ. Macrophage-mediated degradation of crosslinked collagen scaffolds. Acta Biomater 2011;7:278-286.

[27] Henson PM. Mechanisms of exocytosis in phagocytic inflammatory cells. Am J Pathol 1980;101:494-511.

[28] Brodbeck WG, Anderson JM. Giant cell formation and function. Curr Opin Hematol 2009;16:53-57.

[29] Gough JE, Scotchford CA, Downes S. Cytotoxicity of glutaraldehyde crosslinked collagen/poly(vinyl alcohol) films is by the mechanism of apoptosis. J Biomed Mater Res 2002;61:121-130.

[30] Hass V, Luque-Martinez IV, Gutierrez MF, Moreira CG, Gotti VB, Feitosa VP, et al. Collagen cross-linkers on dentin bonding: Stability of the adhesive interfaces, degree of conversion of the adhesive, cytotoxicity and in situ MMP inhibition. Dent Mater 2016;32:732-741.

[31] McGregor C, Byrne G, Rahmani B, Chisari E, Kyriakopoulou K, Burriesci G. Physical equivalency of wild type and galactose α 1,3 galactose free porcine pericardium; a new source material for bioprosthetic heart valves. Acta Biomater 2016;41:204-209.

[32] Fahrenholtz MM, Wen S, Grande-Allen KJ. Development of a heart valve model surface for optimization of surface modifications. Acta Biomater 2015;26:64-71.

[33] Brown BN, Londono R, Tottey S, Zhang L, Kukla KA, Wolf MT, et al. Macrophage phenotype as a predictor of constructive remodeling following the implantation of biologically derived surgical mesh materials. Acta Biomater 2012;8:978-987.

[34] Taguchi T, Xu L, Kobayashi H, Taniguchi A, Kataoka K, Tanaka J. Encapsulation of chondrocytes in injectable alkali-treated collagen gels prepared using poly(ethylene glycol)-based 4-armed star polymer. Biomaterials 2005;26:1247-1252.

[35] Collin EC, Grad S, Zeugolis DI, Vinatier CS, Clouet JR, Guicheux JJ, et al. An injectable vehicle for nucleus pulposus cell-based therapy. Biomaterials 2011;32:2862-2870.

[36] Zeugolis DI, Paul GR, Attenburrow G. Cross-linking of extruded collagen fibres - A biomimetic three-dimensional scaffold for tissue engineering applications. J Biomed Mater Res A 2009;89:895-908.

[37] Zeugolis DI, Paul RG, Attenburrow G. The influence of a natural cross-linking agent (Myrica rubra) on the properties of extruded collagen fibres for tissue engineering applications. Mater Sci Eng C Mater Biol Appl

2010;30:190-195.

[38] Antunes A, Attenburrow G, Covington A, Ding J. Utilisation of oleuropein as a crosslinking agent in collagenic films. J Leather Sci 2008;2:1-12.

[39] Zeugolis D, Paul R, Attenburrow G. Factors influencing the properties of reconstituted collagen fibers prior to self-assembly: Animal species and collagen extraction method. J Biomed Mater Res A 2008;86:892-904.

[40] Lareu R, Zeugolis D, Abu-Rub M, Pandit A, Raghunath M. Essential modification of the Sircol collagen assay for the accurate quantification of collagen content in complex protein solutions. Acta Biomater 2010;6:3146-3151.

[41] Zeugolis D, Li B, Lareu R, Chan C, Raghunath M. Collagen solubility testing, a quality assurance step for reproducible electro-spun nano-fibre fabrication. A technical note. J Biomater Sci Polym Ed 2008;19:1307-1317.

[42] Satyam A, Subramanian G, Raghunath M, Pandit A, Zeugolis D. In vitro evaluation of Ficoll-enriched and genipin-stabilised collagen scaffolds. J Tissue Eng Regen Med 2014;8:233-241.

[43] Sanami M, Sweeney I, Shtein Z, Meirovich S, Sorushanova A, Mullen A, et al. The influence of poly(ethylene glycol) ether tetrasuccinimidyl glutarate on the structural, physical, and biological properties of collagen fibers. J Biomed Mater Res B Appl Biomater 2016;104:914-922.

[44] Ward J, Kelly J, Wang W, Zeugolis DI, Pandit A. Amine functionalization of collagen matrices with multifunctional polyethylene glycol systems. Biomacromolecules 2010;11:3093-3101.

[45] Zeugolis D, Raghunath M. The physiological relevance of wet versus dry differential scanning calorimetry for biomaterial evaluation: A technical note. Polym Int 2010;59:1403-1407.

[46] Helling A, Tsekoura E, Biggs M, Bayon Y, Pandit A, Zeugolis D. In vitro enzymatic degradation of tissue grafts and collagen biomaterials by matrix metalloproteinases: Improving the collagenase assay. ACS Biomater Sci Eng In Press.

[47] Daigneault M, Preston JA, Marriott HM, Whyte MK, Dockrell DH. The identification of markers of macrophage differentiation in PMA-stimulated THP-1 cells and monocyte-derived macrophages. PLoS One 2010;5:e8668.

[48] Helary C, Browne S, Mathew A, Wang W, Pandit A. Transfection of macrophages by collagen hollow spheres loaded with polyplexes: A step towards modulating inflammation. Acta Biomater 2012;8:4208-4214.

[49] Fuller K, Gaspar D, Delgado L, Pandit A, Zeugolis D. Influence of porosity and pore shape on structural, mechanical and biological properties of poly ϵ-caprolactone electro-spun fibrous scaffolds. Nanomedicine 2016;11:1031-1040.

[50] Zeugolis DI, Raghunath M. Collagen: Materials analysis and implant uses. In: Ducheyne P, Healy KE, Hutmacher DW, Grainger DW, Kirkpatrick CJ, editors. Comprehensive Biomaterials. Oxford: Elsevier; 2011. p. 261-278.

[51] Ye Q, Harmsen MC, van Luyn MJ, Bank RA. The relationship between collagen scaffold cross-linking agents and neutrophils in the foreign body reaction. Biomaterials 2010;31:9192-9201.

[52] Ye Q, van Amerongen MJ, Sandham JA, Bank RA, van Luyn MJ, Harmsen MC. Site-specific tissue inhibitor of metalloproteinase-1 governs the matrix metalloproteinases-dependent degradation of crosslinked collagen scaffolds and is correlated with interleukin-10. J Tissue Eng Regen Med 2011;5:264-274.

[53] Bellon JM, Rodriguez M, Gomez-Gil V, Sotomayor S, Bujan J, Pascual G. Postimplant intraperitoneal behavior of collagen-based meshes followed by laparoscopy. Surg Endosc 2012;26:27-35.

[54] Sundararaghavan HG, Monteiro GA, Lapin NA, Chabal YJ, Miksan JR, Shreiber DI. Genipin-induced changes in collagen gels: Correlation of mechanical properties to fluorescence. J Biomed Mater Res A 2008;87:308-320.

[55] Fessel G, Cadby J, Wunderli S, van Weeren R, Snedeker JG. Dose- and time-dependent effects of genipin crosslinking on cell viability and tissue mechanics – Toward clinical application for tendon repair. Acta Biomater 2014;10:1897-1906.

[56] Cote M, Doillon C. Wettability of cross-linked collagenous biomaterials: *In vitro* study. Biomaterials 1992;13:612-616.

[57] Nomura Y, Toki S, Ishii Y, Shirai K. Effect of transglutaminase on reconstruction and physicochemical properties of collagen gel from shark type I collagen. Biomacromolecules 2001;2:105-110.

[58] Sionkowska A, Wess T. Mechanical properties of UV irradiated rat tail tendon (RTT) collagen. Intern J Biolog Macromol 2004;34:9-12.

[59] Christiansen D, Silver F. Mineralization of an axially aligned collagenous matrix: A morphological study. Cells Materials 1993;3:177-188.

[60] Grover C, Gwynne J, Pugh N, Hamaia S, Farndale R, Best S, et al. Crosslinking and composition influence the surface properties, mechanical stiffness and cell reactivity of collagen-based films. Acta Biomater 2012;8:3080-3090.

[61] Sionkowska A, Skopinska-Wisniewska J, Gawron M, Kozlowska J, Planecka A. Chemical and thermal cross-linking of collagen and elastin hydrolysates. Int J Biol Macromol 2010;47:570-577.

[62] Madhavan K, Belchenko D, Motta A, Tan W. Evaluation of composition and crosslinking effects on collagen-based composite constructs. Acta Biomater 2010;6:1413-1422.

[63] Zhang X, Chen X, Yang T, Zhang N, Dong L, Ma S, et al. The effects of different crossing-linking conditions of genipin on type I collagen scaffolds: An in vitro evaluation. Cell Tissue Bank 2014;15:531-541.

[64] Scheffel D, Bianchi L, Soares D, Basso F, Sabatini C, de Souza Costa C, et al. Transdentinal cytotoxicity of carbodiimide (EDC) and glutaraldehyde on odontoblast-like cells. Oper Dent 2015;40:44-54.

[65] Salvatore L, Madaghiele M, Parisi C, Gatti F, Sannino A. Crosslinking of micropatterned collagen-based nerve guides to modulate the expected half-life. J Biomed Mater Res A 2014;102:4406-4414.

[66] Zhu J, Marchant RE. Design properties of hydrogel tissue-engineering scaffolds. Expert Rev Med Devices 2011;8:607-626.

[67] Lammers G, Tjabringa G, Schalkwijk J, Daamen W, van Kuppevelt T. A molecularly defined array based on native fibrillar collagen for the assessment of skin tissue engineering biomaterials. Biomaterials 2009;30:6213-6220.

[68] Haparanta A, Koivurinta J, Hamalainen E, Kellomaki M. The effect of cross-linking time on a porous freeze-dried collagen scaffold using 1-ethyl-3-(3-dimethylaminopropyl)carbodiimide as a cross-linker. J Appl Biomater Biomech 2008;6:89-94.

[69] Gratzer PF, Lee JM. Control of pH alters the type of cross-linking produced by 1-ethyl-3-(3-dimethylaminopropyl)-carbodiimide (EDC) treatment of acellular matrix vascular grafts. J Biomed Mater Res 2001;58:172-179.

[70] Zeugolis DI, Paul GR, Attenburrow G. Cross-linking of extruded collagen fibers - A biomimetic three-dimensional scaffold for tissue engineering applications. J Biomed Mater Res A 2009;89:895-908.

[71] Haugh M, Murphy C, McKiernan R, Altenbuchner C, O'Brien F. Crosslinking and mechanical properties significantly influence cell attachment, proliferation, and migration within collagen glycosaminoglycan scaffolds. Tissue Eng Part A 2011;17:1201-1208.

[72] Steffens GC, Yao C, Prevel P, Markowicz M, Schenck P, Noah EM, et al. Modulation of angiogenic potential of collagen matrices by covalent incorporation of heparin and loading with vascular endothelial growth factor. Tissue Eng 2004;10:1502-1509.

[73] Konno K, Hirayama C, Yasui H, Nakamura M. Enzymatic activation of oleuropein: A protein crosslinker used as a chemical defense in the privet tree. Proc Natl Acad Sci U S A 1999;96:9159-9164.

[74] Kurniawan NA, Wong LH, Rajagopalan R. Early stiffening and softening of collagen: Interplay of deformation mechanisms in biopolymer networks. Biomacromolecules 2012;13:691-698.

[75] Gupta HS, Seto J, Krauss S, Boesecke P, Screen HR. In situ multi-level analysis of viscoelastic deformation mechanisms in tendon collagen. J Struct Biol 2010;169:183-191.

[76] Depalle B, Qin Z, Shefelbine SJ, Buehler MJ. Influence of cross-link structure, density and mechanical properties in the mesoscale deformation mechanisms of collagen fibrils. J Mech Behav Biomed Mater 2014;In Press.

[77] Wenger MP, Bozec L, Horton MA, Mesquida P. Mechanical properties of collagen fibrils. Biophys J 2007;93:1255-1263.

[78] Fratzl P, Misof K, Zizak I, Rapp G, Amenitsch H, Bernstorff S. Fibrillar structure and mechanical properties of collagen. J Struct Biol 1997;122:119-122.

[79] Jarvinen TAH, Jarvinen TLN, Kannus P, Jozsa L, Jarvinen M. Collagen fibres of the spontaneously ruptured human tendons display decrease thickness and crimp angle. J Orthop Res 2004;22:1303-1309.

[80] Puxkandl R, Zizak I, Paris O, Keckes J, Tesch W, Bernstorff S, et al. Viscoelastic properties of collagen: Synchrotron radiation investigations and structural model. Philos Trans R Soc Lond B Biol Sci 2002;357:191-197.

[81] Misof K, Rapp G, Fratzl P. A new molecular model for collagen elasticity based on synchrotron X-ray scattering evidence. Biophys J 1997;72:1376-1381.

[82] Purslow PP, Wess TJ, Hukins DWL. Collagen orientation and molecular spacing during creep and stress-relaxation in soft connective tissues. J Exp Biol 1998;201:135-142.

[83] Silver FH, Christiansen DL, Snowhill PB, Chen Y. Transition from viscous to elastic-based dependancy of mechanical properties of self-assembled type I collagen fibers. J Appl Polym Sci 2001;79:134-142.

[84] Pins GD, Christiansen DL, Patel R, Silver FH. Self-assembly of collagen fibers. Influence of fibrillar alignment and decorin on mechanical properties. Biophys J 1997;73:2164-2172.

[85] Sasaki N, Odajima S. Elongation mechanism of collagen fibrils and force-strain relations of tendon at each level of structural hierarchy. J Biomech 1996;29:1131-1136.

[86] Kato YP, Christiansen D, Hahn RA, Shieh S-J, Goldstein JD, Silver FH. Mechanical properties of collagen fibres: a comparison of reconstituted and rat tail tendon fibres. Biomaterials 1989;10:38-42.

[87] Kato YP, Silver FH. Formation of continuous collagen fibres: evaluation of biocompatibilily and mechanical properties. Biomaterials 1990;11:169-175.

[88] Knorzer E, Folkhard W, Geercken W, Boschert C, Koch MH, Hilbert B, et al. New aspects of the etiology of tendon rupture. An analysis of time-resolved dynamic-mechanical measurements using synchrotron radiation. Arch Orthop Trauma Surg 1986;105:113-120.

[89] Awang M, Firdaus M, Busra M, Chowdhury S, Fadilah N, Wan Hamirul W, et al. Cytotoxic evaluation of biomechanically improved crosslinked ovine collagen on human dermal fibroblasts. Biomed Mater Eng 2014;24:1715-1724.

[90] Chen C, Mao C, Sun J, Chen Y, Wang W, Pan H, et al. Glutaraldehyde-induced remineralization improves the mechanical properties and biostability of dentin collagen. Mater Sci Eng C Mater Biol Appl 2016;67:657-665.

[91] Perez-Puyana V, Romero A, Guerrero A. Influence of collagen concentration and glutaraldehyde on collagen-based scaffold properties. J Biomed Mater Res A 2016;104:1462-1468.

[92] Powell H, Boyce S. EDC cross-linking improves skin substitute strength and stability. Biomaterials 2006;27:5821-5827.

[93] Park S, Park J, Kim H, Song M, Suh H. Characterization of porous collagen/hyaluronic acid scaffold modified by 1-ethyl-3-(3-dimethylaminopropyl)carbodiimide cross-linking. Biomaterials 2002;23:1205-1212.

[94] Lee C, Grodzinsky A, Spector M. The effects of cross-linking of collagen-glycosaminoglycan scaffolds on compressive stiffness, chondrocyte-mediated contraction, proliferation and biosynthesis. Biomaterials 2001;22:3145-3154.

[95] McGann M, Bonitsky C, Jackson M, Ovaert T, Trippel S, Wagner D. Genipin crosslinking of cartilage enhances resistance to biochemical degradation and mechanical wear. J Orthop Res 2015;33:1571-1579.

[96] Bonitsky C, McGann M, Selep M, Ovaert T, Trippel S, Wagner D. Genipin crosslinking decreases the mechanical wear and biochemical degradation of imacted cartilage in vitro. J Orthop Res 2017;35:558-565.

[97] Avila M, Navia J. Effect of genipin collagen crosslinking on porcine corneas. J Cataract Refract Surg 2010;36:659-664.

[98] Fessel G, Wernli J, Li Y, Gerber C, Snedeker J. Exogenous collagen cross-linking recovers tendon functional integrity in an experimental model of partial tear. J Orthop Res 2012;30:973-981.

[99] Jeong S, Yoon E, Lim H, Sung S, Kim Y. The effect of space fillers in the cross-linking processes of bioprosthesis. Biores Open Access 2013;2:98-106.

[100] Enea D, Henson F, Kew S, Wardale J, Getgood A, Brooks R, et al. Extruded collagen fibres for tissue engineering applications: Effect of crosslinking method on mechanical and biological properties. J Mater Sci Mater Med 2011;22:1569-1578.

[101] Fratzl P, Misof K, Zizak I, Rapp G, Amenitsch H, Bernstorff S. Fibrillar structure and mechanical properties of collagen. J Struct Biol 1998;122:119-122.

[102] Purslow P, Wess T, Hukins D. Collagen orientation and molecular spacing during creep and stress-relaxation in soft connective tissues. J Exp Biol 1998;201:135-142.

[103] Rigby B, Hirai N, Spikes J, Eyring H. The mechanical properties of rat tail tendon. J Gen Physiol 1959;43:265-283.

[104] Saito H, Murabayashi S, Mitamura Y, Taguchi T. Characterization of alkali-treated collagen gels prepared by different crosslinkers. J Mater Sci Mater Med 2008;19:1297-1305.

[105] Wissink M, van Luyn M, Beernink R, Dijk F, Poot A, Engbers G, et al. Endothelial cell seeding on crosslinked collagen: Effects of crosslinking on endothelial cell proliferation and functional parameters. Thromb Haemost 2000;84:325-331.

[106] Xing S, Waddell J, Boynton E. Changes in macrophage morphology and prolonged cell viability following exposure to polyethylene particulate in vitro. Microsc Res Tech 2002;57:523-529.

[107] Buchacher T, Ohradanova-Repic A, Stockinger H, Fischer M, Weber V. M2 polarization of human macrophages favors survival of the intracellular pathogen Chlamydia pneumoniae. PLoS One 2015;10:e0143593.

[108] Féréol S, Fodil R, Labat B, Galiacy S, Laurent VM, Louis B, et al. Sensitivity of alveolar macrophages to substrate mechanical and adhesive properties. Cell Motil Cytoskeleton 2006;63:321-340.

[109] Sridharan R, Cameron AR, Kelly DJ, Kearney CJ, O'Brien FJ. Biomaterial based modulation of macrophage polarization: A review and suggested design principles. Materials Today 2015;18:313-325.

[110] Patel N, Bole M, Chen C, Hardin C, Kho A, Mih J, et al. Cell elasticity determines macrophage function. PLoS One 2012;7:e41024.

[111] Blakney A, Swartzlander M, Bryant S. The effects of substrate stiffness on the in vitro activation of macrophages and in vivo host response to poly(ethylene glycol)-based hydrogels. J Biomed Mater Res A 2012;100:1375-1386.

[112] Christo S, Bachhuka A, Diener K, Mierczynska A, Hayball J, Vasilev K. The role of surface nanotopography and chemistry on primary neutrophil and macrophage cellular responses. Adv Healthc Mater 2016;5:956-965.

[113] Refai A, Textor M, Brunette D, Waterfield J. Effect of titanium surface topography on macrophage activation and secretion of proinflammatory cytokines and chemokines. J Biomed Mater Res A 2004;70:194-205.

[114] Christo S, Bachhuka A, Diener K, Vasilev K, Hayball J. The contribution of inflammasome components on macrophage response to surface nanotopography and chemistry. Sci Rep 2016;6:26207.

[115] Lim J, Donahue H. Cell sensing and response to micro- and nanostructured surfaces produced by chemical and topographic patterning. Tissue Eng 2007;13:1879-1891.

[116] Bayrak A, Tyralla M, Ladhoff J, Schleicher M, Stock UA, Volk HD, et al. Human immune responses to porcine xenogeneic matrices and their extracellular matrix constituents in vitro. Biomaterials 2010;31:3793-3803.

[117] Umashankar PR, Mohanan PV, Kumari TV. Glutaraldehyde treatment elicits toxic response compared to decellularization in bovine pericardium. Toxicol Int 2012;19:51-58.

[118] Hey KB, Lachs CM, Raxworthy MJ, Wood EJ. Crosslinked fibrous collagen for use as a dermal implant: Control of the cytotoxic effects of glutaraldehyde and dimethylsuberimidate. Biotechnol Appl Biochem 1990;12:85-93.

[119] Chapman JA, Tzaphlidou M, Meek KM, Kadler KE. The collagen fibril -- A model system for studying the staining and fixation of a protein. Electron Microsc Rev 1990;3:143-182.

[120] Lee CR, Grodzinsky AJ, Spector M. The effects of cross-linking of collagen-glycosaminoglycan scaffolds on compressive stiffness, chondrocyte-mediated contraction, proliferation and biosynthesis. Biomaterials 2001;22:3145-3154.

[121] Levy RJ, Schoen FJ, Sherman FS, Nichols J, Hawley MA, Lund SA. Calcification of subcutaneously implanted type I collagen sponges. Effects of formaldehyde and glutaraldehyde pretreatments. Am J Pathol 1986;122:71-82.

[122] McPherson JM, Sawamura S, Armstrong R. An examination of the biologic response to injectable, glutaraldehyde cross-linked collagen implants. J Biomed Mater Res 1986;20:93-107.

[123] Liang HC, Chang Y, Hsu CK, Lee MH, Sung HW. Effects of crosslinking degree of an acellular biological tissue on its tissue regeneration pattern. Biomaterials 2004;25:3541-3552.

[124] Giner E, Andujar I, Recio MC, Rios JL, Cerda-Nicolas JM, Giner RM. Oleuropein ameliorates acute colitis in mice. J Agric Food Chem 2011;59:12882-12892.

[125] Kontturi L, Järvinen E, Muhonen V, Collin E, Pandit A, Kiviranta I, et al. An injectable, in situ forming type II collagen/hyaluronic acid hydrogel vehicle for chondrocyte delivery in cartilage tissue engineering. Drug Deliv Transl Res 2014;4:149-158.

[126] Kato M, Taguchi T, Kobayashi H. An attempt to construct the stroma of cornea using primary cultured corneal cells. J Nanosci Nanotechnol 2007;7:748-751.

Chapter 4: Collagen sterilisation

Sections of this chapter are under submission at:

Delgado LM, Fuller K, Zeugolis DI. *The influence of cross-linking method and sterilisation treatment on the structural, biophysical, biochemical and biological properties of collagen devices*. Submitted.

4.1. Introduction

Collagen is widely used in in tissue engineering due to its natural composition, well-tolerated degradation products, suitable mechanical stability and appropriate biological response [1-3]. International standards are in place to govern / regulate medical devices sterilisation [4-8], including collagen [9]. Similarly to any other implantable device, ensuring sterility of collagen-based devices is essential for the device success and safety. However, there is no gold standard sterilisation method for collagen-based devices; the selection of the most appropriate sterilisation method is device-dependent and is determined primarily by the physical state of the device and the influence of the sterilisation treatment on the properties of the device to be sterilised [10].

Given the thermosensitive nature of collagen, common sterilisation methods, such as dry heat or steam, cannot be used, as they would denature it. As such, physical (e.g. gamma or e-beam irradiation) and chemical (e.g. ethylene oxide) are the sterilisation methods of choice. However, all come with drawbacks. Gamma irradiation, for example, has been shown to cause structural changes and to induce significant reduction in mechanical properties, resistance to degradation and cell attachment [11-13]. E-beam irradiation at low and high doses significantly decreased the ultimate strain and toughness of human cortical bone [14], whilst high doses of e-beam irradiation negatively impacted on bone regeneration of octacalcium phosphate collagen composites [15]. Ethylene oxide has been shown to reduce stability and cell attachment of collagen-based devices [13, 16]. In recent years, sterilisation through hydrogen peroxide gas plasma has been advocated, as it can be conducted at temperatures (< 50 ºC) well tolerated even by non-cross-linked collagen devices [17] and has demonstrated minimal detrimental effects in comparison to ethylene oxide

sterilisation [18, 19]. Ethanol / alcohol treatments are also gaining pace, as they do not affect structural, degradation and mechanical properties [20-22]. It is however worth noting that alterations in pore size, due to shrinkage, have been reported [21, 23] and it is not used extensively in clinical setting, as it cannot eliminate spores and viruses [24].

Considering that sterilisation treatments may negatively impact on the mechanical and enzymatic stability of collagen-based devices, cross-linking thereof has been proposed as means to minimise the damage [25-27]. However, cross-linking influences biological responses, including inflammatory and wound healing processes [28]. It is therefore essential to correlate the influence of cross-linking / sterilisation method on the properties of collagen-based devices. Herein, we assessed the influence of no sterilisation (NS) and gas plasma (GP), gamma irradiation (GI), ethylene oxide (EO) and ethanol (ET) sterilisation on the biophysical, biochemical and biological properties of non-cross-linked (NCL) and cross-linked with 4-arms polyethylene glycol succinimidyl glutarate (4SP) and genipin (GEN) collagen films. We chose 4SP [29-32] and GEN [33-36], as their beneficial effects in the stabilisation of collagen-based devices have been well documented in the literature.

4.2. Materials and methods

4.2.1. Materials

Bovine Achilles tendons were collected from a local abattoir (steers aged 24 months). 4SP (Mw 10 kDa) and GEN were purchased from JenKem Technology (USA) and Challenge Bioproducts (Taiwan), respectively. All other materials and reagents were purchased from Sigma-Aldrich (Ireland), unless otherwise stated.

4.2.2. Collagen type I isolation and film fabrication

Bovine type I collagen was extracted as has been described previously [37] with slight modifications. Briefly, bovine Achilles tendons were cryomilled, washed with 1x phosphate buffered saline (PBS) solution and dissolved in 1.0 M acetic acid with 80 U / mg wet weight tendon of pepsin from porcine gastric mucosa (lyophilized powder, 3,200-4,500 units/mg protein) at 4 °C. The supernatant obtained following filtration (1 mm pore size nylon screen) and centrifugation (9,000 rpm at 4 °C, Thermo Fisher Scientific, Ireland) was purified by repeated salt precipitation (0.9 M NaCl), centrifugation (9,000 rpm at 4 °C) and re-suspension in 1.0 M acetic acid. Finally, the resultant atellocollagen solution was dialysed (Mw 8,000 cut off) against 1 mM acetic acid; the collagen concentration was adjusted to ~6 mg/ml and kept at 4 °C.

Collagen films were fabricated and cross-linked as has been described previously [30, 33] with slight modifications. Briefly, 10 ml 10x PBS, 3-4 ml of 1.0 M NaOH, 100 ml of collagen (6 mg/ml) and 5 ml of 4SP (20 mM in x1 PBS) or 5 ml of GEN (0.625 % in x1 PBS) were mixed together in ice (final solution pH ~7.3). The solutions were placed in silicone moulds and incubated at 37 °C for 1 h to induce

self-assembly. The films were let to evaporate overnight at 25 °C. Non-cross-linked (NCL) films were used as control.

4.2.3. Collagen film sterilisation

Collagen films were sterilised as follows using the minimum dose reported to obtain sterile films: Gas plasma (GP) of 58 % hydrogen peroxide at 6 mg/l for 45 min diffusion and 20 min radiofrequency excitation [18, 38]; Gamma irradiation (GI) at 8.8 kGy at room temperature [39, 40]; Ethylene oxide (EO) at 750 mg/ml at 40 °C for 12 h [41, 42] and 70 % ethanol (ET) for 30 min at room temperature [31, 43]. Non-sterile (NS) films were used as control. The sterilisation cycle of GP and GI was ensured with a dosimeter indicator. The sterility of each treatment was confirmed as per ISO 11737-2:2009 [6]. Briefly, collagen films were incubated in tryptic soy broth (TSB) at 37 °C for 7 and 14 days. Sterile TSB medium was used as negative control. TSB medium, inoculated with 10 colony forming units (CFU) per ml of *Escherichia coli* (Catalogue Number: 25922, ATCC, UK), was used as positive control. Sterile samples should maintain medium transparency, whilst non-sterile samples should show turbidity. In our case, no sample showed microbial growth (**Figure 4.1**).

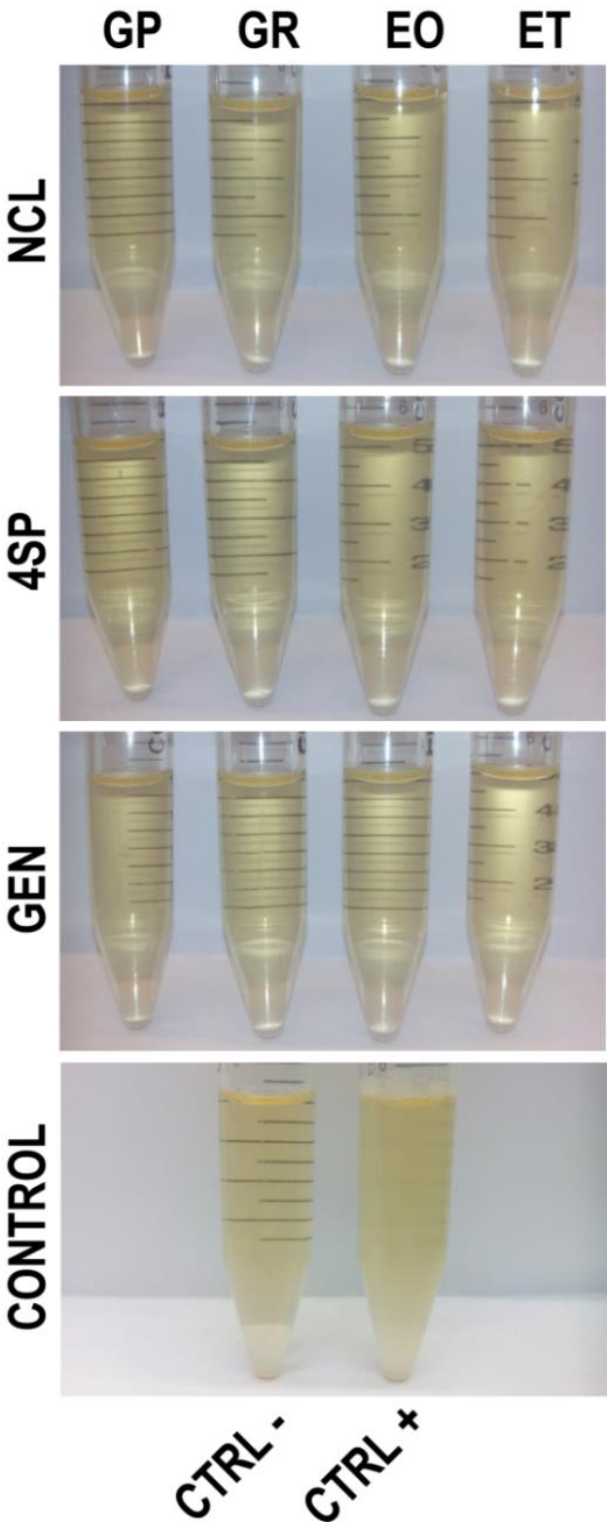

Figure 4.1. Sterility assessment as a function of cross-linking method and sterilisation treatment. No sample showed microbial growth.

4.2.4. Structural characterisation

Morphological characterisation was conducted using a stereo microscope (SZX16, Olympus, UK) and a Hitachi S-4700 scanning electron microscope (SEM, Hitachi, UK). Prior to SEM analysis, collagen films were incubated in 1x PBS overnight, dehydrated in increasing ethanol concentrations (50 %, 70 %, 90 %, 96 % and 100 %) and gold-coated (Emitech K-550X Sputter Coater, Emitech, UK).

4.2.5. Quantification of swelling capacity

Collagen films were incubated in 1x PBS at room temperature overnight. Prior to being weighed, films were quickly blotted with filter paper to remove excess surface water. The swelling ratio (%) was calculated as [(wet weight – dry weight) / dry weight] * 100 %.

4.2.6. Quantification of enzymatic degradation

Resistance to enzymatic degradation was assessed as described previously [44]. Briefly, collagen films were weighed and hydrated for 2 h in 0.1 M Tris-HCl and 5 mM $CaCl_2$ at pH 7.4. Subsequently, the films were incubated with bacterial collagenase type IV (*Clostridium histolyticum*), previously reconstituted in the same buffer at 10 U/ml. After 24 h of incubation at 37 °C, centrifugation was carried out (10,000 g for 5 min), the supernatant was removed, and the remaining films were freeze-dried and weighed. Enzymatic degradation was quantified as a percentage of remaining mass using the following equation: % Remaining mass = [1 – (Initial weight – Final weight) / Initial weight)] * 100 %.

4.2.7. Quantification of solubility

Collagen film solubility was assessed via sodium dodecyl sulphate polyacrylamide gel electrophoresis (SDS-PAGE) and complementary densitometric analysis [45, 46], as has been described previously [47]. Briefly, collagen films were suspended in 1 M acetic acid solution containing 1 mg/ml pepsin from porcine gastric mucosa (lyophilized powder, 3,200-4,500 units/mg protein) at 1 mg/ml concentration for 7 days. The bovine type I collagen solution from which the films were made was used as control. A 3 % stacking gel and a 5 % separation gels were used in a Mini-Protean® 3 apparatus (Bio-Rad Laboratories, UK). Protein bands were stained using the SilverQuest™ kit (Invitrogen, USA) according to the manufacturer's protocol. Densitometric analysis of gels was performed using Image J software (National Institute of Health, USA). Collagen bands were quantified by defining each band with the rectangular tool with background subtraction.

4.2.8. Quantification of denaturation temperature

The denaturation temperature was studied using a differential scanning calorimeter (DSC-60, Shimadzu, Japan), as has been described previously [48]. Briefly, collagen films were incubated in 1x PBS at room temperature overnight and then they were quickly blotted using filter paper to remove unbound surface PBS. Following this, samples were hermetically sealed in aluminium crucibles (Mettler Toledo, UK) and were subjected to a single constant heating ramp at 5 °C/min in the range of 25 to 90 °C. An empty pan was used as reference. The endothermic transition was recorded as a typical peak. The onset (temperature at which the tangent to the initial power versus temperature line crosses the baseline) and peak (temperature of maximum

power absorption during denaturation) temperatures, as well as the denaturation enthalpy (area under the denaturation peak, using a straight base line) were recorded.

4.2.9. Quantification of mechanical properties

Uniaxial tensile test of wet films was performed using an electromechanical testing machine (Z2.5, Zwick, Germany) as has been described previously [49, 50] with slight modifications. Briefly, uniform strips were prepared and their width and thickness were measured using a micrometre. The grips of the testing machine were covered with a rubber film to avoid breakage at contact points; samples that broke at contact points were excluded. The grips were set at 20 mm distance. The samples were tested to complete failure (deformation rate of 10 mm/min, 10 N static load cell). The following parameters were assessed: force at break, stress at break, strain at break and elastic modulus.

4.2.10. Human skin fibroblast and macrophage response

Basic cell response was assessed using WS1 human skin fibroblasts (ATCC, UK) and THP1 human derived leukemic monocyte cells (ATCC, UK). WS1 fibroblasts were grown in Dulbecco's modified Eagle's medium (DMEM) supplemented with 10 % foetal bovine serum (FBS) and 1 % penicillin and streptomycin. WS1 fibroblasts were seeded onto the samples at 16 x 10^3 cells/cm^2 density and incubated at 37 °C, 5 % CO_2 and 95 % humidified air for 1, 3 and 7 days. THP1 cells were grown in RPMI-1640 media supplemented with 10 % FBS and 1 % penicillin and streptomycin. THP1 cells were seeded onto the samples at 26 x 10^3 cells/cm^2 density and mature macrophage-like state was induced through treatment with phorbol 12-myristate 13-acetate (PMA) at 100 ng/ml for 6 h, as has been described previously

[51-53]. Subsequently, adherent cells were washed with Hanks' Balanced Salt solution (HBSS) and incubated with supplemented media at 37 °C, 5 % CO_2 and 95 % humidified air for 1 and 2 days. Activated positive control phenotype was induced with 100 ng/ml of LPS in supplemented media for 24 h.

Cell proliferation was assessed using Quant-iT™ PicoGreen® dsDNA kit (Invitrogen, USA), as per manufacturer's guidelines. Cell metabolic activity was assessed after 2 h incubation at 37 °C with 10 % alamarBlue® (Invitrogen, USA), as per manufacturer's protocol. Cell metabolic activity was expressed in terms of % reduction of alamarBlue® and normalised considering metabolic activity of cells in tissue culture plastic (TCP) at each time point as 100 %. Cell viability was quantified using CytoTox 96® Non-Radioactive Cytotoxicity Assay (Promega, USA) to measure released lactate dehydrogenase (LDH) in the supernatant from dead cells.

4.2.11. Statistical analysis

All experiments were carried out in triplicate, except swelling, denaturation temperature and tensile test assays which were carried out in quintuplicate. Numerical data are expressed as mean ± standard deviation. Statistical analysis was performed using MINITAB® (version 16.2, Minitab Inc., USA). One way analysis of variance (ANOVA) followed by Fisher's post-hoc test were employed after confirming normal distribution from each sample population (Anderson-Darling normality test) and the equality of variances (Bartlett's and Levene's tests for homogeneity of variance). Nonparametric statistics were used when either or both of the above assumptions were violated and, consequently, Kruskal-Wallis for multiple comparison analysis or Mann-Whitney test for 2-samples were carried out. Statistical significance was accepted at $p < 0.05$.

4.3. Results

4.3.1. Structural characterisation

NS NCL and 4SP films were colourless and completely transparent; whilst the GEN films were dark blue and totally opaque (**Figure 4.2**). Following sterilisation, EO-4SP films became brownish and semi-transparent (gross visual assessment), whilst no macroscopic differences were observed in the other treatments (**Figure 4.2**). SEM analysis revealed similar surface morphology for all NS treatments (**Figure 4.3**). Sterilisation differentially affected the surface morphology of the collagen films: GP altered the morphology of NCL and 4SP films; GI altered the morphology of GEN films; EO altered the morphology of 4SP films; and ET altered the morphology of NCL and 4SP films (**Figure 4.3**). Moreover, GP induced wrinkles in the 4SP films that could be associated with collagen mass loss due to the gas treatment (the weight variation induced by each sterilisation method was not studied in this study).

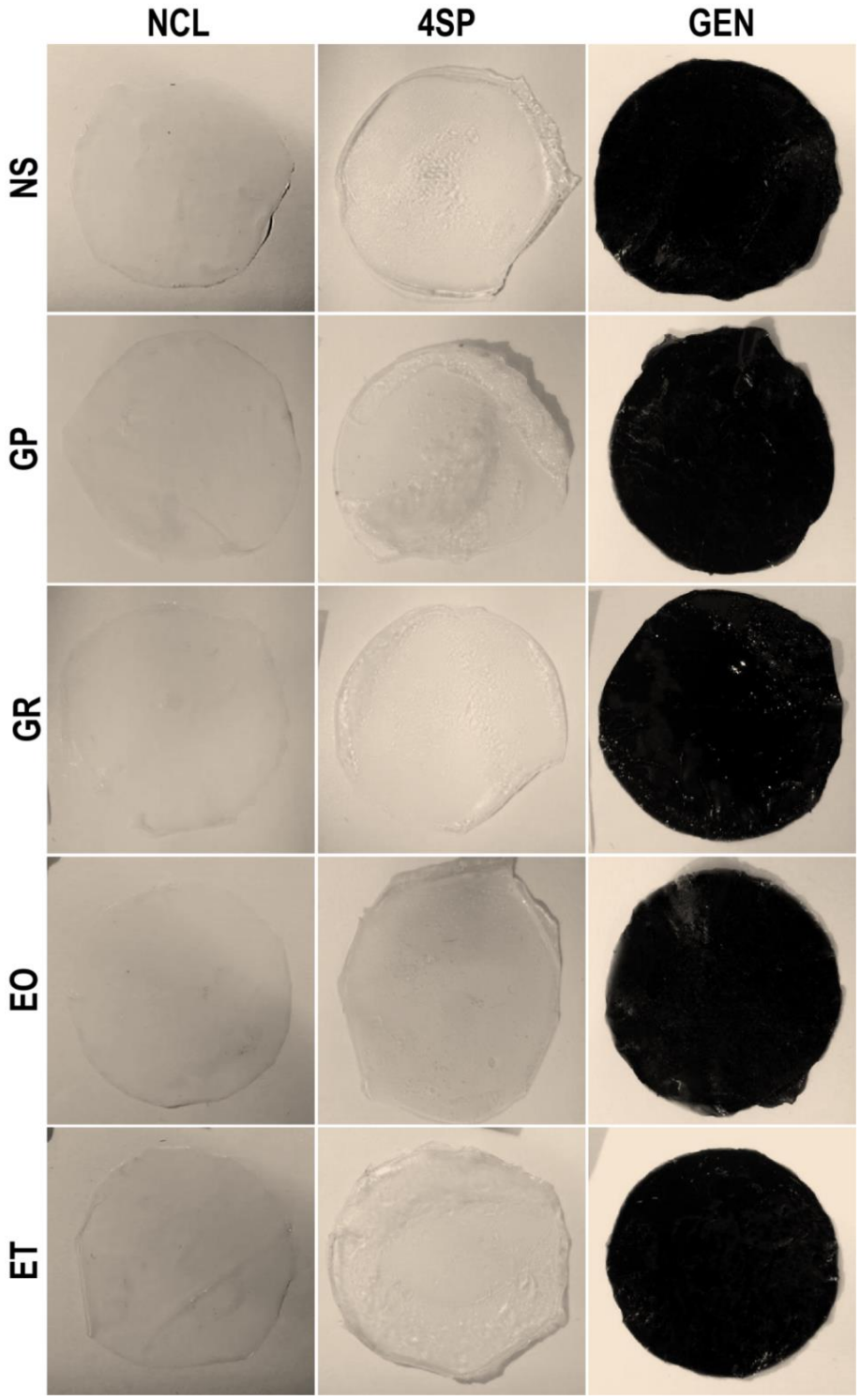

Figure 4.2. Qualitative morphology assessment as a function of cross-linking method and sterilisation treatment. NS NCL and 4SP films were colourless and transparent, whilst GEN produced dark blue films. After sterilisation, the EO-4SP films became brownish, whilst no macroscopic differences were observed in the other treatments.

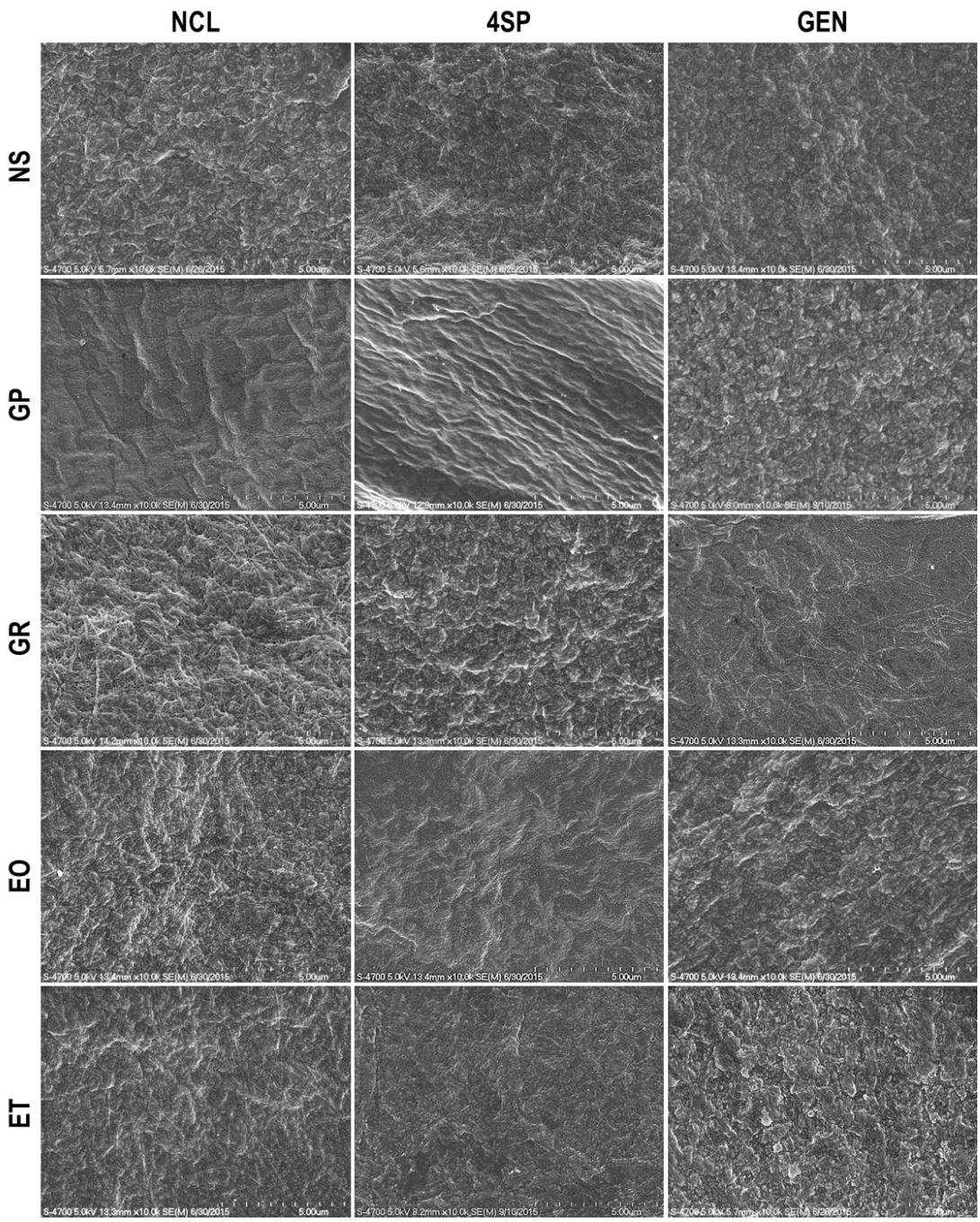

Figure 4.3. Scanning electron micrographs of collagen films as a function of cross-linking method and sterilisation treatment. Cross-linking did not affect the morphology of the non-sterilised samples. Sterilisation differentially affected the surface morphology of the collagen films.

4.3.2. Swelling, enzymatic degradation, solubility and denaturation temperature characterisation

GP sterilisation significantly increased ($p < 0.001$) the swelling ratio of the NCL and the 4SP films, whilst no significant difference ($p > 0.05$) was observed as a function of the sterilisation method for the for the GEN films (**Figure 4.4a**). Collagenase degradation analysis via weigh loss revealed that only the enzymatic resistance of the GP 4SP films was significantly ($p < 0.001$) decreased (**Figure 4.4b**). SDS-PAGE (**Figure 4.5a**) and complementary densitometric (**Figure 4.5b**) analysis revealed no solubility for the 4SP and GEN treated samples, whilst between the NCL samples, NS, ET and GI exhibited the highest solubility ($p < 0.001$). DSC analysis (**Table 4.1**) revealed that between the NCL treatments, GP and EO significantly ($p < 0.001$) decreased the denaturation temperature of the films; between the 4SP treatments, the GP and the EO significantly ($p < 0.001$) decreased the denaturation temperature of the films; and between the GEN treatments, only the GP significantly ($p < 0.05$) decreased the denaturation temperature of the films.

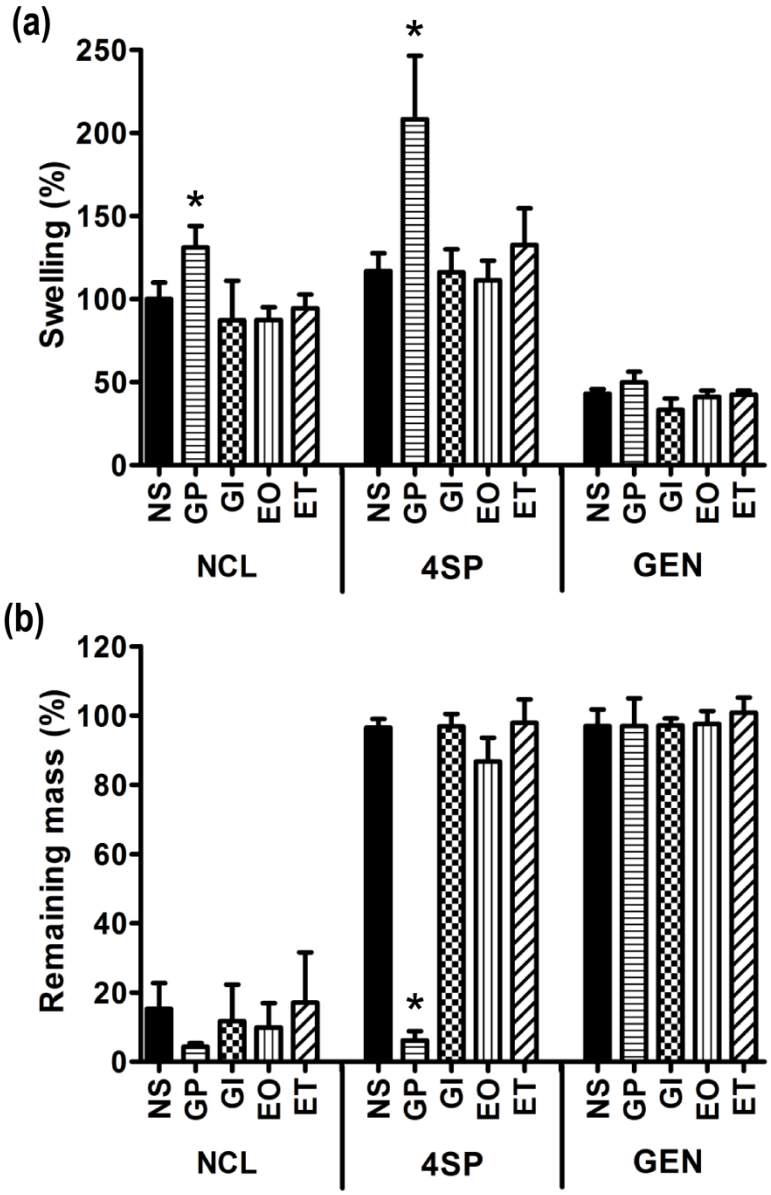

Figure 4.4. Swelling and enzymatic resistance as a function of cross-linking method and sterilisation treatment. **(a)** GP sterilisation significantly increased ($p < 0.001$) % swelling for the NCL and 4SP groups. For the GEN group, no significant difference ($p > 0.05$) was observed between the different sterilisation methods. **(b)** No significant difference, between the sterilisation methods, was observed in susceptibility to collagenase digestion for the NCL and GEN samples ($p > 0.05$). Within the 4SP sample, the GP treated exhibited the lowest ($p < 0.001$) resistance to collagenase digestion.

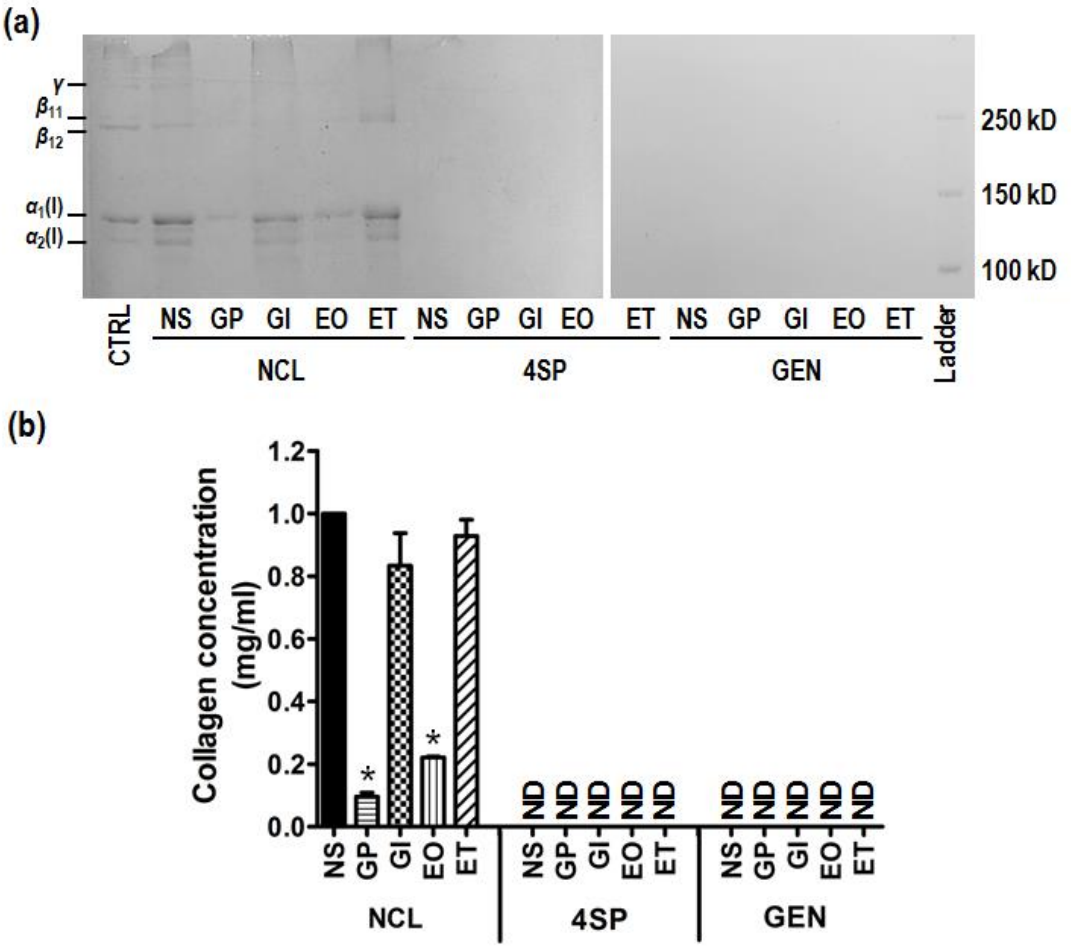

Figure 4.5. Solubility assessment as a function of cross-linking method and sterilisation treatment. SDS-PAGE **(a)** and complementary densitometric analysis **(b)** revealed no detectable (ND) differences in solubility of the 4SP and GEN films as a function of the sterilisation method. Within the NCL films, the highest ($p < 0.001$) solubility was observed for the GP and EO treated films.

Table 4.1. Differential scanning calorimetry data of collagen films as a function of cross-linking method and sterilisation treatment. In general, GP treatment yielded films with the lowest denaturation temperature, independently of the cross-linking state. *: Significant difference at $p < 0.001$. #: Significant difference at $p < 0.05$.

Condition	Onset temperature (ºC)	Peak temperature (ºC)	Energy (J/g)
NS NCL	47.5 ± 0.5	51.3 ± 1.1	7.7 ± 1.4
GP NCL	33.4 ± 3.6*	43.7 ± 1.1*	11.3 ± 0.9*
GR NCL	46.6 ± 1.1	50.4 ± 0.3	8.7 ± 1.1
EO NCL	41.6 ± 0.5*	46.0 ± 0.9*	8.6 ± 1.1
ET NCL	46.7 ± 0.1	50.8 ± 0.1	6.9 ± 0.3
NS 4SP	51.3 ± 2.2	56.6 ± 3.6	2.4 ± 1.4
GP 4SP	29.7 ± 4.0*	37.2 ± 2.2*	5.4 ± 0.9*
GR 4SP	51.6 ± 1.8	57.1 ± 0.8	1.2 ± 0.0
EO 4SP	44.1 ± 1.2*	47.7 ± 0.9*	1.8 ± 0.2
ET 4SP	51.5 ± 2.1	57.4 ± 5.8	0.9 ± 0.5
NS GEN	70.3 ± 0.9	73.8 ± 0.9	1.5 ± 0.2

Condition	Onset temperature (ºC)	Peak temperature (ºC)	Energy (J/g)
GP GEN	63.5 ± 6.3#	69.2 ± 1.5#	2.1 ± 0.5
GR GEN	70.2 ± 2.2	73.0 ± 0.9	1.4 ± 0.4
EO GEN	69.3 ± 2.8	73.4 ± 2.7	1.4 ± 1.3
ET GEN	69.3 ± 0.7	73.1 ± 0.7	1.6 ± 0.5

4.3.3. Biophysical assessment

In general, similar in shape (a small toe region, followed by a rising stress region and a long region of constant gradient until fracture) stress-strain curves were obtained for all treatments, but NCL GP, 4SP GP and 4SP EO, which failed too early (**Figure 4.6**). The GEN treatments exhibited a steeply rising stress region (**Figure 4.6**). **Table 4.2** provides the biomechanical data of the produced scaffolds. Within the NCL groups, the GP treatment resulted in the lowest ($p < 0.05$) stress, strain and force at break and elastic modulus values, whilst the GI treatment resulted in the second lowest ($p < 0.05$) strain at break values. Within the 4SP cross-linked groups, the EO treatment resulted in the lowest ($p < 0.05$) stress, strain and force at break and elastic modulus values, whilst the GP treatment resulted in the second lowest ($p < 0.05$) stress, strain and force at break values. Within the GEN groups, the GP treatment resulted in the lowest ($p < 0.05$) stress and strain at break and elastic modulus values.

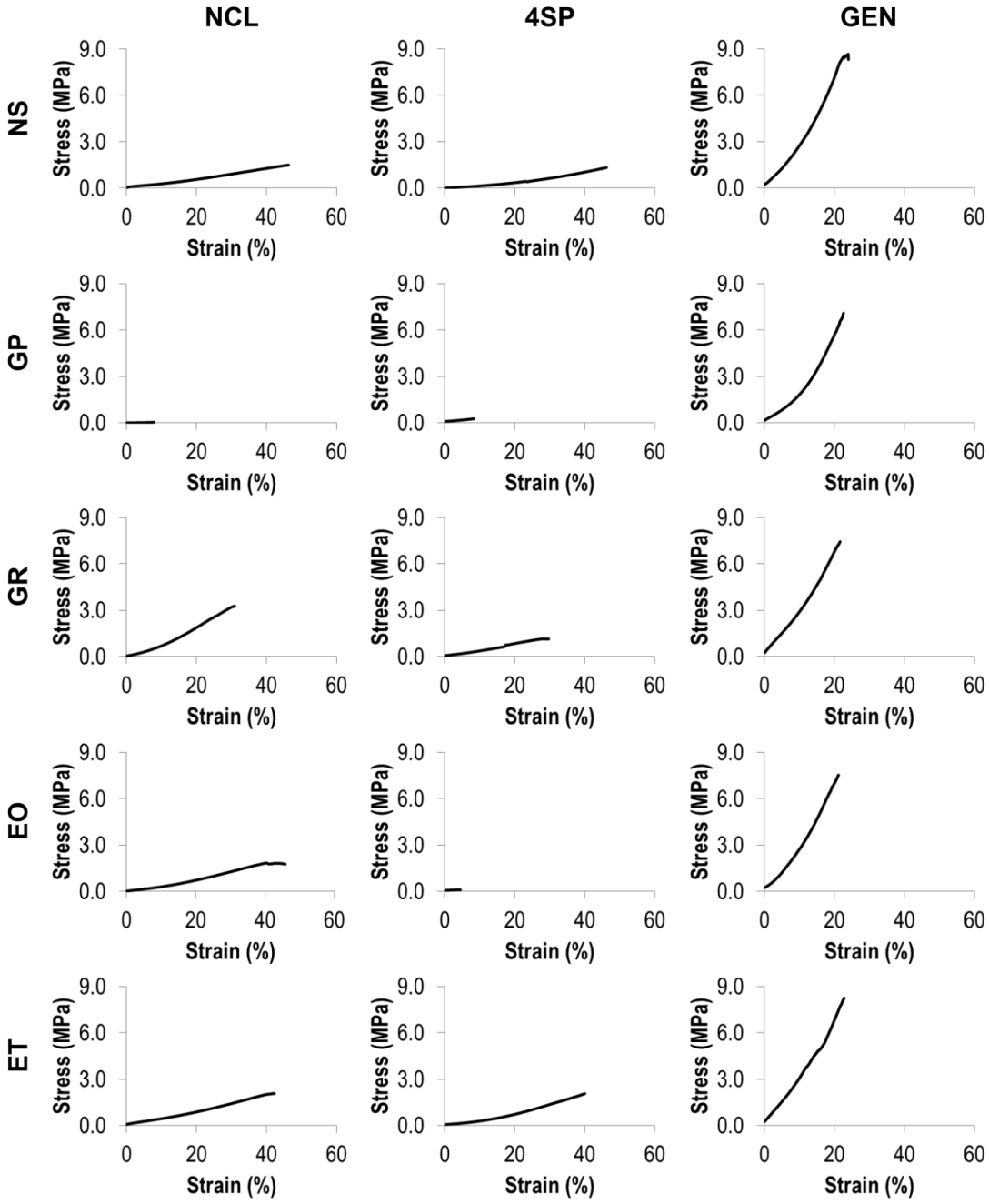

Figure 4.6. Indicative stress-strain curves as a function of cross-linking method and sterilisation treatment. In general, similar in shape (a small toe region, followed by a rising stress region and a long region of constant gradient until fracture) stress-strain curves were obtained for all treatments, apart from the NCL GP, 4SP GP and 4SP EO, which failed too early. The GEN films exhibited a steeply rising stress region.

Table 4.2. Tensile test data of collagen films as a function of cross-linking method and sterilisation treatment. GP treatment yielded films with the lowest mechanical properties for the NCL and GEN films. For the 4SP, the EO yielded the lowest in mechanical properties films. *: Significant difference at $p < 0.001$. #: Significant difference at $p < 0.05$.

Condition	Stress at break (MPa)	Strain at break (%)	Force at break (N/cm)	E Modulus (MPa)
NS NCL	2.08 ± 0.74	51.94 ± 8.11	2.54 ± 0.67	2.43 ± 0.44
GP NCL	0.66 ± 0.20*	7.40 ± 2.55*	0.92 ± 0.29*	0.35 ± 0.15*
GR NCL	3.33 ± 0.48	27.74 ± 7.95*	3.54 ± 0.65	4.14 ± 0.73#
EO NCL	2.19 ± 0.31	40.45 ± 7.89	3.49 ± 0.6	2.92 ± 0.30
ET NCL	2.31 ± 0.28	42.09 ± 3.53	2.70 ± 0.58	3.39 ± 0.52
NS 4SP	1.57 ± 0.43	48.38 ± 14.98	6.06 ± 1.55	1.62 ± 0.42
GP 4SP	0.29 ± 0.19*	14.79 ± 9.00*	0.81 ± 0.49*	1.36 ± 0.50
GR 4SP	1.23 ± 0.21	33.21 ± 7.91	4.61 ± 0.77	1.91 ± 0.26
EO 4SP	0.13 ± 0.06*	6.21 ± 3.23*	0.45 ± 0.20*	0.97 ± 0.12*
ET 4SP	2.35 ± 0.63	43.02 ± 8.89	6.25 ± 2.00	1.96 ± 0.20

Condition	Stress at break (MPa)	Strain at break (%)	Force at break (N/cm)	E Modulus (MPa)
NS GEN	8.19 ± 1.56	27.41 ± 3.54	7.28 ± 1.12	25.27 ± 3.33
GP GEN	4.48 ± 1.43#	19.98 ± 2.55#	5.54 ± 2.19	12.16 ± 2.15#
GR GEN	8.09 ± 0.89	22.28 ± 3.48	8.44 ± 1.48	21.84 ± 3.09
EO GEN	8.73 ± 1.64	23.90 ± 6.38	7.98 ± 0.82	26.43 ± 3.13
ET GEN	8.47 ± 2.15	22.93 ± 5.88	8.29 ± 2.08	22.93 ± 3.04

4.3.4. Biological assessment

Phase contrast microscopy analysis demonstrated that human skin fibroblasts maintained their spindle-shaped morphology, independently of the cross-linking method, sterilisation method or culture time (**Figure 4.7**). DNA concentration, metabolic activity and viability of human skin fibroblasts were not affected ($p > 0.05$) as a function of cross-linking method or sterilisation treatment (**Figure 4.8**).

Regarding to THP1 cells, phase contrast microscopy analysis revealed that most macrophages, independently of the cross-linking method, sterilisation treatment and time in culture, adopted a round morphology (**Figure 4.9**). Only the 4SP films did not exhibit under any sterilisation method elongated cells after 2 days in culture (**Figure 4.9**). Only the 4SP films, independently of the sterilisation method, promoted macrophage aggregates (5 or more cells) after 2 days in culture (**Figure 4.9**). DNA concentration, metabolic activity and viability were significantly ($p < 0.05$) reduced as a function of the cross-linking method, but they were not statistically ($p > 0.05$) affected as a function of the sterilisation treatment (**Figure 4.10**).

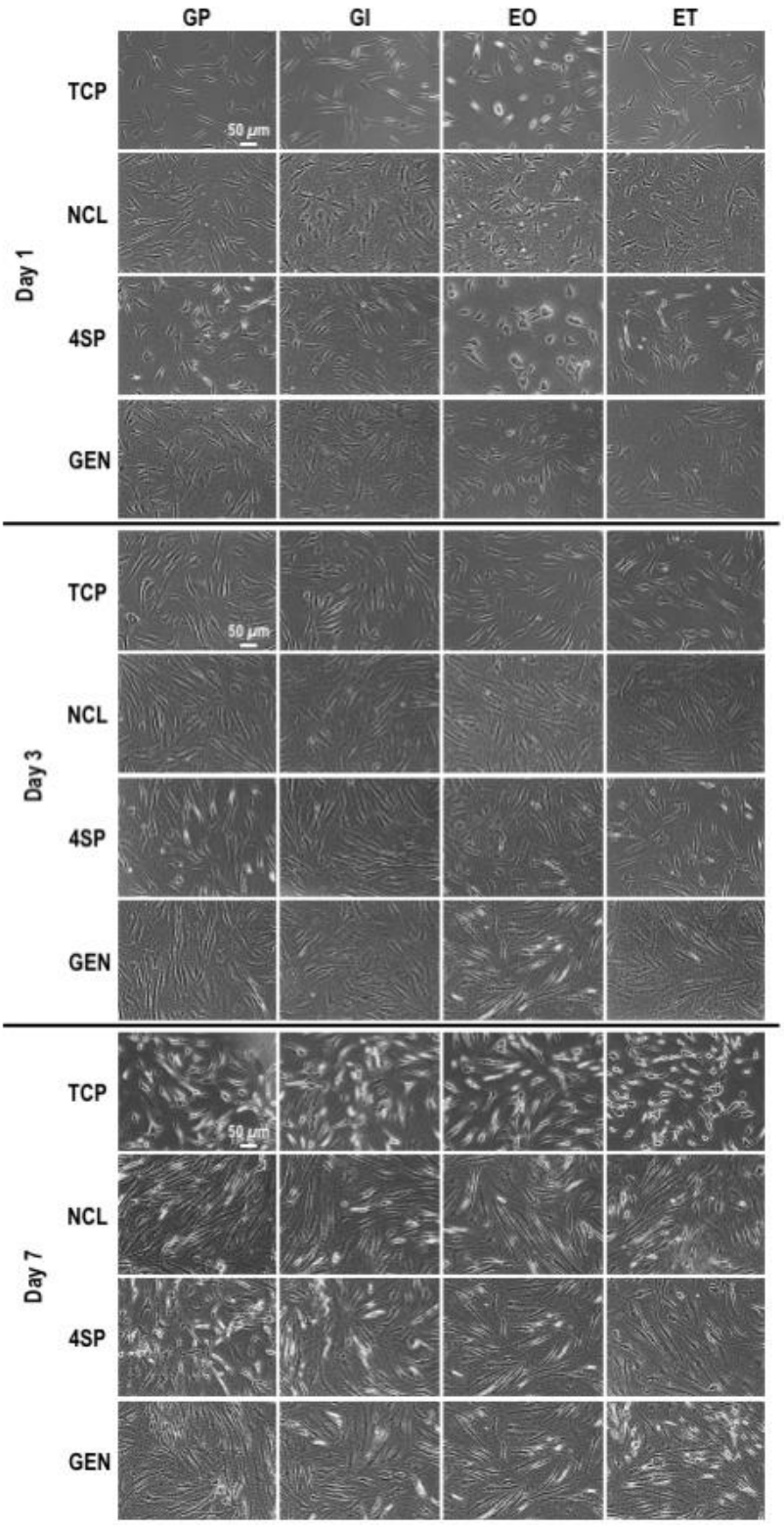

Figure 4.7. Phase contrast microscopy of human skin fibroblasts as a function of cross-linking method and sterilisation treatment. The cells maintained their spindle-shaped morphology, independently of the cross-linking method, sterilisation method or culture time.

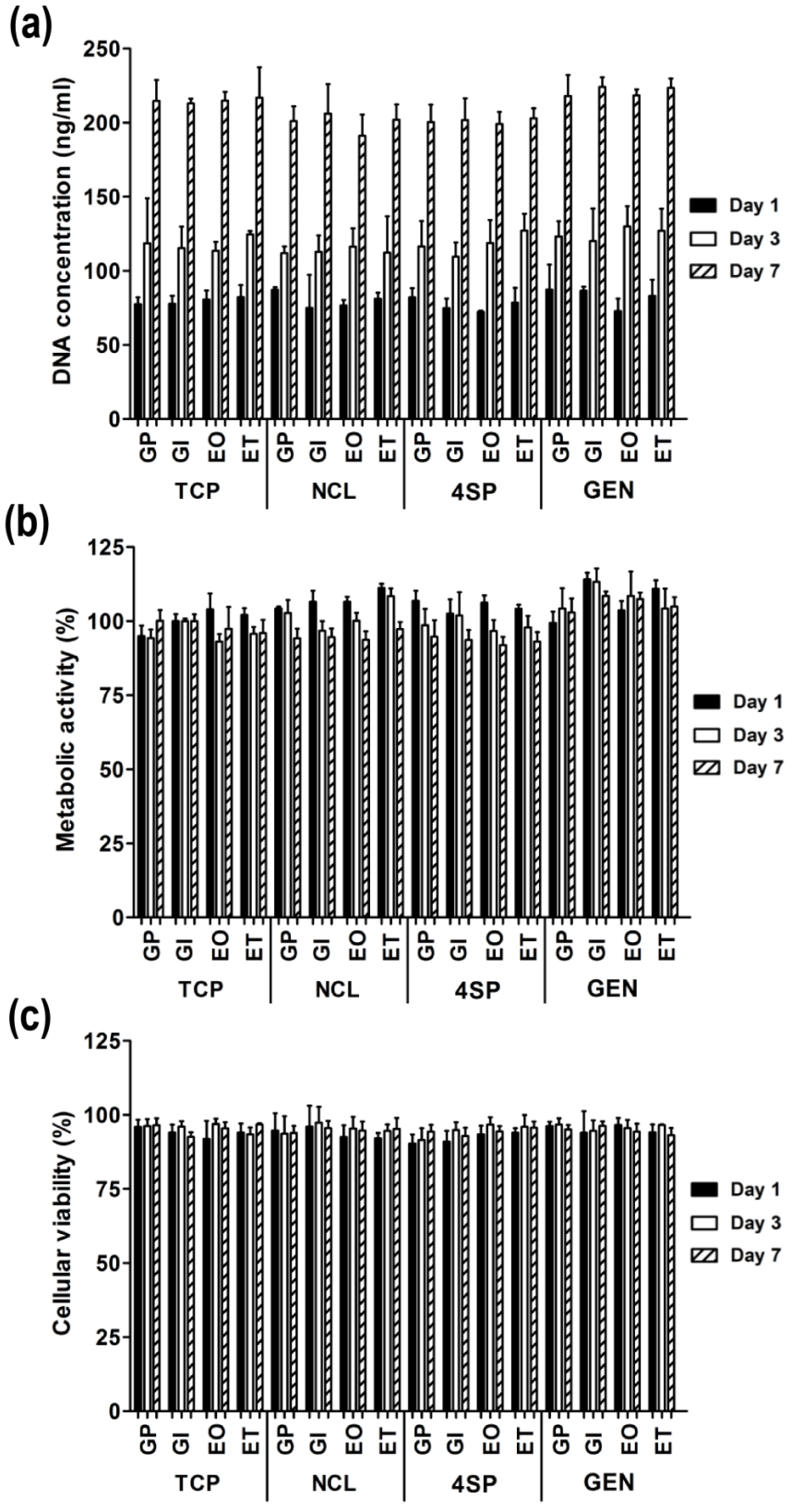

Figure 4.8. Biological assessment, using human skin fibroblasts, as a function of cross-linking method and sterilisation treatment. No significant difference ($p > 0.05$) was observed in DNA concentration **(a)**, metabolic activity **(b)** and cell viability **(c)**.

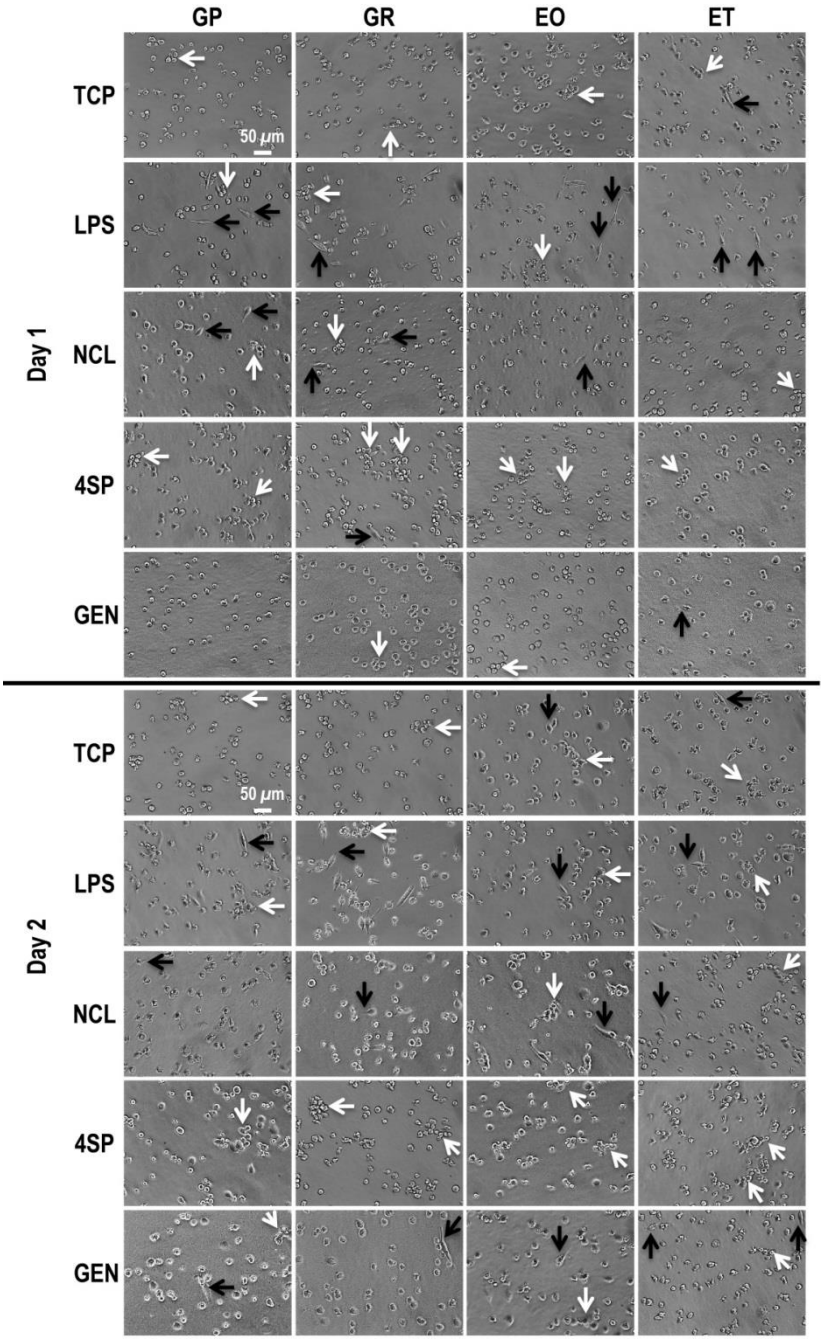

Figure 4.9. Phase contrast microscopic images of THP1 cells as a function of cross-linking method and sterilisation treatment. Most macrophages, independently of the cross-linking method, sterilisation treatment and time in culture, adopted a round morphology. Only the 4SP films did not exhibit under any sterilisation method elongated cells after 2 days in culture. Only the 4SP films, independently of the sterilisation method, promoted macrophage aggregates (5 or more cells) after 2 days in culture. Black arrows: elongated cells. White arrows: cell aggregates.

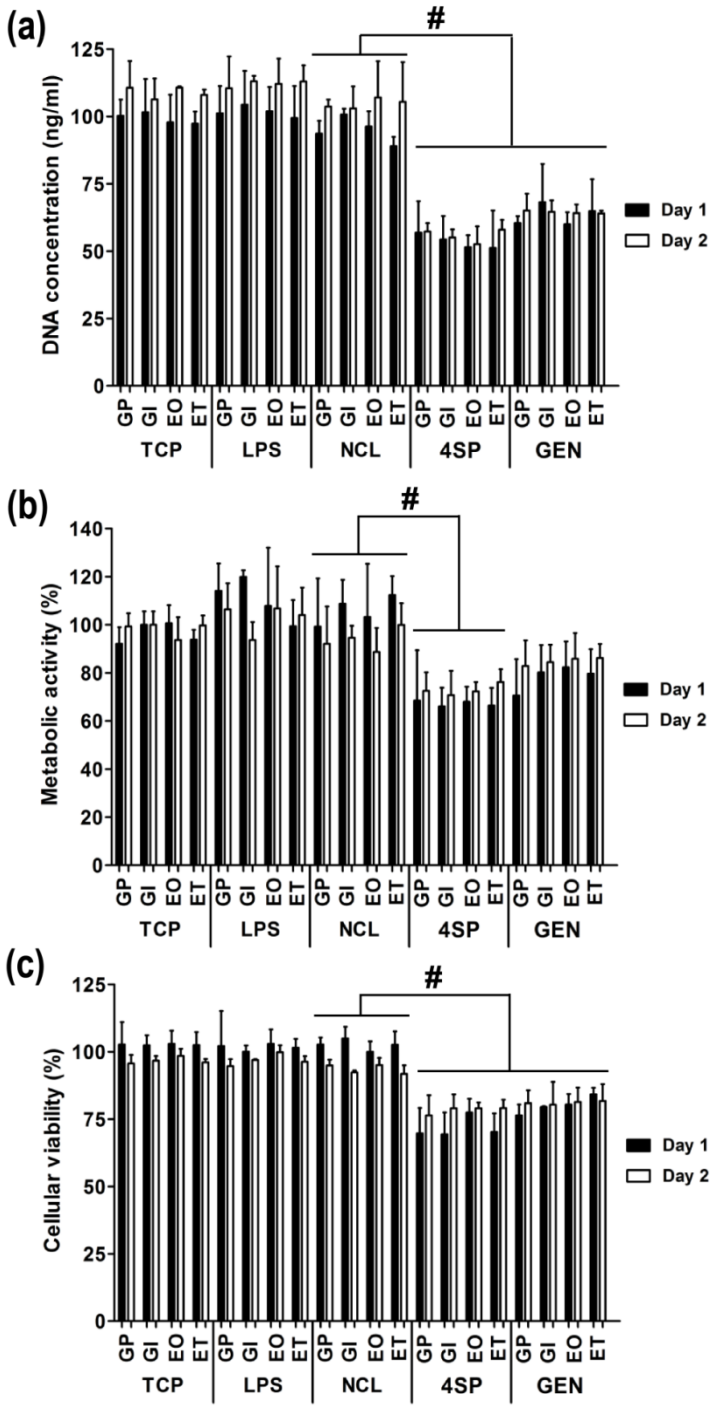

Figure 4.10. Biological assessment, using THP1 cells, as a function of cross-linking method and sterilisation treatment. 4SP significantly reduced ($p < 0.001$) DNA concentration (a), metabolic activity (b) and cell viability (c), whilst GEN significantly reduced ($p < 0.001$) DNA concentration and cell viability, in comparison to the NCL groups. No significant differences ($p > 0.05$) were observed between the sterilisation methods for a given cross-linking state.

4.4. Discussion

Currently available sterilisation treatments are associated with either toxicity (e.g. chemical treatments) or degradation (e.g. physical treatments) of collagen-based devices [10]. Similarly, current potent chemical cross-linking methods (e.g. glutaraldehyde, carbodiimide) of collagen are associated with toxicity and inflammation at the effective concentration [28]. Although the cross-linking potential of 4SP [29-32] and GEN [33-36] has been well-established, their capacity to protect collagen-based devices against sterilisation-induced degradation has yet to be assessed.

Starting with structural analysis, it became apparent that both chemical (EO and ET) and physical (GP, GI) methods were capable of altering the surface morphology of both NCL and 4SP and GEN cross-linked collagen films. In contrast to our data, previous studies have shown EO to not alter the porous structure of collagen sponges [54] and cylindrical collagen scaffolds with longitudinally oriented pore channels [27]. However, EO treatment yielded aggregation of gentamicin loaded PLGA micro-particles, carried by a collagen device, resulting in increased initial release of gentamicin [55]. Similarly to our observations, ET treatment has been shown to induce morphological changes due to dehydration / shrinkage of collagen-based materials [21, 23]; GP has been shown to modify the surface morphology of PCL films [56]; and GI has been shown to damage the structure of various non-cross-linked and cross-linked, even with glutaraldehyde, collagen-based devices [54, 57]. However, it is worth noting that neither morphological changes nor gentamicin release changes were observed when collagen / gentamicin-loaded PLGA micro-particles were subjected to GI treatment [55].

The physicochemical properties of the collagen films appeared to depend on the cross-linking and sterilisation method used. Cross-linking with 4SP was not sufficient to protect against collagenase degradation of GP sterilised collagen films. Cross-linking was not able to avoid thermal denaturation of EO (only for 4SP) and GP (for 4SP and GEN) sterilised films. With respect to the biomechanical properties, within the 4SP groups, the EO and the GP treatments resulted in the lowest stress, strain and force at break values, whilst within the GEN groups, the GP treatment resulted in the lowest stress and strain at break and elastic modulus values. It is evidenced that the more potent the cross-linking method employed, the better the protection against sterilisation induced degradation. Herein, we observed that GEN induced higher stability than 4SP, as judged by higher denaturation temperature, stress at break and elastic modulus values, which is in agreement with previously published data [30]. The great stabilisation capacity of GEN has been attributed to its self-polymerisation capacity that results in efficient binding of primary amines, including those that are relatively far apart [58].

With respect to the influence of the various sterilisation methods on the stability of collagen-based devices, our data are both in agreement, but in contradiction as well, with previous observations. For example, in our hands, GP resulted in profound differences, which is in agreement [56] and disagreement [18, 19, 38] with previous publications. EO treatment of cylindrical collagen scaffolds with longitudinally oriented pore channels resulted in enhanced resistance to denaturation [27]. On the other hand, EO has been shown to decrease shrinkage temperature of non-cross-linked and cross-linked collagen devices [16] and to cause a moderate reduction of enzymatic stability and high reduction of mechanical properties of porcine urinary bladder matrix scaffolds [59]. In contrast to both above studies, no differences were

observed for EO treated collagen materials [18, 54]. GI has been shown to decrease thermal denaturation, but to not affect collagenase resistance and mechanical properties of cross-linked collagen preparations [11, 57, 60]. On the other hand, GI treatment has been shown to decrease resistance against enzymatic degradation [18, 54, 61] and, through chain scission, to decrease mechanical properties of non-cross-linked and cross-linked collagen devices [16, 62]. These contradictive data suggest that the sterilisation method is device dependent and should be appropriately optimised.

With respect to the human dermal fibroblasts cultures, neither the cross-linking method nor the sterilisation treatment appeared to have any effect, which is consistent with previous publications for EO [63-66], ET [66-68], GP [38, 69, 70] and GI [71-74] treated devices. Phase contrast microscopy analysis of THP1 macrophages revealed different polarisation phenotypes: M1 (round morphology; pro-inflammatory), M2 (elongated morphology; anti-inflammatory) and cell aggregates (foreign body response) [75, 76]. Such heterogeneous macrophage response has been previously reported as a function of different collagen cross-linking methods [30], clearly suggesting that the cross-linking method employed, as opposed to the sterilisation treatment used, is more potent modulator of immune response.

4.5. Conclusion

Terminal sterilisation treatments may induce detrimental alterations on the biochemical, biophysical and biological properties of biopolymers. Our data illustrate that gas plasma is not suitable for collagen-based devices. Ethylene oxide should be avoided in conjugation with 4-arms polyethylene glycol succinimidyl glutarate cross-linking, as it significantly alters the mechanical properties of the device. No biomechanical differences were observed for genipin cross-linked and ethylene oxide sterilised collagen-based materials. Gamma irradiation and ethanol did not affect any of the assessed properties. No cytotoxic side effects were brought about by any of the cross-linkers / sterilisation methods. We believe that the cross-linker / sterilisation method to be used are clinical target specific and should be optimised accordingly.

4.6. References

[1] Fratzl P, Weinkamer R. Nature's hierarchical materials. Progress Mat Sci 2007;52:1263-1334.

[2] Friess W. Collagen -- Biomaterial for drug delivery. Eur J Pharm Biopharm 1998;45:113-136.

[3] Browne S, Zeugolis D, Pandit A. Collagen: Finding a solution for the source. Tissue Eng Part A 2013;19:1491-1494.

[4] Sterilization of medical devices -- Microbiological methods -- Part 1: Determination of a population of microorganisms on products. ISO; 2006.

[5] Sterilization of health care products -- Radiation -- Part 2: Establishing the sterilization dose. ISO; 2013.

[6] Sterilization of medical devices -- Microbiological methods -- Part 2: Tests of sterility performed in the definition, validation and maintenance of a sterilization process. ISO; 2009.

[7] Sterilization of health-care products -- Ethylene oxide -- Requirements for the development, validation and routine control of a sterilization process for medical devices. ISO; 2014.

[8] Sterilization of health care products -- General requirements for characterization of a sterilizing agent and the development, validation and routine control of a sterilization process for medical devices. ISO; 2009.

[9] Standard guide for characterization of type I collagen as starting material for surgical implants and substrates for tissue engineered medical products (TEMPs). ASTM International; 2011.

[10] Delgado LM, Pandit A, Zeugolis DI. Influence of sterilisation methods on collagen-based devices stability and properties. Expert Rev Med Devices 2014;11:305-314.

[11] Cheung DT, Perelman N, Tong D, Nimni ME. The effect of gamma-irradiation on collagen molecules, isolated alpha-chains, and crosslinked native fibers. J Biomed Mater Res 1990;24:581-589.

[12] Chen Z, Du T, Tang X, Liu C, Li R, Xu C, et al. Comparison of the properties of collagen-chitosan scaffolds after γ-ray irradiation and carbodiimide cross-linking. J Biomater Sci Polym Ed 2016;27:937-953.

[13] Matuska AM, McFetridge PS. The effect of terminal sterilization on structural and biophysical properties of a decellularized collagen-based scaffold; implications for stem cell adhesion. J Biomed Mater Res B Appl Biomater 2015;103:397-406.

[14] Kaminski A, Grazka E, Jastrzebska A, Marowska J, Gut G, Wojciechowski A, et al. Effect of accelerated electron beam on mechanical properties of human cortical bone: influence of different processing methods. Cell Tissue Bank 2012;13:375-386.

[15] Kajii F, Iwai A, Tanaka H, Matsui K, Kawai T, Kamakura S. Influence of electron beam irradiation doses on bone regeneration by octacalcium phosphate collagen composites. J Tissue Eng Regen Med In Press.

[16] Olde Damink L, Dijkstra P, Van Luyn M, PB VW, Nieuwenhuis P, Feijen J. Influence of ethylene oxide gas treatment on the in vitro degradation behavior of dermal sheep collagen. J Biomed Mater Res 1995;29:149-155.

[17] Moisan M, Barbeau J, Moreau S, Pelletier J, Tabrizian M, Yahia LH. Low-temperature sterilization using gas plasmas: A review of the experiments and an analysis of the inactivation mechanisms. Int J Pharm 2001;226:1-21.

[18] Geutjes PJ, van der Vliet JA, Faraj KA, de Vries N, van Moerkerk HT, Wismans RG, et al. Preparation and characterization of injectable fibrillar type I collagen and evaluation for pseudoaneurysm treatment in a pig model. J Vasc Surg 2010;52:1330-1338.

[19] Mikhael MM, Huddleston PM, Zobitz ME, Chen Q, Zhao KD, An KN. Mechanical strength of bone allografts subjected to chemical sterilization and other terminal processing methods. J Biomech 2008;41:2816-2820.

[20] Sung HW, Hsu HL, Hsu CS. Effects of various chemical sterilization methods on the crosslinking and enzymatic degradation characteristics of an epoxy-fixed biological tissue. J Biomed Mater Res 1997;37:376-383.

[21] Youngstrom DW, Barrett JG, Jose RR, Kaplan DL. Functional characterization of detergent-decellularized equine tendon extracellular matrix for tissue engineering applications. PLoS One 2013;8:e64151.

[22] Zeugolis D, Paul R, Attenburrow G. Post-self-assembly experimentation on extruded collagen fibres for tissue engineering applications. Acta Biomater 2008;4:1646-1656.

[23] Siritientong T, Srichana T, Aramwit P. The effect of sterilization methods on the physical properties of silk sericin scaffolds. AAPS PharmSciTech 2011;12:771-781.

[24] Rutala WA, Weber DJ. Guideline for desinfection and sterilization in healthcare facilities. North Carolina: Department of Health & Human Services and Centers for Disease Control and Prevention - USA; 2008.

[25] Seto A, Gatt CJ, Jr., Dunn MG. Radioprotection of tendon tissue via crosslinking and free radical scavenging. Clin Orthop Relat Res 2008;466:1788-1795.

[26] Seto A, Gatt CJ, Jr., Dunn MG. Improved tendon radioprotection by combined cross-linking and free radical scavenging. Clin Orthop Relat Res 2009;467:2994-3001.

[27] Monaco G, Cholas R, Salvatore L, Madaghiele M, Sannino A. Sterilization of collagen scaffolds designed for peripheral nerve regeneration: Effect on microstructure, degradation and cellular colonization. Mater Sci Eng C Mater Biol Appl

2017;71:335-344.

[28] Delgado L, Bayon Y, Pandit A, Zeugolis DI. To cross-link or not to cross-link? Cross-linking associated foreign body response of collagen-based devices. Tissue Eng B 2014;In Press.

[29] Collin EC, Grad S, Zeugolis DI, Vinatier CS, Clouet JR, Guicheux JJ, et al. An injectable vehicle for nucleus pulposus cell-based therapy. Biomaterials 2011;32:2862-2870.

[30] Delgado LM, Fuller K, Zeugolis DI. Collagen cross-linking: Biophysical, biochemical, and biological response analysis. Tissue Eng Part A 2017;Epub.

[31] Sanami M, Shtein Z, Sweeney I, Sorushanova A, Rivkin A, Miraftab M, et al. Biophysical and biological characterisation of collagen/resilin-like protein composite fibres. Biomed Mater 2015;10:065005.

[32] Sanami M, Sweeney I, Shtein Z, Meirovich S, Sorushanova A, Mullen A, et al. The influence of poly(ethylene glycol) ether tetrasuccinimidyl glutarate on the structural, physical, and biological properties of collagen fibers. J Biomed Mater Res B Appl Biomater 2016;104:914-922.

[33] Satyam A, Subramanian G, Raghunath M, Pandit A, Zeugolis D. In vitro evaluation of Ficoll-enriched and genipin-stabilised collagen scaffolds. J Tissue Eng Regen Med 2014;8:233-241.

[34] Zeugolis DI, Paul GR, Attenburrow G. Cross-linking of extruded collagen fibers - A biomimetic three-dimensional scaffold for tissue engineering applications. J Biomed Mater Res A 2009;89:895-908.

[35] Wang Y, Bao J, Wu X, Wu Q, Li Y, Zhou Y, et al. Genipin crosslinking reduced the immunogenicity of xenogeneic decellularized porcine whole-liver matrices through regulation of immune cell proliferation and polarization. Sci Rep 2016;6:24779.

[36] Alfredo-Uquillas J, Kishore V, Akkus O. Genipin crosslinking elevates the strength of electrochemically aligned collagen to the level of tendons. J Mech Behav Biomed Mater 2012;15:176-189.

[37] Zeugolis D, Paul R, Attenburrow G. Factors influencing the properties of reconstituted collagen fibers prior to self-assembly: Animal species and collagen extraction method. J Biomed Mater Res A 2008;86:892-904.

[38] Markowicz M, Koellensperger E, Steffens GC, Frentz M, Schrage N, Pallua N. The impact of vacuum freeze-drying on collagen sponges after gas plasma sterilization. J Biomater Sci Polym Ed 2006;17:61-75.

[39] Chu G, Harrell CR, Gomez HJ. Terminal sterilization of injectable collagen products. Patent US 7902145 B2 / WO 2006124988 A2; 2011.

[40] Bayon Y, Gravagna P. Preparation of terminally-sterilized collagen that is soluble at neutral pH. Patent EP 2238163 A1 / WO2009095790A1; 2010.

[41] Mendes GC, Brandao TR, Silva CL. Ethylene oxide sterilization of medical devices: A review. Am J Infect Control 2007;35:574-581.

[42] Faraj KA, Brouwer KM, Geutjes PJ, Versteeg EM, Wismans RG, Deprest JA, et al. The effect of ethylene oxide sterilisation, beta irradiation and gamma irradiation on collagen fibril-based scaffolds. J Tissue Eng Reg Med 2011;8:460-470.

[43] Daly WT, Yao L, Abu-rub MT, O'Connell C, Zeugolis DI, Windebank AJ, et al. The effect of intraluminal contact mediated guidance signals on axonal mismatch during peripheral nerve repair. Biomaterials 2012;33:6660-6671.

[44] Helling A, Tsekoura E, Biggs M, Bayon Y, Pandit A, Zeugolis D. In vitro enzymatic degradation of tissue grafts and collagen biomaterials by matrix metalloproteinases: Improving the collagenase assay. ACS Biomater Sci Eng In Press.

[45] Satyam A, Kumar P, Fan X, Gorelov A, Rochev Y, Joshi L, et al. Macromolecular crowding meets tissue engineering by self-assembly: A paradigm shift in regenerative medicine. Adv Mater 2014;26:3024-3034.

[46] Kumar P, Satyam A, Fan X, Rochev Y, Rodriguez B, Gorelov A, et al. Accelerated development of supramolecular corneal stromal-like assemblies from corneal fibroblasts in the presence of macromolecular crowders. Tissue Eng Part C Methods 2015;21:660-670.

[47] Zeugolis D, Li B, Lareu R, Chan C, Raghunath M. Collagen solubility testing: A quality assurance step for reproducible electro-spun nano-fibre fabrication. A technical note. J Biomater Sci Polym Ed 2008;19:1307-1317.

[48] Zeugolis D, Raghunath M. The physiological relevance of wet versus dry differential scanning calorimetry for biomaterial evaluation: A technical note. Polym Int 2010;59:1403-1407.

[49] Zeugolis D, Paul R, Attenburrow G. Extruded collagen-polyethylene glycol fibers for tissue engineering applications. J Biomed Mater Res B Appl Biomater 2008;85:343-352.

[50] Zeugolis D, Paul R, Attenburrow G. Extruded collagen fibres for tissue-engineering applications: Influence of collagen concentration and NaCl amount. J Biomater Sci Polym Ed 2009;20:219-234.

[51] Daigneault M, Preston JA, Marriott HM, Whyte MK, Dockrell DH. The identification of markers of macrophage differentiation in PMA-stimulated THP-1 cells and monocyte-derived macrophages. PLoS One 2010;5:e8668.

[52] Helary C, Browne S, Mathew A, Wang W, Pandit A. Transfection of macrophages by collagen hollow spheres loaded with polyplexes: A step towards modulating inflammation. Acta Biomater 2012;8:4208-4214.

[53] Fuller KP, Gaspar D, Delgado LM, Pandit A, Zeugolis DI. Influence of porosity and pore shape on structural, mechanical and biological properties of poly-caprolactone electro-spun fibrous scaffolds. Nanomedicine 2016;11:1031-1040.

[54] Noah EM, Chen J, Jiao X, Heschel I, Pallua N. Impact of sterilization on the porous design and cell behavior in collagen sponges prepared for tissue engineering. Biomaterials 2002;23:2855-2861.

[55] Friess W, Schlapp M. Sterilization of gentamicin containing collagen/PLGA microparticle composites. Eur J Pharm Biopharm 2006;63:176-187.

[56] Ghobeira R, Philips C, Declercq H, Cools P, De Geyter N, Cornelissen R, et al. Effects of different sterilization methods on the physico-chemical and bioresponsive properties of plasma-treated polycaprolactone films. Biomed Mater 2017;12:015017.

[57] Roe SC, Milthorpe BK, True K, Rogers GJ, Schindhelm K. The effect of gamma irradiation on a xenograft tendon bioprosthesis. Clin Mater 1992;9:149-154.

[58] Mi F-L, Shyu S-S, Peng C-K. Characterization of ring-opening polymerization of genipin and pH-dependent cross-linking reactions between chitosan and genipin. J Polym Sci Part A: Polym Chem 2005;43:1985-2000.

[59] Freytes DO, Stoner RM, Badylak SF. Uniaxial and biaxial properties of terminally sterilized porcine urinary bladder matrix scaffolds. J Biomed Mater Res B 2008;84B:408-414.

[60] Hara M, Koshimizu N, Yoshida M, Haug IJ, Ulset AS, Christensen BE. Cross-linking and depolymerisation of gamma-irradiated fish gelatin and porcine gelatin studied by SEC-MALLS and SDS-PAGE: A comparative study. J Biomater Sci Polym Ed 2010;21:877-892.

[61] De Deyne P, Haut RC. Some effects of gamma irradiation on patellar tendon allografts. Connect Tissue Res 1991;27:51-62.

[62] Mitchell EJ, Stawarz AM, Kayacan R, Rimnac CM. The effect of gamma radiation sterilization on the fatigue crack propagation resistance of human cortical bone. J Bone Joint Surg Am 2004;86-A:2648-2657.

[63] Vink P, Pleijsier K. Aeration of ethylene oxide-sterilized polymers. Biomaterials 1986;7:225-230.

[64] França R, Mbeh D, Samani T, Le Tien C, Mateescu M, Yahia L, et al. The effect of ethylene oxide sterilization on the surface chemistry and in vitro cytotoxicity of several kinds of chitosan. J Biomed Mater Res B Appl Biomater 2013;101:1444-1455.

[65] Dimitrievska S, Petit A, Doillon C, Epure L, Ajji A, Yahia L, et al. Effect of sterilization on non-woven polyethylene terephthalate fiber structures for vascular grafts. Macromol Biosci 2011;11:13-21.

[66] de Moraes M, Weska R, Beppu M. Effects of sterilization methods on the physical, chemical, and biological properties of silk fibroin membranes. J Biomed Mater Res B Appl Biomater 2014;102:869-876.

[67] Escudero-Castellanos A, Ocampo-García B, Domínguez-García M, Flores-Estrada J, Flores-Merino M. Hydrogels based on poly(ethylene glycol) as scaffolds for tissue engineering application: Biocompatibility assessment and effect of the sterilization process. J Mater Sci Mater Med 2016;27:176.

[68] Zhao L, Mei S, Wang W, Chu P, Wu Z, Zhang Y. The role of sterilization in the cytocompatibility of titania nanotubes. Biomaterials 2010;31:2055-2063.

[69] Bertoldi S, Fare S, Haugen HJ, Tanzi MC. Exploiting novel sterilization techniques for porous polyurethane scaffolds. J Mater Sci Mater Med 2015;26:182.

[70] Dai Y, Xia Y, Chen H-B, Li N, Chen G, Zhang F-M, et al. Optimization of sterilization methods for electrospun poly(ε-caprolactone) to enhance pre-osteoblast cell behaviors for guided bone regeneration. J Bioact Compat Polym 2016;31:152-166.

[71] Gorham S. Collagen. In: Byrom D, editor. Biomaterials. New York: Stockton Press; 1991. p. 55-122.

[72] Galante R, Rediguieri C, Kikuchi I, Vasquez P, Colaço R, Serro A, et al. About the sterilization of chitosan hydrogel nanoparticles. PLoS One 2016;11:e0168862.

[73] Hogg P, Rooney P, Leow-Dyke S, Brown C, Ingham E, Kearney JN. Development of a terminally sterilised decellularised dermis. Cell Tissue Bank 2015;16:351-359.

[74] Hu T, Yang Y, Tan L, Yin T, Wang Y, Wang G. Effects of gamma irradiation and moist heat for sterilization on sodium alginate. Biomed Mater Eng 2014;24:1837-1849.

[75] McWhorter FY, Wang T, Nguyen P, Chung T, Liu WF. Modulation of macrophage phenotype by cell shape. Proc Natl Acad Sci U S A 2013;110:17253-17258.

[76] Yahyouche A, Zhidao X, Czernuszka JT, Clover AJ. Macrophage-mediated degradation of crosslinked collagen scaffolds. Acta Biomater 2011;7:278-286.

Chapter 5: Summary and future studies

5.1. Summary

The extracellular matrix has native biophysical, biochemical and biological properties, which provide cell support, protection and signalling that determine cell behaviour [1, 2]. Therefore, tissue engineering strategies focus on developing biomaterials that mimic extracellular matrix properties. In this sense, collagen-based materials are attractive due to their natural composition, well-tolerated degradation products and cell instructive cues [3, 4]. However, clinical translation and commercialisation are limited by some relevant challenges that need to be addressed, such as batch-to-batch variability [5], mechanical resilience [6], degradation resistance [7], cross-linking strategies that lead to a chronic inflammation or foreign body response instead of a more pro-wound healing response [8], or degradation during sterilisation treatments [9].

In this sense, macrophages have defined as a rapid response cell type with plasticity that support tissue repair [10]. Our aim was to assess the influence of collagen extraction, cross-linking and sterilisation on macrophage response to collagen-based devices.

The assessment of the different collagen extraction protocols (in chapter 2) revealed that pre- and post- extraction method variables have been shown to influence the biochemical properties of collagen and the *in vitro* macrophage response. Collagen extraction with acetic acid and pepsin exhibited the highest yield, purity and free amine content and the lowest denaturation temperature, with no differences in resistance to collagenase digestion. Although all treatments exhibited similar macrophage morphology comprised of round cells (M1 phenotype), elongated cells (M2 phenotype) and cell aggregates (foreign body response), significantly more elongated cells were observed on acetic acid films. Moreover, the most significant

finding herein was that hydrochloric acid treatments induced significantly higher release of pro-inflammatory cytokines (IL-1β and TNF-α) with respect to acetic acid treatments, while salt precipitation and pepsin treatment did not appear to influence the macrophage response. These findings indicate that acid strength, surface energy or ion presence may determine macrophage response.

Regarding the chemical cross-linking of collagen to enhance mechanical and enzymatic stability (in chapter 3), all cross-linking methods reduced free amine groups, showing some formation of covalent bonds between the free amine or carboxyl groups of collagen with the cross-linking agent. However, only 4-arm polyethylene glycol succinimidyl glutarate (4SP) and genipin cross-linking increased biochemical and biophysical resistance as glutaraldehyde cross-linking control. With respect to biological analysis, fibroblast cultures showed no significant differences between the cross-linking treatments. Although direct cultures with human macrophages clearly demonstrated the cytotoxic effect of glutaraldehyde, cultures supplemented with conditioned media from the various groups showed no significant differences between the different treatments. With respect to cytokine profile, no significant difference in secretion of pro-inflammatory (e.g. IL-1β, IL-8, TNF-α) and anti-inflammatory (e.g. IL-10, VEGF) cytokines was observed between the non-cross-linked and the 4-arm polyethylene glycol succinimidyl glutarate and genipin cross-linked groups, suggesting the suitability of these agents as collagen cross-linkers. Once more, the obtained results suggested that multifactorial approaches (e.g. collagen extraction optimisation, collagen self-assembling, collagen cross-linking) should be employed to modulate *in vitro* macrophage response.

Finally, chemical cross-linking was assessed as a tool to control degradation resistance to ethylene oxide, ethanol, gamma irradiation and gas plasma sterilisation

(in chapter 4). Our data showed that gas plasma altered the structural, biophysical and biochemical properties of non-cross-linked collagen films and cross-linked counterparts with 4SP and genipin. On the other hand, ethylene oxide resulted in a significant reduction of the mechanical properties of the collagen films. However, gamma irradiation and ethanol sterilisation did not significantly affect thermal, degradation, solubility and mechanical properties of the collagen films. Regarding cell response, human skin fibroblast and macrophage cultures did not reveal any considerable differences as a function of the cross-linking method or sterilisation treatment. We believe that the choice of cross-linking and sterilisation method is device and clinical target dependent and should be optimised accordingly.

Overall, we provide evidence that mechanical and enzymatic resistance of collagen-based devices, such as films, can be improved without compromising human macrophage response or wound healing by controlling collagen extraction and purification, self-assembling, cross-linking, sterilisation, among other parameters. This work provides a new perspective in the field of tissue engineering by demonstrating that fabrication parameters of collagen scaffolds are specific for each clinical indication and they should be optimised accordingly.

5.2. Future studies

The design of bioengineered biomaterials for tissue engineering that can modulate macrophage polarisation to pro-healing and tissue remodelling functions is still under investigation [11]. We explored some of the factors, such as collagen extraction method, exogenous cross-linking or ultimate sterilisation, which can affect inflammatory response upon a reconstituted collagen-based scaffold upon implantation. However, other factors could have an effect on macrophage response such as collagen source, scaffold form and structure, topography, degradation period and products, substrate stiffness, among other factors. Moreover, there are several remarkable strategies in tissue engineering (such as controlled release of growth factors, gene vectors or small molecule drugs) that could be used to modulate macrophage response and consequently enhance tissue repair. Based on the findings and limitations encountered during this thesis, some project proposals are formulated in this section.

5.2.1. Structured collagen films to control macrophage response

Biophysical features, such as stiffness, topographical patterns, pore size or fibre diameter have been demonstrated to impact macrophage function. Regarding the influence of stiffness on macrophage function, macrophages showed a preferential phagocytosis through the stiffest polyacrylamide particles [12], higher spreading and elasticity on the stiffest polyacrylamide gels [13, 14] and increased pro- and anti-inflammatory cytokines *in vitro* and thicker fibrotic encapsulation *in vivo* at stiffest polyethylene glycol–RGD hydrogels (840 kPa) in comparison to the softer hydrogels (130 kPa) [15]. Moreover, topographical patterns on poly(dimethyl siloxane) or Pluronics F127 with fibronectin demonstrated to control macrophage function and

polarisation [16, 17]. Similarly, pore size or fibre diameter and alignment at poly(2-hydroxyethyl methacrylate-co-methacrylic acid) or poly(L-lactic) scaffolds determined macrophage phenotype [18-20]. It is imperative to identify the optimal biophysical features for collagen-based devices in order to modulate macrophage response and to enhance wound healing.

It can be hypothesised that biophysically engineered collagen films will preferentially promote macrophage polarisation from M1 phenotype to M2 phenotype, whilst maintaining mechanical and enzymatic resistance. The influence of collagen stiffness on macrophage response can be assessed using hydrogels with different collagen concentrations and compared to polyacrylamide hydrogels coated with a monolayer of collagen. Collagen stiffness can be also controlled using different degree of cross-linking. Topographical features (groove or pins with different sizes and distribution) can be introduced by soft-lithography onto collagen films alone or in combination with the optimised collagen stiffness to control macrophage response. The influence of pore size on macrophage response can be studied using moulds with pins. Alternatively, pore size could be assessed using collagen sponges obtained by controlled freeze-drying [21].

5.2.2. Functionalised collagen films to control macrophage response

Macrophage response is highly sensitive to biochemical and biological signals [22, 23]. Among others, biomaterial functionalisation approaches with glycosaminoglycans (GAGs), proteoglycans (PGs) and/or carbohydrates (CHs) are extensively studied as means to modulate macrophage response [24-26]. GAGs, PGs and CHs have the specific function of cytokine and growth factor retention due to

their specific binding sites [27-30]. The sulphate group and the extent of sulphation dramatically influence cytokine and growth factor retention [30, 31].

It can be hypothesised that functionalised collagen films will induce a pro-wound healing macrophage M2 phenotype, whilst maintaining collagen fibrillar structure and enzymatic resistance. Different sulphated and non-sulphated GAGs and CHs (e.g. hyaluronic acid, heparin sulphate, chondroitin sulphate, dermatan sulphate, Ficoll, carrageenan), as well as PGs will be incorporated into collagen solution before self-assembly and their influence on the structural, biophysical, biochemical and biological properties of collagen-based biomaterials will be assessed.

5.2.3. Controlled release of therapeutics to control macrophage response

In designing an immune-modulated and regenerative biomaterials, the most targeted method is the controlled release of IL-4 or IL-10 cytokines or DNA plasmids, as these anti-inflammatory cytokines can induce macrophage polarisation [32-34]. Other potential, yet less studied moieties, are synthetic drugs (e.g. steroids) [35, 36], microRNAs (miR, e.g. miR9, miR106, miR146, miR466) [37-40] and short RNA molecules involved in silencing and post-transcriptional regulation of gene expression [41]. The ideal cargo and carrier have yet to be identified.

It can be hypothesised that optimally cross-linked collagen scaffolds can afford sustained and localised delivery of such cargos at the site of injury. Collagen scaffolds will be stabilised with variable starPEG moieties (e.g. molecular weight, number of arms, concentration) and loaded with appropriate cargo(s). The structural, biophysical, biochemical and biological properties of the produced scaffolds will be assessed *in vitro* and *in vivo* in suitable preclinical model. Of interest would also be the simultaneous delivery of multiple cargos from one carrier.

5.3. References

[1] Capulli AK, MacQueen LA, Sheehy SP, Parker KK. Fibrous scaffolds for building hearts and heart parts. Adv Drug Deliv Rev 2016;96:83-102.

[2] Fernandez-Yague MA, Abbah SA, McNamara L, Zeugolis DI, Pandit A, Biggs MJ. Biomimetic approaches in bone tissue engineering: Integrating biological and physicomechanical strategies. Adv Drug Deliv Rev 2015;84:1-29.

[3] Friess W. Collagen--biomaterial for drug delivery. Eur J Pharm Biopharm 1998;45:113-136.

[4] Abou Neel EA, Bozec L, Knowles JC, Syed O, Mudera V, Day R, et al. Collagen--emerging collagen based therapies hit the patient. Adv Drug Deliv Rev 2013;65:429-456.

[5] Baez J, Olsen D, Polarek JW. Recombinant microbial systems for the production of human collagen and gelatin. Appl Microbiol Biotechnol 2005;69:245-252.

[6] Kumar VA, Caves JM, Haller CA, Dai E, Li L, Grainger S, et al. Collagen-based substrates with tunable strength for soft tissue engineering. Biomater Sci 2013;1.

[7] Dearth CL, Keane TJ, Carruthers CA, Reing JE, Huleihel L, Ranallo CA, et al. The effect of terminal sterilization on the material properties and in vivo remodeling of a porcine dermal biologic scaffold. Acta Biomater 2016;33:78-87.

[8] Brown BN, Badylak SF. Expanded applications, shifting paradigms and an improved understanding of host-biomaterial interactions. Acta Biomater 2013;9:4948-4955.

[9] Meyer M, Prade I, Leppchen-Fröhlich K, Felix A, Herdegen V, Haseneder R, et al. Sterilisation of collagen materials using hydrogen peroxide doted supercritical carbon dioxide and its effects on the materials properties. J Supercritical Fluids 2015;102:32-39.

[10] Badylak SF. A scaffold immune microenvironment. Science 2016;352:298.

[11] Sridharan R, Cameron AR, Kelly DJ, Kearney CJ, O'Brien FJ. Biomaterial based modulation of macrophage polarization: A review and suggested design principles. Materials Today 2015;18:313-325.

[12] Beningo KA, Wang YL. Fc-receptor-mediated phagocytosis is regulated by mechanical properties of the target. J Cell Science 2002;115:849-856.

[13] Patel NR, Bole M, Chen C, Hardin CC, Kho AT, Mih J, et al. Cell elasticity determines macrophage function. PLoS One 2012;7:e41024.

[14] Féréol S, Fodil R, Labat B, Galiacy S, Laurent VM, Louis B, et al. Sensitivity of alveolar macrophages to substrate mechanical and adhesive properties. Cell Motil Cytoskeleton 2006;63:321-340.

[15] Blakney AK, Swartzlander MD, Bryant SJ. The effects of substrate stiffness on the in vitro activation of macrophages and in vivo host response to poly(ethylene glycol)-based hydrogels. J Biomed Mater Res A 2012;100A:1375-1386.

[16] Chen S, Jones JA, Xu Y, Low HY, Anderson JM, Leong KW. Characterization of topographical effects on macrophage behavior in a foreign body response model. Biomaterials 2010;31:3479-3491.

[17] McWhorter FY, Wang T, Nguyen P, Chung T, Liu WF. Modulation of macrophage phenotype by cell shape. Proc Natl Acad Sci U S A 2013;110:17253-17258.

[18] Madden LR, Mortisen DJ, Sussman EM, Dupras SK, Fugate JA, Cuy JL, et al. Proangiogenic scaffolds as functional templates for cardiac tissue engineering. Proc Natl Acad Sci U S A 2010;107:15211-15216.

[19] Saino E, Focarete ML, Gualandi C, Emanuele E, Cornaglia AI, Imbriani M, et al. Effect of electrospun fiber diameter and alignment on macrophage activation and

secretion of proinflammatory cytokines and chemokines. Biomacromolecules 2011;12:1900-1911.

[20] Garg K, Pullen NA, Oskeritzian CA, Ryan JJ, Bowlin GL. Macrophage functional polarization (M1/M2) in response to varying fiber and pore dimensions of electrospun scaffolds. Biomaterials 2013;34:4439-4451.

[21] Stokols S, Tuszynski MH. The fabrication and characterization of linearly oriented nerve guidance scaffolds for spinal cord injury. Biomaterials 2004;25:5839–5846.

[22] Hynes RO. Extracellular matrix: Not just pretty fibrils. Science 2009;326:1216-1219.

[23] Boersema GSA, Grotenhuis N, Bayon Y, Lange JF, Bastiaansen-Jenniskens YM. The effect of biomaterials used for tissue regeneration purposes on polarization of macrophages. Biores Open Access 2016;5:6-14.

[24] Gao A, Hang R, Li W, Zhang W, Li P, Wang G, et al. Linker-free covalent immobilization of heparin, SDF-1alpha, and CD47 on PTFE surface for antithrombogenicity, endothelialization and anti-inflammation. Biomaterials 2017;140:201-211.

[25] Franz S, Allenstein F, Kajahn J, Forstreuter I, Hintze V, Moller S, et al. Artificial extracellular matrices composed of collagen I and high-sulfated hyaluronan promote phenotypic and functional modulation of human pro-inflammatory M1 macrophages. Acta Biomater 2013;9:5621-5629.

[26] Taraballi F, Corradetti B, Minardi S, Powel S, Cabrera F, Van Eps JL, et al. Biomimetic collagenous scaffold to tune inflammation by targeting macrophages. J Tissue Eng 2016;7:2041731415624667.

[27] Sasisekharan R, Raman R, Prabhakar V. Glycomics approach to structure-function relationships of glycosaminoglycans. Annu Rev Biomed Eng 2006;8:181-231.

[28] Schultz GS, Wysocki A. Interactions between extracellular matrix and growth factors in wound healing. Wound Repair Regen 2009;17:153-162.

[29] Taylor KR, Gallo RL. Glycosaminoglycans and their proteoglycans: Host-associated molecular patterns for initiation and modulation of inflammation. FASEB J 2006;20:9-22.

[30] Salek-Ardakani S, Arrand JR, Shaw D, Mackett M. Heparin and heparan sulfate bind interleukin-10 and modulate its activity. Blood 2000;96:1879-1888.

[31] Gama CI, Tully SE, Sotogaku N, Clark PM, Rawat M, Vaidehi N, et al. Sulfation patterns of glycosaminoglycans encode molecular recognition and activity. Nat Chem Biol 2006;2:467-473.

[32] Browne S, Monaghan MG, Brauchle E, Berrio DC, Chantepie S, Papy-Garcia D, et al. Modulation of inflammation and angiogenesis and changes in ECM GAG-activity via dual delivery of nucleic acids. Biomaterials 2015;69:133-147.

[33] Browne S, Pandit A. Biomaterial-mediated modification of the local inflammatory environment. Front Bioeng Biotechnol 2015;3:67.

[34] Dash BC, Thomas D, Monaghan M, Carroll O, Chen X, Woodhouse K, et al. An injectable elastin-based gene delivery platform for dose-dependent modulation of angiogenesis and inflammation for critical limb ischemia. Biomaterials 2015;65:126-139.

[35] Boehler C, Kleber C, Martini N, Xie Y, Dryg I, Stieglitz T. Actively controlled release of dexamethasone from neural microelectrodes in a chronic in vivo study. Biomaterials 2017;129:176-187.

[36] Vacanti NM, Cheng H, Hill PS, Guerreiro JDT, Dang TT, Ma M, et al. Localized delivery of dexamethasone from electrospun fibers reduces the foreign body response. Biomacromolecules 2012;13:3031-3038.

[37] Taganov K, Boldin M, Chang K, D B. NF-kappa B-dependent induction of microRNA miR-146, an inhibitor targeted to signaling proteins of innate immune responses. Proc Natl Acad Sci U S A 2006;103:12481-12486.

[38] Sharma A, Kumar M, Aich J, Hariharan M, Brahmachari S, Agrawal A, et al. Posttranscriptional regulation of interleukin-10 expression by hsa-miR-106a. Proc Natl Acad Sci U S A 2009;106:5761-5766.

[39] Rouse JG, Van Dyke ME. A review of keratin-based biomaterials for biomedical applications. Materials 2010;3:999-1014.

[40] Sonkoly E, Pivarcsi A. MicroRNAs in Inflammation. Int Rev Immunol 2009;28:535-561.

[41] Rupaimoole R, Slack FJ. MicroRNA therapeutics: Towards a new era for the management of cancer and other diseases. Nature Rev Drug Discover 2017;16:203-222.

Appendices: Protocols and supplementary information

A. List of components and reagents

Material	Supplier	Reference
2-(N-Morpholino) ethanesulfonic acid	Sigma Aldrich, Ireland	M3671
2-ethoxyethanol	Sigma Aldrich, Ireland	02540
4-(Dimethylamino) benzaldehyde	Sigma Aldrich, Ireland	39070
4arm PEG Succinimidyl Glutarate MW 10,000 (4S-StarPEG)	Jenkem Technology, China	4ARM-SG-10K
Acetic acid glacial	Fischer Chemical, Ireland	A/0360/PB17
Acrylamide/bis-acrylamide 30% solution	Sigma Aldrich, Ireland	A3699-100ML
All Tissue culture consumable	SARSTEDT, Ireland NUNC, Ireland	-
almarBlue reagent	Ireland	DAL1100
Ammonium persulfate	Sigma Aldrich, Ireland	A3678
Bovine tendons	Local abattoirs, Ireland	-
Bromophenol blue	Bio-Rad, UK	161-0404
Calcium chloride	Sigma Aldrich, Ireland	C5080
Chloramine T hydrate	Sigma Aldrich, Ireland	857319
Citric acid monohydrare	Sigma Aldrich, Ireland	33114
Collagen type I standard	Symatese Biomateriaux, France	CBPE2US500

Material	Supplier	Reference
Collagen type I standard	BD Bioscience, France	354231
Collagenase type I from Clostridium histolyticum	Sigma Aldrich, Ireland	C0130
Collagenase type IV from Clostridium histolyticum	Sigma Aldrich, Ireland	C5138
Cytokine panel 1 (human) kit V-PLEX	Meso Scale Discovery (MSD), USA	K15050D
CytoTox 96® Non-Radio-active Cytotoxicity Assay	Promega, USA	G1780
Dialysis tubing cellulose membrane	Sigma Aldrich, Ireland	D9527
Dulbecco's modified eagle's medium	Sigma Aldrich, Ireland	D6429
Foetal bovine serum	Sigma Aldrich, Ireland	F7524
Genipin	Challenge Bioproducts Company (CBC), Taiwan	-
Glutaraldehyde	Sigma Aldrich, Ireland	G5882
Glycine	Fisher Scientific, Ireland	9891
Hank's Balanced Salt Solution	Sigma Aldrich, Ireland	H6648
Human derived leukemic monocyte cells, THP-1	ATCC, LGC Standards, UK	TIB-202
Human skin fibroblasts, WS1	ATCC, LGC Standards, UK	CRL-1502
Hydrochloric acid 37%	Sigma Aldrich, Ireland	320331

Material	Supplier	Reference
Isopropanol	Sigma Aldrich, Ireland	I9516
L-hydroxyproline	Panreac AppliChem, UK	A17050025
Lipopolysaccharides	Sigma Aldrich, Ireland	L9641
Live/Dead® reagent	Invitrogen, Thermo Fisher Scientific, Ireland	L-3224
N-(3-Dimethylaminopropyl)-N'-ethylcarbodiimide (EDC)	Sigma Aldrich, Ireland	39391
N,N,N\'N\'-Tetramethyl-ethylenediamine (TEMED)	Bio-Rad, UK	161-0800
N-hydroxysuccinimide (NHS)	Sigma Aldrich, Ireland	56480
Ninhydrin	Sigma Aldrich, Ireland	N4876
Oleuropein	Extrasynthese, France	0228 S
Penicillin / streptomycin	Sigma Aldrich, Ireland	P4333
Pepsin from porcine gastric mucosa	Sigma Aldrich, Ireland	P6887
Perchloric acid	Sigma Aldrich, Ireland	244252
Phenol red	Sigma Aldrich, Ireland	P3532
Phorbol 12-myristate 13-acetate	Sigma Aldrich, Ireland	P8139
Phosphate buffered saline	Fischer Bioreagents, Ireland	BP399-4
Porcine tendons	Local abattoirs, Ireland	-
Precision plus™ protein std.	Bio-Rad, UK	161-0373
Proinflammatory panel 1	Meso Scale Discovery, USA	K15049D

Material	Supplier	Reference
(human) kit V-PLEX		
Quant-iT™ PicoGreen® dsDNA kit	Invitrogen, Thermo Fisher Scientific, Ireland	P11496
RPMI-1640 medium	Sigma Aldrich, Ireland	R8758
SilverQuest™ Silver Staining Kit	Invitrogen, Life Technologies, Ireland	LC6070
SimplyBlue SafeStain	Invitrogen, Thermo Fisher Scientific, Ireland	LC6060
Sodium acetate anhydrous	Sigma Aldrich, Ireland	71183
Sodium chloride	Sigma Aldrich, Ireland	S7653-5KG
Sodium dodecyl sulphate	Bio-Rad, UK	1610302
Sodium hydroxide	Sigma Aldrich, Ireland	S8045
Tin(II) chloride	Sigma Aldrich, Ireland	452335
Tris Base	Fisher Scientific, Ireland	BP152-1
Trisodium citrate dihydrate	Sigma Aldrich, Ireland	S1804
Trypan blue	Gibco, Thermo Fisher Scientific, Ireland	15250061
Trypsin/ EDTA	Sigma Aldrich, Ireland	T4049
Tryptic Soy Broth	Sigma Aldrich, Ireland	22092
β-Glucosidase from almonds	Sigma Aldrich, Ireland	49290

B. Type I collagen isolation protocol

B.1. Materials

- Frozen Bovine Tendons.
- 1x PBS.
- Glacial Acetic Acid.
- Pepsin (high activity >3000 U/mg, stored at -20ºC).
- Muslin.
- Sodium Chloride.

B.2. Equipment

- Surgical scalpel.
- Cryo-milling machine.
- Magnetic stirrer and magnetic stirring bar.
- Sieve.
- Centrifuge, 250 ml centrifuge tubes and 500 ml centrifuge bottles.
- Weighing scales.

B.3. Method

NOTE: Tendons and collagen solutions have to be kept around 4ºC, use ice or the cold room for all the steps.

1. Cut the frozen tendons into small pieces (1x1x1 cm^3) using a scalpel. Freeze the resulting small pieces until milling step.
2. Cryo-mill the chopped tendon using a Freezer/Mill 6870 (SPEX SamplePrep). Grinding vials should be filled to 2/3 parts of the total capacity (50 g of tendon approximately). The cryo-milling program (for Freezer/Mill 6870) is 10 min of

pre-cooling and 6 cycles of milling for 2 min and cooling for 2 min. Freezer/Mill 6770 program is 5 min of cooling and 4 min of milling.

3. Weigh and record the desired amount of tendon. This weight (milled tendon) is going to be used during other steps.
4. Wash the milled tendon with 1x PBS (40 ml 1x PBS/g milled tendon) and gently stirring in the cold room. Wash it three times for 40 min each.
5. Suspend the washed tendon in 0.5M Acetic Acid for 72h under stirring in the cold room. (400ml Acetic Acid/g milled tendon).
6. Add Pepsin at a ratio of 80,000 U/g Tendon (milled tendon weight) at room temperature (bench) for 2h and leave it for 48h in the cold room under stirring.
7. Filter through a sieve and scab to remove all the big pieces of tendon that did not come into solution. Alternatively, solution can be centrifuged at 10000 rpm for 20 min.
8. Add 0.9M NaCl to the filtered solution and stirring manually every 2hrs (if possible) for 18h (overnight). Any mechanical stirring should be as light as possible to ensure that the precipitated collagen does not break up into small pieces which are too small to collect.
9. The precipitated collagen should collect at the top of the solution with a sieve. Collect as much of the collagen as little as possible of the liquid. Centrifuge at 10000 rpm for 20 min to remove as much liquid as possible. Weigh the collagen.
10. Re-suspend in 1M Acetic Acid (50ml Acetic Acid/g wet collagen). Store at 4ºC until all comes into solution (24h). Light stirring is recommended.
11. Centrifuge at 10000 rpm for 20 min. Collect only the top liquid, discard any precipitated or pellet for in the centrifuge tubes.
12. Add 0.9M NaCl to the re-suspended collagen solution, stirring manually every

2h and leave for 18h (overnight).

13. The precipitated Collagen should collect at the top of the solution. Collect as much as possible of the collagen with a sieve. Centrifuge at 10000 rpm for 20min to remove as much liquid as possible. Weigh the Collagen.
14. Re-Suspend in minimum volume of 1M Acetic Acid to produce highly concentrated collagen solution.
15. Once fully suspended, dialyse the collagen against 1mM Acetic Acid at least 4 times, changing the Acetic Acid every two hours. Last one should be overnight.
16. Check the final acid concentration (titration), collagen concentration (dry weight, hypro assay) and purity (SDS-PAGE).

C. Collagen film fabrication and cross-linking

C.1. Materials

- Collagen solution 6.0 mg/ml.
- 10x PBS.
- 1x PBS.
- 5M NaOH.
- 1M NaOH.
- pH meter.
- Centrifuge.
- Tubes.
- Silicone mould.

C.2. Method

NOTE: All solutions have to be kept at 4-8ºC. Therefore, keep them in ice during the film preparation. The volumes indicate in the table are for 12 films with a final collagen concentration of ~5 mg/ml.

1. Mix 10X PBS and the type I collagen. Each component of the hydrogel needs to be added in the order indicated in Table C1.
2. Add 5M NaOH.
3. Adjust pH 7.2-7.4 with 1M NaOH checking it with the pH meter.
4. Centrifuge at 3,000 rpm to remove bubbles (Cross-linkers can be added just before this step).
5. Add 10 ml of the neutralized solution to each well of the silicone mould.
6. Incubate at 37ºC for 1 hour.

7. Remove the hydrogel from the silicone mould and place them in a non-stick surface.
8. Dry samples in the flow hood at room temperature for at least 18 hours.
9. Wash films three times with 1x PBS for 20 minutes (each time).
10. Finally, dry films again and keep at room temperature avoiding light exposure.

Table C1. 5% Separation Gel for 1 mm thickness for collagen for mini gel (Protean II Bio-Rad).

Component	Order	Concentration	Volume
PBS	1	10 X	6 ml
NaOH	2	5 M	3 ml
Collagen type I	3	6.0 mg/ml	120 ml
NaOH	4	1 M	Adjust pH 7.4

C.3. Cross-linking methods (0.5 ml per 10 ml collagen sample):

1. GTA (Glutaraldehyde): 0.5 ml of 0.625% v/v in 1X PBS (Stock solution: 25%).
2. EDC+NHS (1-ethyl-3-(3-dimethylaminopropyl)carbodiimide) + N-Hydroxy-succinimide): 0.5 ml of 0.05M 2-(N-morpholino) ethanesulfonic acid (MES) buffer containing 1000 mM EDC and 200 mM NHS in distilled water (pH 5.5) (final concentration 50 mM EDC - 10 mM NHS).
3. 4S-StarPEG (4-arm polyethylene glycol succinimidyl glutarate MW 10,000): 0.5 ml of 20 mM in 1X PBS (Stock solution: powder. Final concentration 1mM).
4. GEN (Genipin): 0.5 ml of 0.625% w/v in 1X PBS (Stock solution: powder).
5. OLE (Oleuropein): 0.5 ml of 5.0 % w/v of activated oleuropein in 1X PBS (Final concentration 0.25%).

Oleuropein activation:

a) Dissolve 0.5 U/ml of β-Glucosidase in 1X PBS.

b) Add 5% oleuropein in 1X PBS and vortex vigorously.

c) Mix at 150 rpm at 25ºC for 2 hours.

d) Ready to add into collagen solution.

D. Freeze-drying protocol

This is an alternative protocol to freeze at – 20°C and dry at high vacuum. This freeze-drying protocol for collagen solutions or samples attempts to ensure homogeneity between samples by controlling ice crystal formation, increasing the reproducibility between different batches. The last drying step should be repeated until samples are totally dry.

D.1. Materials

- Virtis Advantage 2.0.
- Silicone (diameter 4.5 cm) for collagen solutions or eppendorf tubes for other assays such as collagenase.

D.2. Method

1. Add 10-15 ml of collagen solution to each well or introduce samples in eppendorf tubes.
2. Introduce samples in the freeze-drier and set-up the following parameters:

Table D1. Freeze-drying parameters.

Freezing			**Drying**			
R/H	**Temp (ºC)**	**Time (min)**	**R/H**	**Temp (ºC)**	**Time (min)**	**Vacuum (mTorr)**
H	4	10	R	-30	10	200
R	-15	60	H	-30	5	200
H	-15	30	R	-20	10	200
R	-40	60	H	-20	5	200
H	-40	60	R	-10	10	200
			H	-10	1250	150
			R	-5	30	100
			H	-5	1250	50
			R	0	1250	50
			H	0	1250	50
			Repeat last step until samples are dry			

Freeze-drying parameters: ‘R’ is a ramp while ‘H’ is isotherm.

E. Hydroxyproline assay for collagen quantification

E.1. Materials

- Citrate buffer (500 ml): 17.19 g of sodium acetate anhydrous, 18.75 g of tri-sodium citrate-$2H_2O$, 2.75 g of citric acid, 200 ml of distilled water and 200 ml of isopropanol. Dissolve solids in the distilled water, add the isopropanol and make up the volume with distilled water.
- Chloramine T reagent: 50 ml of citrate buffer, 0.70 g of Chloramine T and 10 ml of distilled water.
- Ehrlics reagent: 6 g 4-(Dimethylamino)benzaldehyde, 9 ml of perchloric acid and 50 ml of isopropanol. The solids were dissolved in the perchloric acid and the isopropanol was added immediately prior to use.
- Diluent isopropanol: distilled water; 2 to 1 ratio.
- Hydroxyproline standards: 10 mg/ml.

E.2. Method

1. Place 0.75 ml of the collagen solution in a eppendorf tube.
2. Add 0.75 ml of concentrated HCl.
3. Incubate the tubes at 100 ºC for 4 hours.
4. After that, leave tubes to cool down and then transfer into volumetric flasks (50ml) containing approximately 10 ml distilled water. Rinse tubes with distilled water (3 times with 1 ml) and add the washings the volumetric flask.
5. Add water up to 50 ml and mix.
6. Dilute 1, 2 and 3 ml of the hydrolysed solution in 15 ml volumetric flasks, add water up to 10 ml and mix.

7. Prepare a hydroxyproline standard curve at 0, 1, 2.5, 5, 10, 15 and 20 µg/ml in water.
8. Add in a eppendorf tube 240 µl of standard or sample, 550 µl of diluent and 380 µl Chloramine T reagent.
9. Mix and then leave the samples to settle for 20 minutes at room temperature.
10. Add 1000 µl of Ehrlichs reagent and mix.
11. Incubate at 70 ºC for 10 minutes in a hot plate or water bath.
12. Finally, cool down, mix and read the absorbance in a spectrophotometer at 555nm.

F. SDS-PAGE

F.1. Materials

- 1.875 M Tris-HCl, pH 8.8. Dissolve 22.70 g Tris-base in 80 ml milliQ H_2O; add 2 ml concentrated HCl, leave it overnight to equilibrate, adjust pH to 8.8 with a few drops concentrated HCl, make it up to 100 ml with ddH_2O. Keep it at 4-8ºC.
- 1.25 M Tris-HCl, pH 6.8. Dissolve 15.14 g Tris-base in 70 ml milliQ H2O; add 7 ml concentrated HCl, leave it overnight to equilibrate, adjust pH to 6.8 with a few drops concentrated HCl, make it up to 100 ml with ddH_2O. Keep it at 4-8 ºC.
- 5x sample buffer. Dissolve completely 0.25 g SDS in 0.625 ml 1.25 M Tris-HCl, pH 6.8 and 2 ml milliQ H_2O. Leave it overnight for the foam to settle. Top up with glycerol to 5 ml (approximately 2.3ml). Add 2.5 mg bromophenol blue per 10 ml buffer.
- 5x running buffer. Dissolve 15.1 g Tris-base, 72 g glycine and 5 g SDS in 1 litre milliQ H_2O. Store at 4ºC. 1x running buffer is made to run the gel from 5x running buffer by diluting in milliQ H_2O.
- 30% Acrylamide/Bis (37.5:1).
- 10% SDS.
- 100 mg/ml Ammonium persulphate in milliQ H_2O. Dissolve 500mg APS in 5ml ddH_2O, aliquot it in eppendorf tubes and keep it at - 20ºC. The solution is active for a few months.
- TEMED.
- 10% and 70% Ethanol in dH_2O.

F.2. Method – gels preparation

1. Defrost an aliquot of APS.
2. Clean glass plates with 70% ethanol and tissue papers.
3. Set the gel making system, ensuring that the glass plates fit tightly to the rubber base.
4. Check for any leak by placing into some water.
5. Add the different reagents in a conical tube to make the 5% gel according to the Table F1 below. Follow the reagent order of the table.
6. Pipette the mixture into the space between the 2 glass plates to reach about 1 cm from the bottom of the well comb (keep the excess solution to check the polymerisation).
7. Overlay the gel with 10% ethanol to cut off oxidation.
8. Leave it aside for approximately 30 minutes, a phase separation ethanol-gel can be observed when the mixture becomes a gel, check with the excess solution remained.
9. During the setting period, prepare the 3% stacking gel according to the Table F2 (except APS and TEMED).
10. Discard 10% ethanol and remove any traces using filter paper.
11. Add the APS and TEMED to the stacking gel mixture and carefully pipette on top of the previous gel. Immediately, insert the well comb, avoid trapping air bubbles formation (keep the excess solution to check the polymerisation).
12. After the gels have been set (10-15 minutes, check it with the excess solution), keep them at 4-8ºC covered with running buffer or use it immediately.

Table F1. 5% Separation Gel for 1 mm thickness for collagen for mini gel (Protean II Bio-Rad).

	1 Gel	**2 Gels**	**4 Gels**
30% Acrylamide/Bis (37.5:1)	830 μl	1660 μl	3320 μl
1.875M Tris-HCl pH 8.8	1000 μl	2000 μl	4000 μl
10% SDS	50 μl	100 μl	400 μl
ddH2O	3070 μl	6140 μl	12280 μl
APS (100mg/ml)	42 μl	84 μl	168 μl
TEMED	5 μl	10 μl	20 μl
Total	5000 μl	10000 μl	20000 μl

Table F2. 3% Stacking Gel for 1mm thickness) for collagen for mini gel (Protean II Bio-Rad).

	1 Gel	**2 Gels**	**4 Gels**
30% Acrylamide/Bis (37.5:1)	200 μl	400 μl	800 μl
1.25M Tris-HCl pH 6.8	200 μl	400 μl	800 μl
10% SDS	33 μl	66 μl	132 μl
ddH2O	1550 μl	3100 μl	6200 μl
APS (100mg/ml)	17 μl	33 μl	66 μl
TEMED	3 μl	6 μl	12 μl
Total	2000 μl	4000 μl	8000 μl

F.3. Method – sample preparation

1. Mix 100 µl of sample (~0.5 mg/ml) with 5 µl Phenol red.
2. Neutralised sample with 1M NaOH until colour change.
3. Mix 12 µl of sample buffer with 48 µl of sample. Vortex and spin.
4. Denature samples at 95°C for 5 min. Vortex and spin.

F.4. Method – running gels

1. Remove slowly the combs.
2. Assemble the electrophoresis apparatus, for small gel apparatus, fit the gel plates on the electrode bar and fit the set into the inner chamber and clamp them.
3. Fill the upper chamber with 1x running buffer. If no leaks, fill the inner chamber.
4. Load the standards, samples and markers using a 20 μl micropipette and a narrow tip.
5. Close the lid and run the gels.
6. Run at constant voltage: 50V until the front reaches the end of the stacking gel (± 30-40 min), then 120V until the front reaches the end of the separating gel (±1 hour).
7. Remove the glass using the wonder wedge, cut the lower right hand corner and release the gel slowly into milliQ H_2O.
8. Proceed with Coomassie or Silver staining (refer to SafeBlue or SilverQuest, Invitrogen Protocols respectively).

G. Silver staining of SDS-PAGE gels

Adapting the manufacturer instructions for the SilverQuest™ Silver Staining Kit, the method is briefly described in the following table:

Table G1. Silver staining method step by step. Volumes are indicated per gel.

Step	Reagent	Incubation time
Fix	Ethanol 10 ml Acetic acid 2.5 ml Water up to 25 ml	20 min
Wash	Ethanol 7.5 ml Water up to 25 ml	10 min
Sensitize	Ethanol 7.5 ml Sensitizer 2.5 ml Water up to 25 ml	10 min
First wash	Ethanol 7.5 ml Water up to 25 ml	10 min
Second wash	Water 25 ml	10 min
Stain	Stainer 0.25 ml Water up to 25 ml	15 min
Wash	Water 25 ml	1 min
Develop	Developer 2.5 ml Developer enhancer 1 drop Water up to 25 ml	4-8 min

Step	Reagent	Incubation time
Stop	Stopper 10 ml (add directly to developing solution)	10 min
Wash	Water 25 ml	10 min

H. Densitometry analysis of SDS-PAGE

1. Scan the stained gels on using HP Scanjet 7400C scanner and the active transparency adapter HP Scanjet XPA c7671b.
2. Densitometry analysis is performed with ImageJ software.
3. Open ImageJ
4. Go to File/Open/select the desired images
5. Transform image to 16 bits: go to Image/Type/16-bits
6. Select the rectangle tool, and draw a box around the lane from above gamma band until below alpha bands.
7. Select first lane: go to Analyze/Gels/Select first lane or press Ctrl+1
8. Move the rectangle to the next lane and go to Analyze/Gels/Select next lane or press Ctrl+2. Repeat this for each lane.
9. After all the lanes have been marked, go to Analyze/Gels/Plot lanes or press Ctrl+3.
10. Use the line tool to draw a straight line at the bottom of each peak to close the area under each peak.
11. Select the magic wand from the tool menu and click it on each peak.
12. A new box with all the results will be displayed.

I. Ninhydrin assay for free amine quantification

I.1. Materials

- Collagen samples.
- Ninhydrin powder.
- 2-ethoxyethanol.
- 200 mM Citric acid.
- Tin II Chloride.
- Glycine.

I.2. Method

1. Cut collagen sample to small pieces of 3 mg ± 10%.
2. Place into a labelled eppendorf tube.
3. Add 200 μL dH_2O to each sample.
4. Prepare an standard curve of glycine at 0, 0.01, 0.05, 0.1, 0.2 and 0.5 mg/ml.
5. Prepare one tube of 4% Ninhydrin powder in 2-ethoxyethanol and protect from light.
6. Prepare a second tube of 200 mM Citric acid, 0.16 w/v% Tin II Chloride, pH 5.0.
7. Mix both solutions together.
8. Add 1 ml Ninhydrin solution to each tube.
9. Incubate tubes at 95-100ºC for 30-35 minutes, protecting from light.
10. Allow tubes to cool to room temperature.
11. Add 250 μL of 50% isopropanol and vortex.
12. Read using plate reader at 570 nm.

J. Collagenase: degradation/stability assay

J.1. Materials

- Collagen samples.
- 0.1M Tris-HCl pH 7.4 (Tris Base MW = 121.14 g/mol).
- 50 mM CaCl2 (CaCl2 MW = 111 g/mol).

J.2. Method

1. Sample preparation: cut pieces of films with a dry weight between 1.0-1.5 mg and introduce it in 1.5 ml eppendorf (n=5).
2. Prepare the buffer 0.1M Tris-HCl pH 7.4 + 50 mM CaCl2.

   i.e.: 0.25 L*0.1 mol/L* 124.14 g/mol = 3.03 g Tris Base

   i.e.: 0.25 L*0.05 mol/L* 111 g/mol = 1.39 CaCl2
3. Incubate samples in 500 µl of buffer for 30 minutes.
4. Prepare a 20 U/ml solution collagenase in 0.1M Tris-HCl pH 7.4 + 50 mM CaCl2.
5. Add 500 µl of reconstituted collagenase (the concentration of the collagenase buffer is 10 U/ml).
6. Incubate at 37°C and orbital agitation (150 rpm) for 24h.
7. Centrifuge at 11,000 rpm for 10 minutes.
8. Remove buffer and freeze it.
9. Weigh the dry samples and compare with the initial weigh.

K. Scanning electron microscopy (SEM) - sample preparation

K.1. Materials

- Collagen samples.
- 1x PBS.
- 50%, 70%, 90%, 96% and 100% ethanol.

K.2. Method

1. Hydrate samples at room temperature overnight.
2. Dehydrated in ascending ethanol concentration (50%, 70%, 90%, 96% and 100%), 30 minutes for each concentration.
3. Evaporate ethanol overnight at room temperature.
4. Dry sample at the vacuum chamber for at least 12 hours.
5. Gold coating using Emitech K-550X sputtering system for 2 minutes.

L. Protocol of fibroblasts cell culture

The entire protocol should be performed in aseptic conditions. All materials should be sprayed with 70% ethanol before putting into the biological safety cabinet.

L.1. Expansion

- EMEM supplemented with 10% FBS and 1% P/S or DMEM high glucose supplemented with 10% FBS and 1% P/S.
- Media was changed every two-three days.

L.2. Splitting

When cells reach approximately 80 % confluence, they are split into two or more flasks or frozen for later use, as follow:

1. The media is removed from the flask and place in the waste container.
2. The cells are washed with HBSS twice.
3. Trypsin-EDTA is added to the flask, ensuring complete coverage of the flask.
4. The flask is returned to the incubator for 5 minutes (enzyme is active at 37 °C).
5. Then, flask is examined under the microscope to see if cells detach from the surface and are floating in the media. If not, lightly tapping.
6. Once cells are detached, equal volume of media supplemented with 10 % serum is added to the flask to deactivate the trypsin.
7. All media is then collected and placed into a sterile centrifuge tube.
8. Centrifuge for 5 minutes at 1200 rpm.
9. Discard supernatant and the pellet is re-suspended in fresh media.
10. Finally, cells are counted using Neubauer chamber and seed into new flasks.

L.3. Cell freezing

To freeze cell perform the splitting protocol with a modification at the end

1. Instead of re-suspending the pellet in to media, cells are re-suspended in media supplemented with 10 % FBS and 10 % filtered DMSO.
2. Cell concentration should be adjusted at 0.5-1.0 million cells per ml.
3. Transfer 1 ml of media with cells into each vial.
4. Place vial into a Mr Frosty container and place it into the –80 °C freezer for 24 hours.
5. Then, vials should be kept in the liquid nitrogen container.

L.4. Cell thawing

1. Remove vials from the liquid nitrogen container.
2. Thaw the vial by gentle agitation in water bath at 37 °C. Keep the O-ring and cap out of the water to reduce potential contamination.
3. Transfer the content of the vials in a falcon with pre-warmed media.
4. Centrifuge at 1200 rpm for 5 minutes.
5. Discard supernatant and re-suspended in media.
6. Count cells and seed them at 3000-4000 cells/cm^2.
7. Incubate the cells in an incubator at 37°C and 5% CO_2.

M. Protocol of macrophages cell culture

M.1. Expansion

- RPMI 1640 medium supplemented with 10% FBS, 1% P/S and 1% glutamine.
- Seed at 300,000 cells/ml.
- Daily observation in the optical microscope for morphology check.
- Top up with fresh media every second day or when cell concentration reaches 800,000 cells/ml (Do not allow the cell concentration to exceed 1,000,000 cells/ml).
- Spin down and use fresh media every 7 days.

M.2. Differentiation

1. Use THP-1 cells when their density reaches 800,000-1,000,000 cells/ml.
2. Dilute PMA in DMSO at 5 µg/ml.
3. Add 100 µl PMA at 5 µg/ml for each 50 ml supplemented RPMI 1640 medium (10 ng/ml).
4. Spin down the cells and re-suspend them with the medium of differentiation.
5. Count the THP-1 cells with hematocytometer and trypan blue.
6. Adjust the cell density at 100,000 cells/ml.
7. Seed cells in a 24 well plate by adding 0.5 ml of cell suspension per well.
8. Incubate cells at 37°C for 6 hours.
9. Check the differentiation by observation at the microscope. If you see floating cells (undifferentiated), incubate for 6 hours more.
10. Then, remove the media and replace it by normal medium or activation medium (1ml/well). Activation medium is supplemented RPMI 1640 medium with 100 ng/ml LPS (2.5 µl of LPS stock solution at 2 mg/ml for 50 ml medium).

11. Incubate the cells for 24 hours at 37°C.

12. Replace by normal medium (this is time point 0).

M.3. Cell freezing and thawing

As Appendix K - Protocol of fibroblasts cell culture.

N. Cell metabolic activity assay using alamarBlue™

N.1. Materials

- alamarBlue™ (Invitrogen, USA).
- HBSS.

N.2. Method

1. Prepare a 10 % alamarBlue™ solution in HBSS.
2. Wash the wells with HBSS.
3. Add 0.4 ml of alamarBlue™ in each well and a negative control with 10% alamarBlue™ alone.
4. Incubate at 37°C for 3 hours.
5. Transfer 200 µl of each well in a 96-well clear plate.
6. Measure the absorbance at the wave length of 550 nm and 595 nm.
7. Subtract the absorbance value of media only from the absorbance values of the absorbance values of alamarBlue™ in media. This gives the absorbance of alamarBlue™. Call this value AOLW or the absorbance of oxidised form at lower wavelength. Get the AOHW or absorbance of oxidised form at higher wavelength.
8. Calculate correlation factor: RO.

$$RO = AOLW / AOHW$$

9. Calculate the percentage of reduced alamarBlue™:

$$ARLw = ALw – (AHW \times Ro) \times 100$$

O. Cell proliferation assay using Quant-it™ Picogreen®

O.1. Materials

- HBSS.
- Quant-it™ PicoGreen® dsDNA Reagent and Kits (Invitrogen, USA).

O.2. Method

1. Remove the media and gently rinse with HBSS.
2. Add 200µl of DNase free water.
3. Repeatedly freeze-thaw cells three times.
4. Prepare a 1X TE buffer from the 20X stock solution.
5. Prepare a standard of DNA using DNase free water and the Lambda DNA standard at 100 µg/ml in TE.
6. Make up a 2µg/ml DNA solution (dilution 1:50 from 100µg/ml DNA standard).
7. Make up a 50ng/ml DNA solution (dilution 1:80 from 2µg/ml DNA solution).
8. Transfer 100µl of each sample and DNA standard curve into a 96 well plate for fluorescence assays.
9. Make up diluted PicoGreen solution: 9 ml 1x TE + 45 µl concentrated PicoGreen (enough for a 96 well plate).
10. Add 100µl of diluted PicoGreen to each well.
11. Incubate at room temperature 2-5 minutes in the dark.
12. Read the plate using fluorescent channel (excitation 480 nm, emission 520 nm).

Table O1. Volume for preparing the DNA standard curve.

DNA concentration (ng/ml)	Water volume (µl)	Volume of 2µg/mL DNA stock (µl)	Volume of 50ng/mL DNA stock (µl)
1000	200	200	0
500	300	100	0
100	380	20	0
50	0	0	400
25	200	0	200
10	320	0	80
5	360	0	40
0	400	0	0

P. Cell viability assay using Live/Dead staining

P.1. Materials

- LIVE/DEAD™ Viability/Cytotoxicity Kit, for mammalian cells (Invitrogen, USA).
- 1% Triton X-100.
- HBSS.

P.2. Method

1. For a toxic control, add 5 µl of 1% Triton X-100 per well 30 minutes before.
2. Defrost tubes and quick spin to ensure contents are at the bottom of the tube.
3. Remove media from each well and wash them with HBSS twice.
4. Prepare staining solutions:
    a) Calcein (live) is at 4 mM concentration in the tube and it should be used at 4 µM. Therefore, dilute it at 1:1000 (5 µl in 5 ml HBSS).
    b) Ethidium homoimer-1 (dead) is at 2 mM and it should be used at 2 µM. Therefore, dilute it at 1:1000 (5 µl in 5 ml HBSS with calcein).
5. Protect from light.
6. Add 250 µl of staining solution or enough to cover the film.
7. Incubate for 30 minutes at 37°C.
8. Discard staining solution and wash wells with HBSS twice.
9. Then, stained samples are visualised using the inverted fluorescence microscope (IX 51, Olympus, UK), live cells with the FITC filter and dead cells with the Texas red filter. Five images per sample.
10. Viable/live (green) and dead (red) cells are counted using ImageJ 1.48v software (National Institutes of Health, USA).

Q. Cell viability assay using cytotoxicity kit

Q.1. Materials

- CytoTox 96® Non-Radioactive Cytotoxicity Assay (Promega, USA).

Q.2. Method

1. At each time point transfer the supernatant of each well to eppendorf tubes.
2. Centrifuge at 250 x g for 4 minutes.
3. Transfer supernatant to a new eppendorf tube and keep it at – 80°C until testing.
4. Transfer 50 µl of the supernatant to the corresponding well of a flat-bottom 96-well plate.
5. Add 50 l of a 1:5,000 dilution of LDH Positive Control to 3 separate wells.
6. Reconstitute Substrate Mix using Assay Buffer from the kit.
7. Add 50µl of the reconstituted Substrate Mix to each well of the plate.
8. Cover the plate and incubate at room temperature, protected from light, for 30 minutes.
9. Add 50 µl of the Stop Solution to each well of the plate (NOTE: only perform this step if media is phenol red free).
10. Record absorbance at 490 nm.

R. Optimisation of collagen type I extraction

The extraction of large volumes of collagen solution maintaining high quality standards and reproducibility between batches is still being a challenge. Therefore, we evaluated how different tissues and extraction methods affect the purity collagen type I extractions.

R.1. Materials and methods

Three different mammalian tissues (rat tail tendon, RTT; bovina Achilles tendon, BAT; and porcine Achilles tendon, PAT), two crushing technologies (mincing and cryo-milling) and three solubilisation variables (acid-tendon ratio, temperature and time of the pepsin treatment) were studied. Figure R1 shows the flow diagram that summarises the collagen extraction protocol and the different studied variables.

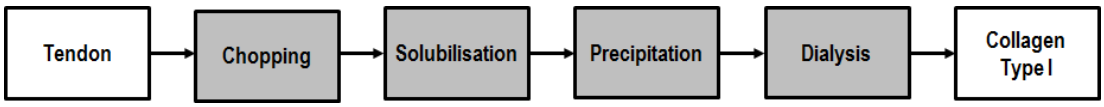

Studied Variables		
Tendon	**Chopping**	**Solubilisation**
RTT BAT PAT	Mincing Cryo-milling	Acid-tendon ratio Temperature and time during pepsin treatment

Figure R1. Flow diagram of collagen extraction and studied variables in the different phases. RTT: rat tail tendon; BAT: bovine Achilles tendon; PAT: porcine Achilles tendon.

BATs and PATs were kindly donated by the local abattoir (steers aged 24 months and pigs aged 6 months, respectively). RATs were obtained from humane sacrificed rats used in other surgical procedures that did not affect rat tails. Collagen type I was extracted from tendons adapting a previous protocol from Zeugolis' group. Briefly, RATs were dissected, washed with 1X phosphate buffered saline (PBS) solution and, subsequently, dissolved in 0.5M acetic acid. On the other hand, BATs and PATs were manually separated from the surrounding fascia, minced or cryo-milled, and washed with 1X PBS solution. Then, 0.5M acetic acid was added progressively to tendons and kept under orbital agitation at 4°C until tendon dissolution. Subsequently, pepsin from porcine gastric mucosa was added in a ratio of 80U/mg of milled tendon and solution was incubated at 22 or 37°C between 2-16 hours. Afterwards, solution was kept at 4°C for 72 hours in order to take profit of all pepsin activity and to increase the efficiency. Insoluble tendon was separated by filtration and centrifugation (21,000g at 4°C for 20 min). Collagen solution was purified by repeated salt precipitation (0.9M NaCl), centrifugation and re-suspension in 1M acetic acid. The final atellocollagen solution was dialysed (Mw 8000 cut off) against 1mM acetic acid.

Collagen concentration was assessed by dry weight after freeze-drying, hydroxyproline assay and/or Sircol assay. Furthermore, collagen purity was examined by sodium dodecyl sulphate polyacrylamide gel electrophoresis (SDS-PAGE) assays.

R.2. Results and discussion

Tendon chopping/crushing phase

Mincing is a common method for breaking tissues before any digestion; however, every single mincing machine, that we used to mince tendons mixed with ice, introduced metallic particles into tendon. The stirring bar used during the solubilisation phase collected the metallic particles and evidenciated their presence, see Figure R2. It could be concluded that the metallic particles come from the mincing machine, as no other metallic tool was used up to this point and degradation marks were observed in the mincers. For that reason, mincing was discarted and cryo-milling was the only method used to extract collagen from bovine and porcine tendon.

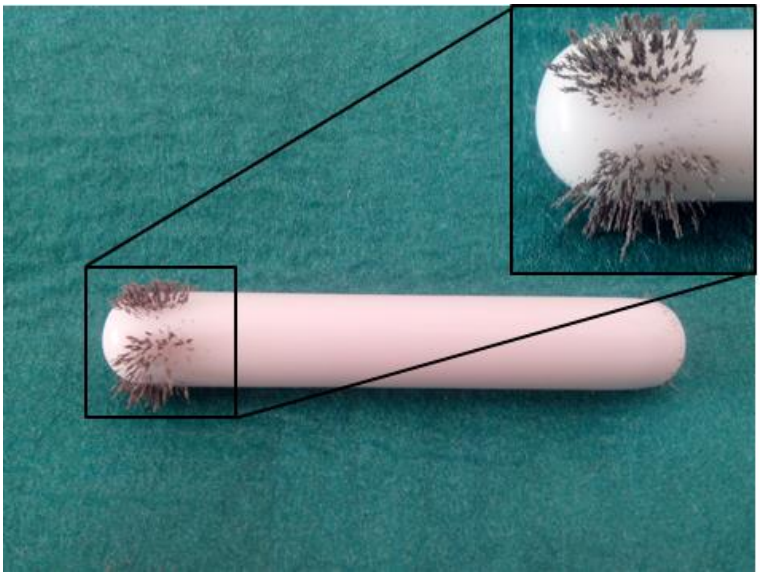

Figure R2. Metallic particles collected by the stirring bar during the solubilisation of minced bovine Achilles tendon in acetic acid. Metallic particles were introduced during mincing step and are partially collected by the stirring bar.

Solubilisation step

The disolution of tendons depended on the animal source, RTTs presented the highest disolution capacity in 0.5 M acetic acid (20 g/litre), followed by PATs (10.5 g/litre) and BATs (3.3 g/litre). This difference is mainly due to the natural cross-linking degree of each tendon source, which is higher as older and bigger are animals.

Regarding the pepsin treatment, increasing of temperature between 22-24°C showed to improve collagen extraction, while 37°C induced collagen denaturation (Figure R3). Moreover, the time increase affected collagen bands, alpha bands increased 12% when treated with pepsin at 22°C for 6 hours, indicating higher collagen extraction efficiency. On the other hand, treatment at 22°C for 16 hours reduced 34% alpha bands which may indicate partially collagen denaturation. Moreover, SDS-PAGE showed that collagen purity for all batches was over 96%.

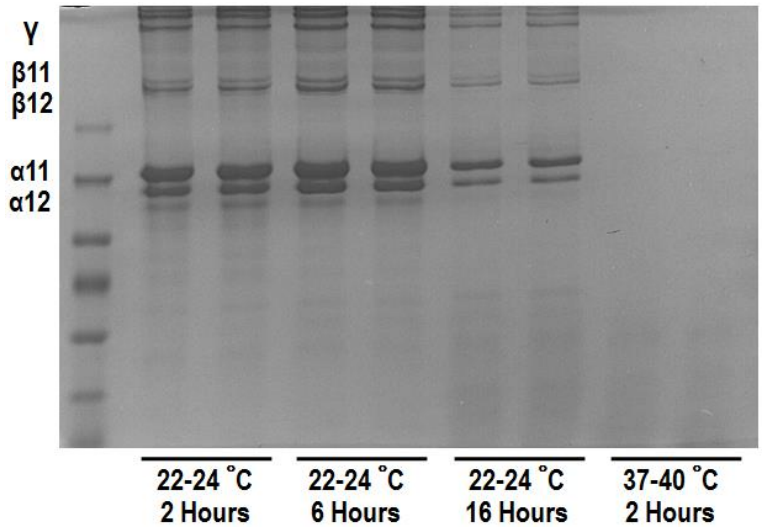

Temperature	Time	Composition (%)			Purity
(°C)	(Hours)	γ	$\beta_{11}+\beta_{12}$	$\alpha_{11}+\alpha_{12}$	(%)
22-24	2	10.6	22.8	62.9	96.3
22-24	6	9.4	23.8	63.5	96.7
22-24	16	14.3	15.6	68.6	98.5
37-40	2	Totally denatured			

Figure R3. SDS-PAGE analysis of bovine pepsin soluble collagen incubated at 22°C or 37°C during pepsin digestion step. Table indicates the distribution of gamma (γ), beta (β) and alpha (α) collagen bands of each collagen batch. Moreover, data shows the high collagen purity.

Once basic parameters of collagen extraction protocol were fixed, collagen type I was extracted from RTT, PAT and BAT. RTT was not cryo-milled because RTT is much less tough than PAT and BAT and, therefore, tendons were directly dissolved in acetic acid without any mincing step. The three different extractions were viscous and smooth with different collagen concentrations, see Figure R4. SDS-PAGE of each collagen extraction demonstrated purities over 90% and similar to commercially available collagen type I BD™ solutions.

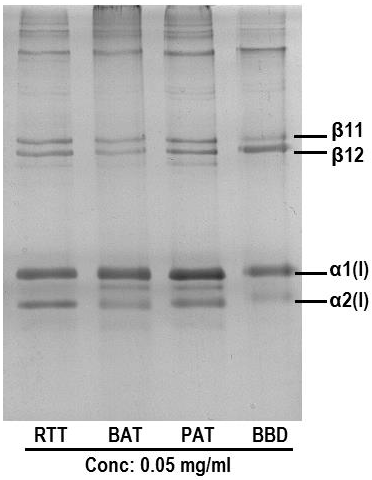

Sample	Final volume	Concentration (mg/ml)			Purity
	(ml)	Dry Weight	Hydroxyproline assay	Sircol assay	(%)
RTT	20	9.4 ± 0.5	8.0 ± 0.1	7.8 ± 0.6	93.9 ± 1.1
BAT	1,200	3.4 ± 0.2	2.7 ± 0.1	2.8 ± 0.4	91.2 ± 0.9
PAT	100	4.6 ± 0.4	4.2 ± 0.1	4.2 ± 0.2	91.5 ± 1.0
BBD	-	3.1 ± 0.3	3.0 ± 0.1	3.0 ± 0.3	95.4 ± 1.0

Figure A4. SDS-PAGE analysis of different collagen type I solutions extracted from RTTs (rat tail tendons), BATs (bovine Achilles tendons) and PATs (porcine Achilles tendons). Commercially available bovine collagen type I BD™ was used as control. Table indicates concentrations of each collagen batch that were measured by dry weight after freeze-drying (D Weight), hydroxyproline assay (Hypro) and Sircol assay. Moreover, table shows the collagen purity obtained from the SDS-PAGE analysis.

Up-scaling of collagen extraction

Last optimisation phase was up-scaling collagen type I extraction maintaining high purity and concentration of protein. This optimisation was only performed with BAT because it is the most complicated source to extract due to its high natural cross-linking degree and it required higher volume of acetic acid to dissolve it; optimised parameters could be used with other tendon sources.

In order to reduce the initial volume, two different concentration of acetic acid (0.5 and 1.0 M) were studied to dissolve milled BAT. 1.0 M acetic acid demonstrated to be more efficient dissolving bovine tendon; ratio tendon-acid was 10 g/litre, while 0.5 M acetic acid was 3.3 g/litre (as above presented). In addition, SDS-PAGE analysis did not show any reduction of purity by the increase of acetic acid concentration, see Figure R5.

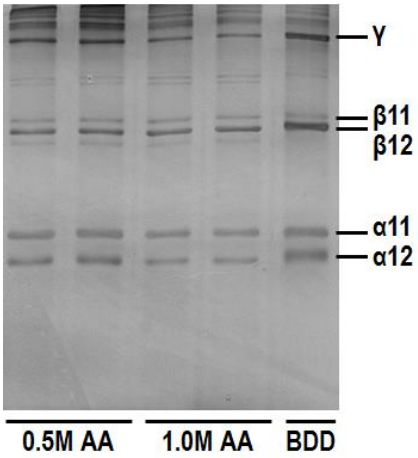

Figure R5. SDS-PAGE analysis of bovine collagen type I solution extracted with 0.5 and 1.0 M acetic acid (AA). Commercially available bovine collagen type I BD™ was used as control (BDD).

Finally, we proceed to extract between 3.5 and 4 litres of collagen type I (5-6 mg/ml) with the reviewed protocol. From the initial 80 grams of cryo-milled BAT, 4.2 litres of collagen type I with a final concetration of 5.1 ± 0.3 mg/ml were obtained, see Figure R6. In addition, collagen purity was not compromised by up-scaling of the extraction and it was similar to commercially available bovine collagen type I BD™, see Figure R6.

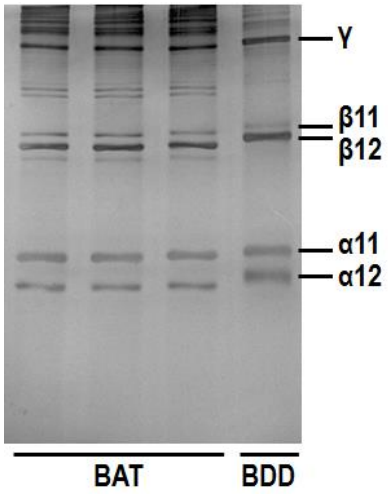

Sample	Final volume	Concentration (mg/ml)		Purity
	(ml)	D Weight	Hypro	(%)
BAT	4,200	5.2 ± 0.1	5.1 ± 0.3	95.6 ± 1.0
BBD	-	3.0 ± 0.1	2.9 ± 0.1	96.8 ± 1.5

Figure R6. SDS-PAGE analysis of pepsin soluble collagen type I extracted from BAT (bovine Achilles tendon). Commercially available bovine collagen type I BD™ was used as control (BDD). Table indicates collagen type I purity (calculated from the densitometric analysis of the SDS-PAGE image) and concentration (measured by dry weight after freeze-drying, D Weight; and hydroxyproline assay, Hypro).

R.3. Conclusions

Pepsin soluble collagen type I solutions with purities over 90% and diverse concentrations have been extracted from rat, bovine and porcine tendons. Cryo-milling of bovine and porcine tendons was an important factor in the extraction as it produced tendon powder free of metallic particles that dissolved fast and homogeneously in all batches. Moreover, the adjustment of temperature and time during pepsin treatment was critical, pepsin treatment at 22°C for 2 hours induced collagen cleavage and improved extraction. This effect was more pronounced when the processing time was 6 hours; it increased 12% collagen alpha bands, which is a sign of better digestion and extraction efficiency. Pepsin treatment at 22°C for 16 hours or at 37°C for 2 hours induced partially or totally collagen denaturation. Finally, bovine collagen extraction up-scaling allowed obtaining about 4 litres of collagen type I with 95% purity, similar to other commercially available collagen type I solutions.

S. Research outputs

S.1. Manuscripts

1. **Delgado LM**, Pandit A, Zeugolis DI. Influence of Sterilisation Methods on Collagen-based Devices Stability and Properties. Expert Rev Med Devices. 2014; 11(3):305-14.
2. Joyce CW, Sugrue C, Chan JC, **Delgado L**, Zeugolis D, Carroll SM, Kelly JL. A barbed suture repair for flexor tendons: a novel technique with no exposed barbs. Plast Reconstr Surg Glob Open. 2014;2(10):e237.
3. Pintado-Sierra M, **Delgado L**, Aranaz I, Marcos-Fernández A, Reinecke H, Gallardo A, Zeugolis D, Elvira C. Surface hierarchical porosity in poly(ε-caprolactone) membranes with potential applications in tissue engineering prepared by foaming in supercritical carbon dioxide. J Supercritical Fluids. 2014;95:273-284.
4. **Delgado LM**, Bayon Y, Pandit A, Zeugolis DI. To cross-link or not to cross-link? Cross-linking associated foreign body response of collagen-based devices. Tissue Eng Part B Rev. 2014;21(3):298-313.
5. Abbah SA*, **Delgado LM***, Azeem A, Fuller K, Shologu N, Keeney M, Biggs M, Pandit A, Zeugolis DI. Harnessing hierarchical nano- and micro- fabrication technologies for musculoskeletal tissue engineering. Adv Healthcare Mat. 2105;16:2488-2499. *These authors share first authorship.
6. Fuller KP, Gaspar D, **Delgado LM**, Pandit A, Zeugolis DI. Influence of porosity and pore shape on structural, mechanical and biological properties of poly ϵ-caprolactone electro-spun fibrous scaffolds. Nanomedicine. 2016; 11(9):1031-40.

7. **Delgado LM**, Fuller K, Zeugolis DI. Collagen cross-linking – Biophysical, biochemical and biological response analysis. Tissue Eng Part A. 2017;23(19-20):1064-1077.
8. **Delgado LM**, Sholugu N, Fuller K, Zeugolis DI. Acetic acid and pepsin result in high yield, high purity and low macrophage response collagen for biomedical applications. Biomedical Mater. 2017;25; 12(6):065009.
9. **Delgado LM**, Fuller K, Zeugolis DI. The influence of cross-linking method and sterilisation treatment on the structural, biophysical, biochemical and biological properties of collagen devices. Submitted.
10. Sorushanova A, **Delgado LM**, Sholugu N, Kshirsagar A, Wu Z, Mullen AM, Raghunath M, Pandit A, Zeugolis DI. New tricks for the old proteins – The next generation of materials. Submitted.

S.2. Outreach manuscripts

1. **Delgado LM**, Pandit A, Zeugolis D. Squeaky clean collagen – device-dependent sterilisation. Medical Device Develop. 2014; Epub.

S.3. Abstract publications

1. Ryan C, Sweeney D, Quinlan L, **Delgado L**, Laighin GO, Pandit A, Zeugolis D. Optimisation of a 3D electrochemically aligned collagen type I scaffold. J Tissue Eng Regen Med. 2014;8:468-69.
2. **Delgado LM**, Pandit A, Zeugolis D. Influence of collagen cross-linking on fibroblast and macrophage response. J Tissue Eng Regen Med, 2014;8:437

3. **Delgado LM**, Fuller K, Gaspar D, Pandit A, Zeugolis D. Collagen cross-linking modulates scaffold stability and pro-inflammatory macrophage response. Tissue Eng Part A. 2015; 21, S12-S13.
4. **Delgado L**, Fuller K, Fernandez-Yague MA, Biggs M, Pandit A, Zeugolis D. Collagen cross-linking increases scaffold stability while modulates pro-inflammatory macrophage response. Front Bioeng Biotechnol, 2016; 10.3389/conf.FBIOE.2016.01.02202.

S.4. Conferences participations

1. Sugrue C, Joyce C, Chan J, **Delgado L**, Zeugolis D, Carroll S, Kelly J. A quick and simple four-strand barbed suture repair technique for flexor tendons: A comparison to a traditional four-strand monofilament repair. The Royal College of Surgeons - BSSH/BAHT Combined Scientific Meeting. 2013, UK.
2. **Delgado LM**, Pandit A, Zeugolis DI. Influence of collagen cross-linking on fibroblast and macrophage response. TERMIS EU. 2014, Italy.
3. Ryan C, Sweeney D, Quinlan L, **Delgado L**, Laighin GO, Pandit A, Zeugolis D. Optimisation of a 3D electrochemically aligned collagen type I scaffold. TERMIS EU. 2014, Italy.
4. Pintado M, **Delgado L**, Aranaz I, Marcos-Fernández A, Reinecke H, Gallardo A, Zeugolis D, Elvira C. Preparation in supercritical carbon dioxide of PCL membranes showing hierarchical porosity and potential applications in tissue engineering. FLUCOMP 2014, Spain.
5. **Delgado LM**, Pandit A, Zeugolis DI. Influence of collagen cross-linking on fibroblast and macrophage response. ESB. 2014, UK.

6. **Delgado LM**, Pandit A, Zeugolis DI. Influence of collagen cross-linking on fibroblast and macrophage response. FIRM. 2014, Spain.
7. **Delgado LM**, Bayon Y, Pandit A, Zeugolis DI. To cross-link or not to cross-link collagen matrix for the reformation of the extracellular matrix? MBI – Meeting. 2014, Ireland.
8. **Delgado LM**, Gaspar D, Fuller K, Pandit A, Zeugolis DI. Collagen cross-linking enhances stability whilst induces pro-inflammatory macrophage response. UKSB 14th Annual Conference and Postgraduate Day. 2015, UK
9. **Delgado LM**, Pandit A, Zeugolis DI. Effect of synthetic and natural cross-linking of collagen films on stability and macrophage response. AFPM. 2015, Ireland.
10. **Delgado LM**, Fuller K, Gaspar D, Pandit A, Zeugolis DI. Collagen Cross-linking modulates scaffold stability and pro-inflammatory macrophage response. TERMIS World. 2015, USA.
11. **Delgado LM**, Fuller K, Fernandez-Yague M, Pandit A, Biggs M, Zeugolis DI. Collagen Cross-Linking Increases Scaffold Stability while Modulates Pro-inflammatory Macrophage Response. World Biomaterials Congress. 2016, Canada.

S.5. Courses

1. Completed LAST course, June-July 2012, Trinity College Dublin.